

**Kingston University London**

**Efficacy of resveratrol metabolites on colon  
cancer cell growth**

**A thesis submitted in partial fulfilment for the degree  
of**

**Doctor of Philosophy**

**By**

**Elena Polycarpou**

**School of Pharmacy and Chemistry**

## **Declaration**

The thesis entitled *Efficacy of resveratrol metabolites on colon cancer cell growth* is based upon the work conducted in the School of Pharmacy and Chemistry, Faculty of Science, Engineering and Computing at Kingston University London. All of the work described here is original unless otherwise acknowledged in the text by references. None of the work presented here has been submitted for another degree in this or any other university.

## Abstract

Resveratrol is a natural polyphenol present in many plant species and derived foods including grapes and red wine. It has been shown to possess chemotherapeutic properties in animal cancer models as well as many biological effects *in vitro*. In this study, the effects of three resveratrol metabolites including resveratrol-3-O-D-glucuronide, resveratrol-4'-O-D-glucuronide and resveratrol-3-O-D-sulphate on the growth of colon cancer cell lines have been investigated.

The growth inhibitory effects of resveratrol, piceatannol, pterostilbene and the glucuronide and sulphate metabolites on Caco-2, CCL-228 and HCT-116 cells were assessed using the neutral red and MTT assays. Resveratrol and its metabolites inhibited the growth of cells with IC<sub>50</sub> values in the range of 9.8-31 µM whilst piceatannol and pterostilbene in the range of 21.7-29.6 µM and 5-34.5 µM respectively. Apoptotic assessment by DAPI staining, Z-VAD-FMK pre-treatment and percentage of cells in sub-G1 by FACS all revealed the absence of apoptosis. Treatment of differentiated Caco-2 monolayers showed that resveratrol was capable of inhibiting the growth of cells following treatment on the apical but not basolateral membrane and the effects were less profound with the metabolites. Only high concentrations (500 µM) of metabolites (not used in any of the growth studies) appeared to be toxic to normal cells as measured by a haemolysis assay.

Resveratrol was capable of causing S phase arrest in all 3 cell lines at 30 µM whilst the two glucuronides caused G0/G1 arrest in Caco-2 and CCL-228 cells only. Resveratrol-3-O-D-sulphate had no effect on the cell cycle. Growth inhibition caused by resveratrol and its two glucuronides was reversed by the addition of an AMP kinase inhibitor (compound C) or an adenosine A<sub>3</sub> receptor antagonist (MRS-1191). Treatment with the highly selective A<sub>3</sub> receptor agonist, 2CI-IB-MECA caused growth inhibition and the A<sub>3</sub> receptor was detected in all 3 cell lines. Levels of cyclin D1 as measured by western blot were significantly reduced at higher concentrations (100 µM) but p-AMPK was not reliably increased in all cases.

Resveratrol glucuronides were shown to inhibit the growth of three colon cancer cell lines by G0/G1 arrest and depletion of cyclin D1. These findings strongly suggest a role of the adenosine A<sub>3</sub> receptor in the observed inhibition therefore, providing a novel target for resveratrol and its metabolites.

## Acknowledgments

The greatest and biggest thank-you goes to my family especially my mum who was and is the greatest inspiration for me. Mum, without you I wouldn't be in this position. My Dad and the best brother and sisters I could have for always being there for me. Frosso, Marina, Petros, thank you for everything. I dedicate this thesis to my grandparents who are not with us today but for always teaching me to have goals in life, achieving them and never giving up.

I would like to thank my Director of Studies, Dr. Mark Carew for all the help, advice, patience and motivation he has provided me with over the past three years. Mark, thank you. I would also like to thank my co-supervisors, Prof. Helmout Modjtahedi, Prof. Elizabeth Tyrrell and Dr. Simon Carrington. My thank you is also extended to the Biomedical and Pharmaceutical Sciences Research Group (BPSRG) of Kingston University for funding my PhD and the Head of Pharmacy and Chemistry, Prof. John Brown and Head of the Doctoral School, Prof. Andy Augousti for covering my conference expenses and providing a completion bursary. I am forever grateful.

I would also like to thank the University of Surrey and more specifically, Dr. Lisiane Meira, Dr. Izabel Villela and Prof. Chris Fry for allowing me to work in their laboratories and providing help and advice. I am also thankful to Prof. Tony Walker and Dr. Alan Seddon (School of Life Sciences) for allowing me to use their facilities and equipment.

Last, but not least, I thank all my friends for their help, support and motivation. More specifically, my greatest gratitude goes to my best friends Dr. Ammara Abdullah and Khatebeh Mazloumi for being here every step of the way. Without you two over the past three years things would not have been possible. Ammara, you are the greatest friend anyone could ask for and I'm glad I met you. I would also like to thank my dear friends Dr. Nikolaos Ioannou, Christina Mintzia, Elisabeth Julie Vargo, Amena Syeda Shah, Salah Breidi, Jason Cranfield and Dr. Peter Brawn for helping me in many ways and also my colleagues in EM213. Also, the person who I met at a later stage but has helped in more ways than he knows, thank you.



## Table of Contents

<b>Abstract.....</b>	<b>i</b>
<b>Acknowledgments .....</b>	<b>ii</b>
<b>Table of Contents .....</b>	<b>iii</b>
<b>List of Figures .....</b>	<b>vii</b>
<b>List of Tables .....</b>	<b>xiii</b>
<b>List of abbreviations .....</b>	<b>xv</b>
<b>Chapter 1. General Introduction .....</b>	<b>1</b>
1.1 Cancer.....	1
1.2 Cancer statistics .....	2
1.3 Hallmarks of Cancer.....	2
1.4 Colorectal Cancer .....	3
1.5 Symptoms .....	3
1.6 Signs and tests .....	4
1.7 Stages.....	4
1.9 Current therapies .....	6
1.10 Chemoprevention .....	6
1.11 Resveratrol.....	10
1.12 The“French Paradox” .....	11
1.12.1 Effects of resveratrol on the cardiovascular system .....	12
1.13 Biological activities of resveratrol .....	14
1.13.1 Resveratrol and longevity .....	15
1.13.2 Resveratrol and cancer.....	16
1.13.3 Inhibition of COX by resveratrol.....	17
1.13.4 Effects of resveratrol on drug metabolism.....	18
1.14 Resveratrol in clinical trials.....	19
1.15 Is bioavailability a problem anymore? .....	22
1.16 Resveratrol metabolites .....	23
1.17Cell cycle.....	27
1.17.1 Cell cycle control.....	28
1.17.2 Cell cycle and cancer .....	30
1.18Apoptosis.....	32

1.18.1 Extrinsic Pathway .....	34
1.18.2 Intrinsic Pathway .....	34
1.18.3 The Common Pathway .....	35
1.18.4 Regulation of apoptosis .....	35
1.18.5 Apoptosis and cancer .....	36
1.18.6 Resveratrol and apoptosis .....	38
1.19 p53 .....	38
1.19.1 Resveratrol and p53 .....	40
1.20 Necrosis .....	41
1.21 Autophagy .....	41
1.22 Signal transduction pathways .....	42
1.22.1 AMPK .....	43
1.22.2 Adenosine receptors .....	44
1.22.3 PI3K .....	46
1.22.4 ERK/MAPK .....	48
1.23 Aims and objectives .....	51
<b>Chapter 2. Materials and Methods .....</b>	<b>52</b>
2.1 Routine cell culture .....	52
2.1.1 Cancer cell lines .....	52
2.1.2 Cell culture .....	53
2.2 Viability assays .....	54
2.2.1 Neutral red uptake assay .....	54
2.2.2 Optimisation of neutral red uptake assay .....	55
2.2.3 Optimisation of incubation time for neutral red uptake .....	56
2.2.4 MTT assay .....	57
2.2.5 Growth of differentiated polarised Caco-2 cells on Transwells .....	57
2.2.6 Haemolysis of red blood cells .....	58
2.3 Growth of cells on chamber slides for microscopic evaluation .....	59
2.4 Growth of cells on chamber slides for immunostaining .....	60
2.4.1 Primary antibody (p53) titration for immunofluorescence .....	60
2.4.2 Immunofluorescence staining of HCT-116 cells for p53 .....	61
2.5 Flow cytometry analysis for cell cycle distribution and apoptosis detection .....	62

2.5.1 Cell cycle distribution using single agents .....	63
2.6 Western Blotting (Method 1).....	64
2.6.1 Preparation of cell lysates .....	64
2.6.2 Protein Quantification of lysates .....	64
2.6.3 Gel preparation .....	67
2.6.4 SDS-PAGE, Immunoblot and developing .....	67
2.7 Western blotting (Method 2) .....	68
2.7.1 Cell lysate preparation .....	68
2.7.2 Protein quantification.....	69
2.7.3 Polyacrylamide Gel Electrophoresis.....	70
2.7.4 Immunoblot (Transfer process) .....	70
2.8 Statistical analysis .....	74

### **Chapter 3. Investigation of the basic effect on growth of resveratrol and its metabolites .....**

**75**

3.1 Effect of resveratrol, piceatannol and pterostilbene on the growth of colorectal cell lines as single agents .....	79
3.2 Effect of resveratrol-3-O-D-glucuronide, resveratrol-4'-O-D-glucuronide and resveratrol-3-O-D-sulphate on the growth of colon cancer cells as single agents .....	84
3.2.1 Using the NRU assay .....	84
3.2.2 Using the MTT assay .....	87
3.3 Effect of resveratrol and its metabolites on polarised Caco-2 cells .....	91
3.4 Investigation of cell growth following drug removal.....	94
3.5 Haemolysis .....	98
3.6 Discussion .....	100

### **Chapter 4. How does resveratrol and its metabolites inhibit cell growth?.....**

**106**

4.1 Involvement of caspases on resveratrol and its metabolites on growth .....	109
4.2 Nuclear morphological evaluation .....	113
4.3 Effect of treatment on p53 expression.....	119
4.3.1 Protein expression of p53 .....	120
4.3.2 Assessment of p53 expression levels by immunofluorescence .....	122
4.4 Cell cycle distribution analysis.....	129
4.4.1 Caco-2 .....	129

4.4.2 CCL-228 .....	137
4.4.3 HCT-116 .....	143
4.4 Cell cycle distribution analysis (concentration-dependent effects using resveratrol and RV-3-G and CCL-228 cells).....	150
4.4 Effects of resveratrol and metabolite treatments on cyclin D1 levels .....	152
4.5 Discussion .....	161
<b>Chapter 5. Mechanism of action of resveratrol metabolites .....</b>	<b>169</b>
5.1 Probing key signalling pathways for a role in the effects of resveratrol and its metabolites.....	172
5.2 Investigation of cell cycle analysis with MRS-1191 co-treatment.....	179
5.3 Investigation of cell cycle analysis with compound C co-treatment.....	182
5.5 Western blot on the presence of Adenosine A3 receptor .....	185
5.6 Adenosine A3 receptor stimulation by 2CI-IB-MECA.....	186
5.7 Co-treatment of cells with 2CI-IB-MECA and MRS-1191.....	188
5.8 Western blots for AMPK and p-AMPK .....	191
5.9 Discussion .....	200
<b>Chapter 6. Discussion .....</b>	<b>206</b>
6.1 Overview .....	206
6.2 Future directions.....	213
6.2.1 Effect of combination studies .....	213
6.2.2 Autophagy.....	214
6.2.3 Involvement of p53 on growth.....	215
6.2.4 Further investigation on the effect of resveratrol and its metabolites on signalling pathways.....	216
6.3 Concluding remarks .....	219
<b>Chapter 7. References.....</b>	<b>220</b>
<b>Chapter 8. Publications and conferences.....</b>	<b>249</b>

## List of Figures

Figure 1.1	Stages of colorectal cancer.....	5
Figure 1.2	Structures of cis- resveratrol (A) and trans-resveratrol (B).....	10
Figure 1.3	Molecular targets of resveratrol for anti-carcinogenic effects.....	14
Figure 1.4	Structures of piceatannol (A), pterostilbene (B), resveratrol-3-O-D-glucuronide (C), resveratrol-4'-O-D-glucuronide (D) and resveratrol-3-O-D-sulphate (E).....	26
Figure 1.5	The cell cycle and the corresponding cyclins in each of the four phases.....	28
Figure 1.6	The intrinsic and extrinsic pathways of apoptosis.....	33
Figure 1.7	Events leading to evasion of apoptosis and consequently cancer.....	37
Figure 1.8	The p53 signalling pathway.....	40
Figure 1.9	The signalling pathway mediated by adenosine receptors.....	45
Figure 1.10	The PI3K signalling pathway and its downstream effectors leading to inhibition of apoptosis or cell growth and proliferation once constitutively activated.....	47
Figure 1.11	The MAPK signalling pathway involved in the process of carcinogenesis.....	50
Figure 2.1	Optimisation of cell seeding density.....	55
Figure 2.2	Optimisation of neutral red dye incubation time.....	56
Figure 2.3	Photomicrographs representing optimisation of the p53 primary antibody.....	61
Figure 3.1	The effect of resveratrol, piceatannol, pterostilbene, actinomycin D and the vehicle control (0.1% DMSO) on the growth of Caco-2 cells after 48 hours using the neutral red assay.....	80
Figure 3.2	The effect of resveratrol, piceatannol, pterostilbene, actinomycin D and the vehicle control (0.1% DMSO) on the growth of CCL-228 cells after 48 hours using the neutral red assay.....	81
Figure 3.3	The effect of resveratrol, piceatannol, pterostilbene, actinomycin D and the vehicle control (0.1% DMSO) on the growth of HCT-116 cells after 48 hours using the neutral red assay.....	82

Figure 3.4	The effect of resveratrol, resveratrol-3-O-D-glucuronide, resveratrol-4'-O-D-glucuronide, resveratrol-3-O-D-sulphate, actinomycin D and the vehicle control (0.1% DMSO) on the growth of Caco-2 cells after 48 hours using the neutral red assay.....	84
Figure 3.5	The effect of resveratrol, resveratrol-3-O-D-glucuronide, resveratrol-4'-O-D-glucuronide, resveratrol-3-O-D-sulphate, actinomycin D and the vehicle control (0.1% DMSO) on the growth of CCL-228 cells after 48 hours using the neutral red assay.....	85
Figure 3.6	The effect of resveratrol, resveratrol-3-O-D-glucuronide, resveratrol-4'-O-D-glucuronide, resveratrol-3-O-D-sulphate, actinomycin D and the vehicle control (0.1% DMSO) on the growth of HCT-116 cells after 48 hours using the neutral red assay.....	86
Figure 3.7	The effect of resveratrol, resveratrol-3-O-D-glucuronide, resveratrol-4'-O-D-glucuronide, resveratrol-3-O-D-sulphate and the vehicle control (0.1% DMSO) on the growth of Caco-2 cells after 48 hours using the MTT assay.....	87
Figure 3.8	The effect of resveratrol, resveratrol-3-O-D-glucuronide, resveratrol-4'-O-D-glucuronide, resveratrol-3-O-D-sulphate and the vehicle control (0.1% DMSO) on the growth of CCL-228 cells after 48 hours using the MTT assay.....	88
Figure 3.9	The effect of resveratrol, resveratrol-3-O-D-glucuronide, resveratrol-4'-O-D-glucuronide, resveratrol-3-O-D-sulphate and the vehicle control (0.1% DMSO) on the growth of HCT-116 cells after 48 hours using the MTT assay.....	89
Figure 3.10	Schematic representation of Transwells and the formation of a monolayer with mucosal and serosal sides.....	91
Figure 3.11	Comparison of the effect of 1 $\mu$ M (A) and 30 $\mu$ M (B) treatments of resveratrol, resveratrol-3-O-D-glucuronide, resveratrol-4'-O-D-glucuronide, resveratrol-3-O-D-sulphate and vehicle control (0.1% DMSO) on the apical or basolateral side of Caco-2 monolayers grown on Transwells for 21 days and treated for 11 days every other day expressed as a percentage of control growth.....	92
Figure 3.12	Comparison of the effect of treatment of Caco-2 cells with IC <sub>50</sub> concentrations of drugs after 48 hours followed by a 48 hour recovery period.....	94

Figure 3.13	Comparison of the effect of treatment of CCL-228 cells with IC <sub>50</sub> concentrations of drugs after 48 hours followed by a 48 hour recovery period.....	95
Figure 3.14	Comparison of the effect of treatment of HCT-116 cells with IC <sub>50</sub> concentrations of drugs after 48 hours followed by a 48 hour recovery period.....	96
Figure 3.15	Effect of resveratrol metabolites on the haemolysis of sheep red blood cells.....	98
Figure 4.1	Effect of treatment with compounds of interest (at IC <sub>50</sub> concentrations) with or without addition of Z-VAD-FMK (50µM) on viability of Caco-2 cells.....	110
Figure 4.2	Effect of treatment with compounds of interest (at IC <sub>50</sub> concentrations) with or without addition of Z-VAD-FMK (50µM) on viability of CCL-228 cells.....	111
Figure 4.3	Effect of treatment with compounds of interest (at IC <sub>50</sub> concentrations) with or without addition of Z-VAD-FMK (50µM) on viability of HCT-116 cells.....	112
Figure 4.4	Morphological evaluation of DAPI stained Caco-2 cell nuclei under a fluorescence microscope.....	114
Figure 4.5	Morphological evaluation of DAPI stained CCL-228 cell nuclei under a fluorescence microscope.....	116
Figure 4.6	Morphological evaluation of DAPI stained HCT-116 cell nuclei under a fluorescence microscope.....	118
Figure 4.7	Western blot analysis of p53 after treatment with 1µM and 10µM treatments of resveratrol, resveratrol-3-O-D-glucuronide, resveratrol-4'-O-D-glucuronide and actinomycin D.....	120
Figure 4.8	Immunofluorescence of HCT-116 for p53 expression after treatment with 10µg/ml actinomycin D (A); untreated in the presence of primary and secondary antibodies (B); untreated (only with primary antibody) (C); and, untreated (only with secondary antibody) (D).....	123
Figure 4.9	Immunofluorescence of HCT-116 for p53 expression after treatment with resveratrol.....	124
Figure 4.10	Immunofluorescence of HCT-116 for p53 expression after treatment with resveratrol-3-O-D-glucuronide.....	125
Figure 4.11	Immunofluorescence of HCT-116 for p53 expression after treatment with resveratrol-4'-O-D-glucuronide.....	126

Figure 4.12	Immunofluorescence of HCT-116 for p53 expression after treatment with resveratrol-3-O-D-sulphate.....	127
Figure 4.13	Photomicrographs of Caco-2 cells after treatment with 10µg/ml actinomycin D (A); control untreated (B); 30µM resveratrol (C); 30µM resveratrol-3-O-D-glucuronide (D); 30µM resveratrol-4'-O-D-glucuronide (E); and, 30µM resveratrol-3-O-D-sulphate (F) for 48 hours.....	130
Figure 4.14	Cell cycle analysis of untreated Caco-2 cells.....	133
Figure 4.15	Histogram representing cell cycle analysis of Caco-2 cells.....	134
Figure 4.16	Photomicrographs of CCL-228 cells after treatment with 10µg/ml actinomycin D (A); control untreated (B); 30µM resveratrol (C); 30µM resveratrol-3-O-D-glucuronide (D); 30µM resveratrol-4'-O-D-glucuronide (E); and, 30µM resveratrol-3-O-D-sulphate (F) for 48 hours.....	138
Figure 4.17	Cell cycle analysis of untreated CCL-228 cells.....	140
Figure 4.18	Histogram representing cell cycle analysis of CCL-228 cells.....	141
Figure 4.19	Photomicrographs of HCT-116 cells after treatment with 10µg/ml actinomycin D (A); control untreated (B); 30µM resveratrol (C); 30µM resveratrol-3-O-D-glucuronide (D); 30µM resveratrol-4'-O-D-glucuronide (E); and, 30µM resveratrol-3-O-D-sulphate (F) for 48 hours.....	144
Figure 4.20	Cell cycle analysis of untreated HCT-116 cells.....	146
Figure 4.21	Histogram representing cell cycle analysis of HCT-116 cells.....	147
Figure 4.22	Effect of 1µM, 3µM, 10µM, 30µM and 100µM resveratrol and resveratrol-3-O-D-sulphate treatments on the cyclin D1 levels of Caco-2 cells.....	153
Figure 4.23	Effect of 1µM, 3µM, 10µM, 30µM and 100µM resveratrol-3-O-D-glucuronide and resveratrol-4'-O-D-glucuronide treatments on the cyclin D1 levels of Caco-2 cells.....	154
Figure 4.24	Effect of 1µM, 3µM, 10µM, 30µM and 100µM resveratrol and resveratrol-3-O-D-sulphate treatments on the cyclin D1 levels of CCL-228 cells.....	156
Figure 4.25	Effect of 1µM, 3µM, 10µM, 30µM and 100µM resveratrol-3-O-D-glucuronide and resveratrol-4'-O-D-glucuronide treatments on the cyclin D1 levels of CCL-228 cells.....	157



Figure 4.26	Effect of 1µM, 3µM, 10µM, 30µM and 100µM resveratrol and resveratrol-3-O-D-sulphate treatments on the cyclin D1 levels of HCT-116 cells.....	159
Figure 4.27	Effect of 1µM, 3µM, 10µM, 30µM and 100µM resveratrol-3-O-D-glucuronide and resveratrol-4'-O-D-glucuronide treatments on the cyclin D1 levels of HCT-116 cells.....	160
Figure 5.1	Schematic representation of key signalling pathways and their possible implication in the effects exerted by resveratrol metabolites.....	172
Figure 5.2	Effect of MRS-1191, compound C, LY294002 and PD98059 on the growth inhibition after treatment with resveratrol and its metabolites in CCL-228 cells.....	173
Figure 5.3	Effect of MRS-1191, compound C, LY294002 and PD98059 on the growth inhibition after treatment with resveratrol and its metabolites in Caco-2 cells.....	175
Figure 5.4	Effect of MRS-1191, compound C, LY294002 and PD98059 on the growth inhibition after treatment with resveratrol and its metabolites in HCT-116 cells.....	177
Figure 5.5	Western blot analysis of untreated Caco-2, CCL-228 and HCT-116 cells to determine the presence of the adenosine A3 receptor.....	185
Figure 5.6	Effect of the highly selective adenosine A3 receptor agonist, 2CI-IB-MECA on the growth of Caco-2, CCL-228 and HCT-116 cells..	186
Figure 5.7	Evaluation of the effects of MRS-1191 and 2CI-IB-MECA co-treatment in Caco-2 cells.....	188
Figure 5.8	Evaluation of the effects of MRS-1191 and 2CI-IB-MECA co-treatment in CCL-228 cells.....	189
Figure 5.9	Evaluation of the effects of MRS-1191 and 2CI-IB-MECA co-treatment in HCT-116 cells.....	190
Figure 5.10	Western blot analysis of total and phosphorylated AMPK levels after treatment with resveratrol and resveratrol-3-O-D-sulphate in Caco-2 cells.....	192
Figure 5.11	Western blot analysis of total and phosphorylated AMPK levels after treatment with resveratrol-3-O-D-glucuronide and resveratrol-4'-O-D-glucuronide in Caco-2 cells.....	193

Figure 5.12	Western blot analysis of total and phosphorylated AMPK levels after treatment with resveratrol and resveratrol-3-O-D-sulphate in CCL-228 cells.....	195
Figure 5.13	Western blot analysis of total and phosphorylated AMPK levels after treatment with resveratrol-3-O-D-glucuronide and resveratrol-4'-O-D-glucuronide in CCL-228 cells.....	196
Figure 5.14	Western blot analysis of total and phosphorylated AMPK levels after treatment with resveratrol and resveratrol-3-O-D-sulphate in HCT-116 cells.....	198
Figure 5.15	Western blot analysis of total and phosphorylated AMPK levels after treatment with resveratrol-3-O-D-glucuronide and resveratrol-4'-O-D-glucuronide in HCT-116 cells.....	199
Figure 6.1	Proposed signalling pathways in the action of resveratrol and its glucuronides on cell growth.....	210

## List of Tables

Table 1.1	List of dietary products and compounds shown to either decrease or increase the risk of colorectal cancer.....	9
Table 1.2	Overview of published and on-going clinical trials involving resveratrol.....	21
Table 2.1	Recipes for making the solutions for the western blot process.....	66
Table 2.2	List of antibodies used for western blotting.....	73
Table 3.1	IC <sub>50</sub> values of resveratrol, piceatannol, pterostilbene, resveratrol-3-O-D-glucuronide, resveratrol-4'-O-D-glucuronide and resveratrol-3-O-D-sulphate using the neutral red and MTT assays.....	90
Table 4.1	ImageJ quantification of p53-immunofluorescence images following treatment with resveratrol and metabolites.....	128
Table 4.2	Cell cycle distribution of Caco-2 human cancer cell line after treatment for 48 hours with DMSO or compounds of interest.....	135
Table 4.3	Representation of the number of gated Caco-2 cells in each phase of the cell cycle per experiment.....	136
Table 4.4	Cell cycle distribution of CCL-228 human cancer cell line after treatment for 48 hours with DMSO or compounds of interest.....	142
Table 4.5	Representation of the number of gated CCL-228 cells in each phase of the cell cycle per experiment.....	143
Table 4.6	Cell cycle distribution of HCT-116 human cancer cell line after treatment for 48 hours with DMSO or compounds of interest.....	148
Table 4.7	Representation of the number of gated HCT-116 cells in each phase of the cell cycle per experiment.....	149
Table 4.8	Cell cycle distribution analysis of CCL-228 cells treated with varying concentrations of resveratrol and resveratrol-3-O-D-glucuronide for 48 hours.....	150
Table 5.1	Summary of significant effects of the inhibitors and their ability to reverse the effects of resveratrol, resveratrol-3-O-D-glucuronide, resveratrol-4'-O-D-glucuronide and resveratrol-3-O-D-sulphate.....	178
Table 5.2	Cell cycle distribution of the CCL-228 human cancer cell line after treatment for 48 hours with resveratrol or metabolites in the presence and absence of the adenosine A <sub>3</sub> receptor antagonist, MRS-1191.....	180

Table 5.3 Cell cycle distribution of the CCL-228 human cancer cell line after treatment for 48 hours with resveratrol or metabolites in the presence and absence of the AMPK inhibitor, compound C..... 183

Table 6.1 Summary of the main findings of this study..... 211

## List of abbreviations

5-FU	5-fluorouracil
ABC	ATP binding cassette
Act. D	actinomycin D
AIF	apoptosis inducing factor
Akt	protein kinase B
AMPK	adenosine monophosphate activated protein kinase
ANOVA	analysis of variance
AP1	activating protein 1
apoE	apolipoprotein E
APS	ammonium persulphate
BSA	bovine serum albumin
CDK	cyclin dependent kinase
CKI	cyclin dependent kinase inhibitors
COX	cyclooxygenase
COX-1	cyclooxygenase 1
COX-2	cyclooxygenase 2
DAPI	4',6-diamidino-2-phenylindole
DIABLO	direct IAP binding protein with low pI
DISC	death-inducing signalling complex
DMEM	Dulbecco's Modified Eagle Medium
DMSO	dimethyl sulphoxide
D-PBS	Dulbecco's Phosphate Buffered Saline
DPPH	2,2-diphenyl-1-picrylhydrazyl
EDTA	Ethylenediaminetetraacetic acid
ERK	extracellular signal-regulated kinases
FADD	Fas associated death domain
Fas-L	Fas ligand
FBS	Foetal Bovine Serum
FSC	forward scatter
HtrA2	Omi/high temperature requirement protein A
IAP	inhibitor of apoptosis

IC50	50% inhibitory concentration
ICAM-1	intracellular adhesion molecule 1
IGF-1	insulin-like growth factor 1
IL-1 $\beta$	interleukin 1 beta
IL-6	interleukin 6
I $\kappa$ B	inhibitors of NF- $\kappa$ B
JNK	c-jun N-terminal kinase
LDL-C	low-density lipoprotein cholesterol
LKB1	liver kinase B1
MAPK	mitogen activated protein kinase
MEME	Minimum Essential Medium Eagle
mTOR	Mammalian target of rapamycin
MTT	3-(4,5-Dimethyl-2-thiazolyl)-2,5-diphenyl-2H-tetrazolium bromide
NaCl	sodium chloride
NAD <sup>+</sup>	nicotinamide adenine dinucleotide
NF- $\kappa$ B	nuclear factor kappa beta
NR	neutral red
NSAIDs	non-steroidal anti-inflammatory drugs
PARP	poly ADP ribose polymerase
PFA	paraformaldehyde
PH	pleckstrin homology
PI	piceatannol
PI/RNase	propidium iodide
PI3K	phosphoinositide 3-kinase
PIP2	phosphatidylinositol-4,5-bisphosphate
PIP3	phosphatidylinositol-3,4,5-triphosphate
PKC	protein kinase C
PKG	protein kinase G
PLC	phospholipase C
PS	pterostilbene
PUMA	p53 upregulated modulator of apoptosis
PVDF	polyvinylidene fluoride
QR1	quinone reductase 1

<b>Rb</b>	<b>retinoblastoma</b>
<b>RNS</b>	<b>reactive nitrogen species</b>
<b>ROS</b>	<b>reactive oxygen species</b>
<b>RPTK</b>	<b>Receptor Protein Tyrosine Kinase</b>
<b>RS</b>	<b>reactive species</b>
<b>RV</b>	<b>Resveratrol</b>
<b>RV-3-G</b>	<b>Resveratrol-3-O-D-glucuronide</b>
<b>RV-3-S</b>	<b>Resveratrol-3-O-D-sulphate</b>
<b>RV-4'-G</b>	<b>Resveratrol-4'-O-D-glucuronide</b>
<b>SDS-PAGE</b>	<b>sodium dodecyl sulphate-polyacrylamide gel electrophoresis</b>
<b>Sir2</b>	<b>sirtuin 2</b>
<b>Smac</b>	<b>second mitochondria-derived activator of caspase</b>
<b>SSC</b>	<b>side scatter</b>
<b>TEMED</b>	<b>N,N,N',N'-tetramethylethylenediamine</b>
<b>TGF-<math>\beta</math></b>	<b>transforming growth factor beta</b>
<b>TNF</b>	<b>tumour necrosis factor alpha</b>
<b>TRADD</b>	<b>TNF receptor associated death domain</b>
<b>Tris-HCl</b>	<b>Tris hydrochloric acid</b>
<b>VCAM-1</b>	<b>vascular cell adhesion molecule 1</b>

# Chapter 1. General Introduction

## 1.1 Cancer

Cancer is a collection of diseases characterised by changes at the genomic level. The identification of mutations that generate oncogenes with a dominant gain of function and the recessive loss of function of tumour suppressor genes are the main characteristics (Hanahan and Weinberg, 2000). Their initial discovery was *via* their modification in both human and animal cancer cells *in vitro* and the cancer phenotype in experimental models (Bishop and Weinberg, 1996). Tumourigenesis is a multi-step process leading to genetic alterations which force the change of normal cells into malignant ones therefore leading to neoplasia (Hanahan & Weinberg, 2000).

The process of carcinogenesis is caused by either one or a mixture of chemical, physical, biological and genetic attack on individual cells (Balmain *et al.*, 1993). These include chemical carcinogens such as aromatic amines, polycyclic hydrocarbons, ultraviolet and ionising radiation which cause major structural mutations in DNA. It has been shown that certain oncogenic viruses, such as adenoviruses are also capable of causing DNA structural modifications (Balmain *et al.*, 1993). Three steps of carcinogenesis have been identified and these include initiation, promotion and progression (Hanahan and Weinberg, 2011, Farber, 1984).



## **1.2 Cancer statistics**

Cancer is one of the leading causes of death in both men and women worldwide (Siegel *et al.*, 2012) with 12.7 million cases being reported in 2008 and death rates reaching approximately 7.6 million (WHO). The latest U.S cancer statistics have reported a total of 1,638,910 new cancer cases and 577,190 deaths from cancer to occur in 2012 (Siegel *et al.*, 2012). In the United Kingdom, 320,000 new cancer cases were reported in 2009 and cancer was responsible for 157,275 deaths in 2010 (Cancer Research UK).

## **1.3 Hallmarks of Cancer**

Hanahan and Weinberg (2000) were the first to characterise the acquired capabilities of cancer. These include: a) self-sufficiency in growth signals, b) insensitivity to antigrowth signals, c) evasion of apoptosis (programmed cell death), d) limitless replicative potential, e) sustained angiogenesis and, f) tissue invasion and metastasis. Recently however, additional hallmarks of cancer involved in the pathogenesis of some if not all cancers have been identified, which are divided into two groups: a) emerging hallmarks (deregulating cellular energy and avoiding immune destruction) and, b) enabling characteristics (genome instability and mutation, and tumour-promoting inflammation) (Hanahan and Weinberg, 2011).

## **1.4 Colorectal Cancer**

Colorectal cancer is a type of tumour that occurs in the large intestine or the rectum and is largely a carcinoma; that is a cancer that is instigated in the skin or in tissues that line internal organs. Certain other types of cancers have been found to affect the colon including lymphoma, melanoma and sarcomas but these are rare. All colon cancers exclusively arise in the glands present in the lining of the colon and rectum (Tortora and Derrickson, 2008). Like all cancers, there is no sole cause of colorectal cancer. The majority of tumours begin as non-malignant or benign polyps that consequently lead to the formation of a tumour.

In the UK in 2009, 41,142 new colorectal cancer cases were reported and colorectal cancer was responsible for 16,013 deaths in the UK (Cancer Research UK). Between the years 2005-2009, 54% of men and 56% of women in England survived their colorectal cancer for 5 years or more. Collectively, these statistics make colorectal cancer the third most common cancer in men after prostate and lung cancer and the second most common in women after breast cancer (Cancer Research UK).

## **1.5 Symptoms**

Most of the cases of colorectal cancer are asymptomatic but certain symptoms may be a sign of colorectal cancer (Sack and Rothman, 2000). These include:

- Pain in the abdomen and tenderness in the lower abdomen
- Presence of blood in the faeces
- Changes in bowel habits, diarrhoea or constipation
- Narrow stools
- Unexpected weight loss

## **1.6 Signs and tests**

With the aid of screening, colon cancer can be detected prior to the development of symptoms and therefore patients have a better prognosis due to the early stage of the tumour. Tests include faecal occult blood test (FOBT) employed for the detection of small amounts of blood in the faeces accompanied by either colonoscopy or sigmoidoscopy (Sack and Rothman, 2000). Blood tests are also employed for the measurement of complete blood count (CBC) (to test for anaemia) and liver function. If there is any indication of colorectal cancer with the fore mentioned tests, further tests will be employed in order to identify whether the tumour has spread. Computed tomography (CT) or magnetic resonance imaging (MRI) scans may be used as well as positron emission tomography (PET) scans for the staging of cancer.

## **1.7 Stages**

There are currently two staging systems in place for colorectal cancer; Dukes' staging system and the TNM staging system (T-tumour size; N-number of lymph nodes affected; and M-presence of metastasis) (Kim *et al.*, 2011). The Dukes' system is subdivided into 4 distinct classes namely, A, B, C and D. Dukes' A corresponds to the cancer which is only present in the innermost lining of the colon or rectum or even characterised by a small growth in the muscle layer. Cancers classified as Dukes' stage B mean that the cancer has grown through the muscle layer of either the colon or the rectum. In Dukes' C the cancer has invaded at least one lymph node in the vicinity of the colon whilst in the final stage, Dukes' D the cancer has metastasised to another organ, usually the liver or lung (Figure 1.1).

The scenario in the TNM (Tumour, Node, Metastases) classification is slightly more complex. This involves the size of the primary tumour (T), the presence of cancer cells in the lymph nodes (N) and whether the cancer has metastasised to another site (M).

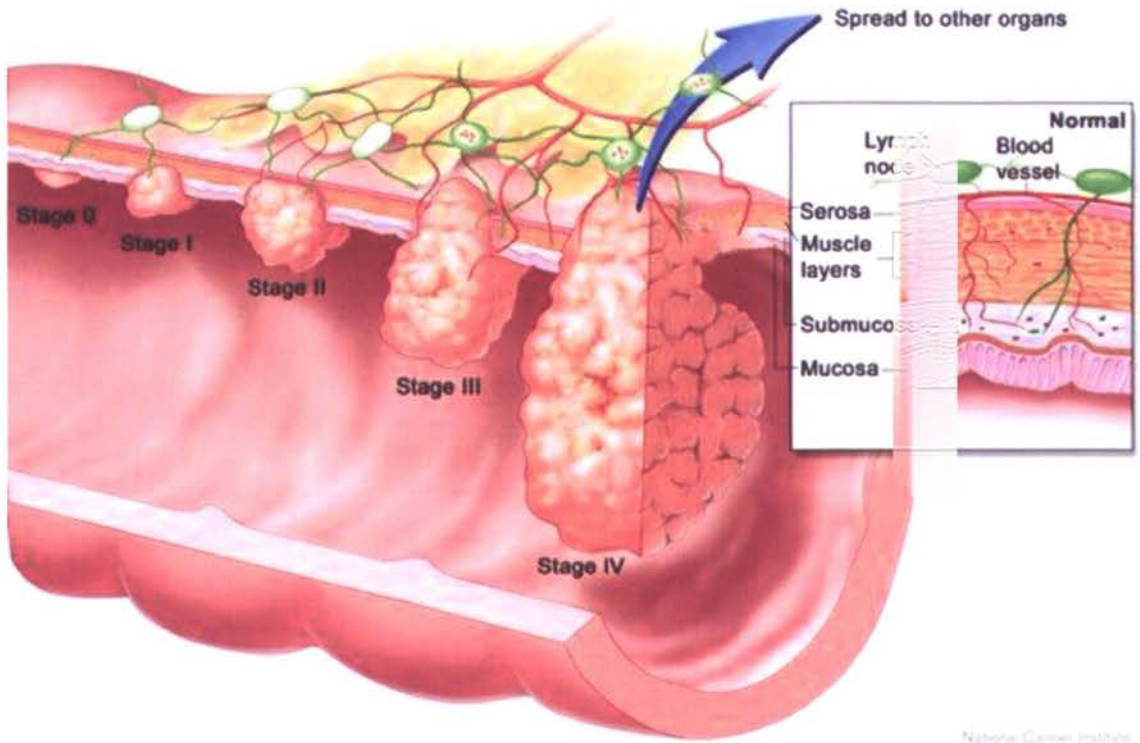


**Figure 1.1** Stages of colorectal cancer. Taken from National Cancer Institute (<http://visualsonline.cancer.gov/details.cfm?imageid=7181>).

## **1.9 Current therapies**

The current treatment options for colorectal cancer include surgery, chemotherapy or radiotherapy. Chemotherapeutic drugs currently being used for the treatment of colorectal cancer include 5-Fluorouracil (5-FU), capecitabine, oxaliplatin, irinotecan and uftoral. These can either be administered neo-adjuvantly (prior to surgery to reduce the size of the tumour) or adjuvantly (after surgery to ensure that any remaining cancer cells are killed) (Meyerhardt and Mayer, 2005). More specifically, 5-fluorouracil and capecitabine belong to a family of chemotherapy drugs known as anti-metabolites that act by blocking the synthesis of DNA and RNA therefore leading to growth inhibition. Oxaliplatin on the other hand is categorised in the 'alkylating agent' group which have an effect on the cell cycle and act by causing crosslinkage of the DNA strands therefore preventing DNA synthesis whilst irinotecan acts by inhibiting the topoisomerase I enzyme therefore blocking the proliferation of cells and halting cell division (André *et al.*, 2004). Uftoral, also known as tegafur-uracil is a combination of chemotherapy drugs (Douillard *et al.*, 2002). Following drug metabolism, tegafur is converted to the active drug (5-Fluorouracil), whilst uracil aids in the delay of the breakdown of 5-FU therefore increasing its half-life.

## **1.10 Chemoprevention**

One of the expanding areas in cancer research is the concept of chemoprevention and the ability of natural products to prevent carcinogenesis. Chemoprevention is characterised by the use of natural products and/or synthetic compounds that are capable of delaying, preventing, or reversing the development and progression of tumours (Pan *et al.*, 2011). The affected targets associated with their chemopreventive effects include the control of signalling pathways, gene expression modulation of proteins involved in

the control of proliferation, differentiation and apoptosis and inhibition of inflammation, metastasis and angiogenesis (Pan *et al.*, 2011).

The most widely known chemopreventive agents are the non-steroidal anti-inflammatory drugs (NSAIDs) including aspirin and sulindac, which have been shown to inhibit cyclooxygenase (COX). The COX inhibitory activity is important in cancer chemoprevention for its ability to catalyse the change of arachidonic acid to pro-inflammatory compounds including prostaglandins that can promote tumour growth, form an inflammatory microenvironment during cancer formation and evade immune control (Jang *et al.*, 1997, Pan *et al.*, 2011). Furthermore, COX enzymes are also capable of activating carcinogens in forms that damage DNA (Jang *et al.*, 1997).

Studies conducted so far, have resulted in noteworthy findings. More specifically, it has been shown that resveratrol is capable of preventing or slowing the development of several illnesses including cancer, cardiovascular disease and ischaemic injuries (Jang *et al.*, 1997, Bradamante *et al.*, 2004, Wang *et al.*, 2002, Sinha *et al.*, 2002). Furthermore, studies have demonstrated that resveratrol is also able to improve stress resistance and prolong the lifespan of different organisms ranging from yeast to vertebrates (Howitz *et al.*, 2003b, Valenzano *et al.*, 2006).

Colorectal cancer risk and its correlation with diet are presented in Table 1.1 (Research, 2011) (World Cancer Research Fund/American Institute for Cancer Research, 2011). Several risk factors for colorectal cancer have been identified so far, including diet, physical activity, alcohol consumption, smoking and family history of which a detailed analysis is depicted in Table 1.1. Studies provide strong evidence to support that

approximately 57% of colorectal cancer cases in men and 52% in women in the United Kingdom are correlated to lifestyle and environmental factors (Parkin *et al.*, 2011).

**Table 1.1** List of dietary products and compounds shown to either decrease or increase the risk of colorectal cancer.

	<b>Effect</b>	<b>References</b>
High intake of red & processed meat	Increased risk	WCRF/AICR, 2011
Fish	No sufficient data for decreased risk	WCRF/AICR, 2011
Dietary fibre	Protective role	WCRF/AICR, 2011
Fruits and vegetables	No sufficient evidence for protection but decreased risk of lung cancer	WCRF/AICR, 2011
High-fat diet	No association	WCRF/AICR, 2011
Milk consumption	Reduced risk	WCRF/AICR, 2011
Dietary sugar intake	Uncertain	WCRF/AICR, 2011
Vitamin B6	Decreased risk/ Increased risk	WCRF/AICR, 2011/(Chan and Giovannucci, 2010)
Vitamin B12	No association/ higher levels reduce the risk	(Eussen <i>et al.</i> , 2010, Key <i>et al.</i> , 2012, Le Marchand <i>et al.</i> , 2011, Kune and Watson, 2011, Dahlin <i>et al.</i> , 2008)
Calcium and vitamin D supplements (combination)	Protection	WCRF/AICR, 2011
Obesity	Increased risk	WCRF/AICR, 2011
Alcohol consumption (even at moderate levels)	Increased risk	WCRF/AICR, 2011
Smoking	Increased risk	WCRF/AICR, 2011
NSAIDs (aspirin)	Reduced risk	WCRF/AICR, 2011
Oestrogen-only HRT/ Oral contraceptives	Protective effect/ no association	WCRF/AICR, 2011
Ulcerative colitis, Crohn's disease and type II diabetes	Increased risk	WCRF/AICR, 2011
Radiation exposure	Increased risk	WCRF/AICR, 2011
Familial adenomatous polyposis (FAP) and hereditary non-polyposis colorectal cancer	Increased risk	(Fearnhead <i>et al.</i> , 2002)



## 1.11 Resveratrol

Resveratrol (3,5,4'-trihydroxy-*trans*-stilbene) (RV) is a natural polyphenol present in red grapes (*Vitis vinifera*), peanuts, and berries, amongst other sources and was first isolated in 1940 from the roots of the white hellebore (*Veratrum grandiflorum* O.Loos) (Takaoka, 1940) and in 1963 from the roots of *Polygonum cuspidatum* (Nonomura *et al.*, 1963). This plant is used in conventional Chinese and Japanese medicine and known as ko-jo-kon, for the treatment of suppurative dermatitis, gonorrhoea, favus, athlete's foot, and hyperlipidemia (Vastano *et al.*, 2000, Cichewicz and Kouzi, 2002, Lee *et al.*, 1998, Takaoka, 1940). Resveratrol is composed of two aromatic rings connected by a methylene bridge. This compound is produced naturally by 72 different plant species and exists in both the *cis*- and *trans*- configurations of which only the *trans*- isoform is biologically active (Figure 1.2) (Catalgol *et al.*, 2012, Soleas *et al.*, 1997).

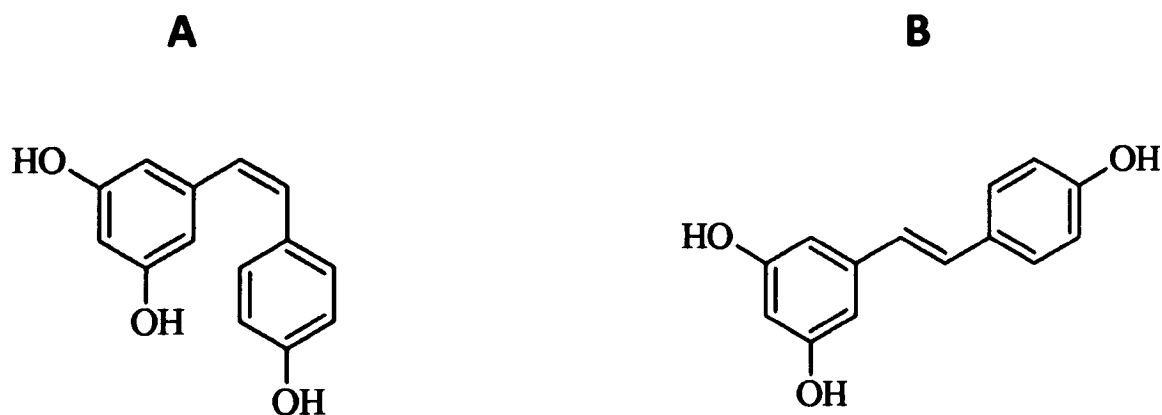


**Figure 1.2** Structures of *cis*-resveratrol (A) and *trans*-resveratrol (B).

In 1976, resveratrol was characterised as a phytoalexin produced in plants other than grapes in response to fungal infection (*Botrytis cinerea*), injury, ultraviolet radiation or other stresses (AGGARWAL et al., 2004, Langcake and Pryce, 1976).

Resveratrol synthesis is limited to the leaf epidermis and grape skin. Since grape skins are not used in the fermentation process during white wine production, the levels of resveratrol are significantly greater in red wine (Catalgol *et al.*, 2012). Studies have shown that fresh grape skins contain 50-100mg resveratrol per gram, corresponding to 5-10% of their biomass, whilst the concentration in wine ranges from 0.2mg/l to 7.7mg/l (Saiko *et al.*, 2008).

Only in 1992 did resveratrol attract further attention when it was suggested to be involved in the cardioprotective effects of red wine (Siemann and Creasy, 1992). Resveratrol was found not only to have cardioprotective effects, but also anti-inflammatory, anti-cancer and other beneficial effects *in vitro*.

### **1.12 The “French Paradox”**

The phenomenon known as the “French Paradox” arose after epidemiological studies identified an inverse correlation between the intake of red wine (alcohol consumption at the level of intake of 20-30g per day) and the occurrence of cardiovascular disease. This is clearly exemplified by the 40% lower incidence of infarction in France compared to the rest of Europe regardless of the very high saturated fat diet (Renaud and de Lorgeril, 1992). The hypothesis however, that drinking red wine will protect against a diet high in fat is yet to be proven and remains inconclusive (Opie et al., 2011).

### 1.12.1 Effects of resveratrol on the cardiovascular system

Multiple *in vitro* studies have been conducted in order to discover the mechanisms of action of resveratrol. Two factors which have been shown to be involved in the pathogenesis of cardiovascular diseases are oxidative damage and reactive species (reactive oxygen species-ROS and reactive nitrogen species-RNS) (Ago *et al.*, 2010, Schiffrin, 2010). The three major ROS which have been shown to be involved in cardiovascular diseases are superoxide ( $O_2^{\cdot-}$ ), hydroxyl (OH) and hydrogen peroxide ( $H_2O_2$ ). The two main RNS are nitric oxide (NO) and peroxynitrite (Catalgol *et al.*, 2012). Studies have shown that resveratrol is capable both of increasing the resistance to vascular oxidative stress by acting as a  $H_2O_2$  scavenger and inhibiting endothelial cell death caused by oxidative stress at concentrations  $10^{-4}$  mol/L and  $10^{-5}$  mol/L respectively, contributing to its cardioprotective properties (Ungvari *et al.*, 2007). However, it is uncertain if polyphenols, including resveratrol or flavonoids, at bioavailable concentrations ( $<1\mu M$ ) have any appreciable antioxidant effects (Halliwell, 2008).

Nitric oxide (NO) plays an important role in the pathogenesis of cardiovascular diseases. It is produced by the endothelial NOS (nitric oxide synthase) and plays a key part in maintaining cardiovascular homeostasis (Catalgol *et al.*, 2012). It is important to point out that low NO concentrations are advantageous to the cardiovascular system (cause vasodilation) but high concentrations have reverse effects due to the reactive characteristics of the compound. Treatment of HUVEC (human umbilical vein endothelial cells) with resveratrol ( $10\text{-}100\mu\text{mol/L}$ ) caused an increased expression of endothelial nitric oxide synthase (eNOS) mRNA which could possibly be responsible for the cardioprotective effects exerted by resveratrol (Wallerath *et al.*, 2002).

Further studies have investigated the antioxidant properties of resveratrol as well as its ability to inhibit oxidation reactions. One such study revealed that resveratrol (20 $\mu$ M) hindered apoptosis related to oxidative stress in peripheral blood mononuclear cells (Losa, 2003). Results from a study by Das and colleagues (2005) showed that resveratrol at concentrations greater than 30 $\mu$ M, is capable of pre-conditioning rat hearts *via* adenosine A<sub>3</sub> receptor signalling, leading to CREB (cAMP response-element binding protein) phosphorylation either through Akt-dependent or –independent mechanisms ultimately leading to cardioprotection (Das *et al.*, 2005).

A study conducted by Robich and colleagues (2010) using the Yorkshire swine hypercholesterolemic model showed that resveratrol administration (100mg/kg/day orally) positively affected certain cardiovascular disease risk factors including high body mass index, cholesterol, glucose tolerance and systolic pressure by decreasing all these parameters (Robich *et al.*, 2010). Another study explored the effects of resveratrol in hypocholesterolemia using apolipoprotein E (apoE) (-/-) mice. It was found that resveratrol supplements (0.02% and 0.06% w/w) induced a decrease in the concentration of total-cholesterol (total-C) and low-density lipoprotein cholesterol (LDL-C) in plasma, decreased the existence of atherosclerotic lesions and periarterial fat accumulation and blocked the expression of the intracellular adhesion molecule-1 (ICAM-1) and vascular cell adhesion molecule-1 (VCAM-1) in atherosclerotic lesions (Do *et al.*, 2008). Furthermore, resveratrol (2.3mg/L) was shown to provide cardioprotection by significantly minimising the infarct size of wild-type mouse hearts relative to control *via* activation of the survivor activating factor enhancement (SAFE) pro-survival signal transduction pathway that consists of the activation of TNF- $\alpha$  and signal transducer and activator of transcription 3 (STAT 3) (Lamont *et al.*, 2011).

1.13 Biological activities of resveratrol

The precise mechanism of action by which resveratrol exerts a variety of beneficial effects in several species and disease conditions is still unknown. It is clear however, that resveratrol exhibits multiple biological activities (Figure 1.3). In the sections that follow, some key molecular and cellular mechanisms affected by resveratrol will be discussed.

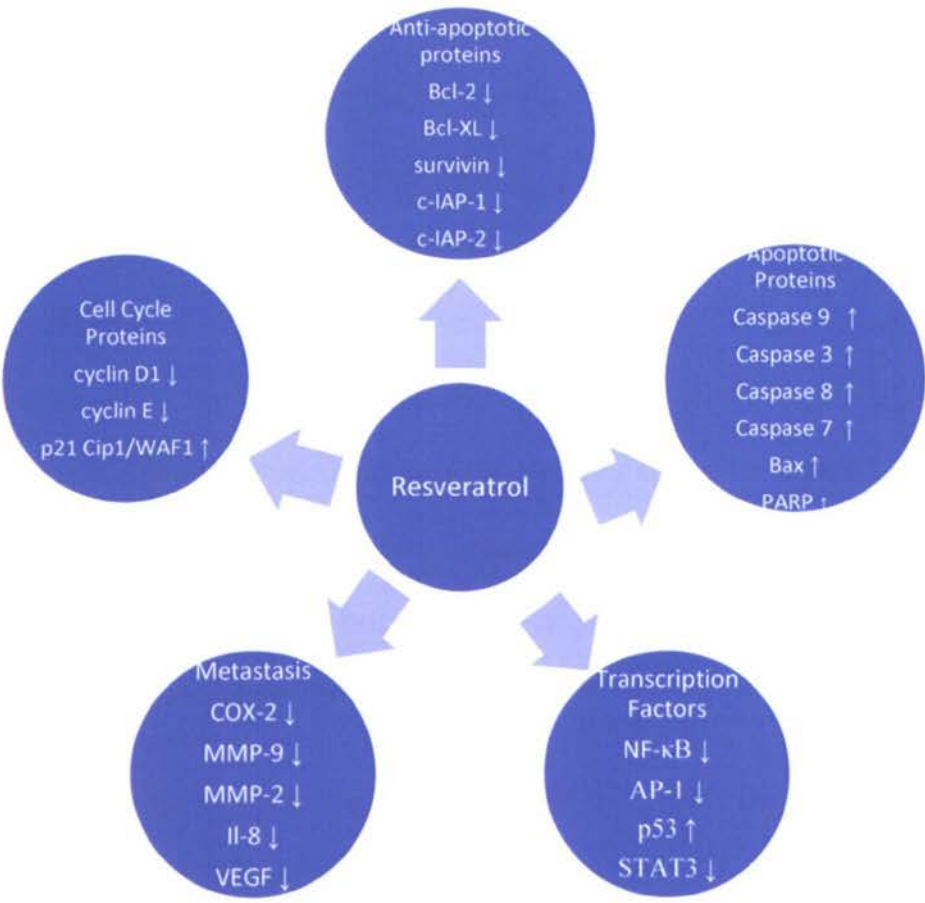


**Figure 1.3** Molecular targets of resveratrol for anti-carcinogenic effects. AP, activator protein; c-IAP, cellular inhibitor of apoptosis protein; NF-κB, nuclear-factor kappa B; PARP, poly (ADP-ribose) polymerase; STAT, signal transducers and activators of transcription; VEGF, vascular endothelial growth factor. Adapted from (Harikumar and Aggarwal, 2008).

### 1.13.1 Resveratrol and longevity

It has been suggested that resveratrol is capable of increasing the lifespan and additionally promotes healthy aging. Studies investigating the effect of resveratrol on the lifespan of several organisms including *Saccharomyces cerevisiae*, *Caenorhabditis elegans* (worm) and *Drosophila melanogaster* (fruit fly) revealed a strong correlation (Wood *et al.*, 2004, Howitz *et al.*, 2003a).

Several studies have shown that caloric restriction leads to overexpression of Sir2 (a conserved NAD<sup>+</sup>-dependent deacetylase) therefore increasing the lifespan in these organisms (Catalgol *et al.*, 2012). Sir2 belongs to the sirtuin (SIRT) pathway which affects the cell cycle, response following DNA damage, apoptosis, metabolism and autophagy (Satoh *et al.*, 2011). Sir2 can become activated by various factors including caloric restriction (by increased intracellular NAD concentration), diminishment of its negative regulator, or by a pharmacological approach by the use of activators including resveratrol (Pearson *et al.*, 2008). One member of the SIRT family, SIRT1 (the mammalian homolog of Sir2) is associated with caloric restriction and the reduction in diseases related with age (Pacholec *et al.*, 2010).

A study by Howitz and colleagues (2003) identified that resveratrol acts as an effector of *in vitro* activity of SIRT1 (increasing SIRT1 activity). This finding was further substantiated by a more recent study by Price *et al.* (2012). Additionally, cell based assays further supported the findings that resveratrol was a direct SIRT1 target *in vivo* and therefore, explained several of the physiological benefits linked to resveratrol.

In addition, resveratrol (12.5µM, 25µM and 50µM) is capable of increasing AMPK levels, mitochondrial number and insulin sensitivity whilst decreasing insulin-like growth factor-1 (IGF-1) levels and improving motor function (Baur *et al.*, 2006).

However, increased longevity was only observed in elderly mice treated with resveratrol leading to decreased inflammation, and apoptosis in the vascular endothelium. Contrary, younger mice on a standard diet did not reveal signs of increased longevity when treated with resveratrol (Pearson *et al.*, 2008).

A study revealed that a moderate dose of resveratrol (25µM) in mice was capable of increasing mitochondrial biogenesis and function whilst also activating AMPK and increasing the levels of NAD<sup>+</sup> in skeletal muscle (Price *et al.*, 2012). Adult mice with a whole-body deletion of SIRT1 however, did not exhibit these health-promoting benefits. AMPK activation with high resveratrol concentrations (50µM) was found to occur independent of SIRT1 thus exemplifying the importance of different resveratrol concentrations. More importantly, there was no evidence of improved mitochondrial function in the SIRT1 knockout group at both resveratrol concentrations (Price *et al.*, 2012). SIRT1 is therefore, an important target in facilitating the effects of resveratrol on the biogenesis of mitochondria.

### **1.13.2 Resveratrol and cancer**

A plethora of studies have been conducted to date investigating the effects of resveratrol in cancer and numerous targets have been identified. Resveratrol is capable of blocking tumourigenesis and inhibits Phase I whilst inducing Phase II enzymes therefore increasing the detoxification of carcinogens (Catalgol *et al.*, 2012). Furthermore, effects include alterations in the cell cycle, the ability to cause apoptosis, suppressing angiogenesis and therefore invasion and metastasis. This natural polyphenol has also been shown to be a good candidate for sensitising cancer cells (HT-29 colorectal cancer cells) to chemotherapeutic agents like etoposide (Kundu and Surh, 2004). The inhibition

in the growth of tumour cells in the *in vitro* scenario has consequently directed to pre-clinical animal studies in order to assess the effects *in vivo* (Bishayee, 2009).

Extensive research over the past decade has identified resveratrol as a good candidate for chemoprevention and cancer therapy (Pezzuto et al., 2006, Aggarwal et al., 2004). Resveratrol is capable of suppressing the growth of a wide range of human cancer cells *in vitro* (extensively reviewed by Aggarwal et al., 2004). The chemotherapeutic potential of resveratrol was shown to be mediated via various cell signalling pathways and include cell cycle arrest, inhibition of cell proliferation, induction of apoptosis, and inhibition of angiogenesis and metastasis where most of these are summarised in the following sections.

Resveratrol was found to possess a dual function on the MAPK pathway. It is capable of activating MAPK at low concentrations (1pM to 10µM) and thus increase proliferation, but, can block the signal transduction of this pathway at higher concentrations ranging from 50µM to 100µM causing a decrease in proliferation (Miloso *et al.*, 1999).

### **1.13.3 Inhibition of COX by resveratrol**

Jang and colleagues were the first to suggest that resveratrol might be a successful candidate for chemoprevention due to its ability to inhibit the enzymatic activity of cyclooxygenase-1 (COX-1, ED<sub>50</sub>= 15µM) and cyclooxygenase-2 (COX-2, ED<sub>50</sub>= 85µM). Epidemiological studies have identified that long-term inhibition of COX decreases the risk of tumour development while the deletion of the gene encoding COX-2 has protective effects in a mouse model of colorectal cancer (Baur and Sinclair, 2006).

Resveratrol is capable of reducing the activity of total COX in both cancerous and normal tissues *in vivo* (Aziz *et al.*, 2005, Khanduja *et al.*, 2004) by modest selective



blockage of COX-1 activity and reduction of the COX-2 mRNA levels (Li *et al.*, 2002, Subbaramaiah *et al.*, 1998, Martín *et al.*, 2004). In addition, Calamini and colleagues (2010) have demonstrated the ability of resveratrol-4'-O-D-sulphate (metabolite of resveratrol) to inhibit COX-1 (IC<sub>50</sub> 5.1µM) and COX-2 (IC<sub>50</sub> 2.5µM) (Calamini *et al.*, 2010). COX-1 is important for sustaining normal physiological activity whilst COX-2 is involved in inflammation and the production of prostaglandins at the site of inflammation (Murias *et al.*, 2004, Zykova *et al.*, 2008). The expression of COX-2 is influenced by different stimuli including oncogenes and tumour promoters (Murias *et al.*, 2004).

#### **1.13.4 Effects of resveratrol on drug metabolism**

The process of drug metabolism is divided into two phases that differ in the enzymes involved. Phase I enzymes are constitutively activated and are composed of cytochrome P450's (CYP's) and flavin monooxygenases but are capable of being expressed further (Baur and Sinclair, 2006). These enzymes are capable of promoting the excretion of foreign compounds by making them more polar by oxidation, reduction or hydrolysis. Phase II enzymes on the other hand consist of conjugating and antioxidant enzymes that become activated and function to detoxify dangerous chemicals. *In vitro* studies have demonstrated that resveratrol (0.18µM) is capable of inhibiting the activity of several Phase I enzymes whilst upregulating Phase II enzymes. The stimulation of Phase II enzymes by resveratrol and other chemopreventive agents is therefore believed to be a promising approach for cancer prevention (Giudice and Montella, 2006).

### 1.14 Resveratrol in clinical trials

To date, there have been 59 clinical trials involving resveratrol, some of these completed whilst others still recruiting volunteers (clinicaltrials.gov). A brief summary of some of these clinical trials is presented in Table 1.2. Of these, several studies have focused on the use of resveratrol in cancer. More specifically, one Phase I study investigated the effect of resveratrol administered at different doses from four distinct sources (resveratrol tablets or grape powder at two different concentrations within each group) on the Wnt signalling pathway in a clinical setting (NCT00256334). The results from this study showed that resveratrol was capable of inhibiting the Wnt target gene expression in normal colonic mucosa, suggesting a chemopreventive activity (Nguyen *et al.*, 2009). A further study currently recruiting participants aims to identify the effects of resveratrol on Notch-1 signalling in patients with low grade gastrointestinal tumours (NCT01476592).

One of the first studies investigating the pharmacokinetics of resveratrol was by Goldberg and colleagues in 2003 who reported the highest serum concentrations of resveratrol and metabolites after 30 minutes oral ingestion with free resveratrol corresponding to 1.7-1.9% in plasma. The low levels of free resveratrol (< 40nmol/L) made the authors conclude that concentrations reached through dietary consumption would not be sufficient to induce any biological effects, according to in vitro findings (5-100 $\mu$ M) (Goldberg *et al.*, 2003).

Clinical pilot studies however, evaluating the safety and pharmacokinetics of resveratrol as a single or repeat dose (0.5, 1.0, 2.5 or 5.0g) on healthy volunteers, identified an average peak plasma concentration of resveratrol of 2.4 $\mu$ M at the single highest dose. The maximum plasma concentration of the two glucuronides however, appeared to be

three-to-eight fold higher and a correlation between the plasma concentration and time curve (area under the curve) has shown a 23-fold increase compared to resveratrol suggesting a greater exposure of the metabolites (Boocock *et al.*, 2007a, Brown *et al.*, 2010). In the follow-up study, administration of resveratrol at the same doses as mentioned above was carried out for 29 days. This identified a 2.4-13 fold increase in peak plasma concentrations of the three main metabolites relative to resveratrol (0.19 to 4.24 $\mu$ M) (Brown *et al.*, 2010). Based on these findings, *in vitro* concentrations of the metabolites up to 55 $\mu$ M appear to be reached *in vivo*. The highest well tolerated repeated dose of resveratrol has been reported to be 1.0g (Boocock *et al.*, 2007). Since resveratrol undergoes extensive metabolism in humans, contribution of the metabolites to this activity could possibly produce plasma concentrations of total resveratrol that are efficacious. Patel *et al.* (2010) have identified that resveratrol levels in human colorectal tissue following a 1.0g oral dose were in agreement with resveratrol concentrations capable of causing anti-tumourigenic effects *in vitro* using cancer cell lines and in the gastrointestinal tract of Apc<sup>min</sup> mice following an effective dose (240mg/kg, 10-14 weeks) leading to a decrease in intestinal adenoma formation (Sale *et al.*, 2005).

Extensive research has identified the anticarcinogenic effects of resveratrol *in vitro* and results from cancer preventive and therapeutic studies in experimental animal models further substantiate these findings (Bishayee, 2009). The current *in vivo* studies have revealed that resveratrol inhibits carcinogenesis in various organ sites including skin, breast, prostate, lung as well as the gastrointestinal tract. One such study has shown that resveratrol (200 $\mu$ g/kg for 100 days in drinking water) was capable of inhibiting AOM-induced colon carcinogenesis in male F344 rats by increasing the expression of Bax and p21 (Tessitore *et al.*, 2000).

**Table 1.2** Overview of published and on-going clinical trials involving resveratrol. The numbers in brackets represent the number of individuals. *Adapted from Patel et al., 2011.*

Cohort	Form of resveratrol	Resveratrol dose	Dosing regime	Study outcome	Reference
Healthy males (12)	White wine, white grapes juice or vegetable juice	25mg/70kg	Single	Similar resveratrol absorption with all three matrices	(Goldberg et al., 2003)
Healthy males (3)	Grape juice (200,400,600 or 1200 ml)	0.32, 0.64, 0.96 or 1.92 mg	Single	Metabolite profile	(Meng et al., 2004)
Healthy males (18) and females (22)	500mg capsules	0.5, 1, 2.5 or 5.0g	Single	Metabolite profile. No serious adverse effects caused.	(Boocock et al., 2007b)
Healthy males (11)	250ml red wine, 1L grapes juice, or 10 tablets	14µg/kg	Single	Resveratrol six fold more bioavailable in red wine and grape juice than tablets	(Ortuño et al., 2010)
Healthy males (12 young) and females (12 elderly)	Capsules	200mg	Single followed by multiple doses three times a day (2 days) and a final single dose	Resveratrol was well-tolerated by young and elderly subjects	(Nunes et al., 2009)
Healthy males (20) and females (20)	Capsules	25, 50, 100 or 150mg	Six times per day, for 13 doses	Well-tolerated except for some mild adverse reactions being reported	(Almeida et al., 2009)
Male (9) and female (11) colorectal cancer patients	500mg caplets	0.5 or 1.0g	Once daily for 8 days prior to surgery	Metabolite profile in tumour tissue	(Patel et al., 2010)
Healthy males (11) and females (31)	500mg caplets	1g	Once daily for 28 days	Modulation of enzymes involved in carcinogen activation and detoxification	(Chow et al., 2010a)

Table 1.2  
continuation

Colon cancer patients (8)	Plant-derived resveratrol tablets (20mg/day or 80mg/day) or grape powder (80g/day or 120g/day)	3.886mg, 15.54mg, 0.073mg (0.32µM) and 0.114mg (0.5µM) respectively	14 days	Inhibition of Wnt signalling in normal colonic mucosa suggesting a beneficial role of resveratrol in colon cancer prevention	(Nguyen et al., 2009)
Patients with gastrointestinal neuroendocrine tumours (estimated enrolment 7)	2.5g	n/a	Twice daily; three months	Effects of resveratrol on Notch-1; safety/efficacy study	On-going NCT01476592

1.15 Is bioavailability a problem anymore?

The efficacy of orally administered resveratrol depends on its absorption, metabolism and tissue distribution. The main problem is the fact that resveratrol is found at nanomolar concentrations in the blood which does not reflect the effects seen *in vitro* which are in micromolar concentrations (Baur and Sinclair, 2006). Bioavailability has been regarded as a major issue and this was illustrated by the very low amount of resveratrol present in wine (0.3-7mg aglycones/L and 15mg glucoside/L in red wine) (Manach *et al.*, 2004). The majority of studies have implicated resveratrol in disease prevention; however, only a few studies have investigated the bioavailability and metabolism of resveratrol (Yu *et al.*, 2002). A small number of *in vivo* studies in animals and humans revealed a very low level of intestinal uptake of resveratrol therefore leading to only minute levels in the bloodstream due to widespread gut and liver metabolism (half-life of ~ 8 to 14 minutes) (Saiko *et al.*, 2008). Resveratrol is accumulated in the intestinal mucosa (Baur and Sinclair, 2006). In humans, the majority of resveratrol after an intravenous dose is converted to sulphate conjugates in

approximately 30 minutes (Saiko *et al.*, 2008). For instance, Calamini *et al.* (2010) reported plasma concentrations as high as 0.5µM for resveratrol and 2-10µM for resveratrol-4'-O-D-sulphate after oral administration of pure resveratrol thus concluding effective *in vivo* inhibition of COX-1 and COX-2. Resveratrol conjugates have not been tested extensively *in vitro* and currently, the active form of resveratrol responsible for the effects reported is still unknown.

Current research however, has provided evidence that the bioavailability of resveratrol is no longer an issue since pharmacokinetic experiments using a mixture of resveratrol-3-O-D-sulphate and resveratrol-4'-O-D-sulphate in mice have shown that resveratrol metabolites are absorbed and undergo hydrolysis thus liberating free resveratrol (Andreadi, 2012). Possible reasons as to why resveratrol exhibits chemopreventive properties in *in vivo* colorectal cancer animal models could be the accumulation of the drug in the colon. It is also possible that resveratrol metabolites in the blood become deconjugated back to free resveratrol in target tissues or even excreted into the bile following enterohepatic circulation leading to deconjugation in the colon by colonic bacteria.

### **1.16 Resveratrol metabolites**

Despite its low bioavailability, *in vivo* evidence has shown that resveratrol has a protective role in rodent models, which suggests that its conjugates (e.g. *trans*-RV-3-O-D-glucuronide, resveratrol-4'-O-D-glucuronide, *trans*-resveratrol-4'-O-D-sulphate and *trans*-resveratrol-3-O-D-sulphate), or other metabolites (e.g. piceatannol), may be active (Figure 1.4). The metabolites reach 3-8 fold greater concentrations than the parent compound after absorption and possess longer half-lives therefore leading to greater

exposure (reaching 23-fold) to the metabolites compared to the aglycone (Patel *et al.*, 2011).

Currently, only one study has investigated the effect of the sulphated metabolites against breast cancer cells (Miksits *et al.*, 2009). The three major sulphated metabolites were tested and these studies demonstrated that unlike resveratrol, the metabolites showed low cytotoxicity in malignant and non- malignant breast cancer cells ( $IC_{50}$ = 202-228 $\mu$ M). This, however, may not be representative of the effects *in vivo* mainly due to the presence of sulphatases which could probably de-conjugate the metabolites back into resveratrol (Miksits *et al.*, 2009). Resveratrol conjugates are not able to enter the cell easily unless bound on a specified transporter. More specifically, p-glycoprotein a member of the ATP-binding cassette (ABC) transporter superfamily, acts as an efflux pump to export resveratrol and its metabolites back into the gut lumen (Lohner *et al.*, 2007).

Studies have shown that resveratrol becomes converted to piceatannol (the tetrahydroxylated form of resveratrol) by the action of cytochrome P450 CYP1B1 (Potter *et al.*, 2002). Piceatannol, a naturally occurring polyphenol (*trans*-3,4,3',5'-tetrahydroxystilbene) is an analogue of resveratrol and like resveratrol is synthesised in plants in response to fungal and other environmental stress, making them phytoalexins (Figure 1.4A) (Wolter *et al.*, 2002). Treatment of Caco-2 cells with increasing concentrations (12.5 to 200 $\mu$ mol/L) of piceatannol led to reduced cell growth in a dose- and time-dependent manner (Wolter *et al.*, 2002). The same study revealed using flow cytometry that Caco-2 cells were reduced in the G0/G1 and G2/M phases of the cell cycle, while an increase was observed in the S phase following a 100 $\mu$ mol/L concentration. These effects were suggested to be mediated by the up-regulation of

positive cell cycle regulators, including cyclin E and cyclin A which are at their highest activity in the S phase.

Pterostilbene (*trans*-3,5-dimethoxy-4'-hydroxystilbene) is a natural dimethylated analogue of resveratrol found most abundantly in blueberries (Figure 1.4B) (Pan *et al.*, 2009). Like resveratrol, it is known to exert anticancer, anti-inflammatory and antiproliferatory effects. Pterostilbene (50 $\mu$ M) has been shown to decrease the expression of COX-2 as well as various cytokines that promote inflammation including TNF- $\alpha$ , IL-1 $\beta$  and IL-6 in HT-29 colorectal cancer cells (Paul *et al.*, 2010). Pterostilbene was also found to be responsible for reducing the levels of cyclin D1 in HT-29 cancer cells, a protein overexpressed in patients with primary colorectal adenocarcinoma, adenomatous polyps and familial adenomatous polyposis (Paul *et al.*, 2010).



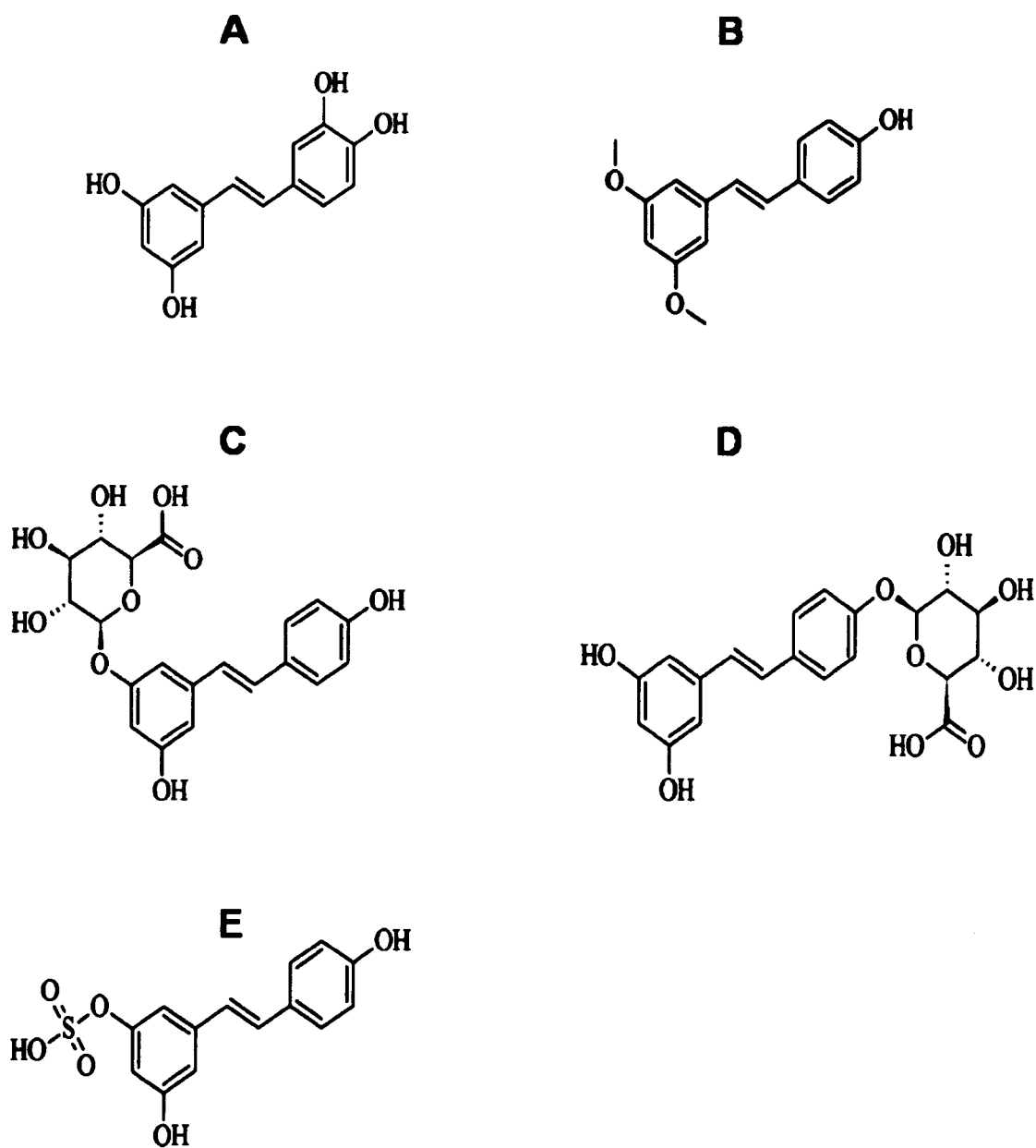


**Figure 1.4** Structures of piceatannol (A), pterostilbene (B), resveratrol-3-O-D-glucuronide (C), resveratrol-4'-O-D-glucuronide (D) and resveratrol-3-O-D-sulphate (E).

## 1.17Cell cycle

The process of cell division comprises of two distinct processes namely, DNA replication and separation of replicated chromosomes into two identical cells (Vermeulen *et al.*, 2003). Cell division is separated into two main stages: mitosis (the actual process of nuclear division) and interphase (the stage in between two mitotic phases). The process of mitosis is further sub-divided into four distinct stages including, prophase, metaphase, anaphase and telophase. More specifically, the interphase includes G1, S and G2 phases where DNA replication occurs in S phase. Prior to S phase, there is a gap phase called G1 at which point the cell is getting ready for DNA synthesis (Figure 1.5). Following the S phase is a further gap phase called G2 where the cell prepares for mitosis. Prior to cells committing to DNA replication, they can enter a resting phase (senescence) called G0. Cells in the body which are not growing or proliferating constitute the majority of cells in this senescent G0 phase.

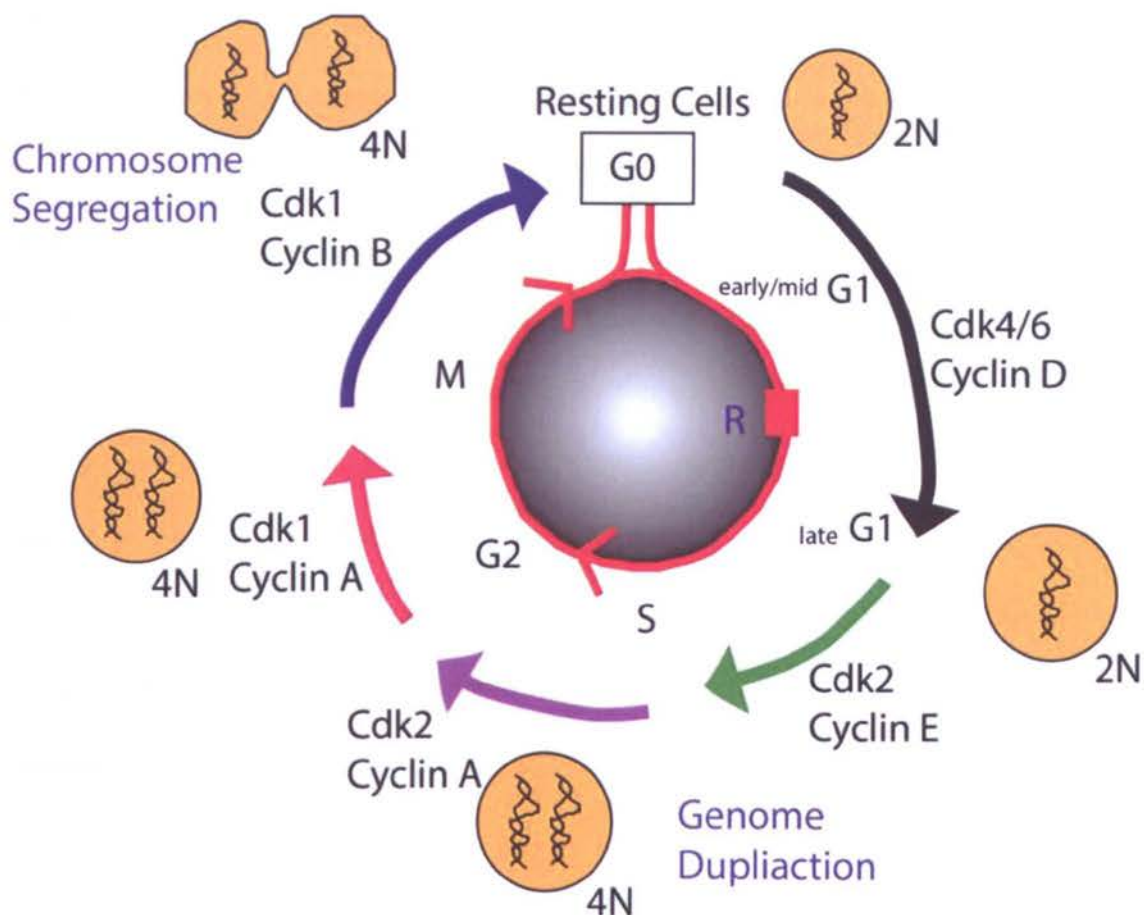


**Figure 1.5** The cell cycle and the corresponding cyclins in each of the four phases. Adapted from (Malumbres and Barbacid, 2001).

### 1.17.1 Cell cycle control

#### 1.17.1.1 Cyclin-dependent kinase (CDK) regulation

The cell cycle is tightly controlled by three distinct entities, the cyclin-dependent kinases (CDK), CDK substrates and through restriction points and checkpoints. Several cellular proteins known as the CDKs are responsible for regulating the passage of cells from one phase of the cell cycle to another. These are a family of serine/threonine protein kinases that become activated at particular points of the cell cycle. More specifically, CDK4, CDK6 and CDK2 are active in the G1 phase whilst CDK2 and CDK1 for S and G2/M phases respectively. Once these CDKs become activated they

cause activation of downstream proteins by phosphorylation (Morgan, 1995, Pines, 1995). Unlike their activating proteins (cyclins), the CDK protein levels remain steady throughout the cell cycle. Depending on the phase of the cell cycle, different cyclins are essential. More specifically, cyclin D, which exists in 3 isoforms (cyclin D1, D2 and D3) is capable of binding to CDK4 and/or CDK6 to form a complex known as the CDK-cyclin D complex, which is required for the entry of cells into G1. Cyclin E is also a G1 cyclin, but, forms a complex with CDK2 that is responsible for the transition from G1 to S phase. Cyclin A on the other hand, binds to CDK2 and is involved in S phase progression but is also capable of complexing with CDK1 in G2/M in order to encourage the transition into M phase. The M phase of the cell cycle is additionally regulated by the cyclin B- CDK1 complex (Vermeulen *et al.*, 2003).

CDK activity is additionally negatively controlled by cell cycle inhibitory proteins known as CDK inhibitors (CKI) which are capable of controlling CDK activity in two ways, either by binding to CDK alone or to the CDK-cyclin complex (Malumbres and Barbacid, 2001). There are two types of CDK inhibitors known as the INK4 family and Cip/Kip family. More specifically, the INK4 family consists of four members, p15, p16, p18 and p19 which are responsible for binding to and forming a stable complex with CDK therefore preventing the binding to cyclin D. The Cip/Kip family consists of p21 (Waf1, Cip1), p27 (Cip2) and p57 (Kip2). The function of these inhibitors is to inactivate G1 CDK-cyclin complexes and less so the CDK1-cyclin B complexes. The inhibitor p21 further exerts its actions by inhibiting DNA synthesis by attaching to and inactivating the proliferating cell nuclear antigen (PCNA). The activity of CDK inhibitors is tightly controlled by internal and external signals. The p21 expression for example, is tightly controlled at the transcriptional level by the tumour suppressor gene

p53. Increased activation of p15 and p27 depends on the transforming growth factor beta (TGF- $\beta$ ) which promotes growth arrest (Vermeulen *et al.*, 2003).

#### **1.17.1.2 CDK Substrates**

Activation of CDK causes phosphorylation of key proteins therefore leading to the progression of the cell cycle. The retinoblastoma tumour suppressor gene (pRb) for example, is the substrate of CDK4/6-cyclin D that becomes phosphorylated during early G1 causing the complex to breakdown and subsequently releasing the two known transcription factors E2F-1 and DP-1 (Malumbres and Barbacid, 2001). These transcription factors function by controlling the gene transcription of key proteins which are essential for progression into S phase. The CDK2-cyclin E complex is responsible for phosphorylating its corresponding inhibitor, p27, causing it to degrade. This complex further phosphorylates histone H1 and this activity is thought to play a role in chromosome condensation during DNA replication. Histone H1 is also a substrate of CDK1-cyclin B (Vermeulen *et al.*, 2003).

#### **1.17.2 Cell cycle and cancer**

In cancer, the tight control of the cell cycle is lost leading to uncontrolled cell proliferation. It is known that mutations that can lead to cancer occur in two families of genes, the proto-oncogenes and tumour suppressor and DNA repair genes. More specifically, mutations in proto-oncogenes encourage cancer growth whilst the inactivation of tumour suppressor genes (*pRB* and *p53*) causes proteins that inhibit the progression of the cell cycle to become dysfunctional (Easton *et al.*, 1998). Mutations also appear in vital proteins involved in the cell cycle. For example, it has been reported that CDK4 is overexpressed in several cell lines whilst mutations in the *CDK4* and *CDK6* genes lead to insufficiency of CKI binding (Wölfel *et al.*, 1995, Easton *et al.*,

1998). Constitutive activation of cyclin D1 and inactivation of CDK inhibitors including p16 and p27 has also been reported (Wölfel et al., 1995).

#### **1.17.2.1 Resveratrol and the cell cycle**

Data from studies on a range of cell lines have suggested that resveratrol has strong anti-proliferative characteristics *in vitro* (Walle *et al.*, 2004, Delmas *et al.*, 2000). Resveratrol prevented the proliferation of tumour cells by directly inhibiting DNA synthesis and by impeding different phases of cell cycle development (Kundu and Surh, 2004). This inhibition is partly attributed to the capability of resveratrol to block the cells from entering mitosis subsequently leading to cell cycle arrest in G1, S or G2/M. This naturally occurring polyphenol also inhibited the expression of cyclin B1 in MCF-7 and SW-480 cells, whilst also down-regulated the expression of cyclins D1 and A in CCL-228 (SW480) cells at concentrations ranging from 12.5µmol/L to 200µmol/L (Wolter *et al.*, 2003). This suggests a cell type-specific effect of resveratrol in blocking the malignant cell cycle progression (Joe *et al.*, 2002). Alternatively, resveratrol inhibited the expression of cyclin D1 and Cdk4 but increased the expression of cyclins E and A in Caco-2 and HCT-116 colorectal cancer cells (Wolter *et al.*, 2001). Resveratrol exerts its inhibitory effects by mediating cell-cycle arrest through up-regulation of p21, p27, p53 and Bax (Rimando and Suh, 2008, Gescher and Steward, 2003).

## 1.18 Apoptosis

Apoptosis, the process of programmed cell death, is a natural process which occurs during development and ageing in order to maintain homeostasis in tissues (Elmore, 2007). It is the most vital cellular mechanism against transformation of 'new growth' that removes a damaged cell whilst also suppressing the development of transformed cells that have been inappropriately stimulated to divide despite the absence of mitotic stimuli (Kundu and Surh, 2004). The apoptotic process also occurs in response to cell damage either by disease and/or toxic agents or as a protective means as in immune reactions (Norbury and Hickson, 2001). Morphological characteristics consistent with apoptosis include cell shrinkage accompanied by a dense cytoplasm and tightly packed organelles (Kroemer *et al.*, 2008). Pyknosis is another characteristic of cells undergoing apoptosis and is caused by chromatin condensation along with nuclear fragmentation (karyorrhexis) (Kroemer *et al.*, 2005). Plasma membrane blebbing is a further morphological change which occurs during apoptosis and subsequently leads to the formation of apoptotic bodies. Because these apoptotic bodies are rapidly phagocytosed by macrophages, they do not shed their cellular parts and no inflammatory reaction is formed.

Apoptosis can occur in three distinct ways: the extrinsic pathway (death receptor), the intrinsic pathway (mitochondrial) and the perforin/granzyme pathway. The process of apoptosis is tightly regulated by a group of proteins which belong to the cysteine protease family called caspases which act as both the initiators and executioners of apoptosis (Wong, 2011). Both the extrinsic and intrinsic pathways converge at the execution phase of apoptosis (Figure 1.6).

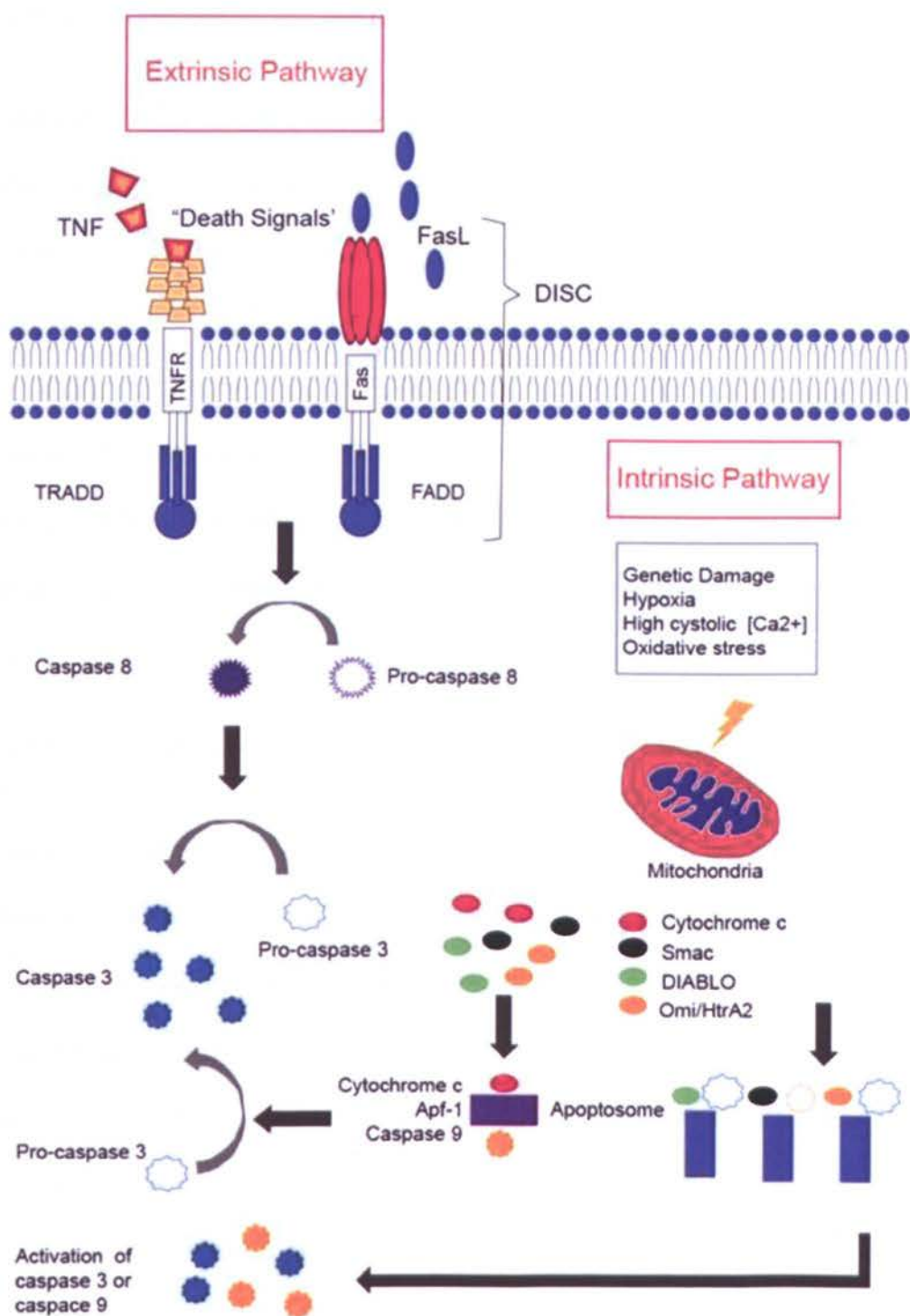


**Figure 1.6** The intrinsic and extrinsic pathways of apoptosis (Adapted from Wong, 2011).



### **1.18.1 Extrinsic Pathway**

The extrinsic death receptor family is initiated following binding of specific death ligands to a death receptor including type I TNF receptor and Fas (CD-95) receptor and their respective ligands, TNF and Fas-L (Fas-ligand). These death receptors possess an intracellular domain which is responsible for employing proteins like the TNF receptor-associated death domain (TRADD), the Fas-associated death domain (FADD) and caspase-8. The attachment of the ligand to the receptor creates a binding site for the adaptor proteins mentioned previously thus forming a complex known as the death-inducing signalling complex (DISC). This in turn causes the activation of pro-caspase 8, an initiator caspase that activates apoptosis by activating further downstream caspases.

### **1.18.2 Intrinsic Pathway**

The second common apoptosis pathway takes place within the cell and is usually initiated subsequently to internal damage like DNA damage and high levels of cytosolic calcium amongst others. Activation of this pathway is due to increased mitochondrial permeability and release of cytochrome c (a pro-apoptotic molecule) into the cytoplasm. Further control proteins include members of the Bcl-2 family consisting of pro- and anti-apoptotic proteins. The pro-apoptotic protein members (Bax, Bak, Bad) promote the release of cytochrome c whilst the anti-apoptotic ones (Bcl-2, Bcl-XL) block this mitochondrial release (Malumbres and Barbacid, 2001). Regardless of this, the initiation of apoptosis is a result of the actual balance of pro- and anti-apoptotic proteins. Further factors are usually released from the mitochondria during this process including apoptosis inducing factor (AIF), second mitochondria-derived activator of caspase (Smac), direct IAP Binding protein with low pI (DIABLO) and Omi/high temperature requirement protein A (HtrA2). Complex formation (consisting of cytochrome c, Apaf-

1 and caspase-9) known as the apoptosome, is the result of cytochrome c release which causes caspase-3 activation. The apoptotic factors, Smac/DIABLO and Omi/HtrA2 on the other hand, function by binding to inhibitor of apoptosis (IAP's) therefore promoting caspase activation by blocking the contact between IAP's and caspase-3 and -9 (Malumbres and Barbacid, 2001).

### **1.18.3 The Common Pathway**

The common pathway also known as the execution phase, involves the activation of certain caspases through which both the intrinsic and extrinsic pathways lead to apoptosis. Caspase-3 is responsible for cleaving the inhibitor of the caspase-activated deoxyribonuclease which is involved in apoptosis. Furthermore, additional caspases that are present downstream of caspase-3 function by cleaving certain protein kinases and DNA repair proteins amongst other targets. These downstream caspases have also been shown to affect the cell cycle and signal transduction pathways which collectively lead to apoptosis (Ghobrial *et al.*, 2009).

### **1.18.4 Regulation of apoptosis**

The main apoptotic pathways are tightly regulated by certain proteins including p53, NF- $\kappa$ B, the ubiquitin proteasome system and the PI3K signalling pathway. p53 also known as the “guardian of the genome”, is a transcription factor which is involved in the regulation of downstream genes responsible for cell cycle arrest, DNA repair and apoptosis (Ghobrial *et al.*, 2009). Under normal circumstances, p53 is capable of causing cell cycle arrest subsequent to DNA damage to allow enough time for repair. If however, the damage is irreparable, p53 is capable of inducing apoptosis.

Nuclear factor kappa beta, (NF- $\kappa$ B) is a nuclear transcription factor which functions by controlling key genes that are involved in key pathways including apoptosis, tumourigenesis and inflammation (Ghobrial *et al.*, 2009). Certain growth factors and cytokines are just two examples of agents causing activation of NF- $\kappa$ B. NF- $\kappa$ B remains inactive in the cytoplasm by being bound to proteins of the I $\kappa$ B inhibitor family and the stimuli cause its activation by phosphorylating I $\kappa$ B leading to its degradation. Once released, it translocates to the nucleus, attaches to different genes and subsequently causes their transcription. NF- $\kappa$ B possesses both pro-apoptotic and anti-apoptotic properties either by activation of proteins including c-myc, p53 and caspases or activation of TNF receptor-associated factor and IAP respectively.

PI3K is a protein kinase which has a vital function in signalling pathways involved in cell proliferation, survival and tissue neovascularisation (Ghobrial *et al.*, 2009) which has been shown to be upregulated in many cancers (Cantley, 2002). Second messengers therefore become activated that subsequently lead to the activation of a downstream molecule, Akt. Activation of Akt in turn causes the phosphorylation of specific cell survival proteins and inactivation of pro-apoptotic proteins.

#### **1.18.5 Apoptosis and cancer**

Evasion of apoptosis is an important pre-requisite for the steps of carcinogenesis. Resistance to apoptosis can occur in three distinct manners: a) disturbance in the balance between pro- and anti-apoptotic proteins, b) decreased caspase function and c) non-functional death receptor signalling (Figure 1.7). Altered regulation of the inhibitors of apoptosis (IAPs), the endogenous inhibitors of caspases has been reported in many cancers. For example survivin, a member of the IAP family has been found to

be aberrantly expressed in certain tumours and the dysregulated expression of IAPs leads to chemotherapy resistance (Wong, 2011).

Down-regulation or impairment of caspase activity causes a reduction in apoptosis and therefore leads to carcinogenesis. Defects in the death signalling pathways lead to inhibition of the extrinsic apoptotic pathway. This includes decreased expression or loss of function of the receptor or even a decreased amount of death signals which individually cause a malfunction in signalling and consequently, reduced apoptosis (Wong, 2011).

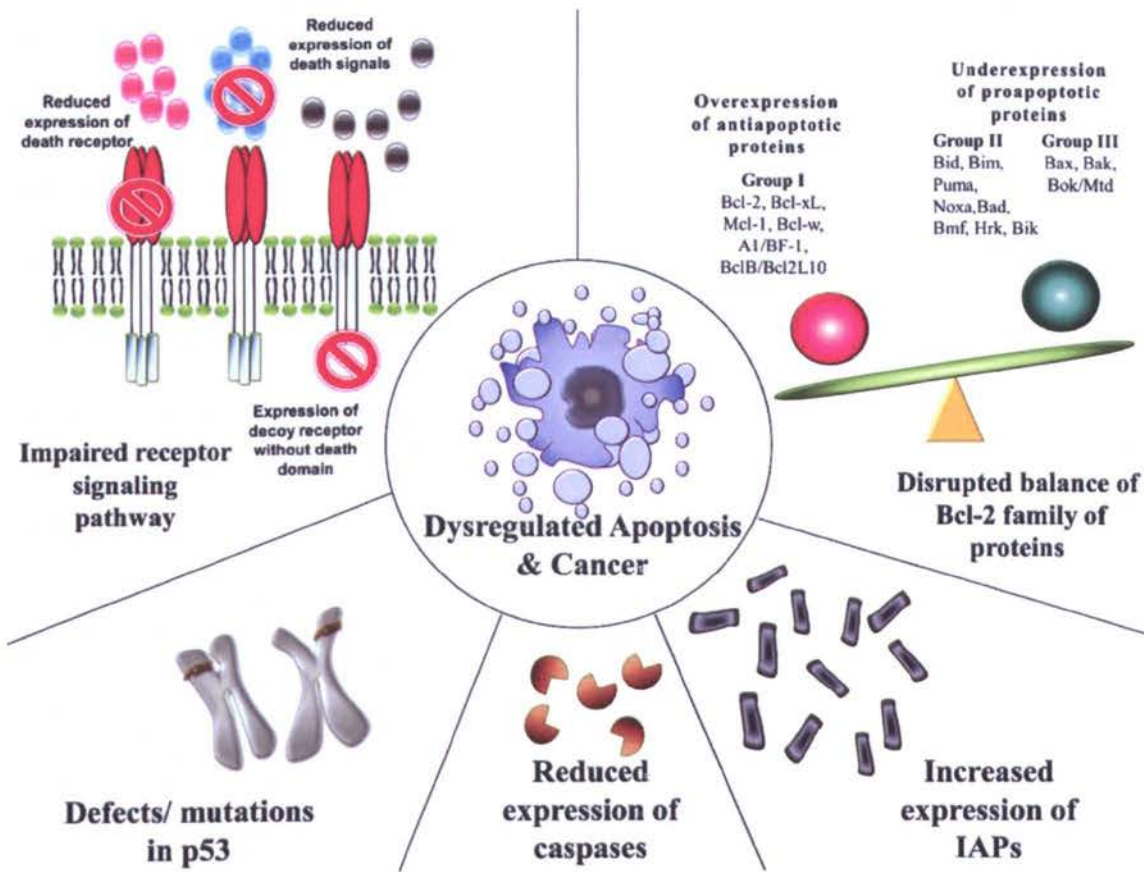


**Figure 1.7** Events leading to evasion of apoptosis and consequently cancer.Taken from Wong, (2011).

### 1.18.6 Resveratrol and apoptosis

Resveratrol at 20µg/ml, is capable of inducing apoptosis by positively regulating the expression of Bax, p53, PUMA and other pro-apoptotic proteins while concurrently reducing the expression of anti-apoptotic proteins including Bcl-2 and surviving (Kuo *et al.*, 2002, Shankar *et al.*, 2007).

It has been revealed that resveratrol can trigger apoptosis in a variety of malignant cell types by encouraging cytochrome c release, up-regulation of the pro-apoptotic Bax protein, down-regulation of the anti-apoptotic Bcl-2 and through activation of the tumour suppressor protein, p53 at a range of 2.3-40µM (Gusman *et al.*, 2001, Dong, 2003). Resveratrol caused apoptosis in HL-60 (Human promyelocytic leukaemia cells) and the T47D breast cancer cell line by eliciting the CD95-CD95L signalling pathway (Clément *et al.*, 1998). Alternatively, studies by Delmas and colleagues (2003) reported that modulation of Fas/FasL was not responsible for resveratrol-induced apoptosis (at 30µM) in SW-480 colorectal cancer cells; rather it was due to caspase activation and up-regulation of Bax and Bak (Delmas *et al.*, 2003).

### 1.19 p53

The p53 protein, also known as tumour protein 53 (TP53) is one of the highly studied tumour suppressor proteins which is encoded by the tumour suppressor gene *TP53* located on chromosome 17 (17p13.1). In addition to its involvement in the regulation of the cell cycle mentioned previously, it is also responsible for inducing apoptosis and is also involved in development, differentiation, gene amplification, DNA recombination, chromosomal segregation and cellular senescence (Oren and Rotter, 1999). Gene abnormalities of p53 have been reported in more than 50% of human cancers (Bai and Zhu, 2006) and aberrant expression of genes controlled by p53 which are implicated in

apoptosis and regulation of the cell cycle cause the anomalous activity of p53 therefore leading to tumour cell proliferation (Avery-Kiejda *et al.*, 2011).

Cell cycle arrest caused by DNA damage at the G1/S checkpoint is highly dependent on p53. This leads to increased expression of p53 which in turn promotes the transcription of key genes like p21, Mdm2 and Bax. p21 causes cell cycle arrest and blocks the replication of damaged DNA (Figure 1.8). Mdm2 acts by promoting a negative feedback loop for p53 by binding to it and inhibiting its transcription therefore causing p53 degradation. On the other hand, p19 is capable of binding to Mdm2 therefore inhibiting the p53 degradation, subsequently causing p53 ubiquitination (Aylon and Oren, 2011). If DNA damage is irreparable, p53 induces cell death by activating certain genes including Bax and Fas amongst others. Cells are capable of initiating cell cycle arrest when DNA damage occurs in the G2 phase. This is either dependent on or independent of p53 and is achieved by constant inhibition of CDK1.

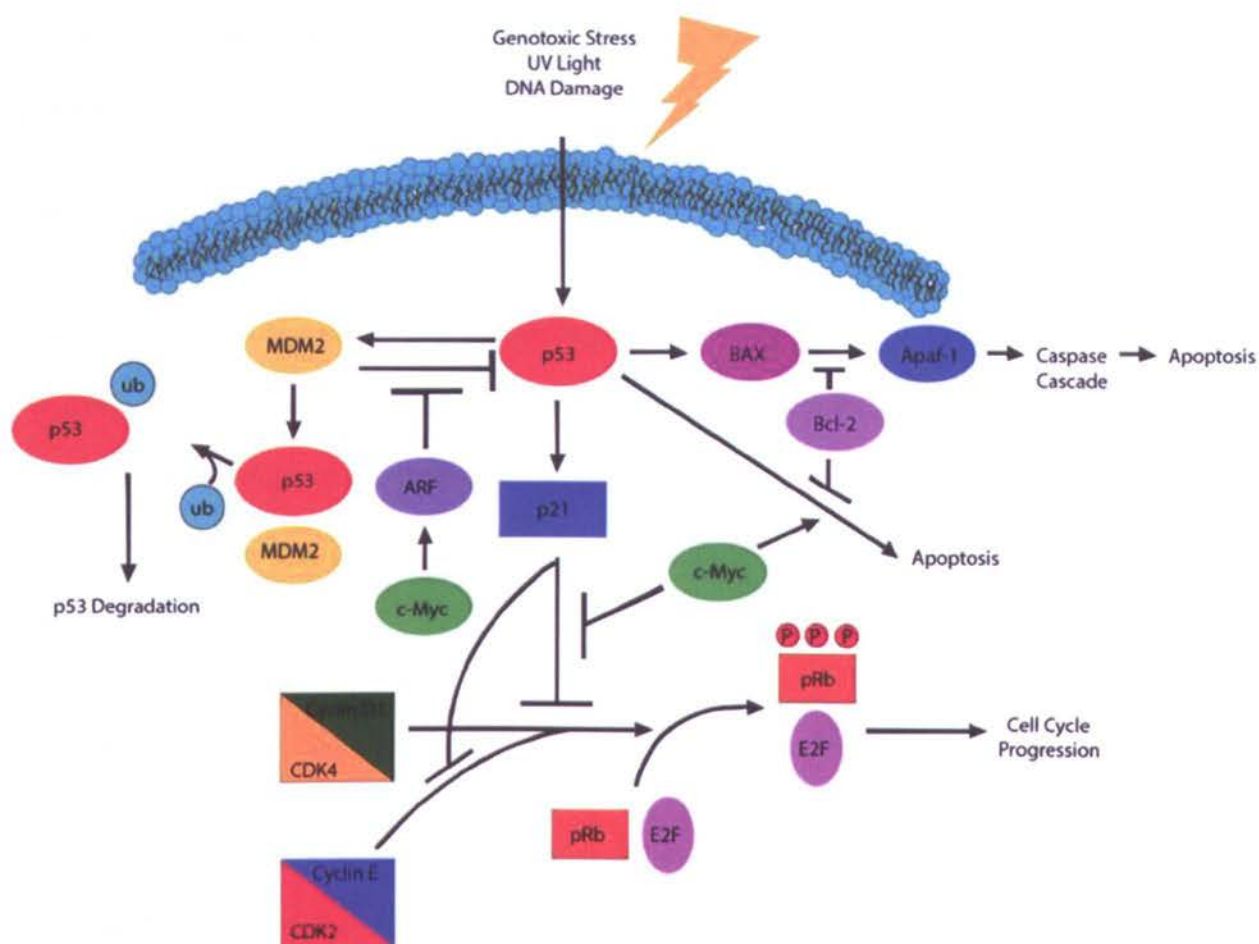


**Figure 1.8** The p53 signalling pathway. Adapted from Sigma-Aldrich.

(<http://www.sigmaaldrich.com/life-science/cell-biology/learning-center/pathway-slides-and/the-p53-signaling-pathway.html>).

### 1.19.1 Resveratrol and p53

The mechanisms responsible for the induction of apoptosis using resveratrol seem to be cell-type specific, either p53-dependent or p53-independent. This was observed through a study by Mahyar-Roemer *et al.* (2001) where it was suggested that resveratrol-induced apoptosis of HCT-116 colorectal cells is by a p53-independent mechanism at concentrations between 10 $\mu$ M-100 $\mu$ M (Mahyar-Roemer *et al.*, 2001). Furthermore, the apoptotic effect of resveratrol was concurrent with caspase activation (mainly by

caspase-3 cleavage) and PARP cleavage, of which both events are important in the apoptotic pathway.

### **1.20 Necrosis**

Unlike apoptosis and cell death by autophagy, necrosis is portrayed by an increase in the size of the cell (oncosis), membrane fragmentation, swelling of organelles followed by loss of intracellular constituents (Kroemer *et al.*, 2008). Necrosis is regarded as a toxic process that does not involve energy and inflammation is usually present (Elmore, 2007).

### **1.21 Autophagy**

The most common type of programmed cell death is apoptosis (Debnath *et al.*, 2005) but recently however, there has been a spur of interest in different pathways of cell death. More specifically, autophagy has been suggested to be a vital component of non-apoptotic cell death and is classified as a form of cell death that takes place without the presence of chromatin condensation (Kroemer *et al.*, 2005). Rather, autophagy is escorted by the accumulation of the cytoplasmic components in vacuoles known as autophagosomes leading to immense breakdown by lysosomes. These vacuoles are two-membraned and present within them are degenerating cytoplasmic organelles or cytosol (Levine and Kroemer, 2008, Levine and Klionsky, 2004). The autophagic process is completed after the blending of the autophagosomes with the lysosomes therefore forming autolysosomes followed by the subsequent degradation by lysosomal hydrolases (Kroemer *et al.*, 2008).



However, the importance of autophagy as one of the main types of cell death is still an issue of great debate. The main reason for this is the highly recognised function of autophagy as a survival mechanism during states of scarce nutrients. Therefore, by cytoplasmic degradation, the process of autophagy is used to conserve nutrients and energy in the stressed cells (starved cells) (Tsukada and Ohsumi, 1993, Straub *et al.*, 1997, Schlumpberger *et al.*, 1997). The autophagic process in these conditions therefore serves to sustain the viability of cells (Debnath *et al.*, 2005).

There are three distinct types of autophagy in cells including: a) macroautophagy (usually called autophagy) which involves the sequestration of the cytoplasmic constituents into autophagosomes and subsequently delivered to the lysosomes for degradation, b) microautophagy where the cytoplasm is swallowed up directly by the lysosomal membrane and, c) chaperone-mediated autophagy where proteins are conveyed to the lysosome via a receptor-mediated process. Of the three routes mentioned above, only macroautophagy has been linked to type 2 programmed cell death (autophagy) (Debnath *et al.*, 2005).

### **1.22 Signal transduction pathways**

Several key proteins of signal transduction pathways involved in maintaining homeostasis by controlling the degree of cell proliferation and cell death, become dysregulated in human cancers either by constitutive activation, overexpression or inhibition. In the sections that follow below only the pathways investigated in this study will be described.

### 1.22.1 AMPK

Adenosine monophosphate (AMP)-activated protein kinase (AMPK) is a eukaryotic heterotrimeric protein kinase that is activated in response to nutritional and environmental stresses therefore functioning as a metabolic switch (Hardie and Carling, 1997). It consists of an  $\alpha$ -catalytic and  $\beta$ - and  $\gamma$ -regulatory subunits (Rashid *et al.*, 2011). Some key functions of AMPK include controlling carbohydrate and lipid metabolism and cell proliferation (Rashid *et al.*, 2011). AMPK is capable of identifying increased levels of the AMP/ATP ratio in the stress conditions mentioned above. It therefore, preserves energy via inhibition of protein synthesis and mTOR (mammalian target of rapamycin) and additionally acts as a checkpoint leading to cell cycle arrest through p53 (Jones *et al.*, 2005). The activity of AMPK is controlled allosterically by AMP and via phosphorylation at the Thr172 residue of the  $\alpha$ -subunit (Lin *et al.*, 2010).

AMPK has been shown to be responsible for controlling several processes that could influence the proliferation and/or survival of tumour cells (Shackelford and Shaw, 2009). LKB1, a serine/threonine kinase (liver kinase B1) and a known tumour suppressor protein was found to be the main upstream activator of AMPK by direct phosphorylation and activation of AMPK (Shackelford and Shaw, 2009).

The mammalian target of rapamycin (mTOR) has been identified as a downstream target of the LKB1-AMPK pathway and has been shown to control cell growth and is deregulated in the majority of human cancers (Guertin and Sabatini, 2007). LKB1 and AMPK have also been linked to p53. Studies have additionally identified that AMPK affects p53-dependent apoptosis and directly causes p53 phosphorylation at Ser15.

### 1.22.2 Adenosine receptors

The signalling molecule adenosine is capable of affecting various pathophysiological processes like cell proliferation via the involvement with one of the four cell-surface receptors, namely A<sub>1</sub>, A<sub>2A</sub>, A<sub>2B</sub> and A<sub>3</sub>. The regulation of adenosine levels is dependent on two mechanisms; the release of adenosine from metabolically active cells and its extracellular production by degradation of released ATP (Gessi *et al.*, 2007).

The four receptor isoforms can be distinguished from one another based on their pharmacological properties and in their ability to couple to second messengers (Fredholm *et al.*, 2001). For example, A<sub>1</sub> and A<sub>3</sub> inhibit the activity of adenylyl cyclase via G<sub>i</sub> proteins, whilst A<sub>2A</sub> and A<sub>2B</sub> activate it via G<sub>s</sub> proteins (Fredholm, 2003).

A<sub>1</sub>, A<sub>2B</sub> and A<sub>3</sub> receptors have also been demonstrated to activate several effector proteins including phospholipase (PLC) and K<sup>+</sup> channels (Yaar *et al.*, 2004) while all receptor subtypes regulate the phosphorylation of ERK1/2 (Schulte and Fredholm, 2000) (Figure 1.9). Adenosine is capable of controlling several processes including cell proliferation, differentiation and apoptosis in cancer cells but this depends on its extracellular concentration, the adenosine receptor subtype expression and the various signalling pathways activated subsequent to binding of specific agonists (Fishman *et al.*, 2000, Merighi *et al.*, 2002, Mujoomdar *et al.*, 2004).

Due to the focus of this study on the adenosine A<sub>3</sub> receptor, the other subtypes will only be briefly described. Potent A<sub>3</sub> agonists and highly specific antagonists recognised that the A<sub>3</sub> subtype plays a vital role in the control of tumour cell proliferation caused by adenosine (Bar-Yehuda *et al.*, 2001, Merighi *et al.*, 2005). Depending on the

concentration of the agonist and the cell type,  $A_3$  receptor activation possesses a dual function, either by promoting cell growth or inducing cell death (Merighi *et al.*, 2003). Indeed, the  $A_3$  receptor is over-expressed on the cell surface of cancer cells including colorectal cancer tissue (Gessi *et al.*, 2004).  $A_3$  receptor activation stimulates an intracellular cascade that induces the activation of phospholipase C and increases intracellular calcium concentration (Abbracchio *et al.*, 1995).

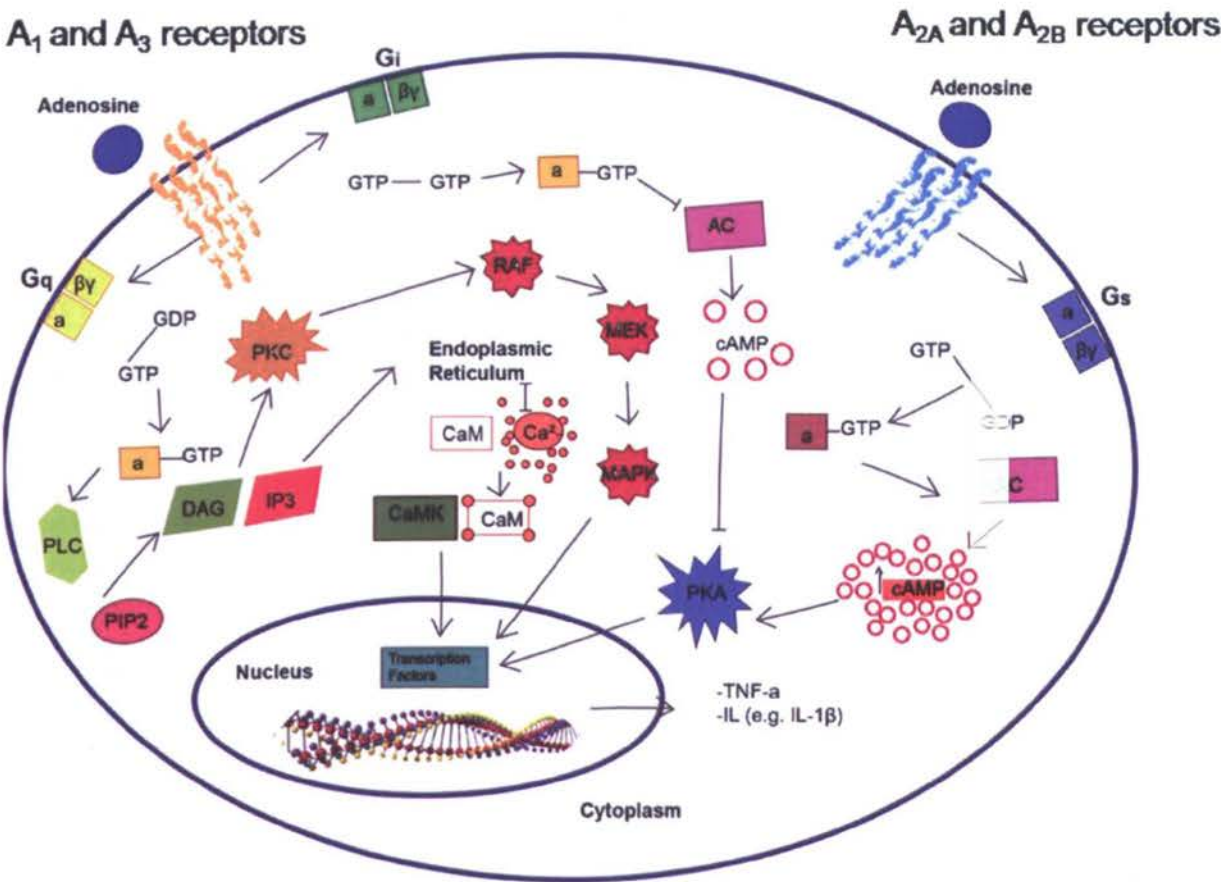


**Figure 1.9** The signalling pathway mediated by adenosine receptors (Adapted from Varani *et al.*, 2010).

### 1.22.3 PI3K

Phosphatidylinositol-3 kinases (PI3Ks) are a family of lipid kinases that are capable of phosphorylating the inositol ring 3'-OH group in inositol phospholipids. Class I PI3Ks are heterodimers which consist of a catalytic subunit (p110) and a regulatory subunit (p85). Class I is further subdivided in IA which is induced by receptors that possess a protein tyrosine kinase activity (Receptor Protein Tyrosine Kinase, RPTK) and class IB which requires receptors coupled with G protein for activation (Vara *et al.*, 2004). In order for a second messenger to be formed, in this case phosphatidylinositol-3,4,5-triphosphate (PI-3,4,5-P<sub>3</sub>), a substrate is required (phosphatidylinositol-4,5-bisphosphate, PI-4,5-P<sub>2</sub>).

The activation of RPTK causes the PI3K to bind to the receptor via one or two SH2 domains and subsequently causes allosteric activation of the catalytic p110 subunit. PIP<sub>3</sub> brings further signalling molecules with pleckstrin homology (PH) domains to the cell surface like PDK1 and Akt. PTEN, a PI-3,4,5-P<sub>3</sub> phosphatase, negatively regulates the PI3K/Akt pathway (Vara *et al.*, 2004). Upon activation, Akt controls the activation and inhibition of certain proteins, ultimately leading to cell proliferation and evasion of apoptosis.

The Akt family consists of three members, PKB $\alpha$  (Akt1), PKB $\beta$  (Akt2) and PKB $\gamma$  (Akt3) (Murthy *et al.*, 2000). In order for a successful activation of Akt to occur, phosphorylation of a threonine residue (Thr308) in the kinase region is required. For maximal Akt activation, phosphorylation of a further site at Serine 473 should occur on the C-terminal tail (Alessi *et al.*, 1996).

The activation of Akt activates several pathways promoting cell survival, growth and progression of the cell cycle (Figure 1.10) (Testa and Bellacosa, 2001). Specific targets include the pro-apoptotic proteins Bad, procaspase-9 and p21. The main modification of the PI3K/Akt pathway in cancer is gene amplification of the PI3K gene, *PIK3C* (Vara *et al.*, 2004). Further changes involved in the carcinogenic process include overexpression or constitutive activation of Akt, consequently leading to resistance to anti-proliferative signals, evasion of apoptosis, limitless replicative ability, angiogenesis and invasion and metastasis (Testa and Bellacosa, 2001).

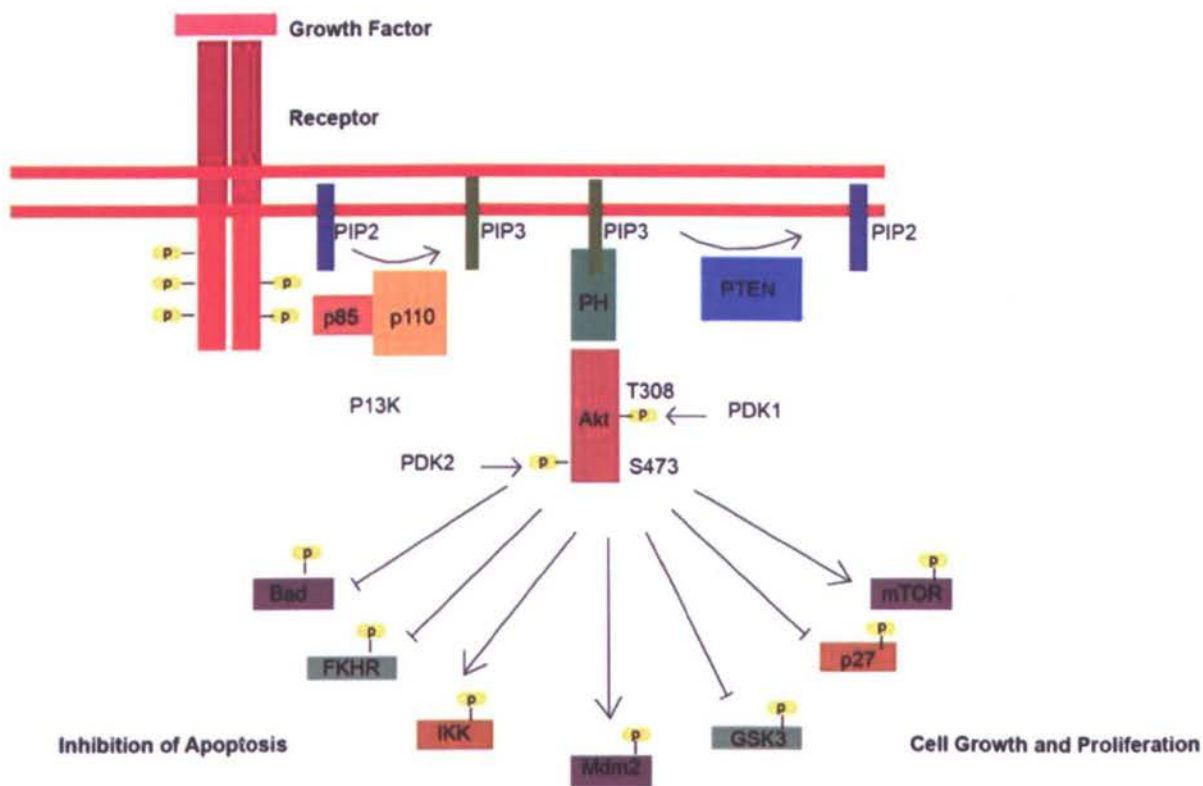


**Figure 1.10** The PI3K signalling pathway and its downstream effectors leading to inhibition of apoptosis or cell growth and proliferation once constitutive activated (Adapted from Varas *et al.*, 2004).

#### 1.22.4 ERK/MAPK

The extracellular signal-regulated kinase/ mitogen activated protein kinase (MAPK) is a member of a larger family of serine/threonine kinases which create important cell proliferation signalling pathways starting from the cell membrane and leading to the nucleus (Dong *et al.*, 2002). The MAPK family consists of three main subfamilies, the extracellular signal-regulated kinases (ERK/MAPK), the c-jun N-terminal kinase (JNK) and MAPK14 (Fang and Richardson, 2005). The activity of ERK/MAPK is responsible for conveying extracellular signals into intracellular responses. MAPKs phosphorylate several intracellular targets including transcription factors, membrane transporters and other kinases (Lawrence *et al.*, 2008).

The ERK transduction pathway is activated by signals being passed on through protein kinase C (PKC) or Ras. This triggers the activation of Raf1 which consequently activates a pathway consisting of MEK and ERK (Dong *et al.*, 2002). The binding of GTP to Ras family members is encouraged by PKC which causes the eventual Raf1 and MAPK activation (Wang *et al.*, 2004b). Raf causes phosphorylation of MEK1 and MEK2 at serine residues which also phosphorylate ERK. The ERK enzymes function by phosphorylating certain targets in the cytoplasm or are capable of migrating to the nucleus and cause phosphorylation and consequent activation of several transcription factors like c-Fos (Treisman, 1994). These transcription factors regulate specific genes which are involved in cell proliferation and anti-apoptotic signals (Lewis *et al.*, 1998).

Following ERK/MAPK activation, the production of cyclin D1 is induced leading to increased cell division. This effect is balanced out by the cell cycle inhibitor protein (INK4). The activation of the cyclin-dependent kinase inhibitor 1 for example, is

controlled by the Ras/Raf/MEK/ERK pathway (Sato *et al.*, 2004). The ERK/MAPK pathway plays a vital role in cell proliferation and multiple growth factors and proto-oncogenes convey the signals favouring growth and differentiation (DeFazio *et al.*, 2000). Findings from numerous studies have concluded that activation of ERK MAPK is implicated in the carcinogenesis and progression of colorectal cancer (Wang *et al.*, 2004a).

In conjunction with ERK1/2, JNK appears to be vital for the phosphorylation of activating protein 1 (AP1) (Ip and Davis, 1998). Unlike the ERK pathway however, JNK proteins are activated by protein kinase G (PKG)/MEKK1/SEK1/JNK cascade and play a role in cell proliferation and induction of apoptosis (Figure 1.11) (Soh *et al.*, 2001). MAPK14 on the other hand, plays a role in the control of cell proliferation and differentiation (Fang and Richardson, 2005) with studies now indicating an anti-apoptotic role (Liao and Hung, 2003).

It has been shown that approximately 30% of cancers possess a deregulated cascade. The existing evidence of the involvement of the ERK/MAPK pathway in cancer lies on several observations including:

- a) Mutation of Ras in 36% of colorectal cancers, *KRAS* proto-oncogene mutations occurring early in the development of these cancers and increased activity of Ras is concomitantly associated with increased ERK activity
- b) Increased kinase activity as a consequence of mutations of *BRAF* (serine/threonine kinase of the Raf family)
- c) The activation of the transcription factor c-Jun
- d) Lastly, the up-regulation of the EGF receptor leads to increased activation of ERK/ MAPK signalling.



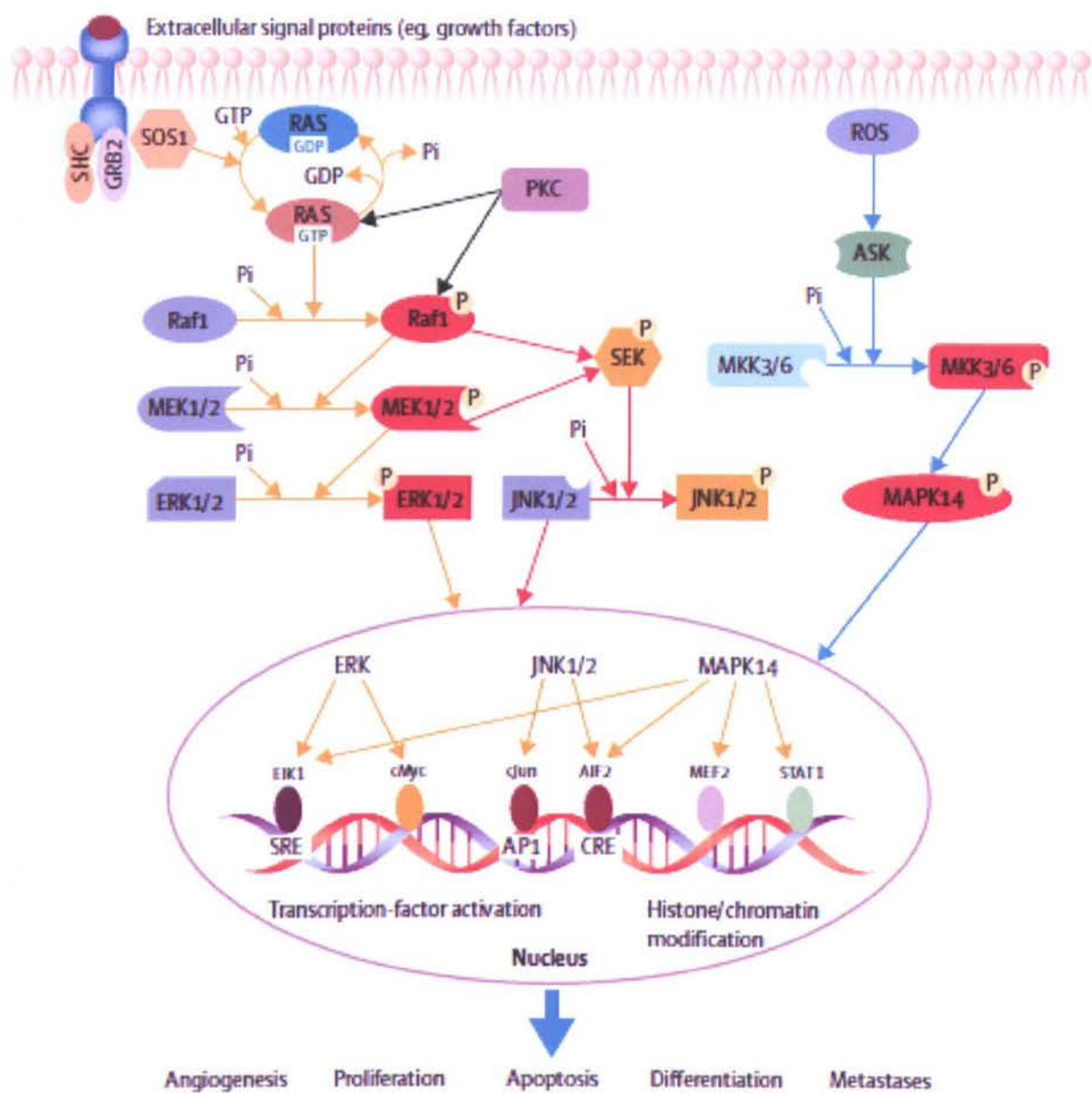


**Figure 1.11** The MAPK signalling pathway involved in the process of carcinogenesis. Taken from Fang and Richardson (2005).

### **1.23 Aims and objectives**

The initial aim of this study was to investigate the effect of the parent compound, resveratrol, two of its analogues (piceatannol and pterostilbene) and its three main metabolites on the growth of human colorectal cell lines *in vitro* using two well established viability assays.

This project further aimed to examine the mechanism of action of the metabolites on the cell cycle and its effects, if any, on inducing programmed cell death (apoptosis) using a range of techniques. The possible involvement of various molecular targets of key signalling cascades discussed previously (e.g AMPK, A<sub>3</sub> receptor, MAPK and PI3K) were also investigated in order to identify the mechanism of action of resveratrol and its metabolites.

## **Chapter 2. Materials and Methods**

### **2.1 Routine cell culture**

#### **2.1.1 Cancer cell lines**

The human colorectal cancer cell line Caco-2 was purchased from the European Collection of Cell Cultures (Salisbury, UK). The HCT-116 and CCL-228 human cell lines were kindly provided by Prof. Modjtahedi, Kingston University and were purchased from the American Tissue Culture Collection (Manassas, VA). All cell lines were cultured in Minimum Essential Eagle's medium (MEME; Sigma- Aldrich, Poole, United Kingdom), supplemented with 10% Foetal Bovine Serum (FBS; Sigma-Aldrich, Poole, United Kingdom), 10,000U penicillin, 10mg streptomycin/mL in 0.9% NaCl and 200 mM L-glutamine (Sigma-Aldrich), and were maintained at 37°C in a humidified atmosphere with 5% CO<sub>2</sub>. Caco-2 is a cell derived from the colon from a Caucasian patient with adenocarcinoma of the colon. These cells form well differentiated adenocarcinomas consistent with colonic primary grade II in nude mice (ECACC). They possess a dysfunctional p53, mutant adenomatous polyposis coli (APC) and  $\beta$ -catenin whilst possess a wild-type k-Ras (Liu and Bodmer, 2006, Nutakul *et al.*, 2011). Similarly, CCL-228 (SW-480) cells are colorectal adenocarcinoma cells with a Dukes' Type B stage. These cells are positive for the epidermal growth factor receptor and for a range of oncogenes including c-myc, K-ras, H-ras, N-ras, myb, sis and fos (Trainer *et al.*, 2006). They do, however, possess a mutated p53 (Yang *et al.*, 1996, Liu and Bodmer, 2006). HCT-116 (CCL-247) cells are epithelial and were isolated from a colorectal carcinoma. They have a wild-type p53 and APC whilst K-ras is mutated (Nutakul *et al.*, 2011). HCT-116 cells, the only cell line studied here to have a wild type p53, are also positive for transforming growth factor beta 1 (TGF- $\beta$ 1) and TGF- $\beta$ 2 expression (Sun *et al.*, 1994).

### 2.1.2 Cell culture

A cryotube of cells was removed from liquid nitrogen (-196°C) and placed in a 37°C waterbath for 1-2 minutes. The cryotube contents were transferred to a cell culture flask containing 10ml of pre-warmed 10% FBS/MEME and maintained in a humidified incubator at 37°C with 5% CO<sub>2</sub> overnight after which the medium was replaced with fresh medium to remove the toxic DMSO present in the freezing down solution. Media was replenished every 3 days until cells reached approximately 70% confluency.

Once the cells reached 70-80% confluency they were trypsinised at passages 8-14 for HCT-116 and CCL-228 and passages 50-60 for Caco-2. The cell flask contents were discarded and five millilitres of Dulbecco's – phosphate buffered saline (D-PBS) (GIBCO, UK) was added to remove any residual media and was later on discarded. Three millilitres of 0.25% trypsin-EDTA solution (Sigma-Aldrich) was then added and flasks incubated for 5-6 minutes at 37°C in order for the cells to detach. The cell culture flask contents were supplemented with 9ml 10% FBS MEME for trypsin deactivation and the solution was transferred in a 25ml universal tube for centrifugation at 1500rpm for 5 minutes. The supernatant was discarded and the pellet was re-suspended in 5ml 10% FBS in MEME. Two-hundred microlitres of the cell suspension was added to an equal volume of trypan blue (Sigma-Aldrich) and of this 30µl were transferred to the haemocytometer and the cells were counted using the Fast Read Method (Immune Systems Ltd, Paignton, UK).

$$\text{counts/ml} = \frac{\text{total counts}}{\text{number of complete 4x4 grids counted}} \times 10^4 \times \text{sample dilution(if any)}$$

Approximately  $1 \times 10^6$ - $2 \times 10^6$  cells were added to each flask for all three cell lines and allowed to grow in a humidified atmosphere at 37°C and 5% CO<sub>2</sub>. Media was replenished every 3 days.

## **2.2 Viability assays**

### **2.2.1 Neutral red uptake assay**

The neutral red uptake assay is one of the most widely used viability assays that provides a quantitative estimation of the number of viable cells. It is a fast and reliable assay with minimal background absorbance when measured in the absence of cells. Viable cells have the ability to incorporate and bind the neutral red supravital dye in the lysosomes which is later extracted (Repetto *et al.*, 2008). Cells were seeded in 96-well plates (20,000 cells/well) and treated for 48 hours after which they were incubated for 2.5 hours with 40µg/ml neutral red (Sigma-Aldrich, Poole, UK) in medium. The cells were subsequently washed with D-PBS (Fisher Scientific, Loughborough, UK) and the dye extracted using de-stain solution (1% acetic acid in 50% ethanol solution) (Fisher Scientific, Loughborough, UK). The absorbance was measured at 540nm using a LabTech (LT-4000) plate reader (Uckfield, UK).

Percent cell growth was calculated relative to the absorbance of untreated cells as shown below:

$$(\text{Abs (treatment)-blank} / \text{abs (control) -blank*}) \times 100\%$$

\*blank- absorbance of neutral red alone

### 2.2.2 Optimisation of neutral red uptake assay

A cell number calibration assay was carried out to relate cell number to absorbance and provide a large dynamic range to read cells. All three cell lines were seeded at densities of 500, 1,000, 2,000, 4,000, 8,000, 16,000, 20,000, 32,000 and 64,000 cells per well supplemented with 10%FBS/MEME. Eight hours post seeding, the media was removed, and 100µl neutral red (40µg/ml) was added per well and the plates incubated for 2 and a half hours. Cells were then washed with 200µl PBS and 150µl of 1% acetic acid in 50% ethanol solution were added to each well. The absorbance was measured at 540nm using a LabTech (LT-4000) plate reader (Uckfield, UK). The final seeding density was decided to be 20,000 cells per well as this falls in the linear portion of the graph. Overall, it seems that HCT-116 cells took up the dye much better as compared to the other two cell lines.

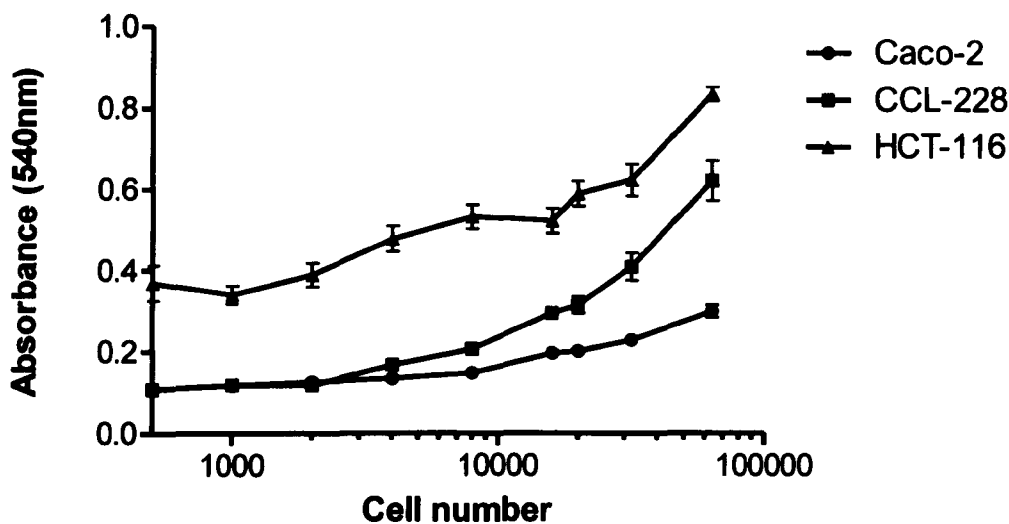


**Figure 2.1** Optimisation of cell seeding density. Different cell numbers were seeded and following 8 hours incubation the absorbance was measured using the neutral red assay. Values represent the means of three independent experiments (6 replicates each)  $\pm$ SEM.

**2.2.3 Optimisation of incubation time for neutral red uptake**

A time uptake assay was incorporated into this study in order to identify the optimum uptake time of the dye giving the highest absorbance. Briefly 20,000 cells were added per well and 48 hours post seeding, 100µl neutral red (40µg/ml) was added per well and incubated for 2, 3, 4 and 5 hours respectively. The dye was subsequently removed and the wells washed with PBS. One percent acetic acid in 50% ethanol solution was added to solubilise the cells and the absorbance measured at 540nm. Since there was no significant difference between the incubation times, 2.5 hours incubation was selected for these experiments. Repetto and colleagues recommended an incubation time varying from 2 hours to no more than 3.5 hours.

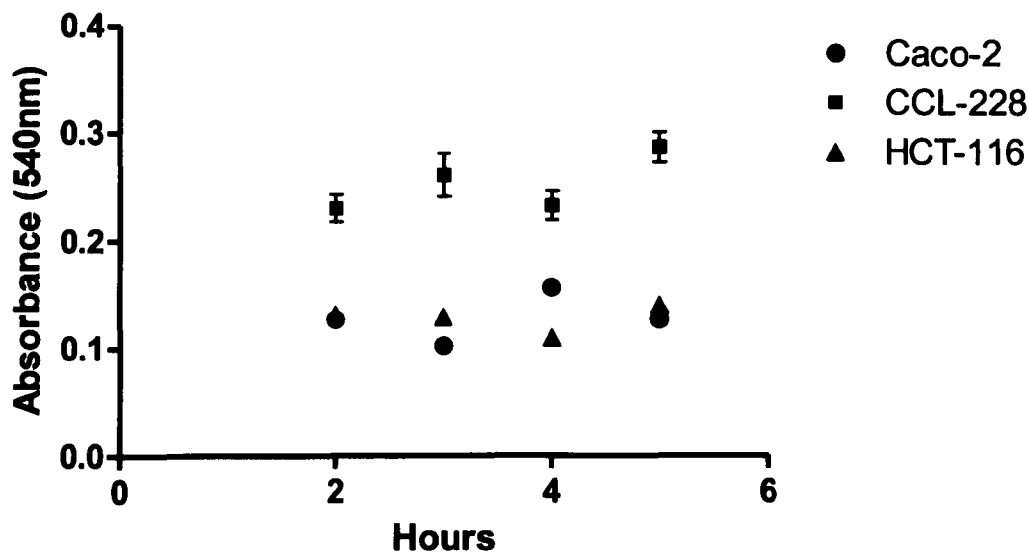


**Figure 2.2** Optimisation of neutral red dye incubation time. Twenty thousand cells were added per well and 48 hours later, cells were incubated with various times of the dye. The absorbance was subsequently measured at 540nm.

#### **2.2.4 MTT assay**

The Thiazolyl Blue Tetrazolium Blue (3-(4,5-Dimethyl-2-thiazolyl)-2,5-diphenyl-2H-tetrazolium bromide) (MTT) assay is a quantitative colorimetric assay used for the measurement of mammalian cell survival and proliferation (Mosmann, 1983). MTT is a yellowish solution which is converted to a purple water-insoluble MTT formazan product by mitochondrial dehydrogenases of living cells. Briefly, cells were seeded as mentioned previously. One hundred microlitres of a 50µg/ml MTT solution (Sigma-Aldrich, Poole, UK) in phenol red free DMEM (GIBCO Fisher Scientific, Loughborough, UK) was added to each well in the dark and incubated for 3 hours. The MTT was removed and the purple crystals were solubilised with 100µl DMSO (Sigma Aldrich, Poole, UK) for 15 minutes in the dark, at room temperature and the intensity was measured colorimetrically at a wavelength of 570 nm using a LabTech (LT-4000) plate reader (East Sussex, UK). Percent growth was calculated as in Section 2.2.3.

#### **2.2.5 Growth of differentiated polarised Caco-2 cells on Transwells**

Caco-2 cells were seeded on Transwell plates (Corning, UK) at  $2 \times 10^5$  cells/well in a final volume of 500µl on the apical side and 3ml of complete media on the basolateral compartment and allowed to grow and differentiate for 21 days. The transepithelial resistance (TEER) was measured using an EVOM meter (epithelial voltohmmeter) and values  $>300 \text{ ohm.cm}^2$  confirmed that the monolayers were suitable for electrophysiological and drug permeability experiments. TEER measurements were employed for determining the permeability of the tight junctions. Caco-2 cells are widely used as a model of the intestinal barrier and culturing them for 21 days leads to the formation of a polarised enterocyte-like monolayer with two distinct compartments,



the apical and basolateral (Leoni et al., 2012). Media was replenished every 2-3 days. The neutral red uptake assay was carried out after the experiments as described previously (Section 2.2) with slight modification. Cells were incubated for 2.5 hours with 300µl of 40µg/ml neutral red dye and subsequently washed with 500µl D-PBS. Three hundred microlitres of 1% acetic acid in 50% ethanol solution was added to each well to solubilise the cells and the contents of the apical compartment transferred to 96-well plates in duplicate. The absorbance was measured at a wavelength of 540nm as mentioned previously.

### **2.2.6 Haemolysis of red blood cells**

A modified protocol was used (Arias *et al.*, 2010). The haemolysis assay has been employed previously (Waheed et al., 2012). A 5ml solution of sheep red blood cells (sheep blood defibrin liquid oxoid) (Fisher Scientific, Loughborough, UK) was taken from the initial 25ml stock for each independent experiment. The solution was centrifuged at 3000rpm for 10 minutes at 4°C and the pellet was re-suspended in 45ml isotonic buffer (120mM NaCl, 10 mM EDTA, 5mM sodium citrate and 5 mM Tris-HCl, pH 7.4) and centrifuged under the same conditions. This step was repeated 6-7 times (using 45ml isotonic buffer) until the supernatant became clear (slightly pink). The final pellet was re-suspended in 5ml of D-PBS and from this 1ml was removed and added to 9ml of PBS to reach an approximate cell number of  $5 \times 10^8$  cells/ml. The desired drug concentrations were prepared in eppendorfs initially in double concentrations to a final volume of 0.5ml which were then diluted two-fold with an equal volume of the red blood cell/D-PBS solution. A vial was also prepared with sheep blood cells in the absence of treatment and a positive control vial with 1% Triton-X100 which would later on serve as 100% haemolysis. The solutions were incubated for 30 minutes on ice after which they were centrifuged at 3000rpm for 10 minutes at 4°C. Two hundred

microlitres of the supernatant was added onto 96-well plates in triplicate and the absorbance/concentration of haemoglobin released was measured at 540nm using a LabTech (LT-4000) plate reader (Uckfield, UK).

### **2.3 Growth of cells on chamber slides for microscopic evaluation**

All cell lines were counted and plated on 8-well culture slides (BD Biosciences, Oxford, UK) (60,000 cells per chamber) at a final volume of 400µl until they reached ~70% confluence. Cells were subsequently treated with the test compounds and incubated for 48 hours. Media was subsequently aspirated, cells washed with 300µl D-PBS and fixed with 3.7% paraformaldehyde (Sigma-Aldrich, Poole, UK) for 10 minutes at room temperature. The PFA was then removed and cells washed thrice with D-PBS. Cells were then permeabilised with 100% cold methanol (Fisher Scientific, Loughborough, UK) for 5 minutes and washed three times with D-PBS. One drop of VECTASHIELD mounting medium with DAPI (Vector Laboratories, Peterborough, UK) was added per chamber and a coverslip was placed on top of the slide and sealed. Cells were then visualised under a fluorescence microscope (Leica DFC 420C) and images acquired using the Leica Application Suite V3.7 software to determine the presence, if any, of nuclear fragmentation.

## **2.4 Growth of cells on chamber slides for immunostaining**

### **2.4.1 Primary antibody (p53) titration for immunofluorescence**

HCT-116 cancer cells were trypsinised and 60,000 cells were added per chamber on a slide at a final volume of 400µl. Cells were then incubated for an according period of time until they reached confluency (usually 3 days). Cells were treated with the relevant concentrations of resveratrol and metabolites for 48 hours in a humidified atmosphere at 37°C with 5% CO<sub>2</sub>. The media plus treatments was subsequently removed and cells washed with 400µl PBS and fixed for 10 minutes at room temperature using 100% ice-cold methanol (Fisher Scientific, Loughborough, UK), washed thrice with D-PBS and solubilised with 0.5% Triton-X100 (Promega UK, Southampton, UK). Cells were washed again three times with D-PBS. Two hundred microlitres of 1% bovine serum albumin (BSA) (Sigma-Aldrich, Poole, UK) in D-PBS was added to the cells and blocked for 30 minutes at room temperature. The solution was then aspirated and cells washed thrice with D-PBS. Two hundred microlitres of primary antibody (p53) (DO-1) (sc-126) [Santa Cruz Biotechnology and bought from Insight Biotechnology Ltd (Middlesex, UK)] in 1% BSA was added in dilutions of (1:50, 1:100 and 1:500) (Figure 2.3). Moreover, 1% BSA alone was added to control chambers where only secondary antibody was to be added (to make sure there was no non-specific binding) and incubated for 1 hour at room temperature. The antibody solutions were subsequently removed and cells were washed three times with D-PBS to ensure no residual antibody was present. Two hundred microlitres of TRITC-conjugated anti-mouse IgG1(1:200, NL007, R&D Systems Abingdon, UK), in 1% BSA was added to cells and incubated for 1 hour at room temperature in the dark after which the cells were washed thrice with D-PBS. The chambers were then removed from the slide and one drop of VECTASHIELD mounting medium with DAPI was added to each compartment. A

coverslip was placed on the slide and sealed. Cell images were acquired using a fluorescent microscope (Leica DFC 420C) using the red and blue filters respectively. Images with DAPI stained and TRITC stained nuclei were overlayed using the Leica Application Suite V3.7 software. From the images in Figure 2.3 below, it is evident that the optimal p53 concentration was 1:100.

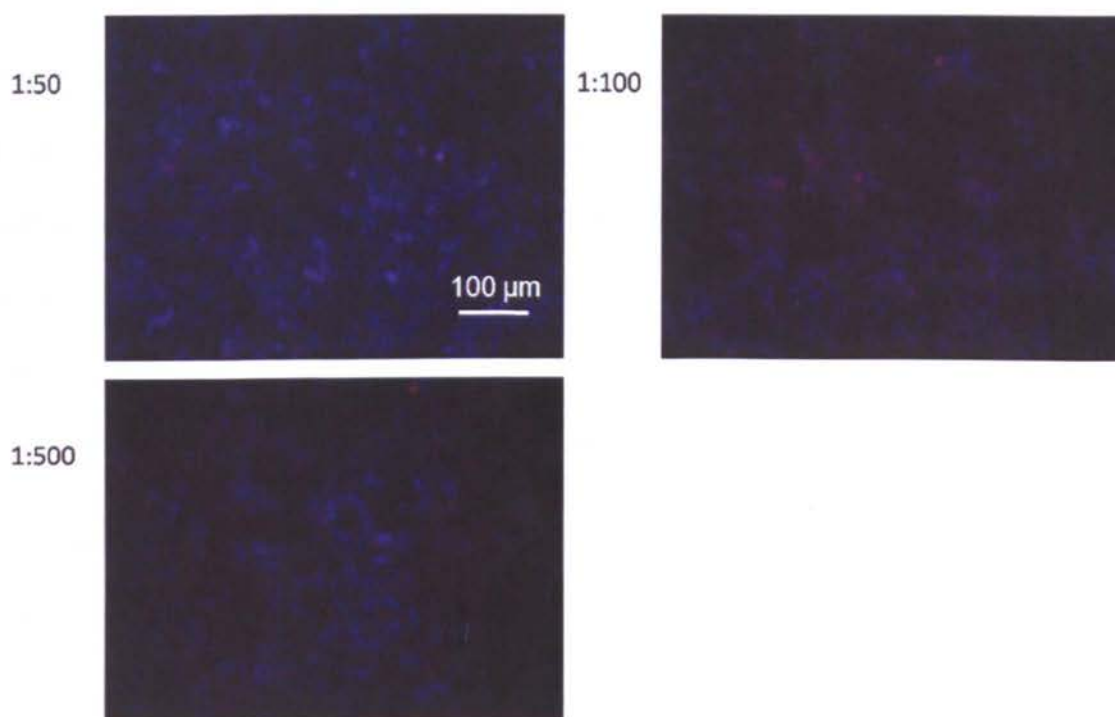


**Figure 2.3** Photomicrographs representing optimisation of the p53 primary antibody. Cells were incubated with 1:50, 1:100 and 1:500 dilutions of the antibody. Blue stain represents DAPI staining and red staining, p53. Magnification x100.

#### **2.4.2 Immunofluorescence staining of HCT-116 cells for p53**

Once the primary antibody (p53) concentration was optimised, experiments were carried out in the same manner as section 2.4.1. From Figure 2.3 it was evident that the 1:100 p53 concentration was the optimum as compared to the other two concentrations. HCT-116 cells were treated with 1 $\mu$ M, 10 $\mu$ M, 30 $\mu$ M and 100 $\mu$ M concentrations of

resveratrol, RV-3-G, RV-4'-G and RV-3-S for 48 hours. Control untreated wells were included containing either primary antibody alone, secondary antibody alone or both. Images were quantified using the ImageJ software and the percentage of p53 stained cells was calculated relative to the total number of DAPI stained cells.

## **2.5 Flow cytometry analysis for cell cycle distribution and apoptosis detection**

A flow cytometer is an instrument that employs an air-cooled argon gas laser which emits a single colour beam at 488nm at 15mV of power. As single cells flow through the light source, this causes light scattering in different directions. Cells stained with a fluorochrome become excited by the laser therefore resulting in a fluorescent emission (Nunez, 2001b). Signals are consequently analysed to collect information about the relative size of the cell (forward light scatter-FSC), the complexity (side light scatter, SSC) as well as diverse cellular structures and antigens exemplified by fluorescence.

Flow cytometry also enables the determination of the relative cellular DNA content and identifies the distribution of cells in the different cell cycle phases (Nunez, 2001a). The cell cycle of proliferating cells consists of 4 distinct phases, G1, S (DNA synthesis), G2 and M (mitosis). The G2 and M phases however have the same DNA content and on that basis cannot be distinguished based on this (Nunez, 2001a).

Propidium iodide (PI) is a fluorogenic nucleic acid dye that stains DNA and can either be measured in the orange or red channel (FL2 or FL3). To avoid any false analysis and hence interpretation, RNAases should be incorporated into the PI solution since PI binds to RNA.

### **2.5.1 Cell cycle distribution using single agents**

Caco-2, CCL-228 and HCT-116 cells were seeded at a density of  $1 \times 10^6$  cells at a final volume of 10ml per T25 flask. The cell number to volume ratio was directly proportional to the cell number to volume ratio for the growth inhibition studies (20,000 cells per 200 $\mu$ l). Cells were directly treated with compounds, vehicle control or medium alone. Forty-eight hours post seeding and treatment (at the point where control cells reached confluency), cells were trypsinised by the addition of 1ml 0.25% trypsin in EDTA (Sigma-Aldrich, Poole, UK). After the cells detached from the flask, 6ml of media were added to deactivate the trypsin and centrifuged at 1500rpm for 4 minutes. Since apoptosis was measured, the supernatant was removed and transferred to a new centrifuge tube to collect any dead cells by centrifuging at 3000rpm for 5 minutes. The pellets were re-suspended in 2ml of D-PBS, and cells washed three times with cold D-PBS by centrifuging at 12000rpm for 5 minutes. The final pellet was re-suspended in 200 $\mu$ l D-PBS and 1ml of cold 70% ethanol (Fisher Scientific) in D-PBS solution was added gradually by vortex. The samples were incubated overnight at -20°C. Cells were then harvested by centrifugation at 3000rpm for 5 minutes and washed once with D-PBS. One hundred microlitres of the cell suspension were added to 100 $\mu$ l of trypan blue (Sigma-Aldrich, Poole, UK) and cells counted. One million cells were included per tube and incubated with 500 $\mu$ l of ribonuclease A/PI (propidium iodide) solution (BD Pharmingen, Oxford, UK) for 30 minutes at room temperature in the dark. Ten thousand events per sample were counted and analysed using the FL3 filter and according FSC/SCC dot plots, cell count/fluorescence intensity histograms and FL3A/FL3W dot plots for exclusion of cell aggregates on a FACS Calibre instrument (Beckton Dickinson, UK). Data was analysed using the CellQuest™ Pro software.

## **2.6 Western Blotting (Method 1)**

Western blotting is a technique where proteins are identified with specific antibodies after being separated from one another according to their molecular weight. Separation is achieved by gel electrophoresis after which the gel is placed next to a membrane (usually nitrocellulose or polyvinylidene fluoride (PVDF) and an electrical current is applied in order to transfer the proteins from the gel onto the membrane where they will remain adhered. The membrane is subsequently stained with an antibody (raised against the protein of interest) and visualised using a chemiluminescent substrate.

### **2.6.1 Preparation of cell lysates**

HCT-116 cells (wild-type p53) were seeded (60,000 cells per well) on 6-well plates (BD Falcon) and allowed to attach and multiply for 24 hours. After treatment with the test compounds at the according concentrations, cells were washed twice with ice-cold D-PBS and lysed in a buffer containing 150mM NaCl, 10mM Tris-HCl pH7.6, 0.1% Triton x-100, 5mM EDTA pH8 and 1% protease inhibitor cocktail (Sigma-Aldrich, Poole, UK). The lysate was then freeze thawed five times (10 minutes in -80°C freezer and 5 minutes at 37°C) and centrifuged at 14,000rpm for 10 minutes at 4°C. The supernatant was transferred to a new eppendorf and stored at -20°C until protein quantification, whilst the pellet was discarded.

### **2.6.2 Protein Quantification of lysates**

One microlitre of sample (supernatant) was added in triplicate on 96-well plates. In separate wells, 5µl of bovine serum albumin (BSA- Sigma-Aldrich, Poole, UK) standards in D-PBS were added in triplicate at increasing concentrations (0.2µg/µl, 0.4µg/µl, 0.6µg/µl, 0.82µg/µl, 1µg/µl and 1.2µg/µl; therefore, 1µg/5µl, 2µg/5µl,

3µg/5µl, 4µg/5µl, 5µg/5µl and 6µg/5µl). Two hundred and fifty microlitres of Bradford reagent (Sigma-Aldrich, Poole, UK) was then added per well and placed on a shaker for approximately 30 seconds after which the plate was left standing for 20 minutes. The absorbance was then measured at 620nm. The absorbencies of the standards were used to calculate a standard curve and the protein concentrations of the samples thus calculated. Samples were then reduced using a 5x loading buffer (5µl to a final volume of 25µl) and heated at 95°C for 5 minutes.



**Table 2.1** Recipes for making the solutions for the western blot process.

<b><u>Product</u></b>	<b><u>Constituents</u></b>	<b><u>Final Volume (ml)</u></b>	<b><u>Final Concentration</u></b>
12.5% resolving gel	40% acrylamide 2% bis-acrylamide 1M Tris-HCl pH8.8 10% SDS Milli H <sub>2</sub> O Total:	7.8ml 4.1ml 9.4ml 0.25ml 3.5ml 25ml	} 12.5% 0.375M 0.1%
6% stacking gel	40% acrylamide 2% bis-acrylamide 1M Tris-HCl pH8.8 10% SDS Milli H <sub>2</sub> O Total:	3.7ml 2.0ml 3.1ml 0.25ml 16ml 25ml	} 6% 0.1%
10x Running Buffer	25g SDS 75.7g Tris 360g Glycerin Adjust pH 8.3 with HCl and make up to 2.5L with distilled water	n/a	
10x TBS-Tween	60.5g Tris 200g NaCl 20ml Tween Make up to 2.5L with distilled water	n/a	
10x Transfer buffer	17.5g Tris 225g Glycine Make up to 2.5L with distilled water	n/a	
5x Loading buffer	2% SDS (w/v) 2-mercaptoethanol 10% Glycerol 0.01% (w/v) Bromophenol Blue 62.5mM Tris-HCl	n/a	
Stripping buffer (Abcam recipe)	15g glycerol 1g SDS 10ml Tween 20 Adjust pH to 2.2 Bring volume to 1 litre with ultrapure water	n/a	

N.B To 20ml of the 12.5% Resolving Gel, 320µl of 10% ammonium persulphate (APS, Sigma-Aldrich, Poole, UK) was added plus 32µl of TEMED (N,N,N',N'-tetramethylethylenediamine, for electrophoresis) (Sigma-Aldrich, Poole, UK). To 10ml of the stacking gel 240µl of 10% APS was added plus 40µl of TEMED.

### **2.6.3 Gel preparation**

The 12.5% resolving gel solution was prepared (see Table 2.1 for ingredients) and 8ml was immediately transferred to the gel formation compartment (1.5mm plates). A few drops of isopropanol were added to remove any bubbles formed. The gel was left to stand for 40 minutes at room temperature in order to polymerise. The 6% stacking gel solution was prepared as mentioned in Table 2.1 and after the isopropanol was removed, 5ml of stacking gel was added followed by the combs and left for 40 minutes to allow for polymerisation. Following polymerisation, the comb was carefully removed and the wells washed with running buffer using a syringe-needle.

### **2.6.4 SDS-PAGE, Immunoblot and developing**

Equal amounts of protein samples (20µg) were separated by sodium dodecyl sulphate-polyacrylamide gel electrophoresis (SDS-PAGE) (150V, 300mA for 90 minutes) using a 12.5% resolving gel and 6% stacking gel. A final volume of 25µl was added per well for the samples and 15µl of the pre-stained protein marker (Broad range 7-175kDa, New England BioLabs, Hitchin, UK). Proteins were subsequently electro-blotted onto Hybond polyvinylidenedifluoride membranes (Amersham, Buckinghamshire, UK) at 4°C (300V, 300mA for 90 minutes). The membranes were then blocked overnight at 4°C in blocking solution (5% (w/v) non-fat dry milk in TBS/Tween). The membranes were washed 3 times (15 minutes each time) with TBS/Tween and incubated with the primary antibody (dilution 1:1000 for p53 and actin) by gently agitating overnight at 4°C. Following that, the membranes were washed with TBS/Tween and incubated with the secondary antibody (HRP-conjugated goat anti-mouse IgG (dilution 1:1000 for p53 and beta-actin) (Dako, Ely, UK) in TBS/Tween and blocking solution) for 1.5 hours at room temperature. The membranes were washed three times (15 minutes each time)

with TBS/Tween and chemiluminescence was detected using the Amersham ECL Western Blotting detection kit (GE Healthcare, Buckinghamshire, UK) by adding 2ml of solution A and 50µl of solution B for 5 minutes and exposing the membranes to Amersham hyperfilm (GE Healthcare, Buckinghamshire, UK) in a cassette. Membranes were subsequently stripped using stripping buffer (see Table 2.1 for constituents) for one hour at room temperature gently shaking and blocked overnight using 10% marvel at 4°C. Following blocking, membranes were washed thrice with TBS/Tween (15 minutes each time) and re-probed for the next antibody of interest as described above. The density of protein bands in blots were analysed relative to beta-actin using ImageJ.

## **2.7 Western blotting (Method 2)**

A different method was carried out here as compared to Method 1. The reason being that Method 1 was optimised in Surrey but moving back to Kingston later on, another protocol was followed. It is important to note however that experiments using Method 1 (expression levels of p53) were completed in Surrey. For all other experiments (described in Chapters 4 and 5), Method 2 was used.

### **2.7.1 Cell lysate preparation**

Caco-2, CCL-228 and HCT-116 cells were seeded at a density of 60,000 cells per well and grown until they reached 70% confluence after which they were treated with the according concentrations in addition to vehicle control, medium alone and positive control for 48 hours. Cells were subsequently washed with D-PBS and lysed for 10 minutes on ice using NuPAGE LDS sample buffer 4x (Invitrogen, Fisher Scientific, Loughborough, UK) diluted in distilled water in the presence of 1% protease inhibitor (Sigma-Aldrich, Poole, UK). The contents were transferred into eppendorfs and heated at 72°C for 10 minutes and then stored at -20°C prior to protein quantification.

### 2.7.2 Protein quantification

For protein quantification a Bio-Rad DC Protein Assay (Bio-Rad Laboratories, Hertfordshire, UK) was used. This is a colorimetric assay for protein concentration detection following solubilisation by a detergent. The reaction is a modified Lowry assay, with shorter maximum colour development and longer colour stability after the addition of reagents. The assay is dependent on the reaction of protein with an alkaline copper tartrate solution and Folin reagent (Lowry *et al.*, 1951, Peterson, 1979). Similar to the Lowry assay, the development of colour involves two steps; firstly, the reaction between copper and protein in an alkaline solution and secondly, the consequent reduction of the Folin reagent by the copper-treated protein from the first step. The presence of proteins cause the Folin reagent to undergo reduction by losing up to 3 oxygen atoms thus producing a species with a characteristic blue colour with a maximum absorbance at 750nm.

For the preparation of the working reagent, 20µl of reagent S was added to each ml of reagent A (alkaline copper tartrate solution) making solution A' (Bio-Rad Laboratories, Hertfordshire, UK). Six dilutions of the protein standard bovine serum albumin (BSA) were prepared in distilled water (0mg/ml, 0.25mg/ml, 0.50mg/ml, 0.70mg/ml, 1.0mg/ml and 1.4mg/ml protein) and placed on ice. Five microlitres of sample lysates were added to an equal volume of distilled water (this was the sample working solution for protein quantification) and placed on ice. Five microlitres of standards and samples were added in duplicate on a 96-well plate. Twenty-five microlitres of solution A' were added to each well followed by 200µl of reagent B (dilute Folin reagent). The plate was then slowly shaken in order to mix the reagents taking care that no bubbles formed. After 15 minutes the absorbance was measured at 750nm. The standard curve of the BSA

standards was created each time and the protein concentration of the samples calculated based on it. Calculations were made in order to load 30µg of protein per well.

### **2.7.3 Polyacrylamide Gel Electrophoresis**

To every 90µl of sample lysate, 10µl of reducing agent (NuPAGE sample reducing agent 10x Invitrogen, Fisher Scientific, Loughborough, UK) was added. Thirty micrograms of protein were loaded in each well and 15µl of pre-stained protein marker after the wells were washed with running buffer. Proteins were separated according to size by gel electrophoresis run at a constant voltage of 195V for 1 hour using a 4-12% tris-gel(Invitrogen).The running buffer was made up using 50ml running buffer (20x), and 950ml ultrapure water. From this, 200ml were taken for the inner compartment to which 500µl of antioxidant was added.

### **2.7.4 Immunoblot (Transfer process)**

The gel was electroblotted onto a PVDF membrane (pre-wet with methanol for five minutes and rinsed in transfer buffer) and run at 30V (500mA) for 2 hours and 45 minutes. The transfer buffer was made up using 50ml transfer buffer (20x), 850ml ultrapure water, 100ml methanol and 1ml antioxidant as per the manufacturer's instructions. Post-transfer, the membrane was blocked overnight at room temperature gently shaking in blocking solution (5ml ultra filtered water, 2ml blocker/diluent A and 3ml blocker/diluent B, Invitrogen). The blocking solution was then decanted and the membrane washed twice with 20ml of water for 5 minutes each time. The membrane was subsequently incubated with the antibody of interest at a final volume of 10ml of primary antibody solution (7ml ultra filtered water, 2ml blocker/diluent A and 1ml blocker/diluent B) for 1.5 hours at room temperature or overnight at 4°C at the according antibody concentrations (see Table 2.2) and then decanted. The membrane

was again washed 3 times for 5 minutes each time with 20ml of antibody wash solution [150ml ultra filtered water and 10ml antibody wash solution (16x)], followed by a 30 minute incubation at room temperature with 10ml secondary antibody solution gently shaking. The membrane was again rinsed 3 times with 20ml of antibody wash for 5 minutes followed by two 20ml washes with distilled water for 2 minutes per wash. Without allowing the membrane to dry out completely, approximately 2.5ml of Chemiluminescent substrate was added to the membrane and the reaction allowed to develop for 5 minutes after which images were captured for an analogous time depending on the antibody being probed for using the GeneGnome bio-imaging system (Syngene, Cambridge, UK). For re-probing with other antibodies, the membranes were stripped for 1 hour at room temperature gently shaking. The membranes were then washed twice with 20ml distilled water followed by three washings with 20ml wash solution (5 minutes each time). Probing for antibodies was repeated as mentioned previously. Blots were analysed relative to beta-actin using ImageJ (NIH free software). ImageJ analysis is a quantitative analysis of the band intensities. Values were normalised relative to the loading control beta-actin and comparisons made with untreated cells.

All reagents for western blotting (method 2) were from Invitrogen, purchased from Fisher Scientific (Loughborough, UK) and listed below: NuPAGE LDS Sample Buffer (4x) Invitrogen (VXNP0007), NuPAGE sample reducing agent (10x) Invitrogen (VXNP0004), Novex sharp pre-stained protein standard Invitrogen (VXLC5800), Bis-tris gel NuPAGE Novex 15 well for SDS-PAGE 4 to 12% (VXNP0336), NuPAGE antioxidant Invitrogen (VXNP0005), Transfer buffer (20x) Invitrogen (VXNP0006), MOPS SDS Running Buffer (VXNP0001), Western Breeze chemiluminescent kit anti-

mouse (VXWB7104), and filter paper sandwich PVDF membrane (VXLC2005).  
Protease Inhibitor cocktail (P8340) was from Sigma-Aldrich (Poole, UK).

**Table 2.2** List of antibodies used for western blotting. Concentrations, incubation periods and product codes for each antibody are also stated.

<u>Antibody</u>	<u>Dilution</u>	<u>Source</u>	<u>Incubation Period</u>	<u>Product Code</u>	<u>Supplier</u>
p53 (DO-1)	1:1000	Mouse monoclonal	Overnight at 4°C	Sc-126	Santa Cruz Biotechnology
AMPK-α (23A3)	1:1000	Rabbit monoclonal	Overnight at 4°C	#2603	Cell Signaling
p-AMPK-α (Thr172)	1:1000	Rabbit monoclonal	Overnight at 4°C	#2535	Cell Signaling
Adenosine A3 receptor	1:500	Rabbit polyclonal	1.5 hours at room temperature	A3R32-A	Alpha Diagnostic International
Cyclin D1[DCS-6]	1:500	Mouse monoclonal	1.5 hours at room temperature	ab10540	Abcam
Beta-actin(8H10D10)	1:2000	Mouse monoclonal	1.5 hours at room temperature	#3700	Cell Signaling
secondary antibody solution alkaline phosphatase conjugated	10ml	anti-rabbit	30 minutes at room temperature	VXWP20 007	Invitrogen
secondary antibody solution alkaline phosphatase conjugated	10ml	Anti-mouse	30 minutes at room temperature		Invitrogen



## 2.8 Statistical analysis

For the growth studies, all values represent the means of 3 independent experiments  $\pm$ SEM (3-6 replicates per experiment). Group comparisons were conducted using ANOVA and Tukey's post test where,  $p < 0.05$  was the criterion for statistical analysis.  $IC_{50}$  values were calculated using non-linear regression graph where values were constrained to 0%- 100%. For ImageJ analysis, results were analysed by repeated measures ANOVA and Dunnett's test whilst statistical differences for cell cycle distribution experiments were assessed by  $\chi^2$  test of the number of cells in one phase compared to the remaining phases. For all analyses, the GraphPad Prism statistical software was used (GraphPad Prism 5.0.4 Software, Inc. USA).

### **Chapter 3. Investigation of the basic effect on growth of resveratrol and its metabolites**

During the past decade there has been a burst of interest in the potential health benefits associated with dietary consumption of naturally occurring polyphenols (Athar *et al.*, 2007). More specifically, in 1997, Jang and colleagues published a paper describing the ability of resveratrol to inhibit various cellular events associated with the three main stages of carcinogenesis (initiation, promotion and progression) (Jang, 1997, King *et al.*, 2006). The main reason for this interest is speculated to have commenced following the identification of anti-oxidant properties, their abundance in our diet, and their probable role in the prevention of various diseases such as cancer and cardiovascular diseases (Rimando and Suh, 2008, Manach *et al.*, 2004, Wenzel and Somoza, 2005).

A study conducted by Jang and colleagues (1997) has reported reduced numbers of skin tumours by up to 98% after topical resveratrol administration on mice. There are exceptions however, despite the fact that most *in vivo* studies have demonstrated a chemopreventive effect. More specifically, it has been shown that a resveratrol dose of 1-5mg per kg (body weight) daily did not succeed in affecting the growth or metastasis of breast cancer in mice, regardless of the *in vitro* evidence (Baur and Sinclair, 2006). There are currently several Phase I clinical trials for the oral administration of resveratrol in humans with doses reaching 7.5g per day ([clinicaltrials.gov](http://clinicaltrials.gov)).

Yu and colleagues (2002) showed that *trans*-resveratrol-3-*O*-D-glucuronide is the primary metabolite of resveratrol in human liver and that *trans*-resveratrol-3-*O*-D-glucuronide and *trans*-resveratrol-3-*O*-D-sulphate are both significant metabolites in rat urine and mouse serum (Yu *et al.*, 2002). A Phase I clinical trial, however, identified resveratrol-4'-*O*-D-glucuronide and resveratrol-3-*O*-D-glucuronide as the main metabolites following oral administration (Wang *et al.*, 2004a). On the contrary, other

studies identified the presence of resveratrol-3-*O*-D-sulphate, resveratrol-4'-*O*-D-sulphate, resveratrol-3-*O*-4'-*O*-D-disulphate, resveratrol-4'-*O*-D-glucuronide and resveratrol-3-*O*-D-glucuronide where the main conjugates were the sulphates both in the plasma and urine (Maier-Salamon *et al.*, 2006, Miksits *et al.*, 2005).

Currently, only a few studies have investigated the effect of the sulphated metabolites against breast cancer cells (Miksits *et al.*, 2009, Hoshino *et al.*, 2010, Kenealey *et al.*, 2011). Miksits and colleagues specifically investigated the effect of the three major sulphated metabolites and demonstrated that unlike resveratrol, the metabolites showed low cytotoxicity in malignant and non-malignant breast cancer cells (IC<sub>50</sub> 202-228µM). This however may not be representative of the effects *in vivo*, mainly due to the presence of sulphatases which could probably de-conjugate the metabolites back into resveratrol (Miksits *et al.*, 2009). Hoshino *et al.* (2010) also evaluated the biological effect of sulphate-conjugated resveratrol metabolites in MCF-7 cells but found low antiproliferative activity. It is noteworthy to point however, that resveratrol-3-*O*-D-sulphate and resveratrol-4'-*O*-D-sulphate inhibited nitric oxide production by NO scavenging and down-regulation of iNOS expression in RAW264.7 cells. In addition to this, the same metabolites collectively revealed an induction of QR1, DPHH free radical scavenging, COX-1 and COX-2 inhibition and inhibition of NF-κB (Hoshino *et al.*, 2010).

Consistent findings to those of Miksits *et al.* (2009) were reported by Kenealey *et al.* (2011) where resveratrol metabolites did not induce early pro-apoptotic mechanisms in neuroblastoma cells using the Cell Titer Blue reagent (Kenealey *et al.*, 2011). A recent study by Storniolo & Moreno (2012) studied the effects of the three major metabolites namely, resveratrol-3-*O*-D-glucuronide, resveratrol-4'-*O*-D-glucuronide and resveratrol-3-*O*-D-sulphate at concentrations between 10µM-50µM on Caco-2 cells and

found an antioxidant activity similar to the parent compound (using an Antioxidant Assay Kit from Cayman Chemicals), such as growth inhibition and a G0/G1 arrest (Storniolo and Moreno, 2012).

### **Aims and objectives**

The aims of this first chapter were to compare the effects of resveratrol with its metabolites piceatannol and the conjugated metabolites, resveratrol-3-*O*-D-glucuronide, resveratrol-4'-*O*-D-glucuronide, resveratrol-3-*O*-D-sulphate and a resveratrol analogue, pterostilbene, on the growth of three colorectal cell lines, Caco-2, CCL-228 and HCT-116.

The neutral red assay was employed and cells were treated for 48 hours with various concentrations of the drugs (1µM, 3µM, 10µM, 30µM and 100µM) as described in Section 2.2.1. Results were further confirmed with a second viability assay, the MTT assay which used the same concentrations and exposure time.

In addition to the effects of these drugs on colorectal cancer cells, it was vital to identify the effects on a polarised Caco-2 cell monolayer (fully differentiated cells grown for 21 days) using two concentrations (1µM and 30µM) for a period of 11 days as well as the effect on normal cells. The reason being that the epithelium is polarised with two sides (luminal and mucosal), each with different receptors, ion channels and properties. This experiment therefore aimed to mimic the intestinal epithelium. The 11-day treatment experiment was designed to compare the results with those by a study by Schneider *et al.* (2003). In order to investigate the reversibility potential of these agents, cells were incubated at 30µM of drugs for 48 hours and allowed to recover for a further 48 hours in fresh media in the absence of drugs after which cell numbers were determined. The

neutral red uptake assay was employed for the latter two experiments (for method see section 2.2.1).

Any inhibitory effect on cell growth may be due to damage therefore sheep red blood cells were used to check for necrosis. In this instance, higher concentrations than those used previously were also selected (1 $\mu$ M, 10 $\mu$ M, 100 $\mu$ M, 200 $\mu$ M and 500 $\mu$ M) to ensure that the compounds of interest had no cytotoxic effect on normal cells.

### **3.1 Effect of resveratrol, piceatannol and pterostilbene on the growth of colorectal cell lines as single agents**

The effect of resveratrol, piceatannol, pterostilbene and the positive control, actinomycin D (10 $\mu$ g/ml) as well as 0.1% DMSO on the growth of three colorectal cell lines was investigated using the neutral red (NR) colorimetric assay. The HCT-116 cells expressing a wild-type p53 were used, as well as CCL-228 (SW480) and Caco-2 cells which have a mutated p53.

Cells were treated with increasing concentrations of the test compounds (1 $\mu$ M, 3 $\mu$ M, 10 $\mu$ M, 30 $\mu$ M and 100 $\mu$ M) for 48 hours and cell viability was measured using the neutral red uptake assay. Statistical analysis was performed by ANOVA and Tukey's test and  $p < 0.05$  were considered significant relative to the untreated group. It is apparent that following treatment with the three compounds, cell growth was inhibited with increasing concentrations.

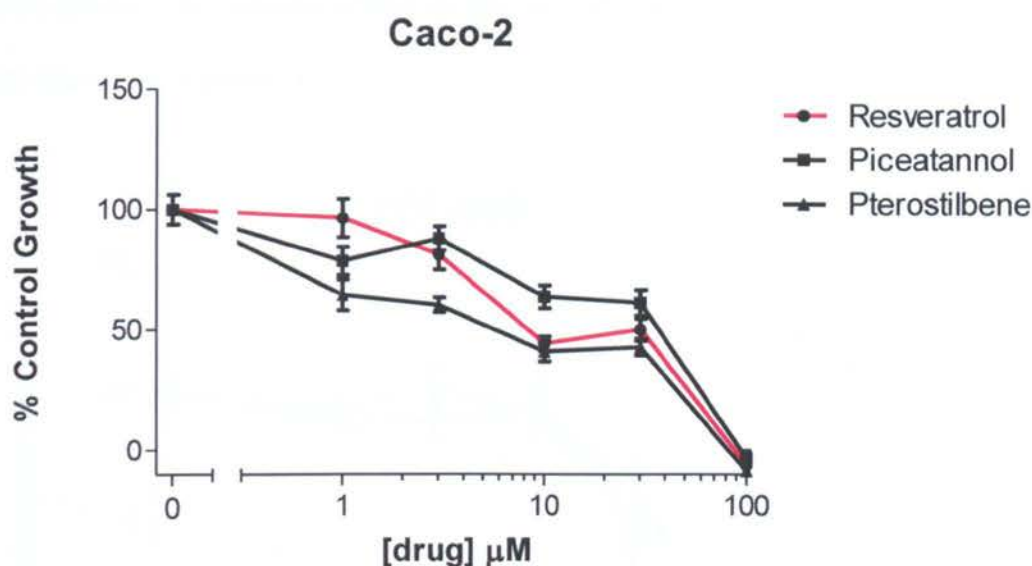


**Figure 3.1** The effect of resveratrol, piceatannol, and pterostilbene on the growth of Caco-2 cells after 48 hours using the neutral red assay. Growth following actinomycin D (10 μg/ml) and vehicle control (0.1% DMSO) treatments reached  $49.1 \pm 4.7\%$  and  $92.4 \pm 7.7\%$  respectively. Points represent mean of  $n=18$  from 3 independent experiments  $\pm$  SEM.  $p \leq 0.05$  for pterostilbene at all five concentrations;  $p \leq 0.05$  at 1 μM, 10 μM, 30 μM and 100 μM piceatannol treatments; and  $p \leq 0.05$  at 10 μM, 30 μM and 100 μM resveratrol treatments.

Overall, the effect of the test compounds on the growth of Caco-2 was very similar. More specifically, at 100 μM RV, PI and PS treatments, the absorbance of cells reached 0.06, 0.06 and 0.02 (data not shown) with complete inhibition suggesting a cytotoxic effect and not cytostatic at this concentration, since the absorbance is near zero and less than that of starting cells (see optimisation in Chapter 2) (Figure 3.1). Administration of 0.1% DMSO had no effect on the growth of cells with growth exceeding  $92.38 \pm 7.65\%$  (SEM) (Figure 3.1). The positive control actinomycin D exerted a significant effect with an inhibition of 51% at 10 μg/ml ( $p \leq 0.05$  relative to untreated). Overall, pterostilbene was the most effective with the lowest percent growth at all the concentrations tested reaching complete inhibition at 100 μM. Cell growth was decreased with increasing drug concentrations. Pterostilbene and resveratrol had lower  $IC_{50}$  values of 5 μM and 12.6 μM respectively and 21.7 μM for piceatannol with the greatest statistical significance seen in

pterostilbene with concentrations as low as 1μM (p<0.05 using ANOVA and Tukey's test relative to untreated).

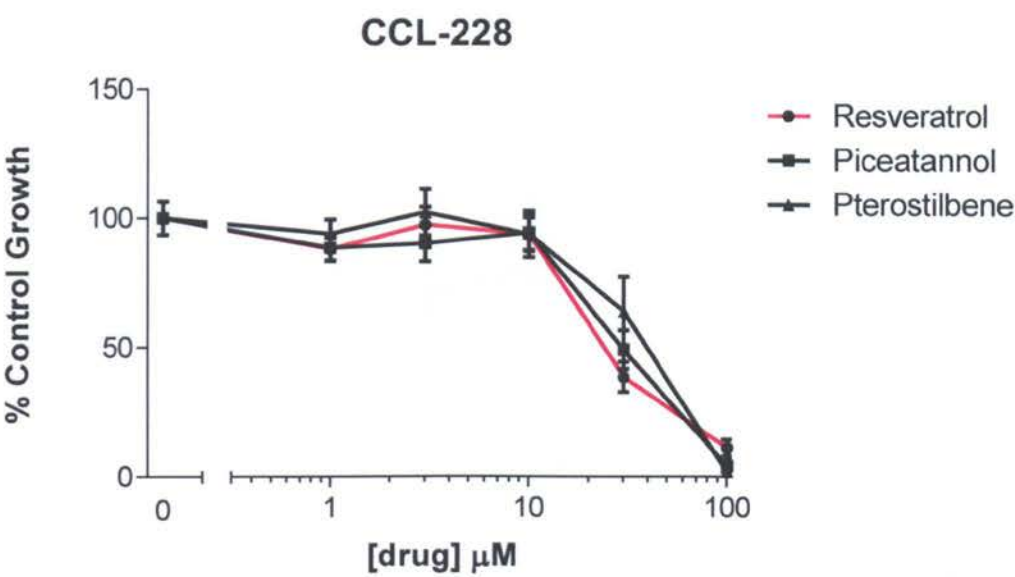


**Figure 3.2**The effect of resveratrol, piceatannol, and pterostilbeneon the growth of CCL-228 cells after 48 hours using the neutral red assay. Growth following actinomycin D (10μg/ml) and vehicle control (0.1% DMSO) treatments reached 41.1±3.2% and 105.8±8% respectively Points represent mean of n=18 from 3 independent experiments ±SEM.p≤0.05 at 30μM and 100μM concentrations for all three treatments.

In the case of the CCL-228 colorectal cell line, a profound effect was evident at 30μM and 100μM for all three treatments (Figure 3.2). Growth was significantly reduced at 30μM treatments with percent growth reaching 38.7±5.8%, 49.2±7.5% and 64.1±13.2% for resveratrol, piceatannol and pterostilbene respectively. A noteworthy point to make is that at 100μM there was almost complete inhibition with piceatannol and pterostilbene but less so for the parent compound, resveratrol (83%±6.2%). Again, there was no significant difference between 0.1% DMSO (vehicle) and control untreated and a significant difference after treatment with 10μg/ml actinomycin D relative to the control (p<0.05). Overall however, the IC<sub>50</sub> values for CCL-228 cells seemed to be



greater after treatment with the three compounds (resveratrol 42.1  $\mu$ M, piceatannol 29  $\mu$ M and pterostilbene 34.5  $\mu$ M) (Table 3.1).

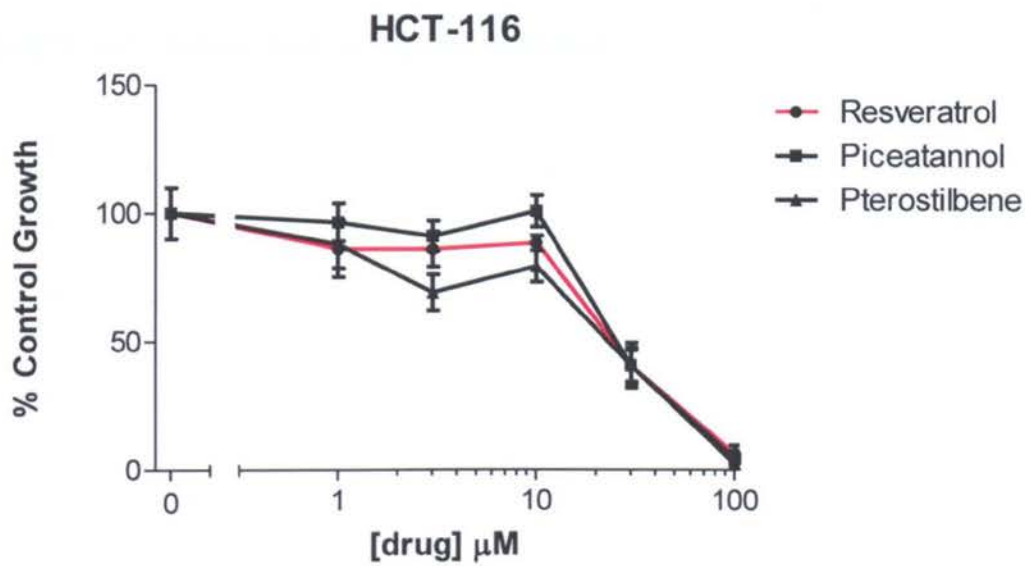


**Figure 3.3**The effect of resveratrol, piceatannol, and pterostilbene on the growth of HCT-116 cells after 48 hours using the neutral red assay. Growth following actinomycin D (10  $\mu$ g/ml) and vehicle control (0.1% DMSO) treatments reached 18.2 $\pm$ 1.9% and 93.7 $\pm$ 7.4% respectively. Points represent mean of n=18 from 3 independent experiments  $\pm$ SEM.  $p\leq0.05$  following treatments with 3  $\mu$ M, 30  $\mu$ M and 100  $\mu$ M pterostilbene;  $p\leq0.05$  with 30  $\mu$ M and 100  $\mu$ M piceatannol treatment; and,  $p\leq0.05$  with 30  $\mu$ M and 100  $\mu$ M resveratrol treatment.

The effect of resveratrol, piceatannol and pterostilbene on the growth of HCT-116 cancer cells was also investigated. Overall, it can be noted that HCT-116 cells were similarly sensitive to all three treatments with a steep decrease in growth at concentrations greater than 10  $\mu$ M (Figure 3.3). At 100  $\mu$ M, >94% inhibition was achieved for all three compounds with IC<sub>50</sub> values of 22.8  $\mu$ M, 28.0  $\mu$ M and 18.3  $\mu$ M for resveratrol, piceatannol and pterostilbene respectively (Table 3.1). DMSO did not exert any inhibitory effect on HCT-116 cells whilst actinomycin D inhibited cells by ~82% as opposed to Caco-2 (45%) with 48 hours incubation ( $p<0.05$ ).

Overall, it is evident that the effects seen in Caco-2 cells were more gradual (linear) as compared to the CCL-228 and HCT-116 cells where a steep decrease in growth was apparent from 10 $\mu$ M to 100 $\mu$ M. These findings suggest that 100 $\mu$ M concentrations are toxic to cells making them not capable to recover.

## 3.2 Effect of resveratrol-3-O-D-glucuronide, resveratrol-4'-O-D-glucuronide and resveratrol-3-O-D-sulphate on the growth of colon cancer cells as single agents

### 3.2.1 Using the NRU assay

The effect of the three main metabolites against the three colorectal cell lines (Caco-2, CCL-228 and HCT-116) was determined using the neutral red uptake assay.

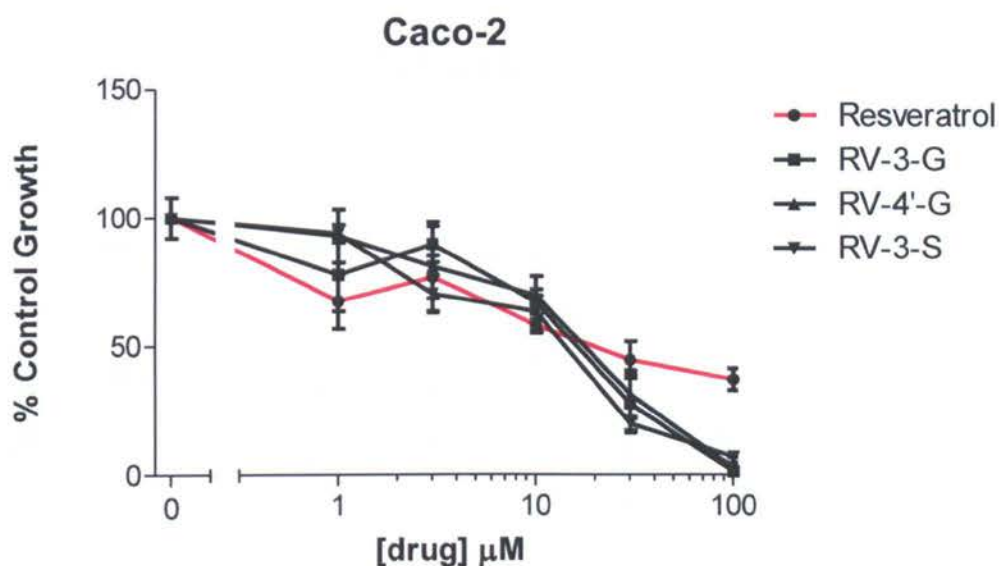


**Figure 3.4** The effect of resveratrol, resveratrol-3-O-D-glucuronide, resveratrol-4'-O-D-glucuronide and resveratrol-3-O-D-sulphate on the growth of Caco-2 cells after 48 hours using the neutral red assay. Growth following actinomycin D ( $10\mu\text{g/ml}$ ) and vehicle control (0.1% DMSO) treatments reached  $40\pm2.5\%$  and  $87.7\pm14.5\%$  respectively. Points represent mean of  $n=18$  from 3 independent experiments  $\pm$ SEM.  $p\leq0.05$  following treatment with resveratrol at all concentrations;  $p\leq0.05$  following treatment with  $10\mu\text{M}$ ,  $30\mu\text{M}$  and  $100\mu\text{M}$  RV-3-G and RV-4'-G' and,  $p\leq0.05$  at  $3\mu\text{M}$ ,  $10\mu\text{M}$ ,  $30\mu\text{M}$  and  $100\mu\text{M}$  RV-3-S.

Depicted in Figure 3.4 above is the effect on Caco-2. A very similar response to treatment with RV-3-S and RV-4'-G is evident with almost complete inhibition in growth at  $100\mu\text{M}$  relative to the control ( $p<0.05$  relative to the control). Interestingly in Figure 3.4 is that at  $100\mu\text{M}$  resveratrol treatment, growth is reduced by

63%±4.3% relative to control untreated and the metabolites are more active. Also, a significant difference is seen at 1µM treatment with resveratrol (p<0.05) and RV-3-G which is not evident with RV-4'-G and RV-3-S. All three metabolites had lower IC<sub>50</sub> values as compared to the parent compound (Table 3.1). In the case of the vehicle control, there is no effect on cell growth and as for actinomycin D (10µg/ml) there is apparent inhibition of ~60% (p<0.05).

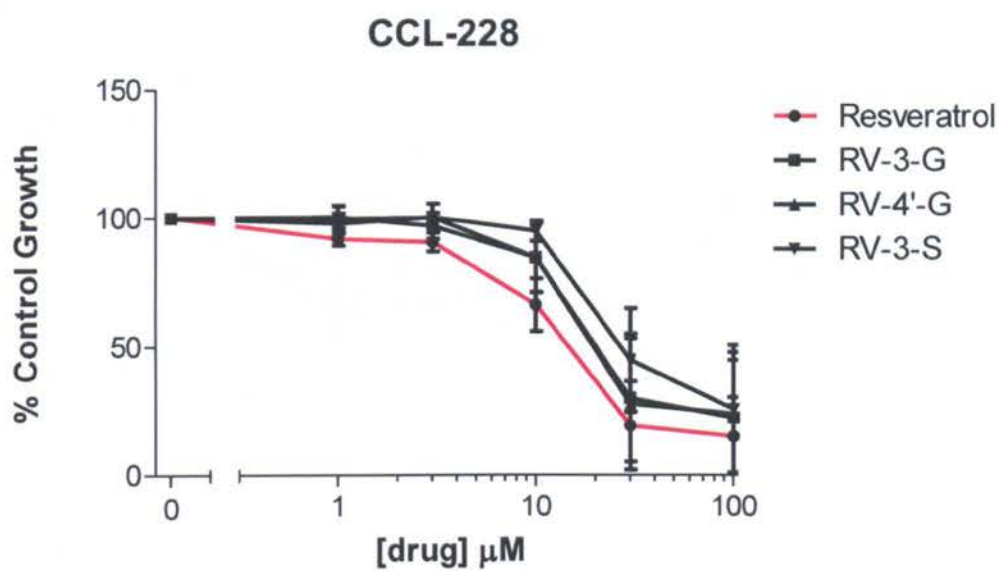


**Figure 3.5**The effect of resveratrol, resveratrol-3-O-D-glucuronide, resveratrol-4'-O-D-glucuronide and resveratrol-3-O-D-sulphate on the growth of CCL-228 cells after 48 hours using the neutral red assay. Growth following actinomycin D (10µg/ml) and vehicle control (0.1% DMSO) treatments reached 47±14.2% and 92.4±4.8% respectively. Points represent mean of n=18 from 3 independent experiments ±SEM. p≤0.05 following treatment with 10µM, 30µM and 100µM resveratrol; p≤0.05 with 30µ and 100µM metabolite treatments.

The trend in Figure 3.5 on the effect of the metabolites on CCL-228 differs from the previous figure (Caco-2). More specifically, at 1µM treatment on CCL-228 there was no effect on growth unlike Caco-2 cells. Seen in Figure 3.5, the effect is more profound at concentrations above 10µM for resveratrol, RV-3-G an RV-4'-G and above 30µM for



RV-3-S. For all compounds there was no significant effect at 1μM and 3μM but CCL-228 cells were more sensitive to treatment as compared to Caco-2. In addition, resveratrol-3-O-D-sulphate seemed to be less effective at concentrations above 10μM but still reached complete growth inhibition at 100μM ( $p<0.05$  relative to untreated cells). Again, growth was not affected after treatment with the vehicle and there was a significant decrease in growth after treatment with actinomycin D ( $53\%\pm14\%$ ).

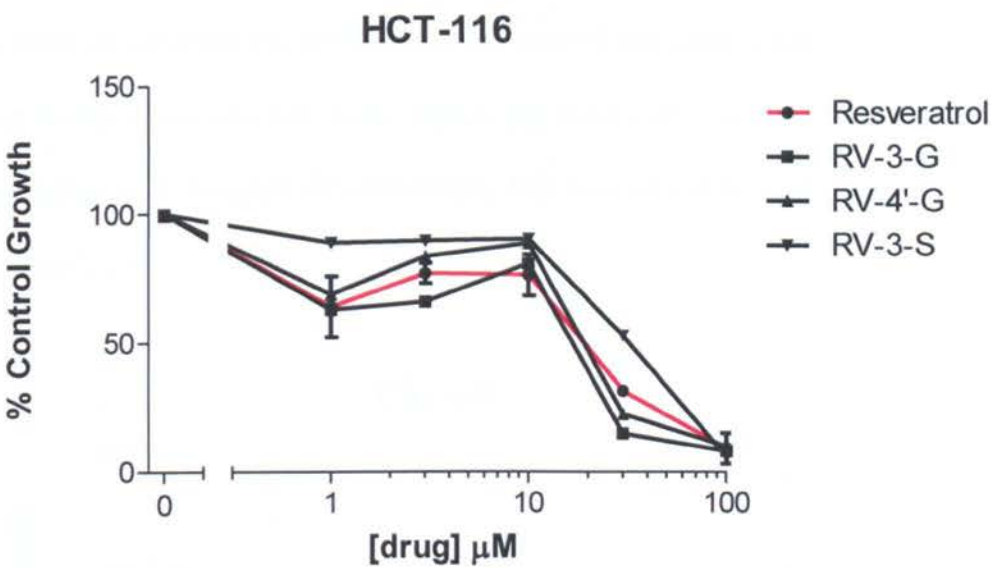


**Figure 3.6**The effect of resveratrol, resveratrol-3-O-D-glucuronide, resveratrol-4'-O-D-glucuronide and resveratrol-3-O-D-sulphate on the growth of HCT-116 cells after 48 hours using the neutral red assay. Growth following actinomycin D (10μg/ml) and vehicle control (0.1% DMSO) treatments reached  $60.1\pm12.5\%$  and  $99.3\pm2.7\%$  respectively. Points represent mean of  $n=18$  from 3 independent experiments  $\pm$ SEM.  $p\leq0.05$  at all resveratrol and RV-3-G concentrations;  $p\leq0.05$  at 1μM, 3μM, 30μM and 100μM RV-4'-G treatments;  $p\leq0.05$  with 30μM and 100μM RV-3-S treatments.

The trend exemplified in Figure 3.6 with HCT-116 cells is non-linear as compared to CCL-228 (Figure 3.5). It seems that the response of CCL-228 cells to treatment is dose-dependent. More specifically, the effect seen after 1μM treatment with resveratrol, RV-3-G and RV-4'-G is greater as compared to 3μM and 10μM ( $p<0.05$ ).In the case of RV-

3-S however, there was no significant effect at the lowest concentrations, but only at 30 $\mu$ M and 100 $\mu$ M ( $p < 0.05$  relative to control). However, even at 30 $\mu$ M, RV-3-S was less effective as compared to the other treatments but the effect was the same at 100 $\mu$ M. Again, there was no effect with the vehicle control while a notable 40% inhibition was observed following treatment with actinomycin D.

### 3.2.2 Using the MTT assay

In order to compare the results from the neutral red assay a second widely used assay was incorporated into this study. Again, the three cell lines were dosed under the same conditions and 50 $\mu$ g/ml of tetrazolium dye was added to each well (as described in Section 2.2.4).

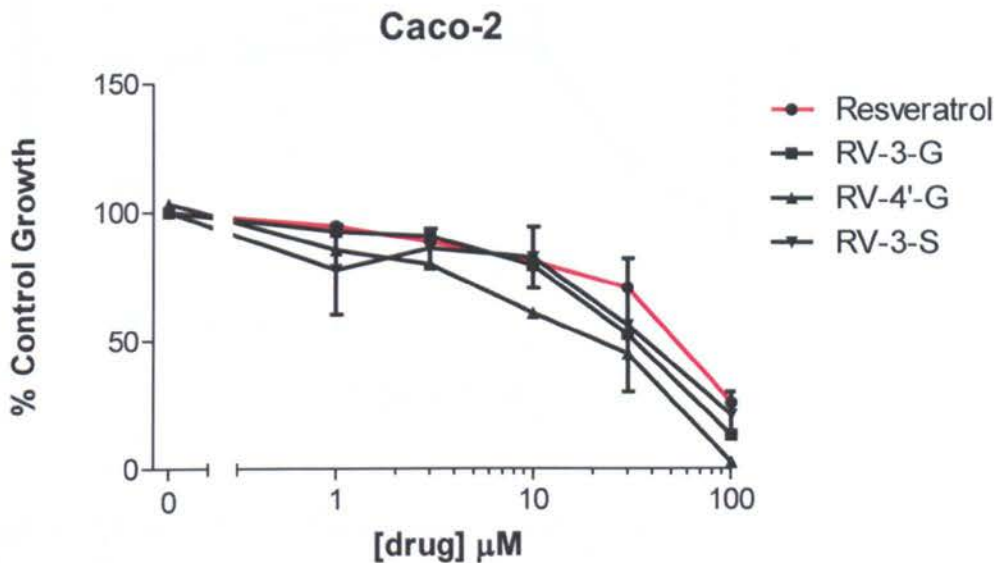


**Figure 3.7** The effect of resveratrol, resveratrol-3-O-D-glucuronide, resveratrol-4'-O-D-glucuronide and resveratrol-3-O-D-sulphate on the growth of Caco-2 cells after 48 hours using the MTT assay. Growth following vehicle control (0.1% DMSO) treatment reached  $91.3 \pm 4.7\%$ . Points represent mean of  $n=18$  from 3 independent experiments  $\pm$  SEM.  $p \leq 0.05$  at 30 $\mu$ M and 100 $\mu$ M treatments with resveratrol, RV-3-G and RV-4'-G; and,  $p \leq 0.05$  at 10 $\mu$ M, 30 $\mu$ M and 100 $\mu$ M treatments with RV-3-S.

It is evident from Figure 3.7 that the general trend of the effects of resveratrol and its metabolites was very similar when comparing the two assays. The  $IC_{50}$  values however, seemed to be slightly higher using the MTT assay (see Table 3.1). For example, the  $IC_{50}$  value for RV-3-G with the neutral red assay for example was  $16.5 \pm 8.1\%$  whilst with the MTT,  $28.9 \pm 1.1\%$ . In addition, at  $100\mu M$ , the growth inhibition after treatment with RV-3-S was 79% whilst for RV-4'-G, 97.4%. The results for RV-4'-G were in agreement with the neutral red whilst those of RV-3-S were slightly less sensitive. Overall, it seemed that the MTT assay was slightly less sensitive than the neutral red assay.

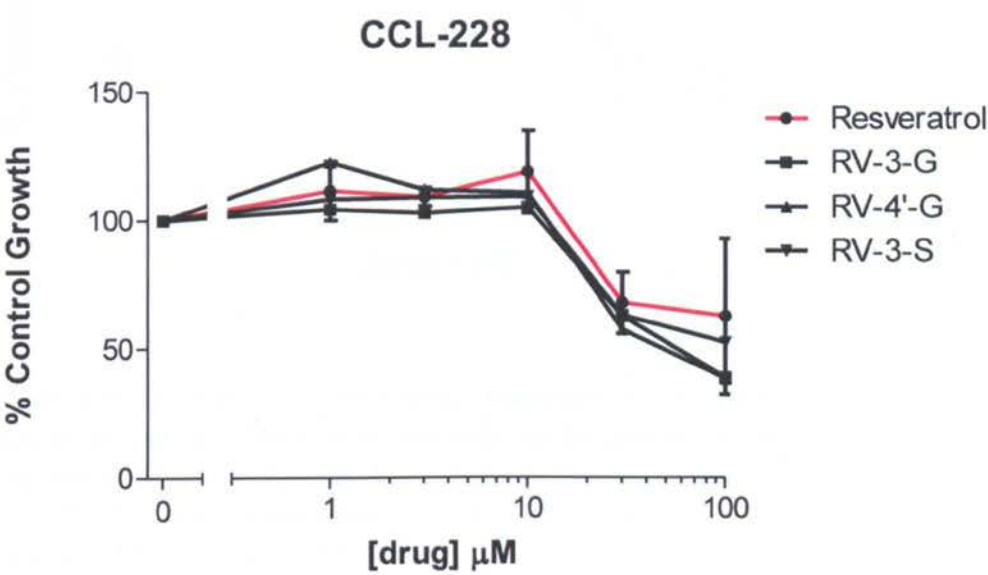


**Figure 3.8**The effect of resveratrol, resveratrol-3-O-D-glucuronide, resveratrol-4'-O-D-glucuronide and resveratrol-3-O-D-sulphate on the growth of CCL-228 cells after 48 hours using the MTT assay. Growth following vehicle control (0.1% DMSO) treatment reached  $91.3 \pm 4.7\%$ . Points represent mean of  $n=18$  from 3 independent experiments  $\pm$ SEM.  $p \leq 0.05$  at  $30\mu M$  and  $100\mu M$  for all treatments except in the case of  $100\mu M$  resveratrol.

In the case of CCL-228 depicted above in Figure 3.8, it was evident that despite the common trend, values were not in agreement with the neutral red uptake assay (Figure 3.5). One hundred micromolar treatments with all four compounds were not sufficient



to completely inhibit the growth of CCL-228 cells, with the lowest observed inhibition of 62%. Differences could be accounted for by the basis of the two assays. The large difference between the means of independent experiments with resveratrol resulted in a very high coefficient of variation and led to the absence significance at 100µM resveratrol treatment.

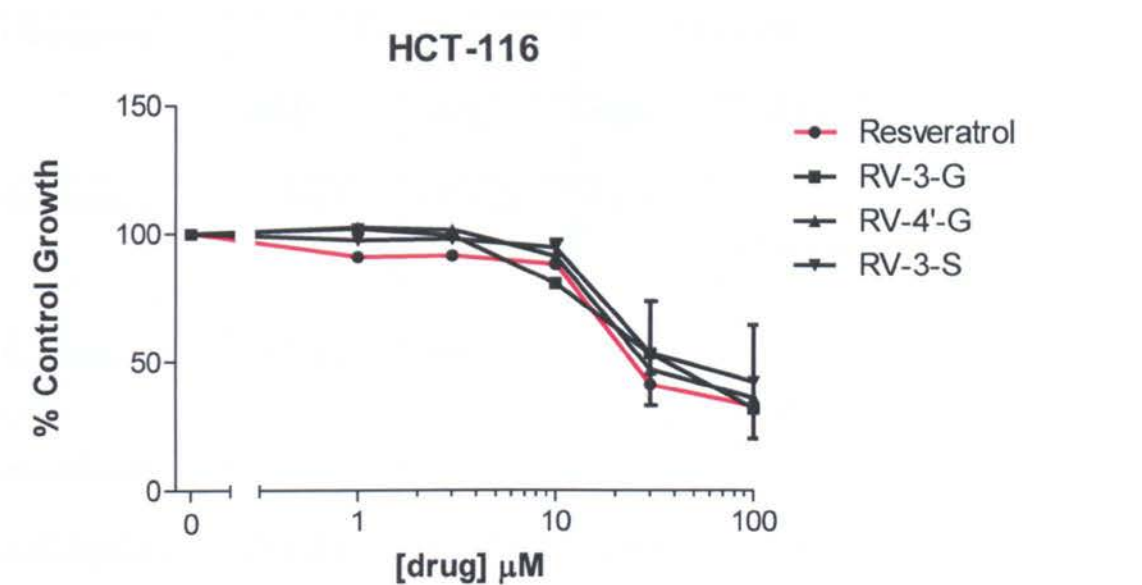


**Figure 3.9**The effect of resveratrol, resveratrol-3-O-D-glucuronide, resveratrol-4'-O-D-glucuronide and resveratrol-3-O-D-sulphate on the growth of HCT-116 cells after 48 hours using the MTT assay. Growth following vehicle control (0.1% DMSO) treatment reached 86±17.1%. Points represent mean of n=18 from 3 independent experiments ±SEM. p≤0.05 at 30µM and 100µM for all four treatments.

Presented in Figure 3.9 are the results of HCT-116 cells being treated with the four compounds of interest. Again, these results like CCL-228 seemed to be less sensitive as compared to the results obtained with the neutral red uptake assay (Figure 3.6). Even at 100µM, complete inhibition was not reached, with the greatest inhibition being 68%. The IC<sub>50</sub> values were 34.6µM, 40.6µM, 42.6µM and 57.0µM for resveratrol, RV-3-G, RV-4'-G and RV-3-S respectively. When comparing these values with the neutral red assay in Table 3.1, it is clear that the values are greater.



**Table 3.1** IC<sub>50</sub> values of resveratrol, piceatannol, pterostilbene, resveratrol-3-O-D-glucuronide, resveratrol-4'-O-D-glucuronide and resveratrol-3-O-D-sulphate using the neutral red and MTT assays. Values were calculated using GraphPad Prism 6.0 by non-linear regression (curve fit) and dose-response inhibition (variable slope, 4 parameters) and values represent means of three independent experiments ± SEM.

	<b>IC<sub>50</sub>mean(±SEM) μM n=3-4 independent experiments</b>					
<b>Compound</b>	<b>Caco-2</b>		<b>CCL-228</b>		<b>HCT-116</b>	
	<b>NRU</b>	<b>MTT</b>	<b>NRU</b>	<b>MTT</b>	<b>NRU</b>	<b>MTT</b>
Resveratrol	23.8±8.0	47.7±1.2	9.8±1	~30-100μM *	15.1±5.3	34.6±1.1
Resveratrol-3-O-D-glucuronide	16.5±8.1	28.9±1.1	15.8±4.2	~30-100μM *	10.1±3.0	40.6±1.2
Resveratrol-4'-O-D-glucuronide	18.6±8.1	15.4±1.2	12.9±1.2	~30-100μM *	24.4±3.4	42.6±1.2
Resveratrol-3-O-D-sulphate	11.2±1.4	33.6±1.2	21±0.04	~30-100μM *	31.0±1.3	57.0±1.2
Piceatannol	21.7±1.1	NT	29±1.0	NT	28.0±1.1	NT
Pterostilbene	5±1.1	NT	34.5±1.1	NT	18.3±1.10	NT

NT- Not tested

\* Not possible to calculate by GraphPad Prism

### 3.3 Effect of resveratrol and its metabolites on polarised Caco-2 cells

Caco-2 cells were grown on permeable Transwells for 21 days in order to form a differentiated polarised monolayer (Figure 3.10). Cells were treated every other day with either resveratrol or its metabolites at  $1\mu\text{M}$  or  $30\mu\text{M}$  on either the apical or the basolateral sides for 11 days. Cell viability was assessed using the neutral red uptake assay as mentioned in Section 2.2.1 and converted to percent of growth relative to untreated cells.

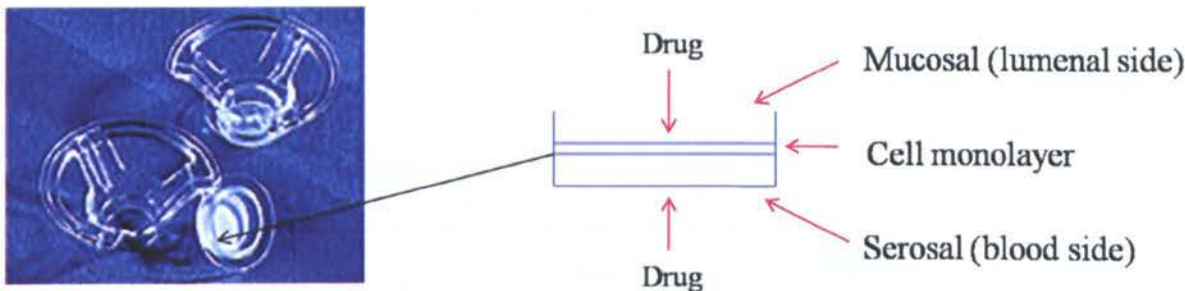


**Figure 3.10** Schematic representation of Transwells and the formation of a monolayer with the mucosal and serosal sides. Image taken from Corning Life Sciences.

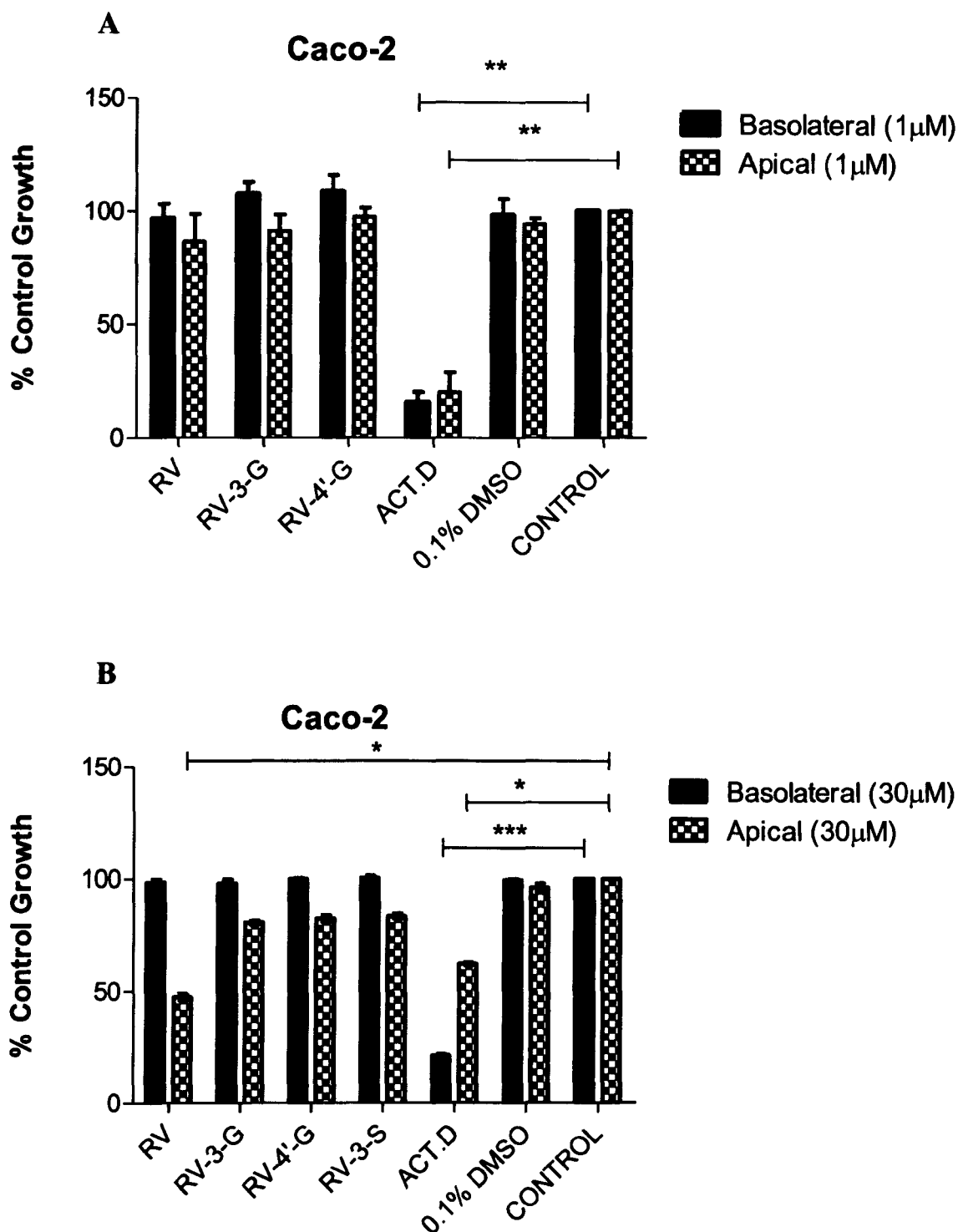


**Figure 3.11** Comparison of the effect of 1µM (A) and 30µM (B) treatments of resveratrol, resveratrol-3-O-D-glucuronide, resveratrol-4'-O-D-glucuronide, resveratrol-3-O-D-sulphate and vehicle control (0.1% DMSO) on the apical or basolateral side of Caco-2 monolayers grown on Transwells for 21 days and treated for 11 days every other day expressed as a percentage of control growth. Points represent means  $n=6$  from 3 independent experiments  $\pm$  SEM. \*  $p<0.05$ , \*\* $p<0.01$ , \*\*\*  $p<0.001$  relative to control untreated.

It is evident from Figure 3.11A that the growth of Caco-2 cells was not affected by low concentrations of the test compounds on either side ( $p>0.05$ ). For example, there was a  $17\% \pm 5.6\%$  reduction in growth with  $1\mu\text{M}$  apical resveratrol as compared to basolateral ( $2\% \pm 15.6\%$ ) but the difference was not statistically significant ( $p>0.05$ ). This contradicts the results from Figure 3.4 where  $1\mu\text{M}$  treatments with RV, RV-3G, and RV-4'-G caused an inhibition by 33%, 23%, and 7% respectively. Differences could be attributed to the biological variability and/or the difference between a polarised and non-polarised scenario. Moreover, addition of  $30\mu\text{M}$  treatments on the basolateral side yielded similar results (Figure 3.11B). Apical delivery however of  $30\mu\text{M}$  resveratrol reduced cell viability to about 50% ( $p<0.05$ ), while the metabolites had a smaller effect (Figure 3.11B). For example,  $30\mu\text{M}$  RV-3-G reduced growth by only  $20\% \pm 0.8\%$ . What is interesting is that the same effect was seen with actinomycin D irrespective of 'side' of treatment at  $1\mu\text{M}$  ( $p<0.01$ ) but apical  $30\mu\text{M}$  actinomycin D was not as effective as  $1\mu\text{M}$ . Despite these observations, all results excluding those for  $30\mu\text{M}$  apical vs  $30\mu\text{M}$  basolateral resveratrol treatments and actinomycin D were not statistically significant ( $p>0.05$ ). One can therefore conclude that the 'sidedness' of treatment was not a major factor at low concentrations but apical  $30\mu\text{M}$  resveratrol was an active treatment, whereas basolateral  $30\mu\text{M}$  resveratrol was not.

### 3.4 Investigation of cell growth following drug removal

Cells were treated with IC<sub>50</sub> concentrations(see Table 3.1 for exact values) of the drugs for 48 hours after which cell numbers were calculated or media replenished for further 48 hours in order to investigate whether the effects seen were reversed. Statistical analysis using ANOVA and Tukey's test was used comparing the 48 hour treatment groups with the corresponding treatments following 48 hour replenishment with fresh media. Only p-values  $\leq 0.05$  were considered statistically significant.

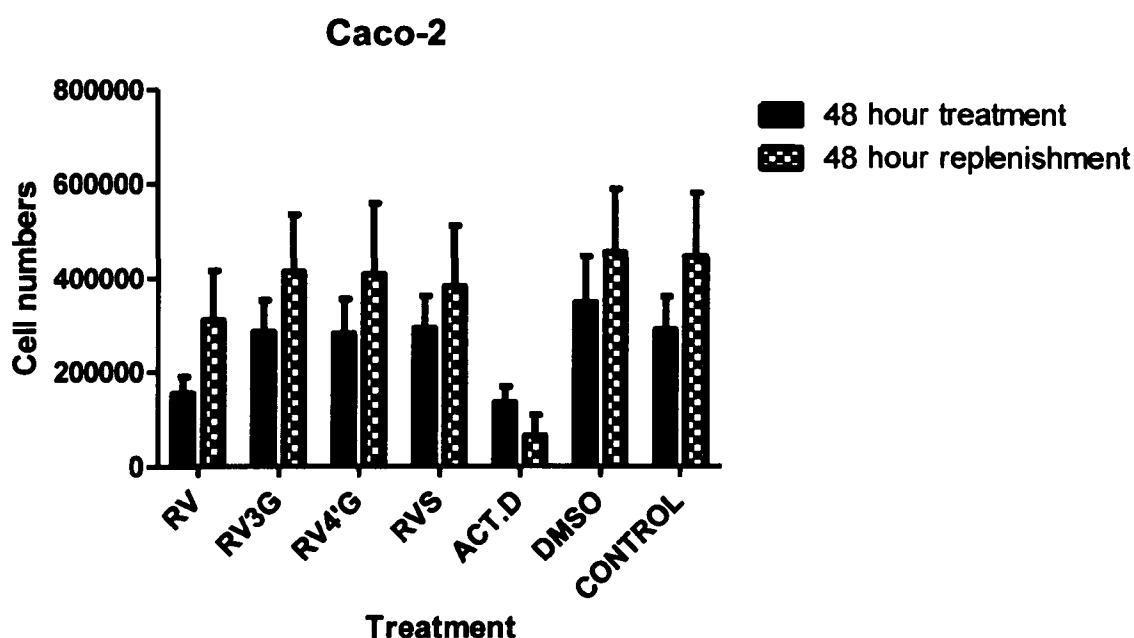


**Figure 3.12** Comparison of the effect of treatment of Caco-2 cells with IC<sub>50</sub> concentrations of drugs after 48 hours followed by a 48 hour recovery period. Values represent mean cell numbers  $n=9$  from 3 independent experiments  $\pm$ SEM. IC<sub>50</sub> values: resveratrol 23.8 $\mu$ M, RV-3-G 16.5 $\mu$ M, RV-4'-G 18.6 $\mu$ M and RV-3-S 11.2 $\mu$ M.

As shown in Figure 3.12, cells numbers decreased after 48 hours incubation with resveratrol but cells were capable of recovering after 48 hours following addition of fresh media in the absence of drug (170,000 cells and 300,000 cells respectively) suggesting that cells can recover from an S phase arrest as will be shown later. The trend in the case of the metabolites was the same but cells numbers were greater

(~280,000 cells) reaching approximately 400,000 cells after the 48 hour recovery period. However, there was little activity of the metabolites overall in these experiments when compared to DMSO and did not correspond to IC<sub>50</sub> concentrations. This was not the case however, for actinomycin D as cell numbers were overall less (~140,000 cells) with cells not being able to recover (~68,000) as expected, since actinomycin D is an irreversible inhibitor of protein synthesis. One possibility for the unexpected effect of the metabolites could be loss of activity. In fact, a recent study has identified that UV exposure and exposure to air and room temperature for a period of 72 hours leads to changes in the emission spectra of resveratrol and its metabolites (Aires et al., 2013). So, despite the fact that exposure to light and air was kept to a minimum, this could be a possibility for the loss of activity.

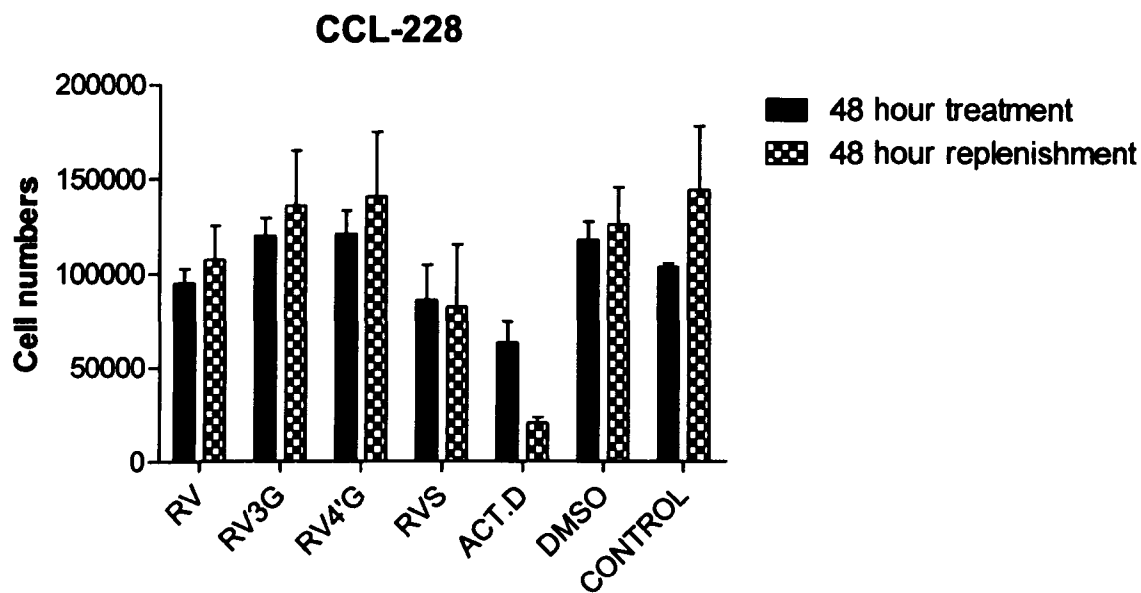


**Figure 3.13** Comparison of the effect of treatment of CCL-228 cells with IC<sub>50</sub> concentrations of drugs after 48 hours followed by a 48 hour recovery period. Values represent mean cell numbers n=9 from 3 independent experiments ±SEM. IC<sub>50</sub> values: resveratrol 9.8μM, RV-3-G 15.8μM, RV-4'-G 15.4μM and RV-3-S 33.6μM.

The trend seen in CCL-228 cells (Figure 3.13) was similar as in the case of Caco-2 cells but the anti-tumour activity of treatments, including resveratrol, was less effective than expected. The concentrations of resveratrol and the two glucuronides used were not sufficient to reduce growth by 50% with the sulphated metabolite being slightly more active suggesting loss of activity of the compounds. Overall, treatment of CCL-228 cells with RV-3-S did not lead to growth reversal. More specifically, after 48 hour drug treatment with RV-3-S, cells were reduced to 85,632 relative to 82,073 after incubation for a further 48 hours with drug-free media. Only in the case of actinomycin D, cells were not capable of recovering after removal of the drug with cell numbers reducing even further.

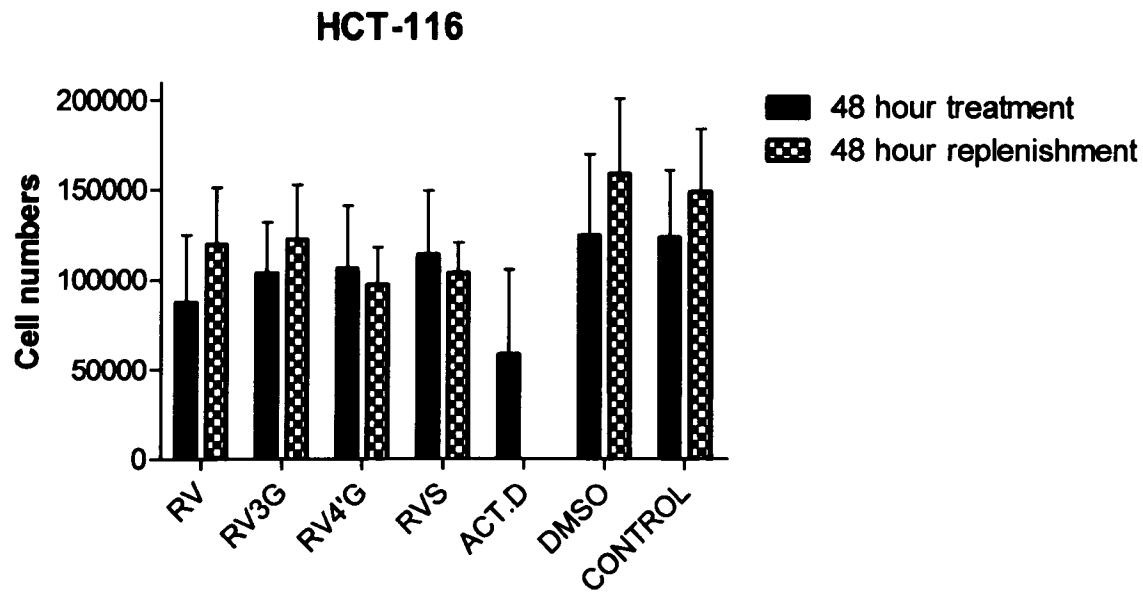


**Figure 3.14** Comparison of the effect of treatment of HCT-116 cells with IC<sub>50</sub> concentrations of drugs after 48 hours followed by a 48 hour recovery period. Values represent mean cell numbers (triplicates) of 3 independent experiments ±SEM. IC<sub>50</sub> values: resveratrol 15.1µM, RV-3-G 10.1µM, RV-4'-G 24.4µM and RV-3-S 31.0µM.

The comparison of 48 hour treatment alone and 48 hour recovery period for HCT-116 cells is shown in Figure 3.14. These results were in agreement with the findings in Caco-2 and CCL-228 cells. Despite that treatment with resveratrol caused a reduction in cell numbers, 48 hour replenishment with fresh media was sufficient to increase cell numbers but this was not statistically significant ( $p>0.05$ ). The same scenario was seen with RV-3-G, the vehicle control and untreated cells. In the case of RV-4'-G and RV-3-S, there was no reversal of the drug effect following 48 hour media replenishment.

The lack of activity of the drugs was surprising, so much that Bertin Pharma was contacted to check the Lot numbers and whether the specific batch of compounds was up to standard. Bertin confirmed the potency of the chemicals. As will be seen, further studies suggest that cell variability in how cells respond to drugs may account for this change in activity.



### 3.5 Haemolysis

In order to investigate the effect of the resveratrol metabolites on normal cells, sheep red blood cells were used and treated for 30 minutes at increasing concentrations (1μM, 10μM, 100μM, 200μM and 500μM). The concentration of haemoglobin released was measured at 540nm and the percent of haemolysis was calculated relative to 1% Triton X-100 (positive control).

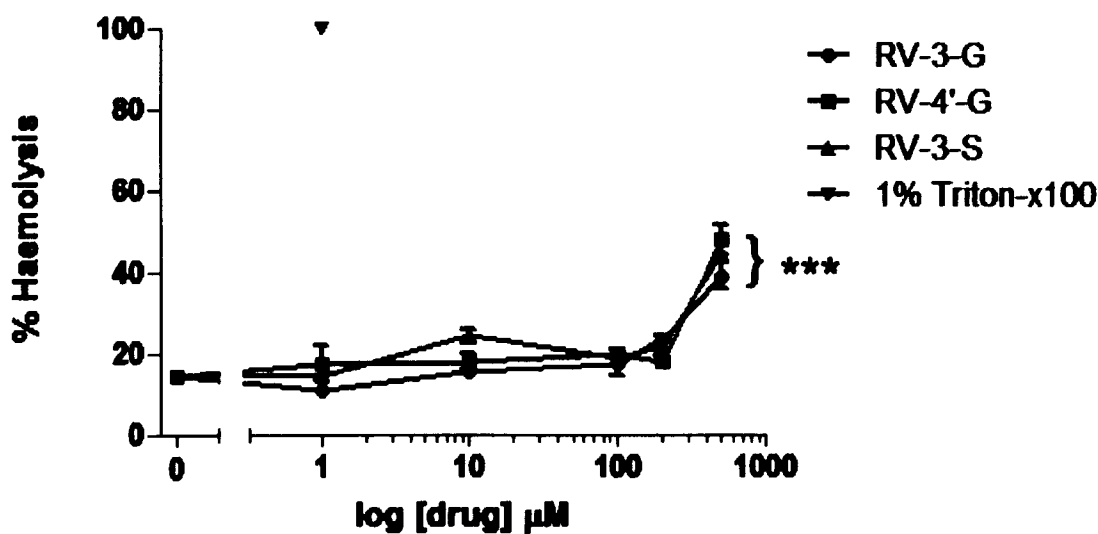


**Figure 3.15** Effect of resveratrol and its metabolites on the haemolysis of sheep red blood cells. RBC's were treated with increasing concentrations of drugs (1μM, 10μM, 100μM, 200μM and 500μM) for 30 minutes and the absorbance measured at 540nm. Percent haemolysis was calculated by using 1% Triton-X100 as 100% haemolysis. Values represent means (triplicates) of two independent experiments ±SEM. \*\*\*p<0.001relative to control by one-way ANOVA followed by Tukey's test.

The extent of haemolysis in the untreated group reached 14.5%±0.8% and the resveratrol metabolites did not cause haemolysis of sheep red blood cells when added up to 200μM (Figure 3.15). More specifically, haemolysis of sheep cells at 1μM RV-4'-G treatments reached 17.5%±4.2% while it was even lower percentages with the other

treatments. These were not significantly different to the non-treated group ( $14.5\% \pm 0.8\%$ ). Even at  $200\mu\text{M}$  treatments (two-fold difference with the highest concentration used for the growth studies), haemolysis was not sufficient to suggest a cytotoxic effect to normal cells. For example, after  $200\mu\text{M}$  treatment with RV-3-G, haemolysis of red blood cells reached  $23.5\% \pm 0.3\%$ . Significant haemolysis was only apparent at concentrations reaching  $500\mu\text{M}$  which was 5-fold the maximum concentration used for the growth studies ( $39.1\% \pm 3.0\%$ ,  $47.9\% \pm 3.5\%$ ,  $44.2\% \pm 1.2\%$  for RV-3-G, RV-4'-G and RV-3-S respectively) ( $p < 0.001$ ). These experiments indicated that resveratrol and its metabolites were not capable of exerting a cytotoxic effect on normal cells, suggesting that growth inhibition of undifferentiated cells was due to a different mechanism.

### 3.6 Discussion

The aim of this chapter was to elucidate and compare the effect on growth of two known analogues of resveratrol, piceatannol (a resveratrol metabolite) and pterostilbene as well as the three main conjugated metabolites. Experiments were also designed to identify whether the growth inhibition was reversible when the drugs were removed. In addition to experiments on growing cells, the effect on cells grown as a polarised epithelium were performed to model the *in vivo* state more closely. Finally, possible non-specific actions of the drugs on cells were tested using a haemolysis assay. Whilst all attempts were made to maintain the stability of the drugs including minimal exposure to light and air and avoidance of continuous freeze-thawing, stability assays were not performed.

#### **Effect of resveratrol analogues on growth**

Results showed that pterostilbene had the lowest  $IC_{50}$  in the range of 5-20 $\mu$ M for the three cell lines. One possibility for the greater observed efficacy could be the substitution of two hydroxyl groups of resveratrol to methoxy groups that are known to increase its permeability in the cell making pterostilbene more lipophilic and increasing the potential for cellular uptake (McCormack and McFadden, 2012). The findings from this study agree with screening assays conducted by Pan *et al.* (2007) on colorectal cancer cell lines using pterostilbene where they reported an  $IC_{50}$  6.25 $\mu$ M using COLO205 cells (Nam *et al.*, 2001, Pan *et al.*, 2007). A study by Wolter and colleagues (2002) reported an  $IC_{50}$  of 25 $\mu$ M when screening piceatannol against Caco-2 and HCT-116 cells after 72 hours (Wolter *et al.*, 2002). This is in tight accordance with results from this study which identified an  $IC_{50}$  of 21.7 $\mu$ M for Caco-2 and 28 $\mu$ M for HCT-116 at 48 hours. The slight differences between the two studies could be due to the different

assay used (Crystal Violet and Neutral Red) as well as the exposure time. Another noteworthy fact about the study by Wolter is that piceatannol hampered the growth of HCT-116 cells (do not express COX-2 and are deficient in COX-1 activity). This suggests that piceatannol has a different mechanism for inhibiting growth compared to resveratrol being independent of COX activity. Murias *et al.* (2004) have demonstrated that piceatannol inhibits COX-2 with a higher efficacy than resveratrol and the clinically established celecoxib making it a good candidate for achieving growth inhibition at lower concentrations (Murias *et al.*, 2004).

A study by Schneider and colleagues (2003) investigated the effect of pterostilbene at low micromolar concentrations (0.1  $\mu$ M-0.6  $\mu$ M) over a period of 11 days on Caco-2 and CCL-228 cells (Schneider *et al.*, 2003). They reported IC<sub>50</sub> values of 0.25  $\mu$ M and 0.23  $\mu$ M respectively. After attempting this experiment using 1  $\mu$ M treatments of resveratrol, its two analogues and the metabolites for 11 days, results were inconclusive possibly owing to the fact that cells became detached from the 96-well plates after this exposure time (data not shown). Therefore only an experiment using 1  $\mu$ M and 30  $\mu$ M for 11 days on Transwells was performed.

### **Effect of conjugated metabolites on growth**

The results presented in this chapter showed for the first time a significant inhibitory effect of the three main resveratrol metabolites. IC<sub>50</sub> values for the parent compound, resveratrol and its metabolites were in the range of 9-31  $\mu$ M for the three cell lines, Caco-2, CCL-228 and HCT-116. The values reported here for resveratrol are in accordance with previous studies, where growth inhibition was reported in the range of 10-100  $\mu$ M (Juan *et al.*, 2012, Pan *et al.*, 2007, Nam *et al.*, 2001) despite them being relatively high when considering the bioavailability of resveratrol (Walle, 2011).

The neutral red assay was mainly employed in this study, which seems to be more sensitive than assays of tetrazolium salts (including MTT), enzyme leakage or protein content (Repetto *et al.*, 2008). This was confirmed by the IC<sub>50</sub> values with the MTT assay which were in the 30-100 µM range. Previous studies used the MTT assay on the three major sulphated metabolites, trans-resveratrol 3-O-D-sulphate, trans-resveratrol 4'-O-D-sulphate and trans-resveratrol-3-O-4'-O-D-disulphate on breast cancer cells (less potent than resveratrol) (Miksits *et al.*, 2009), the sulphorhodamine (SRB) protein assay using resveratrol-3-O-D-sulphate on breast cancer cells (IC<sub>50</sub>>50 µM) (Hoshino *et al.*, 2010) and Promega's Cell Titer Blue assay (oxidation of resazurin, resveratrol glucuronides IC<sub>50</sub>>100 µM on neuroblastoma cells) (Kenealey *et al.*, 2011). One explanation for the greater IC<sub>50</sub> values with the MTT assay in this study as well as the fore mentioned, could lie in the fact that resveratrol and possibly its metabolites increase metabolic activity which caused the considerable variation in these results. It has been shown that resveratrol is capable of protecting against mitochondrial injury and to increase the activity of mitochondrial dehydrogenases (Yousuf *et al.*, 2009). Therefore, it is suggested that injured cells can reduce the MTT and consequently increase the production of the formazan product leading to the under-estimation of the anti-proliferative effects of resveratrol and metabolites.

The results of this study are in contrast to a report stating “the 3-O and 4'-O-D-glucuronide resveratrol metabolites were without effect on colon cancer cell growth, as evidenced by cell proliferation and cell cycle analysis at a concentration of 60µM” (unpublished data) (Delmas *et al.*, 2011). A recent study by Storniolo and Moreno (2012) however, has reported an inhibitory effect with the three metabolites using Caco-

2 cells ( $IC_{50}$  reported to be approximately  $10\mu M$ ) in a concentration-dependent manner which further confirms our findings.

### **Effect on growth using a polarised epithelium**

The work by Schneider and colleagues (2003) was the inspiration for this experiment. These authors found that low concentrations ( $1\mu M$ ) of resveratrol and its trimethoxy derivative for a period of 11 days were sufficient to inhibit the growth of Caco-2 cells. This led us to investigate the effect of low concentrations on polarised cells but ultimately contradicted the results from this study using Caco-2 cells and Transwells. It has been previously shown that resveratrol is rapidly metabolised in the liver and intestine via Phase II metabolism, therefore making it less bioavailable (Walle, 2011). High concentrations like those used in *in vitro* studies are therefore never achieved *in vivo*. Therefore, the effect of the drugs on a polarised monolayer experiment was designed to investigate the effect of two concentrations of resveratrol and its metabolites over a period of 11 days on the growth of Caco-2 cells. Only Caco-2 cells were used for this experiment because these adenocarcinoma cells are capable of forming monolayers and are the gold standard model in drug permeation studies. In order to mimic the polarised epithelium of the intestinal tract, cells were loaded onto Transwell plates to create a polarised monolayer and treatment was applied to either the apical or basolateral compartment as cells exist in a polarised form *in vivo*. The effect of resveratrol and its metabolites on fully differentiated polarised Caco-2 monolayers has not been investigated so far except for this study. It has been shown that apical or basolateral treatment of resveratrol and its metabolites for a period of 11 days at low concentrations ( $1\mu M$ ) did not have any effect on the growth of proliferating Caco-2 cells. Thirty micromolar resveratrol delivered on the apical side of the monolayer

significantly inhibited the growth of cells by ~50%. The effect of the metabolites however was less profound with only about 25% inhibition. These results suggest that the apical side is more sensitive and raise the possibility that these events are receptor-mediated. For example, the activation of the adenosine A<sub>3</sub> receptor could be a target that causes activation of downstream signalling pathways leading to growth inhibition. This however will be discussed further in Chapter 5. Thirty micromolar actinomycin D treatment on the apical side was unexpectedly less effective as compared to 30µM basolateral and 1µM apical and basolateral treatments. This suggests that specific efflux pumps are present which are responsible for actively pumping the high concentrations of actinomycin D outside the cell. One such family of transporters is the ABC (ATP-binding cassette) family and one of its members, P-glycoprotein was previously shown to be present on the apical side of the colon (Balayssac et al., 2005).

#### **Effect following removal of drugs**

In order to gain a further insight into the mechanism of action of the metabolites, the effects after removal of the drugs were attempted to be elucidated. From the results however, it was not possible to draw any conclusions. More specifically, despite the recovery of cells in some instances, the differences were not statistically significant. Contradicting results come from a study by Opiari (2004) however, where A2780 ovarian cancer cells were treated with 50µM resveratrol in increasing amounts of time (0-48 hours) and cells allowed to recover (Opiari, 2004). It has been shown that cell exposure greater than 12 hours caused irreversible growth arrest. One possibility for the variation in effects could be the higher resveratrol concentration as compared to the current study where only 30µM concentrations were employed. Experiments with 100µM treatments were attempted but cells were not able to recover following 24, 48 and 72 hours media replacement (data not shown) which further suggests there is a limit

to the reversibility of the resveratrol effect. These experiments were hampered by the lack of activity of resveratrol and its metabolites. The treatments were added at IC<sub>50</sub> values but 50% inhibition was rarely measured. The stability of the drugs was checked with the manufacturer (Bertin Pharma) and assured there were no problems. There is only limited evidence for a reversible effect of resveratrol.

### **Lack of non-specific effects**

The results of the haemolysis experiment on sheep red blood cells showed no evidence of lytic activity of resvetratrol and its metabolites at concentrations reaching 200µM. This is in close agreement with published studies (Jung *et al.*, 2005). Other studies however, have reported the parent compound, resveratrol to possess cytotoxic effects on human peripheral blood mononuclear cells (PBMCs) at concentrations greater than 30µM but this was absent for the mono-glucuronide metabolites at up to 270µM (Wang *et al.*, 2004a).

### **Conclusion**

The experiments described in this chapter showed the growth inhibitory effects at high concentrations of the metabolites. The next phase of work was to investigate the actual mechanism of action of these metabolites. Further experiments were conducted to elucidate whether these drugs cause the same effects as the parent compound or whether they acted in a different manner. One possibility could be that the metabolites caused cell arrest by inhibiting a specific phase in the cell cycle or that they targeted the cells in a specific manner inducing them to undergo programmed cell death (apoptosis). In the next two chapters, a more mechanistic probe into the effects of these drugs on the cell cycle and the possible involvement of apoptosis was performed.



## **Chapter 4. How does resveratrol and its metabolites inhibit cell growth?**

*In vitro* studies have demonstrated that resveratrol can inhibit cell proliferation, induce apoptosis, and block cell cycle progression in numerous types of human cancer cell lines including colon, skin, breast as well as pancreas (Walle *et al.*, 2004). Resveratrol is capable of causing cell cycle arrest at the G0/G1, S and G2/M phases and has the ability of causing terminal differentiation and eventual apoptosis in various cancer cell lines including colon, breast, liver and prostate (Saiko *et al.*, 2008, Parekh *et al.*, 2011, Hahnvajanawong, 2011).

The most vital cellular mechanism against transformation of ‘new growth’ is apoptosis which removes a damaged cell whilst also suppressing the development of transformed cells that have been inappropriately stimulated to divide despite the absence of mitotic stimuli (Kundu and Surh, 2004). It has been revealed that resveratrol can trigger apoptosis in a variety of malignant cell types by encouraging cytochrome c release, up-regulation of the pro-apoptotic Bax protein, down-regulation of the anti-apoptotic Bcl-2 and through activation of the tumour suppressor protein, p53, known as the guardian of the genome (Gusman *et al.*, 2001, Dong, 2003). RV caused apoptosis in HL-60 (Human promyelocytic leukaemia cells) and the T47D breast cancer cell line by eliciting the CD95-CD95L signalling pathway (Clément *et al.*, 1998). Alternatively, studies by Delmas and colleagues (2003) reported that modulation of Fas/FasL was not responsible for RV-induced apoptosis in SW480 colorectal cancer cells; rather it was due to caspase activation and up-regulation of Bax and Bak. The mechanisms responsible for the induction of apoptosis using resveratrol seem to be cell-type specific, either p53-dependent or p53-independent. This was observed through a study by Mahyar-Roemer *et al.* (2001) where it was suggested that resveratrol-induced apoptosis of HCT-116

colorectal cells is by a p53-independent mechanism (even though this cell line expresses wild type p53).

Data from studies on a range of cell lines have suggested that resveratrol has strong anti-proliferative characteristics. Resveratrol prevented the proliferation of tumour cells by directly inhibiting DNA synthesis and by impeding different phases of cell cycle development (Kundu and Surh, 2004). This naturally occurring polyphenol also inhibited the expression of cyclin B1 in MCF-7 and SW480, whilst also down-regulating the expression of cyclin D1 and cyclin A in SW480 cells only (Wolter *et al.*, 2003). This suggests a cell type-specific effect of resveratrol in blocking the malignant cell cycle progression (Joe *et al.*, 2002). Alternatively, resveratrol inhibited the expression of cyclin D1 and Cdk4 but increased the expression of cyclin E and cyclin A in Caco-2 and HCT-116 colorectal cancer cells (Wolter *et al.*, 2001).

Resveratrol exerts its inhibitory effects by mediating cell-cycle arrest through up-regulation of p21, p27, p53 and Bax and down-regulation of cyclin D1, cyclin E and Bcl-2 (Rimando and Suh, 2008, Gescher and Steward, 2003). Resveratrol is also capable of inducing apoptosis by positively regulating the expression of Bax, p53, PUMA and other pro-apoptotic proteins while concurrently reducing the expression of anti-apoptotic proteins including Bcl-2 and surviving (Shankar *et al.*, 2007). Other signalling pathways include suppression of tumour cell proliferation, reduction of inflammation and angiogenesis and inhibition of adhesion, invasion and metastasis (Bishayee, 2009).

## **Aims and objectives**

The aims of this chapter were therefore, to investigate the effect of treatment and deduce whether there is a link to apoptosis or if in fact the effect lies further downstream in the nuclear level and affects the cell cycle. Experiments were conducted by co-treating cells with IC<sub>50</sub> concentrations of resveratrol and its metabolites and the pan-caspase inhibitor, Z-VAD-FMK (50µM) to identify whether the effects of these drugs were reduced therefore suggesting an apoptotic effect. The morphology of cells was also examined using the DAPI nuclear stain in order to see the effect on the nuclear integrity after treatment. The apoptotic effect was further analysed by flow cytometry by looking at the cell cycle distribution and the percentage of cells in the sub-G1 phase after treatment followed by measurement of the protein levels of cyclin D1 using a range of concentrations. The involvement of p53 on the growth effects after treatment was also investigated by western blot and immunofluorescence staining.

#### **4.1 Involvement of caspases on resveratrol and its metabolites on growth**

In order to investigate whether treatment with resveratrol and its metabolites exerted an apoptotic effect, the pan-caspase inhibitor, Z-VAD-FMK was employed. Z-VAD-FMK is a cell-permeable, irreversible pan-caspase inhibitor. It inhibits caspase processing and apoptosis induction in tumour cells in vitro ( $IC_{50} = 0.0015-5.8mM$ )(Slee *et al.*, 1996, King *et al.*, 1998). Cells were treated for 1 hour with 50 $\mu$ M Z-VAD-FMK prior to treatment with the test compounds at  $IC_{50}$  concentrations and incubated for 48 hours (see Table 3.1 for  $IC_{50}$  values). Z-VAD-FMK (50 $\mu$ M) has been shown previously to be an effective treatment in blocking the caspases (Waheed *et al.*, 2011). If cells died by apoptosis, it was expected that after administration of Z-VAD-FMK the absorbances would be higher than without the inhibitor. If this was the case, one would conclude that the mechanism of action of these compounds was through induction of apoptosis.

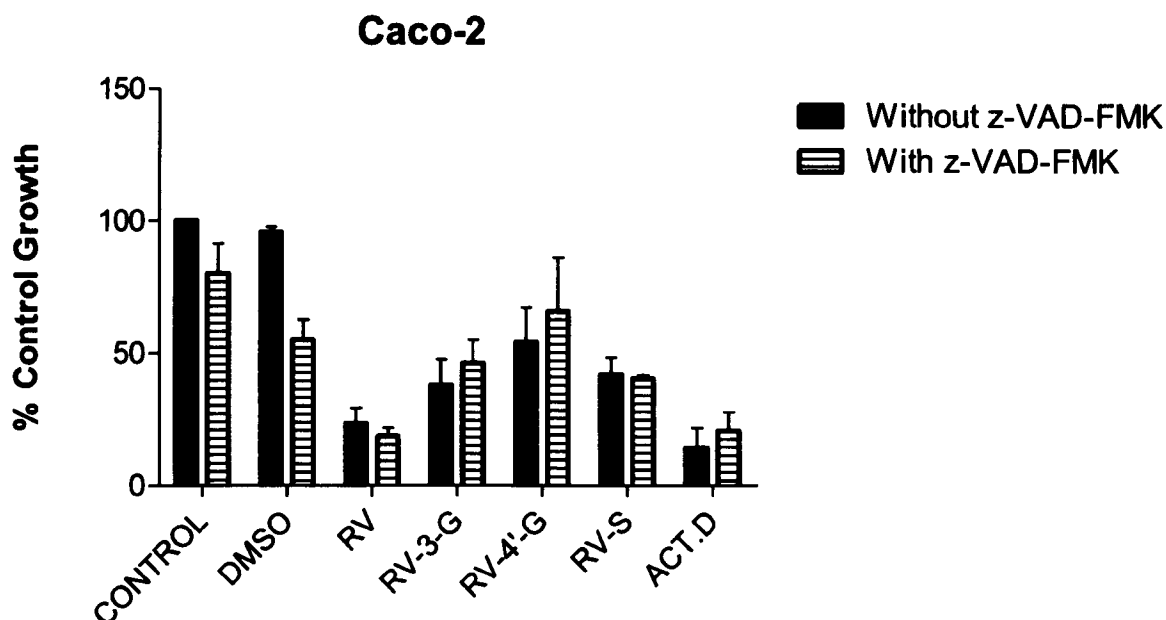


**Figure 4.1** Effect of treatment with compounds of interest (at IC<sub>50</sub> concentrations) with or without addition of Z-VAD-FMK (50µM) on viability of Caco-2 cells. Briefly, cells were incubated with drugs either alone or with Z-VAD-FMK for 48 hours and viability measured using the neutral red uptake assay. Results represent means (n=9) from 3 independent experiments ±SEM.

From the results above it is clear that percent growth values looked similar in the presence or absence of Z-VAD-FMK (Figure 4.1). For resveratrol and RV-3-S, there was a slight but not significant decrease in growth as compared to treatment alone which could be accounted for by variability ( $p>0.05$ ). A noteworthy point to emphasise is the fact that IC<sub>50</sub> concentrations were used for this experiment however, greater than 50% inhibition was achieved in some cases as shown in Figure 4.1. In the case of DMSO in the presence of Z-VAD-FMK, there appears to be a drop in growth due to the presence of outliers from two independent experiments as this was not evident in the other two cell lines (Figures 4.2 and 4.3). Exclusion of these outliers led to growth reaching the levels of the control group in the presence of Z-VAD-FMK (data not shown). Overall, these findings were not statistically significant ( $p>0.05$ ) and therefore suggest no association between the test compounds and induction of apoptosis.

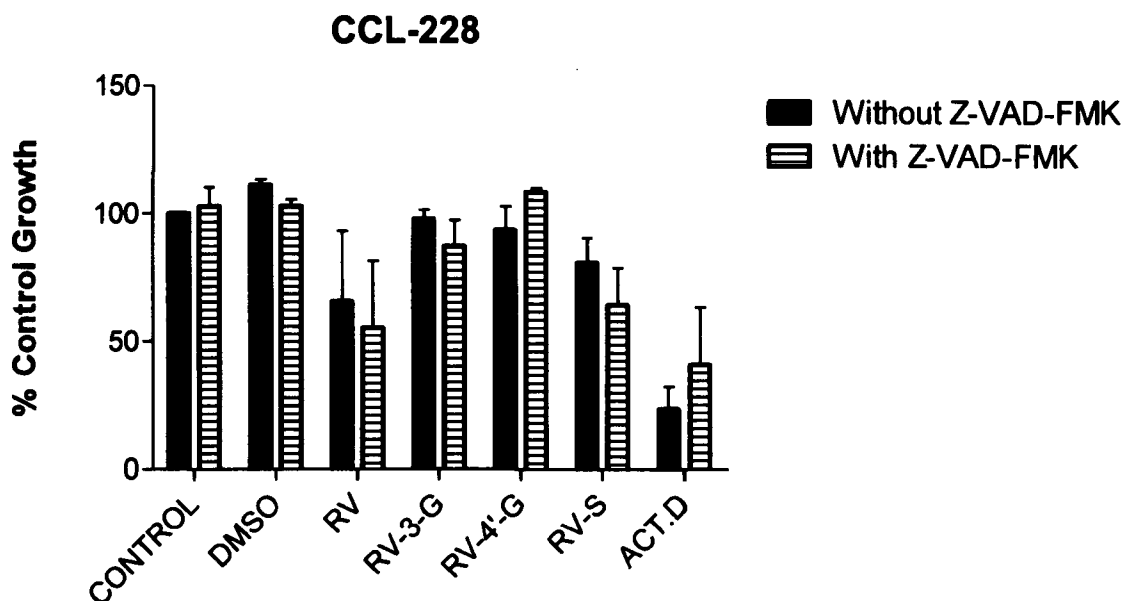


**Figure 4.2** Effect of treatment with compounds of interest (at  $IC_{50}$  concentrations) with or without addition of Z-VAD-FMK ( $50\mu M$ ) on viability of CCL-228 cells. Briefly, cells were incubated with drugs either alone or with Z-VAD-FMK for 48 hours and viability measured using the neutral red uptake assay. Results represent means ( $n=9$ ) from 3 independent experiments  $\pm$ SEM.

Several effects are evident from Figure 4.2 above for CCL-228 colorectal cancer cells. Firstly, there is no significant effect on growth after treatment with RV-3-G and RV-4'-G so, again there was loss of activity. RV and RV-3-S were active, and Z-VAD-FMK did not reverse the inhibitory effects. What is interesting is that even though RV and RV-3-S inhibited growth, 50% inhibition was not achieved. The variable results are seen from the very high error bars. Secondly, in most cases with the exception of actinomycin D the overall percent growth is lower in the pre-treatment group (with Z-VAD-FMK) as compared to the group with treatment alone. Lastly, following ANOVA analysis it was concluded that the two experimental groups i.e. in the presence or absence of Z-VAD-FMK, were not significantly different between themselves ( $p>0.05$ ).

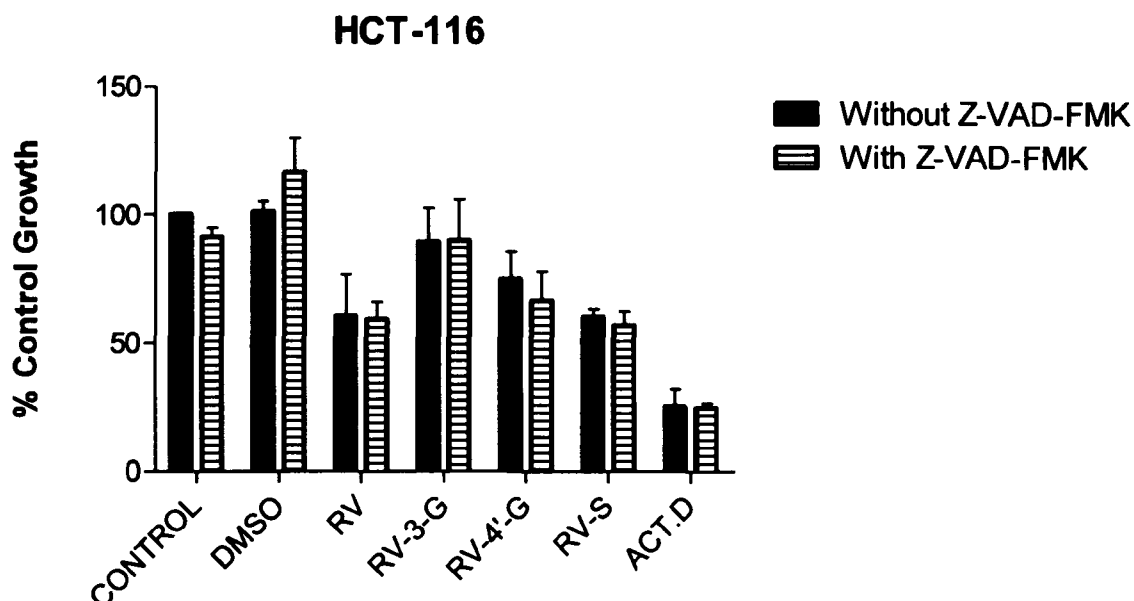


**Figure 4.3** Effect of treatment with compounds of interest (at  $IC_{50}$  concentrations) with or without addition of Z-VAD-FMK ( $50\mu M$ ) on viability of HCT-116 cells. Briefly, cells were incubated with drugs either alone or with Z-VAD-FMK for 48 hours and viability measured using the neutral red uptake assay. Results represent means ( $n=9$ ) from 3 independent experiments  $\pm$ SEM.

The involvement of caspases in the mode of action of resveratrol and its metabolites was also investigated using HCT-116 cells. It is clear that resveratrol, RV-4'-G and RV-3-S appeared active except for RV-3-G where the drug activity was lost again. From Figure 4.3 above it is apparent that there was no difference in growth when cells were pre-treated with the inhibitor and test compound alone. This is best exemplified in the case of resveratrol and actinomycin D. With RV-4'-G and RV-3-S, there was a slight decrease in growth after addition of Z-VAD-FMK. More specifically, with RV-4'-G in the absence of Z-VAD-FMK growth was inhibited by 25% but this increased to 34% in the presence of the caspase inhibitor. After analysis however, all findings were found not be to statistically significant ( $p>0.05$ ). It seems that the caspases are not involved and/or responsible for the effects exerted by resveratrol or the resveratrol metabolites and more studies are warranted to determine the actual molecular pathway. One

suggestion could be that these natural products could be causing cell cycle arrest leading to apoptosis in a caspase-independent manner.

## **4.2 Nuclear morphological evaluation**

Caco-2, CCL-228 and HCT-116 cells were evaluated under fluorescence with DAPI staining under x20 magnification in order to identify any characteristics of apoptosis (nuclear fragmentation for example) and to relate any observations to the Z-VAD-FMK experiment (Section 4.1).

As shown in Figure 4.4, treatment of Caco-2 cells with resveratrol and its metabolites revealed no signs of apoptosis. More specifically, treatment with resveratrol and the three metabolites did not affect the size or fragmentation levels of the nuclei as compared to the untreated and vehicle control groups (Figure 4.4 A&C). Treatment with actinomycin D was sufficient to decrease the number of viable cells and hence the number of nuclei but for all other treatments these numbers remained constant.



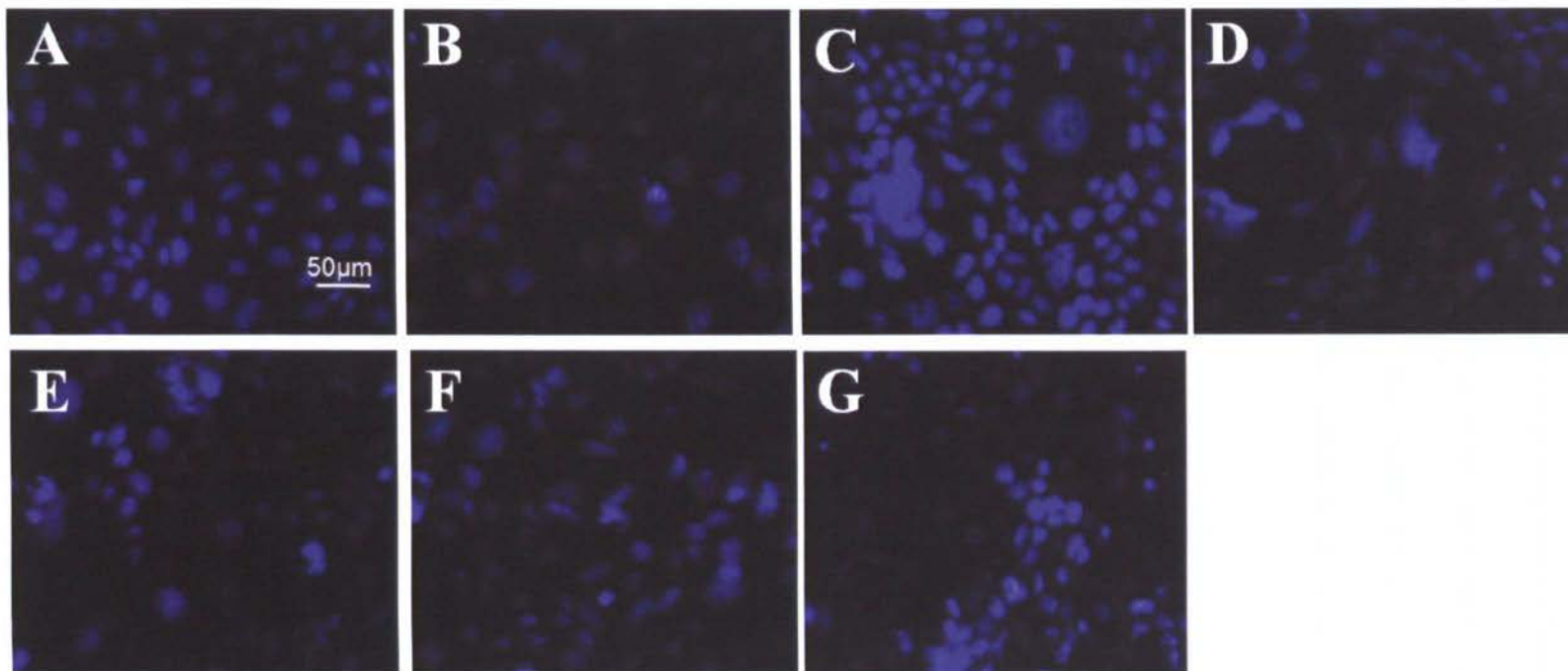


**Figure 4.4** Morphological evaluation of DAPI stained Caco-2 cell nuclei under a fluorescence microscope. Briefly, cells were seeded in chamber slides and 48 hour post treatment cells were fixed and mounting medium containing DAPI was added. Control (A); actinomycin D (B); 0.1% DMSO (C); resveratrol (D); RV3G (E); RV4'G (F); and, RV3S (G). Images are from one experiment but are representative from at least 3 independent experiments. Magnification x200.

In the case of CCL-228 the size of the nuclei were much smaller as compared to Caco-2 primarily due to the smaller size of these cells (Figure 4.5). Untreated cells and those treated with the vehicle displayed no evidence of nuclear fragmentation (Figure 4.5A&C). After treatment with resveratrol and its three metabolites, it was evident that cell numbers were much lower however, cells managed to retain their nuclear size and no signs of apoptosis were evident (Figure 4.5 D-G). In the case of actinomycin D, the number of nuclei was even less compared to all treated and untreated groups (Figure 4.5 B).

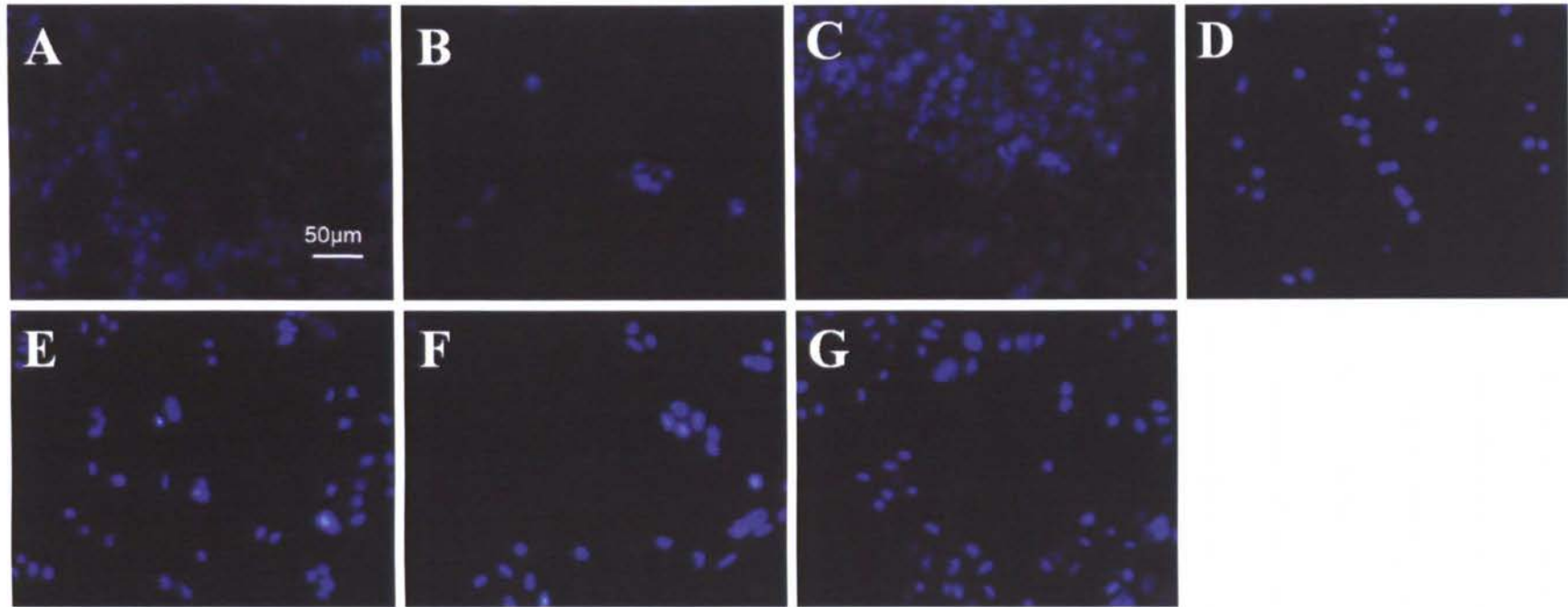


**Figure 4.5** Morphological evaluation of DAPI stained CCL-228 cell nuclei under a fluorescence microscope. Briefly, cells were seeded in chamber slides and 48 hour post treatment cells were fixed and mounting medium containing DAPI was added. Control (A); actinomycin D (B); 0.1% DMSO (C); resveratrol (D); RV3G (E); RV4'G (F); and, RV3S (G). Images are from one experiment but are representative from at least 3 independent experiments. Magnification x200.

DAPI stained untreated HCT-116 nuclei appeared to have the same size as CCL-228 and were more circular with no evidence of cell injury (Figure 4.6A). Treatment with actinomycin D caused a significant reduction in cell numbers but with no sufficient evidence of nuclear fragmentation (Figure 4.6B). Similar morphology to untreated cells was exhibited after treatment with the vehicle control (0.1% DMSO) where the nuclei appeared normal with no signs of damage. In the case of resveratrol treatment, the cell nuclei were significantly less but whether they have undergone injury corresponding to nuclear fragmentation it was not clear (Figure 4.6D). In the case of RV-3-G however, the nuclei were not affected after treatment unlike RV-4'-G where the majority of cells appeared to be like the untreated cells and the vehicle control. With respect to RV-3-S the cell nuclei displayed characteristics similar to untreated cells and those treated with the vehicle control (Figure 4.6G).

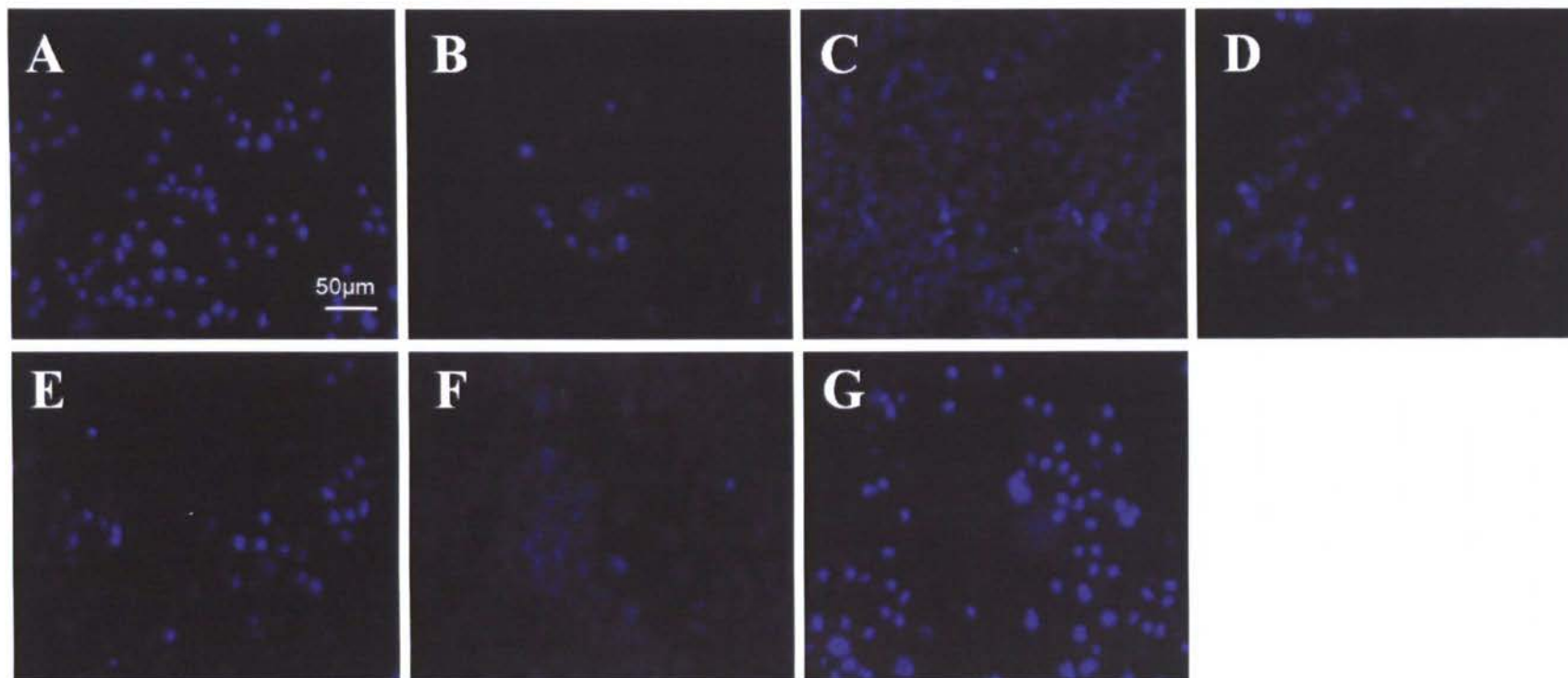


**Figure 4.6** Morphological evaluation of DAPI stained HCT-116 cell nuclei under a fluorescence microscope. Briefly, cells were seeded in chamber slides and 48 hour post treatment cells were fixed and mounting medium containing DAPI was added. Control (A); actinomycin D (B); 0.1% DMSO (C); resveratrol (D); RV3G (E); RV4'G (F); and, RV3S (G). Images are from one experiment but are representative from at least 3 independent experiments. Magnification x200.

### **4.3 Effect of treatment on p53 expression**

In the present study, western blotting and immunostaining were employed in order to determine the p53 expression of treated HCT-116 cells with resveratrol and its metabolites at a range of concentrations. This study was undertaken in order to determine the involvement of the tumour suppressor p53 on the effects seen after treatment with the resveratrol metabolites. HCT-116 was the only cell line used since it expresses a wild-type p53. Caco-2 and CCL-228 on the other hand however possess a mutated p53 status (Liu and Bodmer, 2006).

4.3.1 Protein expression of p53

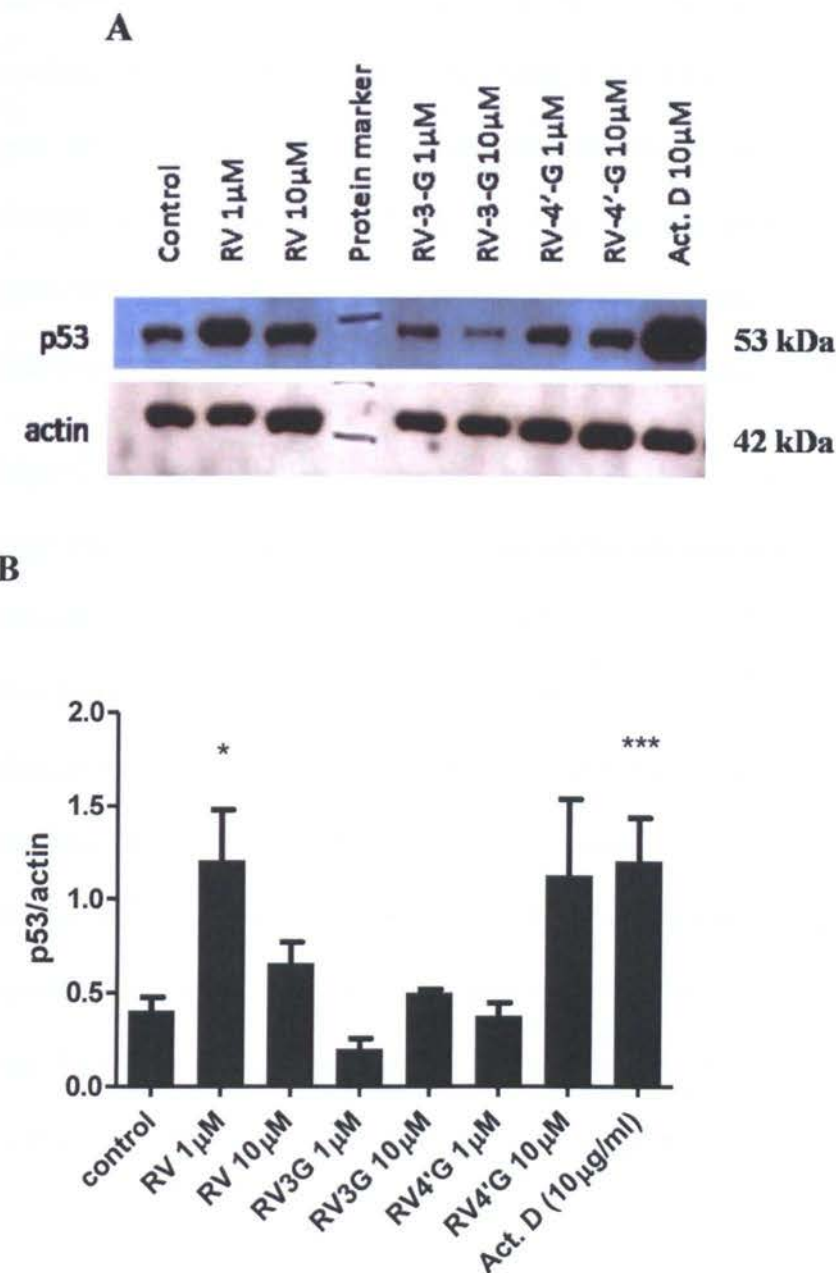


**Figure 4.7** Western blot analysis of p53 after treatment with 1µM and 10µM treatments of resveratrol, RV-3-G, RV-4'-G and actinomycinD. Blot is a representative of at least 3 independent experiments (A); relative values of p53/beta-actin after ImageJ analysis (B). Values represent means of at least 3 independent experiments  $\pm$ SEM. \* $p < 0.05$  and \*\*\* $p < 0.001$  by ANOVA and Tukey's test relative to the control.

From the protein expression profile seen in Figure 4.7 (A) above, it is clear that at 1 $\mu$ M resveratrol treatment the protein levels of p53 increased ( $p<0.05$  compared to the control) as compared to 10 $\mu$ M. In the case of RV-3-G, however, levels were not altered and were comparable to the basal levels (untreated) ( $p>0.05$ ). A greater effect was evident with RV-4'-G at 10 $\mu$ M but, this was not significant after 3 experiments ( $p>0.05$ ). The positive control, actinomycin D, a known p53 inducer (Choong *et al.*, 2009) was shown to considerably increase the protein levels ( $p<0.001$ ).

ImageJ quantification of the protein bands is seen in Figure 4.7 (B). The protein expressions bands were normalised to the respective beta-actin levels. For untreated cells this ratio was approximately  $0.41\pm0.07$  whilst for 1 $\mu$ M RV and 10 $\mu$ g/ml actinomycin D this increased to  $1.21 \pm 0.23$  respectively. At 10 $\mu$ M resveratrol, this was increased slightly to  $0.66\pm0.11$  but in the case of RV-3-G the relative values were comparable to the basal levels ( $0.20\pm0.05$  and  $0.50\pm0.02$  respectively) (Figure 4.7). Analysis of RV-4'-G treatments suggested an increase in p53 with the highest concentration (10 $\mu$ M). More specifically, the relative value increased from  $0.38\pm0.07$  to  $1.13\pm0.41$ . Due to the fact that RV-3-S was not commercially available during this time, protein expression levels of p53 could not be assessed but were included in later immunofluorescent work.



### 4.3.2 Assessment of p53 expression levels by immunofluorescence

Cells were treated for 48 hours and incubated with an antibody raised against p53 and a TRITC conjugated secondary antibody. One image was scored per treatment and DAPI and TRITC stained nuclei were manually counted using ImageJ. Figure 4.8 and Table 4.1 clearly shows the increase in p53 levels after treatment with the positive control, actinomycin D (48%) and also the basal levels of p53 expression in untreated cells (9%). In order to confirm the absence of non-specific binding, untreated cells were incubated with either primary antibody alone (0%) or secondary antibody alone (0%) and the images in Figure 4.8 (C & D) clearly show that cell nuclei were not stained with the red label.

Immunostaining revealed that p53 expression is transient with increasing concentrations of resveratrol, with higher expression at 10 $\mu$ M (19%). At higher concentrations (30 $\mu$ M and 100 $\mu$ M) there was less evidence of p53 activation as for 1 $\mu$ M with the percentage of staining less than the basal levels, suggesting a biphasic response with less effect at higher concentrations (Figure 4.9 A-D). Overall, it is clear that at the two highest concentrations for all treatments, that p53 levels decreased below the basal levels (Figures 4.9, 4.11 and 4.12). Unlike the results from Figure 4.7 above for RV-3-G, the immunofluorescence images suggest that p53 levels are increased after 1 $\mu$ M and 10 $\mu$ M treatments relative to untreated HCT-116 cells (16% and 25% respectively) (Figure 4.10). The images from Figure 4.11 confirm the western blot results for RV-4'-G treatment where p53 levels were greater at 10 $\mu$ M treatments (9%) as compared to 1 $\mu$ M (1%). A noteworthy point for RV-3-S was that with increasing drug concentrations, the expression levels of p53 decreased (Figure 4.12). For example, 1 $\mu$ M and 10 $\mu$ M

treatments led to 45% and 29% of cells being stained with p53 as compared to 30 $\mu$ M (6%).

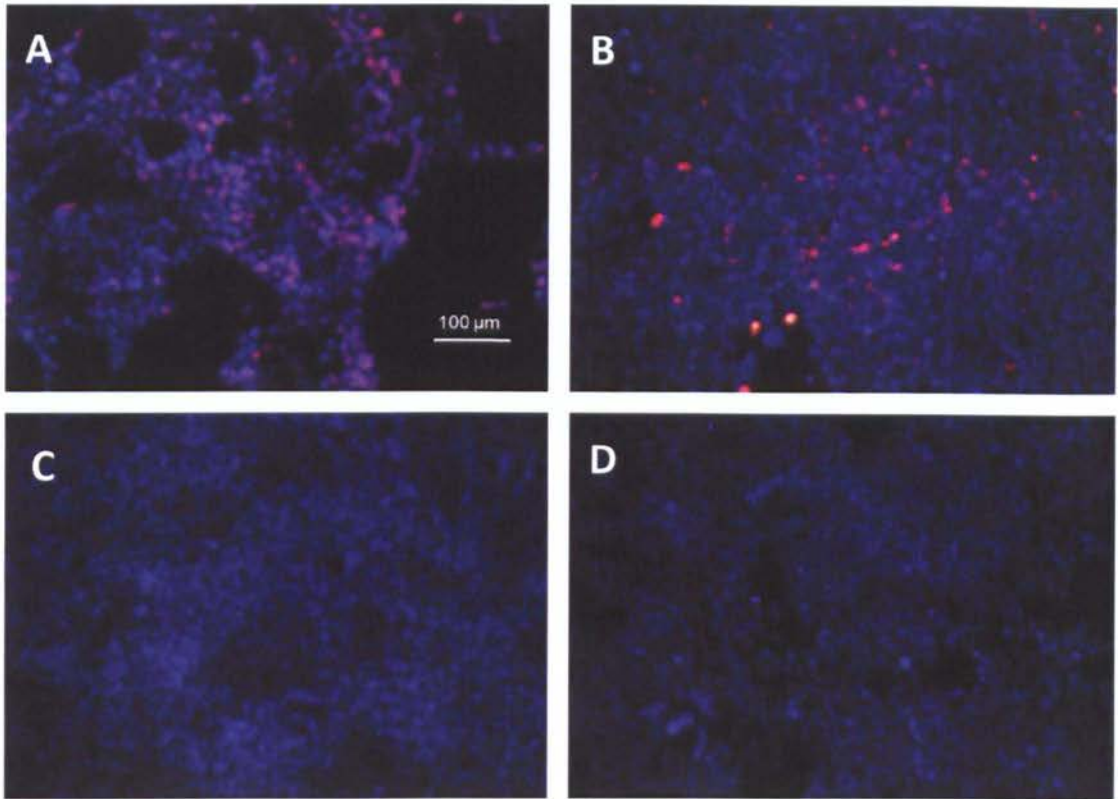


**Figure 4.8** Immunofluorescence of HCT-116 for p53 expression after treatment with 10 $\mu$ g/ml actinomycin D (A); untreated in the presence of primary and secondary antibodies (B); untreated (only with primary antibody) (C); and, untreated (only with secondary antibody) (D). Cells were treated for 48 hours and further incubated with an antibody raised against p53 for one hour followed by a TRITC-labelled anti-mouse secondary antibody. Images were captured at x100 magnification using a fluorescence microscope and are representative of three independent experiments.

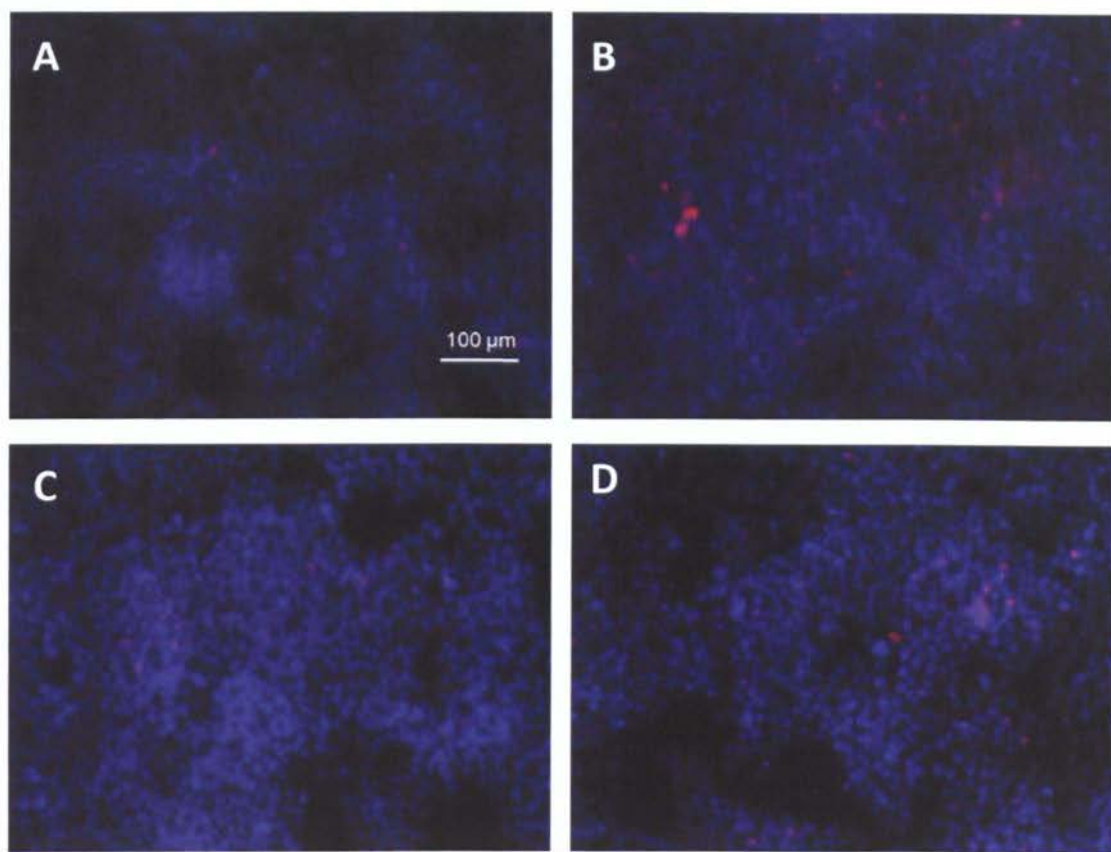


**Figure 4.9** Immunofluorescence of HCT-116 for p53 expression after treatment with resveratrol. Cells were treated for 48 hours and further incubated with an antibody raised against p53 for one hour followed by a TRITC-labelled anti-mouse secondary antibody. (A) resveratrol 1 $\mu$ M; (B) resveratrol 10 $\mu$ M; (C) resveratrol 30 $\mu$ M; and (D) resveratrol 100 $\mu$ M. Images were captured at x100 magnification using a fluorescence microscope and are representative of three independent experiments.

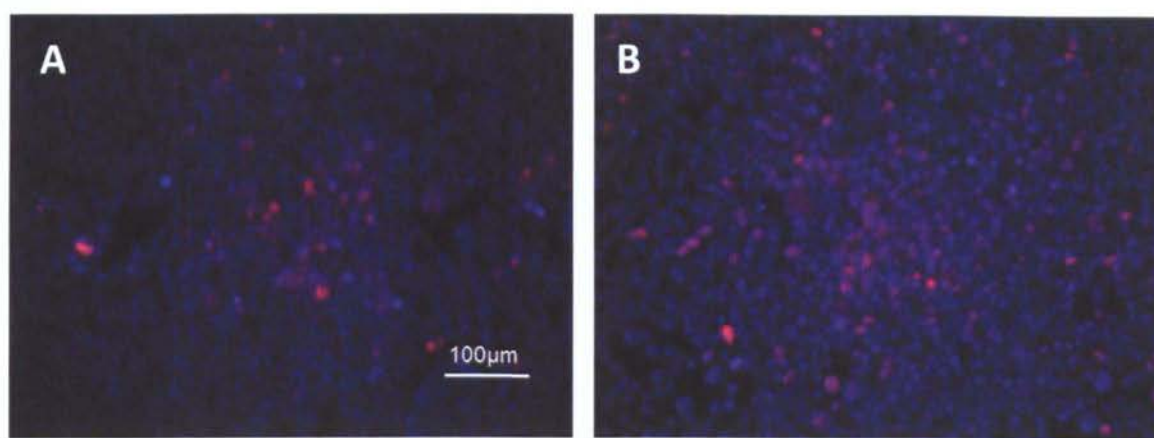


**Figure 4.10** Immunofluorescence of HCT-116 for p53 expression after treatment with resveratrol-3-O-D-glucuronide. Cells were treated for 48 hours and further incubated with an antibody raised against p53 for one hour followed by a TRITC-labelled anti-mouse secondary antibody. (A) RV-3-G 1µM; (B) RV-3-G 10µM. Images were captured at x100 magnification using a fluorescence microscope and are representative of three independent experiments.

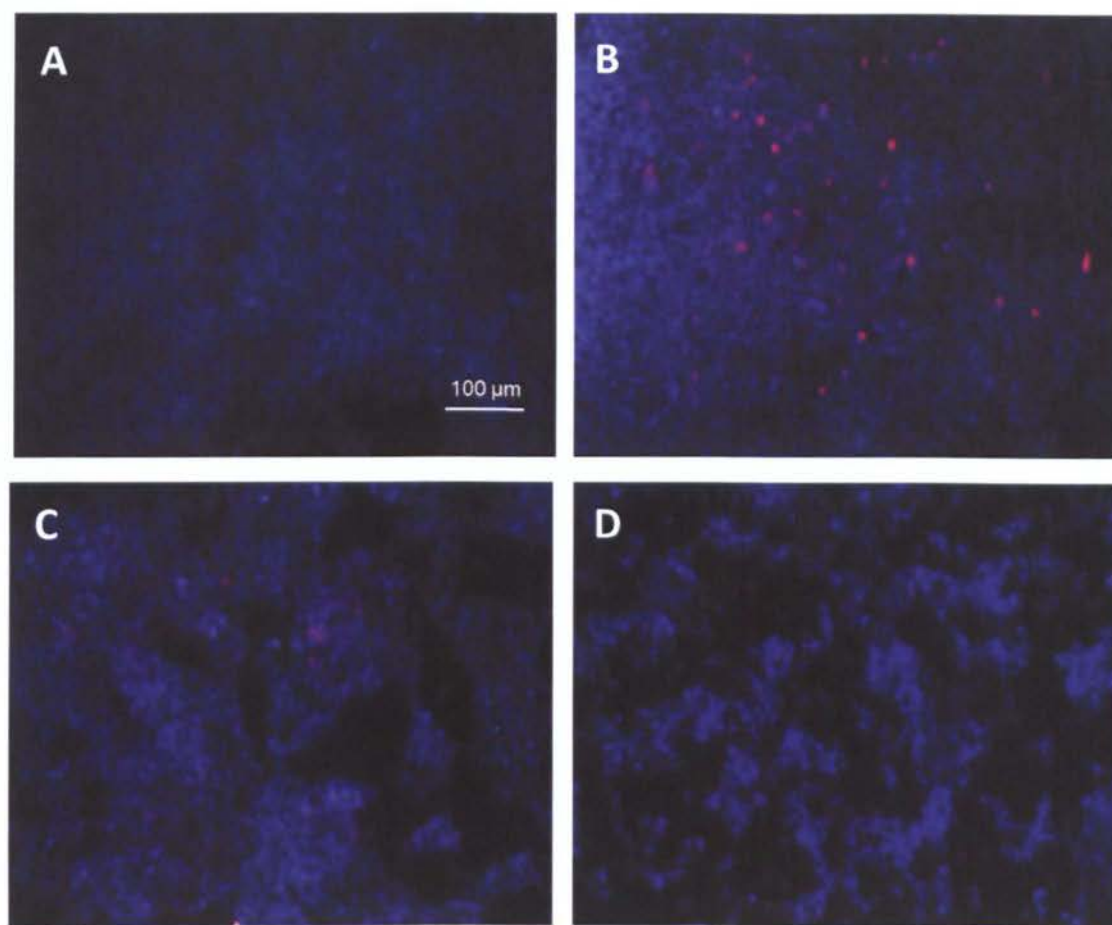


**Figure 4.11** Immunofluorescence of HCT-116 for p53 expression after treatment with resveratrol-4'-O-D-glucuronide. Cells were treated for 48 hours and further incubated with an antibody raised against p53 for one hour followed by a TRITC-labelled anti-mouse secondary antibody. (A) RV-4'-G 1 $\mu$ M; (B) RV-4'-G 10 $\mu$ M; (C) RV-4'-G 30 $\mu$ M; and (D) RV-4'-G 100 $\mu$ M. Images were captured at x100 magnification using a fluorescence microscope and are representative of three independent experiments.



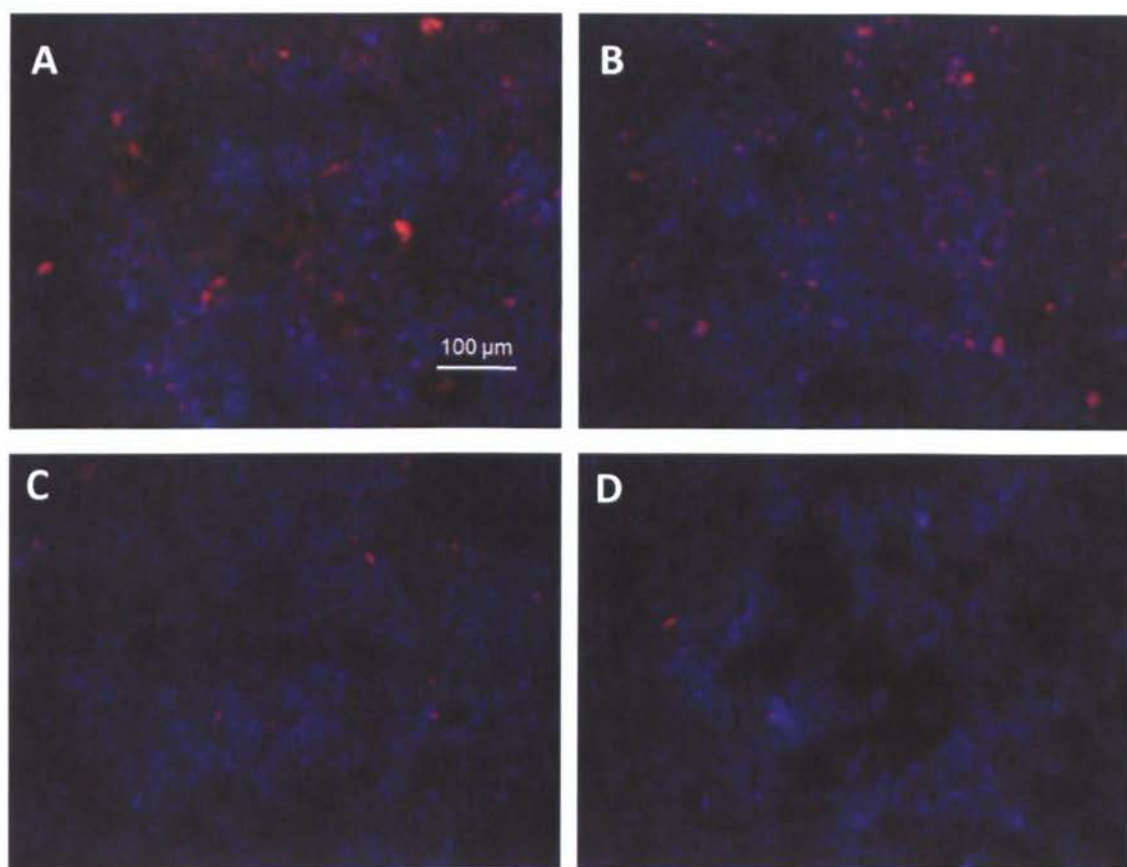


**Figure 4.12** Immunofluorescence of HCT-116 for p53 expression after treatment with resveratrol-3-O-D-sulphate. Cells were treated for 48 hours and further incubated with an antibody raised against p53 for one hour followed by a TRITC-labelled anti-mouse secondary antibody. (A) RV-3-S 1 $\mu$ M; (B) RV-3-S 10 $\mu$ M; (C) RV-3-S 30 $\mu$ M; and (D) RV-3-S 100 $\mu$ M. Images were captured at  $\times 100$  magnification using a fluorescence microscope and are representative of three independent experiments.

**Table 4.1** ImageJ quantification of p53-immunofluorescence images following treatment with resveratrol and metabolites.

<b>Treatment</b>	<b>Number of TRITC stained cells</b>	<b>Number of DAPI stained cells</b>	<b>Percentage of p53 positive TRITC cells</b>
Act. D	253	525	48%
Control (1° and 2° Ab)	100	1133	9%
Control (1° only)	2	1115	0%
Control (2° only)	0	980	0%
RV 1 $\mu$ M	24	1166	2%
RV 10 $\mu$ M	149	803	19%
RV 30 $\mu$ M	50	974	5%
RV 100 $\mu$ M	43	849	5%
RV-3-G 1 $\mu$ M	146	892	16%
RV-3-G 10 $\mu$ M	240	974	25%
RV-4'-G 1 $\mu$ M	8	1013	1%
RV-4'-G 10 $\mu$ M	91	975	9%
RV-4'-G 30 $\mu$ M	47	928	5%
RV-4'-G 100 $\mu$ M	5	647	1%
RV-3-S 1 $\mu$ M	323	725	45%
RV-3-S 10 $\mu$ M	257	891	29%
RV-3-S 30 $\mu$ M	52	809	6%
RV-3-S 100 $\mu$ M	34	693	5%

#### **4.4 Cell cycle distribution analysis**

The main interest in examining the effects of resveratrol and its metabolites on the cell cycle progression in exponentially dividing cells and the degree of apoptosis arose after the findings from the previous sections where it was suggested that the metabolites do not exert any apoptotic effects on cells. This experiment was a follow up of the growth inhibition studies from the previous chapter. Due to the fact that the main interest was the simultaneous investigation of growth inhibition, cell cycle arrest and apoptosis in the three cell lines, only one concentration was used for the subsequent experiments. The chosen concentration is greater than the  $IC_{50}$  ( $\sim IC_{70}$ ) for each cell line used since  $30\mu M$  is the top end of all the  $IC_{50}$  values and a sufficient concentration to observe the maximal effects. Treated cells were labelled with PI/RNase solution and analysed by flow cytometry as described in Section 2.5.1.

##### **4.4.1 Caco-2**

Caco-2 cells were treated with  $30\mu M$  of compounds of interest (resveratrol, RV-3-G, RV-4'-G and RV-3-S),  $10\mu g/ml$  actinomycin D and 0.1% DMSO alone for 48 hours and images acquired prior to analysis (Figure 4.13 A-F). Treatment with  $10\mu g/ml$  actinomycin D clearly shows that cell numbers were significantly reduced, revealing a large number of floating dead cells as compared to untreated cells where the morphology was different; adherent cells (Figure 4.13 A and B respectively). In the case of resveratrol treatment, there was no evidence of dead or apoptotic cells but, cells appeared larger in size. Forty-eight hour treatment with RV-3-G seemed to decrease the number of Caco-2 cells. In agreement with this, treatment with the two other metabolites, RV-4'-G and RV-3-S led to alteration of the morphology. More



specifically, it seemed that cells treated with the metabolites lost their characteristic epithelial morphology.

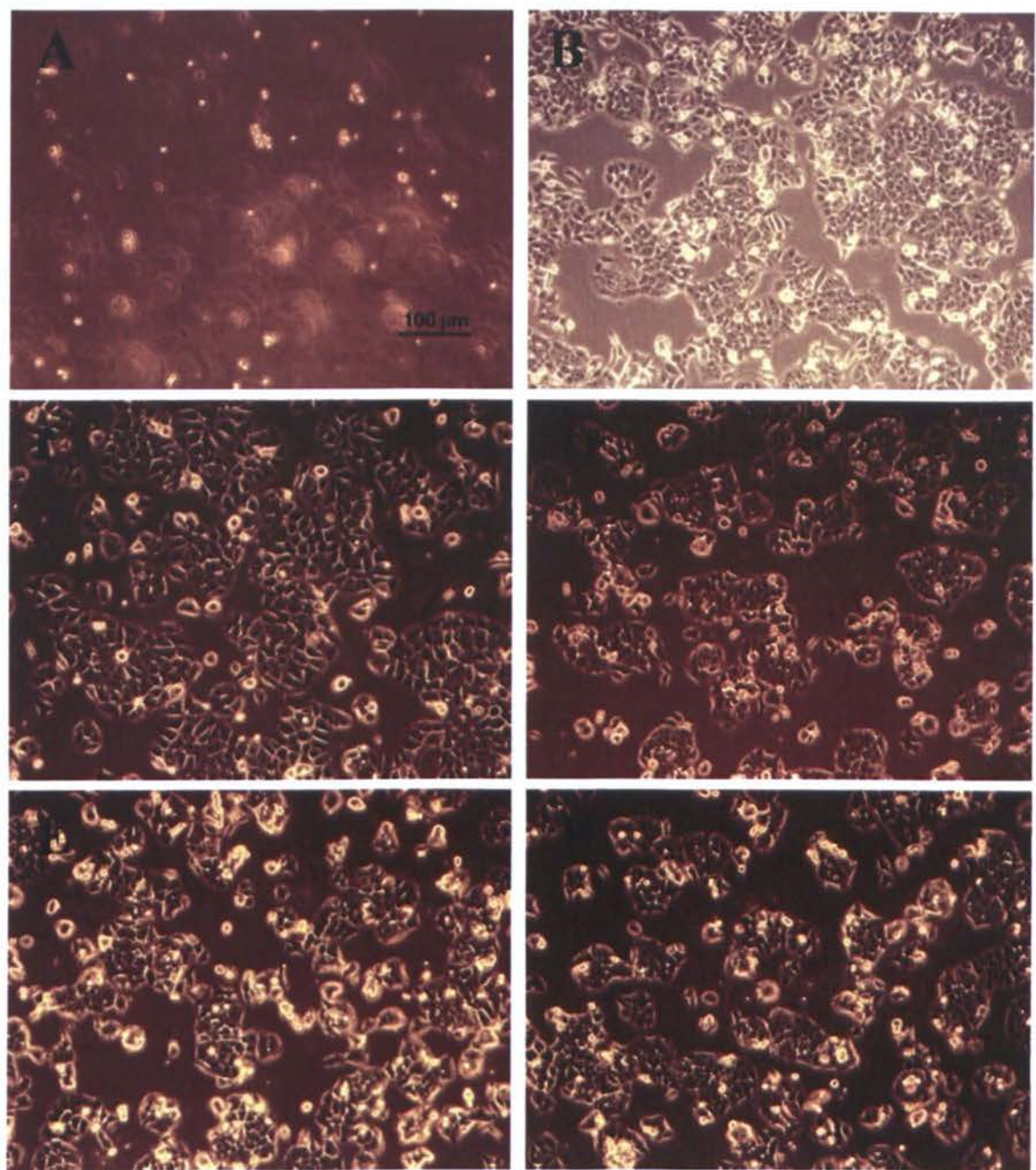


**Figure 4.13**Photomicrographs of Caco-2 cells after treatment with 10µg/ml actinomycin D (A); control untreated (B); 30µM resveratrol (C); 30µM resveratrol-3-O-D-glucuronide (D); 30µM resveratrol-4'-O-D-glucuronide (E); and, 30µM resveratrol-3-O-D-sulphate (F) for 48 hours. Magnification X100.

Figure 4.14 represents the flow cytometry plots after analysis. The first dot plot displays the distribution of cells according to the side and forward scatter where in this instance the cells of interest were labelled red. This cell population was later gated to exclude dead cells, doublets and cell aggregates in order to calculate the cell distribution in the various phases (Figure 4.14B). The FL3-A/FL3-W plot in Figure 4.14B was used to discriminate between single cells and doublets. This was done by plotting the area (FL3-A) of the fluorescence light pulse versus the width (FL3-W). Doublets possess a greater pulse width as compared to single cells primarily due to the fact that they require a longer time to pass through the laser beam. In order to identify the number and percentage of cells in sub-G1 (apoptotic cells), the gate was extended to zero. Any dead cells would therefore appear below 200RFU. Figure 4.14D represents a basic histogram of the distribution of untreated cells. The first peak represents the distribution of cells in G0/G1 appearing at 200RFU. The flat peak following the G0/G1 peak represents the cell population in S phase whilst the last peak just before 400RFU, G2/M. If there any sign of apoptosis, a peak would appear prior to the distinct G0/G1 peak. The same procedure was repeated for all treatments but only histograms and percentages of cells in each phase of the cell cycle are presented here.

Seen in Figures 4.14 and 4.15 are the histogram results for Caco-2 cells. Resveratrol caused a significant increase in the number of cells in S phase of the cell cycle with a subsequent decrease in G0/G1 and G2/M phases respectively, suggesting an S phase arrest (Figure 4.15). In the cases of RV-3-G and RV-4'-G however, it was noteworthy to point that they caused cell arrest in G0/G1 with the percentage of cells reaching even higher levels relative to control untreated and the vehicle control (0.1% DMSO). As for RV-3-S treatment, the histogram was similar to the other metabolites but the difference was not significant relative to the control. The positive control actinomycin D, a

compound known to arrest cells at G0/G1 was also shown here. This arrest was accompanied by a concomitant decrease in S and G2/M phases and a significant portion of cells in sub-G1.

Table 4.2 further illustrated the proportion of cells in each phase of the cell cycle. It is clearly evident that resveratrol caused cell cycle arrest in S phase whilst RV-3-G and RV-4'-G along with actinomycin D, a G0/G1 arrest. The distribution of cells after RV-3-S treatment appears to remain unaltered (comparable to the control untreated group). For example treatment with RV-3-G increased the proportion of cells in G0/G1 from 48.58% to 55.30% (average of 3 independent experiments) ( $p < 0.0001$  for 3/3 experiments using a contingency –chi squared test analysing cell numbers in G0/G1 versus non G0/G1) whilst this was further increased after RV-4'-G treatment (66.05%). Despite the fact that treatment with RV-3-S increased the proportion of cells in G0/G1 by approximately 5.5%, this increase was not significant. In the case of resveratrol the percentage of cells in S phase was increased from 19.88% (vehicle control) to 28.93% ( $p < 0.05$ ).

The percentage of cells in the sub-G1 phase (apoptotic peak) was minimal for the metabolites after 48 hours treatment (RV-3-G- 1.44%  $\pm$  0.86%; RV-3-S- 1.35%  $\pm$  0.78%) as compared to resveratrol (3.07%  $\pm$  1.05%) except in the case of RV-4'-G where apoptosis was greater (3.2%  $\pm$  1.39%) (Tables 4.2 & 4.3). In agreement with the histogram for actinomycin D, apoptosis reached 10.66%  $\pm$  3.55% ( $p < 0.05$ ).

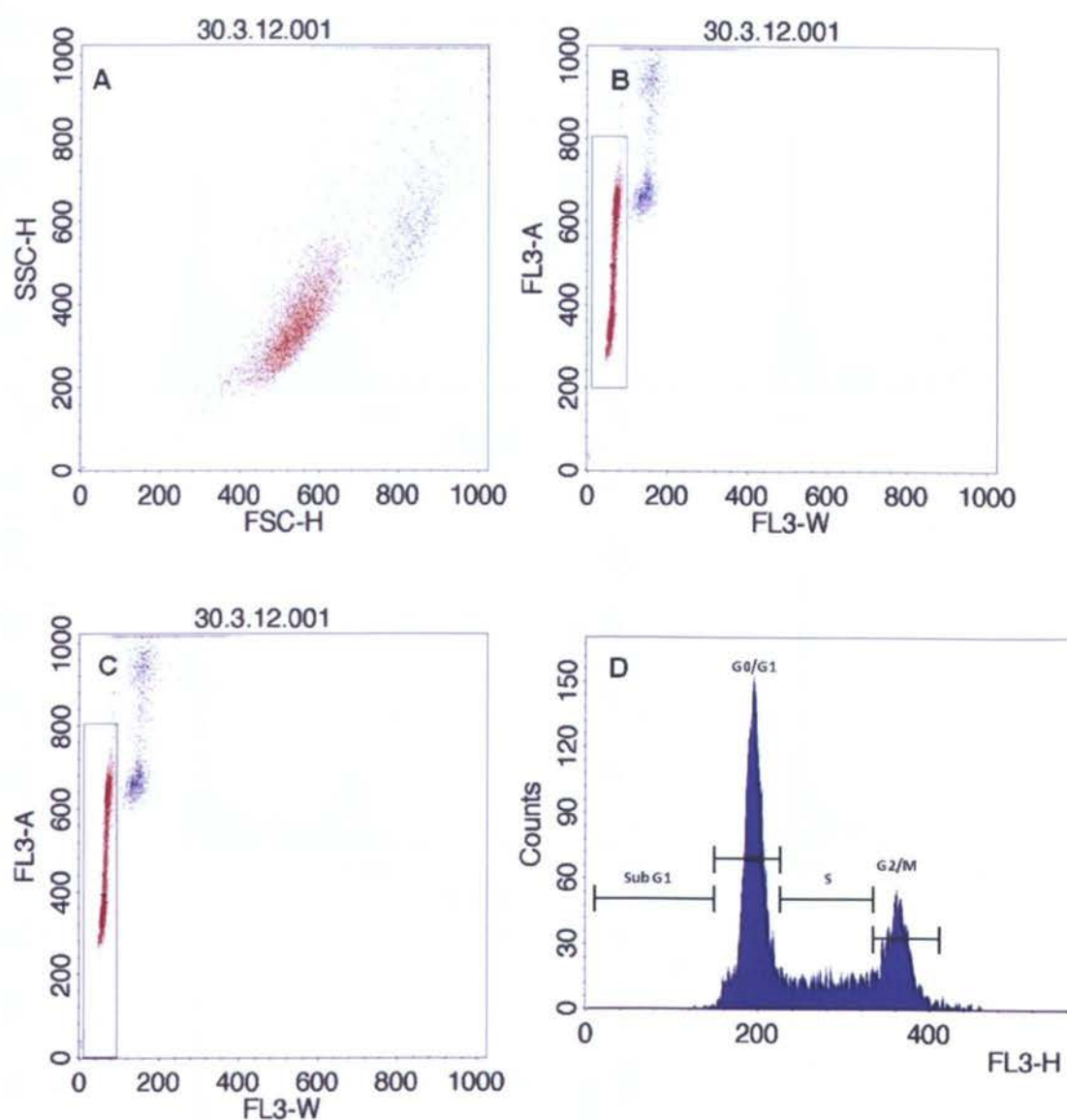


**Figure 4.14** Cell cycle analysis of untreated Caco-2 cells. After 48 hours of incubation, cells were labelled with PI/RNase solution and analysed by flow cytometry. Forward scatter versus side scatter dot plot (A); dot plot of gated cells excluding sub-G1 (B); dot plot illustrating gated cells including dead cells (C); and, histogram representing cell cycle analysis (D). All four figures are given as reference and therefore only histograms are shown for each treatment below.



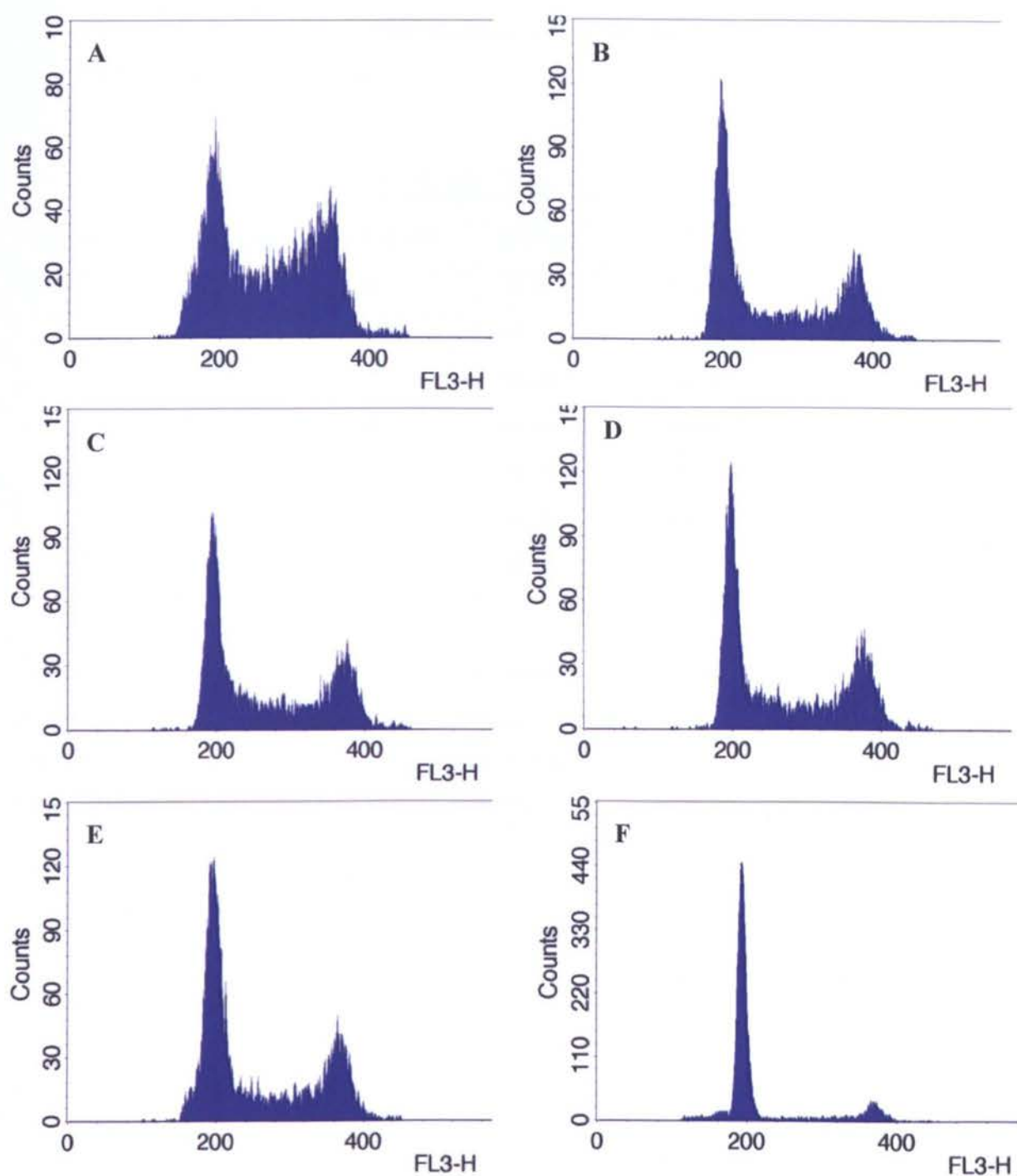


**Figure 4.15** Histogram representing cell cycle analysis of Caco-2 cells. After 48 hours of incubation, cells were labelled with PI/RNase solution and analysed by flow cytometry. Resveratrol (A); resveratrol-3-O-D-glucuronide (B); resveratrol-4'-O-D-glucuronide (C); resveratrol-3-O-D-sulphate (D); DMSO (E); and, Actinomycin D (F). All experiments were performed in triplicate and independent experiments gave similar results.

**Table 4.2** Cell cycle distribution of Caco-2 human cancer cell line after treatment for 48 hours with DMSO or compounds of interest.

Cell line	Treatment	Distribution (% cells) <sup>+</sup>			
		Sub-G1	G0/G1	S	G2/M
Caco-2	DMSO	1.02	48.58	19.88	23.08
	RV	3.07	44.39	<b>28.93*</b>	17.88
	RV3G	1.44	<b>55.30*</b>	18.68	21.47
	RV4'G	3.02	<b>66.05*</b>	13.94	15.48
	RVS	1.35	53.95	20.60	20.90
	Act.D	<b>10.66*</b>	<b>72.28*</b>	8.41	11.24
	Control	1.77	48.46	23.46	24.94

+ DNA content was analysed after staining with PI/RNase solution. The data represent the mean percentage of gated cells of three independent experiments in each phase of the cell cycle.  
\* statistical significance in all three independent experiments relative to the proportion of cells in the specific phase of the cell cycle relative to DMSO.

**Table 4.3** Representation of the number of gated Caco-2 cells in each phase of the cell cycle per experiment. Relative ratios were calculated by dividing cell numbers in each phase by total number of cells. If this ratio was greater than that of vehicle cells, a chi-squared contingency test was carried out per experiment to calculate the significance of treatments per phase of the cell cycle relative to control untreated.

NUMBER OF GATED CELLS PER EXPERIMENT								
		CONTROL	RV	RV3G	RV4'G	RV3S	ACT.D	DMSO
1 <sup>st</sup> experiment	G0/G1	3008	3012	3331	3904	3360	3223	2678
2 <sup>nd</sup> experiment	G0/G1	1258	2490	2592	6106	2329	1831	2844
3rd experiment	G0/G1	3934	2492	3052	3234	3241	6513	3594
1 <sup>st</sup> experiment	S	1511	1911	1056	809	978	514	1220
2 <sup>nd</sup> experiment	S	959	1744	1350	886	1321	253	1212
3 <sup>rd</sup> experiment	S	1167	1557	719	974	1084	395	1019
1 <sup>st</sup> experiment	G2/M	986	225	786	753	867	423	1011
2 <sup>nd</sup> experiment	G2/M	937	1436	1580	867	1418	402	1618
3 <sup>rd</sup> experiment	G2/M	1479	1601	1200	1304	1145	803	1443

The results from the cell cycle distribution were analysed by  $\chi^2$  analysis. The proportion of cells in S phase from one experiment following treatment with resveratrol for example, were divided by the total number of cells from all three phases. So, by considering the results of the first experiment, the number of cells in S phase following resveratrol treatment were divided by the total number of cells (1911+1744+1557). Therefore,  $1911/5148 = 0.371$ .

If this value was greater than the results of the vehicle control (DMSO) (in this case  $1220/4909 = 0.249$ ) this indicated an increase in the number of cells in S phase following treatment (4909 is the total number of cells in the three phases, 1220+1212+1019). Therefore, the total number of cells in S phase vs non S phase for resveratrol were analysed relative to the cells in S phase vs non S phase for DMSO for each independent experiment. Arrest in a specific phase of the cell cycle was only considered significant if all three experiments were statistically significant. In the example presented below, it seemed that treatment of Caco-2 cells with resveratrol caused S phase arrest relative to the vehicle control.

<u>Treatment</u>	<u>S phase</u>	<u>non-S phase</u>
Resveratrol	1911	3237
DMSO	1220	3689

**4.4.2 CCL-228**

The effect on the cell morphology after treatment with various compounds was also investigated in CCL-228 cells (Figure 4.16 A-F). It is apparent that after treatment with actinomycin D for 48 hours, cells were not capable of dividing with a significant reduction in numbers as compared to untreated cells. In the case of untreated cells, numbers were much greater with almost complete confluence (Figure 4.16B). Similar to



the Caco-2 images, following treatment with resveratrol and the three metabolites, the appearance of the cells was similar to those that were untreated (Figure 4.16 D-F).

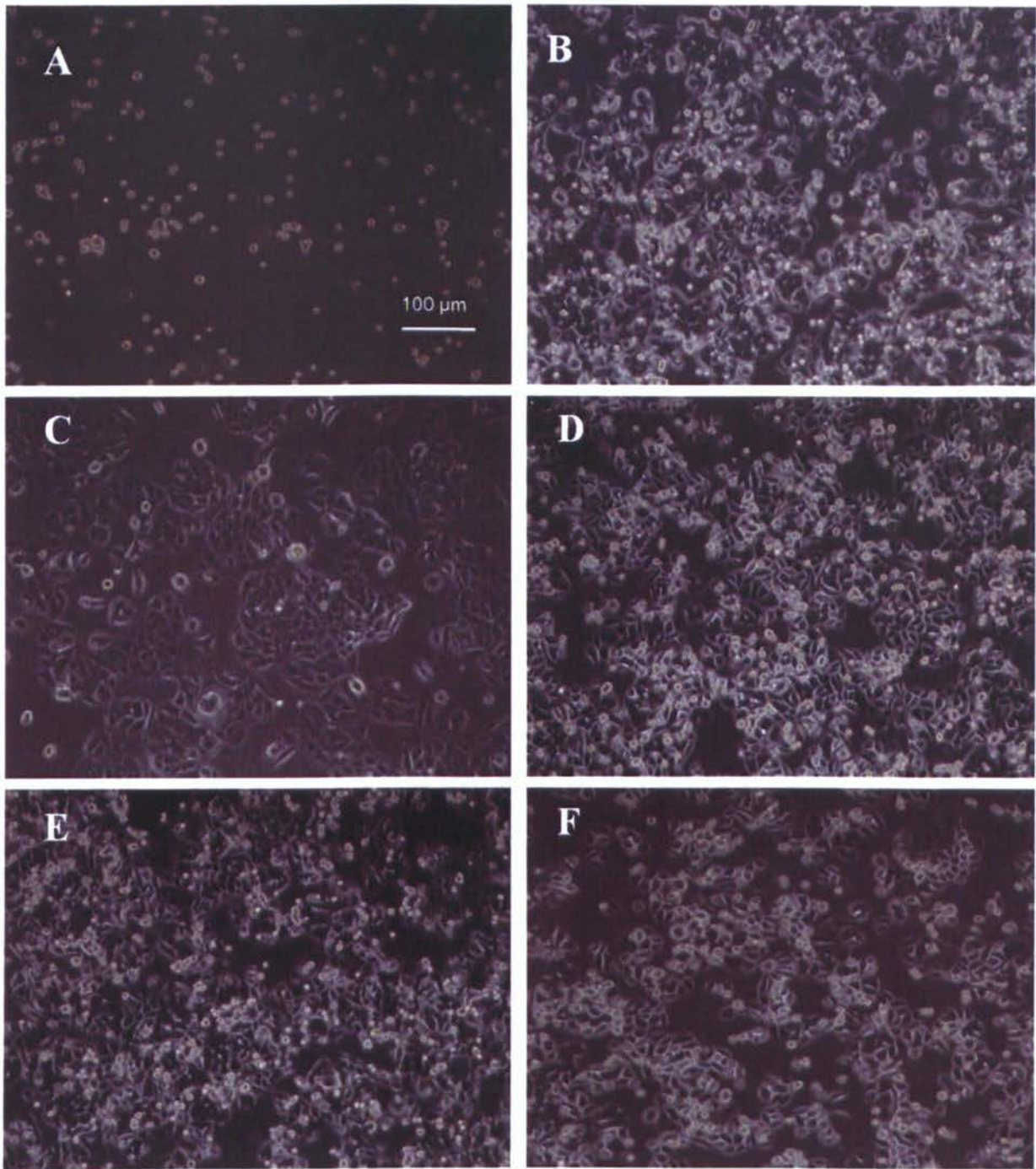


**Figure 4.16** Photomicrographs of CCL-228 cells after treatment with 10µg/ml actinomycin D (A); control untreated (B); 30µM resveratrol (C); 30µM resveratrol-3-O-D-glucuronide (D); 30µM resveratrol-4'-O-D-glucuronide (E); 30µM resveratrol-3-O-D-sulphate (F) for 48 hours. Magnification X100.

The histogram in Figure 4.17D for untreated cells displays the high proportion of cells in G0/G1 phase with a smaller population in S and G2/M accordingly. The distribution of cells after treatment with resveratrol was completely altered; the G0/G1 peak was not a steep distinct peak like the control and the S phase was much greater as compared to the control (Figure 4.18A). It is evident that in all the other histograms (Figure 4.18B-F), the distribution of cells was similar to that of the control except in the case of actinomycin D where there was some degree of apoptosis evident by the presence of cells below 200RFU (G0/G1 peak).

As with the results for Caco-2, treatment with resveratrol caused an arrest in S phase (from 18.9% to 30% relative to untreated cells), followed by a decrease in G0/G1 whilst the G2/M phase was unaffected (Table 4.4). Cells treated with resveratrol metabolites had a different effect as compared to the parent compound. The percentage of CCL-228 cells, like Caco-2 was increased in G0/G1 phase followed by a decrease in S phase. More specifically, in the case of RV-3-G, the percentage of cells in G0/G1 increased from 68% (vehicle control) to 75.2% ( $p < 0.001$  for all 3 independent experiments) whilst for RV-4'-G and RV-3-S, 71.6% ( $p < 0.001$  for all 3 experiments) and 69.1% ( $p > 0.05$ ) respectively (Table 4.4).

As with the Caco-2 cells, the metabolites did not seem to exert a profound effect regarding apoptosis with levels comparable to untreated cells (Table 4.4). More specifically, the percent apoptosis for RV-3-G, RV-4'-G and RV-3-S was 0.45%, 0.39% and 0.41% respectively (Table 4.4). In the case of resveratrol and actinomycin D however, the proportion of cells in sub-G1 corresponded to 6.82% and 3.92% respectively ( $p < 0.05$ ) (Table 4.4). This is an interesting finding which provides an insight into the mechanism of action of the metabolites and suggests that they act

differently to the parent compound. The results also suggest that resveratrol causes apoptosis in CCL-228 cells but, this was not supported by data from the other assays.

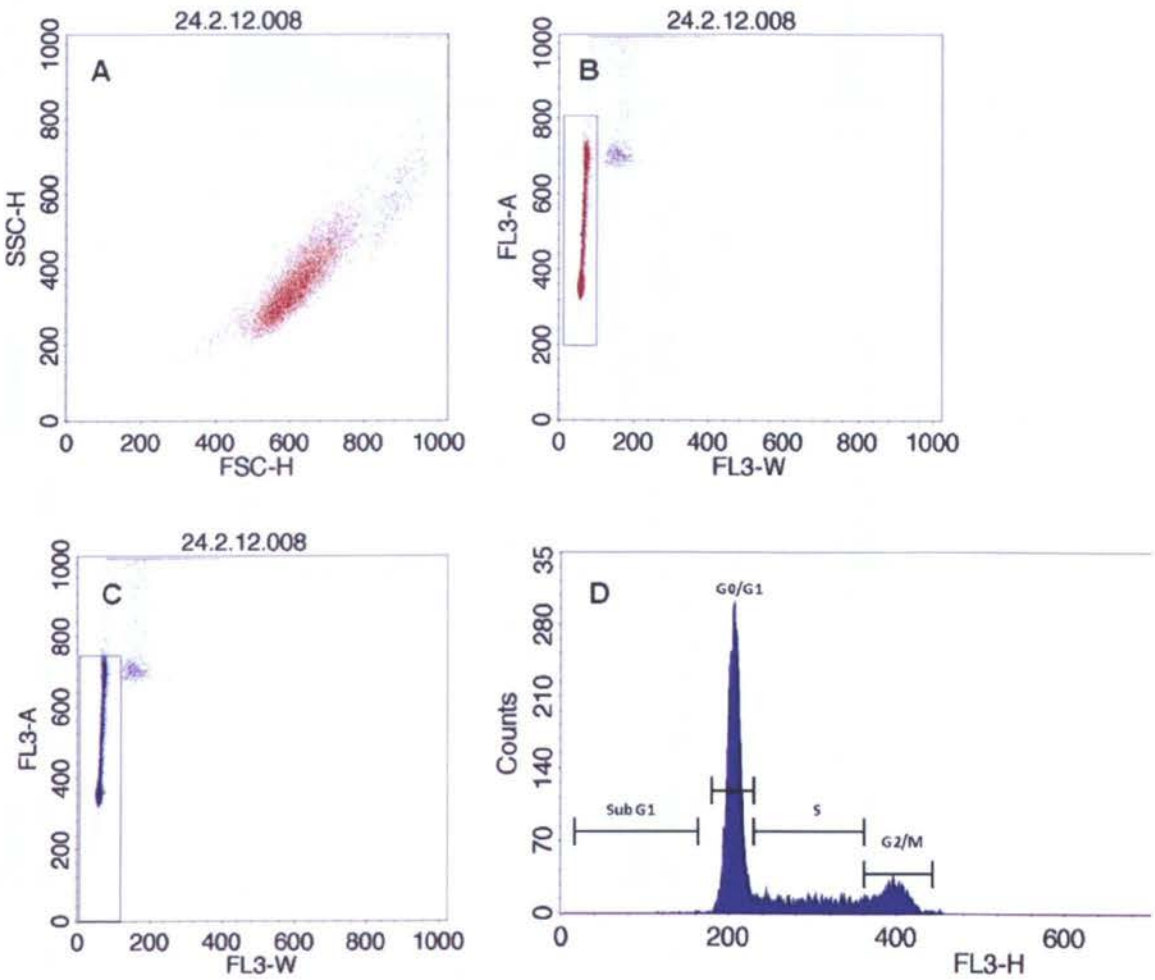


**Figure 4.17** Cell cycle analysis of untreated CCL-228 cells. After 48 hours of incubation, cells were labelled with PI/RNase solution and analysed by flow cytometry. Forward scatter versus side scatter dot plot (A); dot plot of gated cells excluding sub-G1 (B); dot plot illustrating gated cells including dead cells (C); and, histogram representing cell cycle analysis (D). All four figures are given as reference and therefore only histograms are shown for each treatment below.

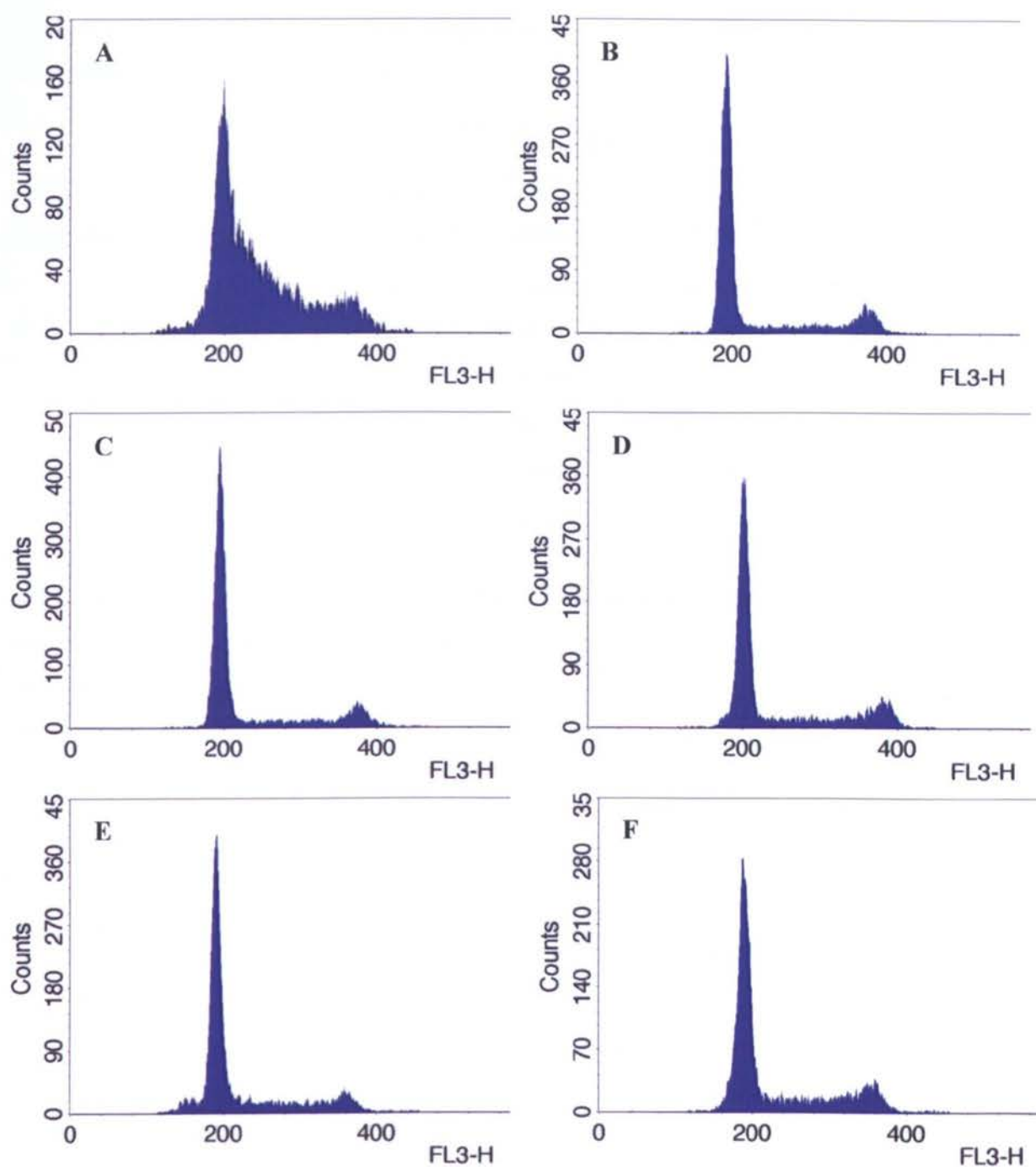


**Figure 4.18** Histogram representing cell cycle analysis of CCL-228 cells. After 48 hours of incubation, cells were labelled with PI/RNase solution and analysed by flow cytometry. Resveratrol (A); resveratrol-3-O-D-glucuronide (B); resveratrol-4'-O-D-glucuronide (C); resveratrol-3-O-D-sulphate (D); Actinomycin D (E); and, DMSO (F). All experiments were performed in triplicate and independent experiments gave similar results. Chi-squared contingency statistical analysis was carried out using GraphPad Prism.

**Table 4.4** Cell cycle distribution of CCL-228 human cancer cell line after treatment for 48 hours with DMSO or compounds of interest.

		Distribution (% cells) <sup>+</sup>			
Cell line	Treatment	Sub-G1	G0/G1	S	G2/M
CCL-228	DMSO	0.88	68.00	18.90	13.10
	RV	<b>6.82*</b>	55.60	<b>30.00*</b>	14.40
	RV3G	0.45	<b>75.20*</b>	10.80	14.00
	RV4'G	0.39	<b>71.60*</b>	13.30	15.10
	RVS	0.41	69.10	15.30	15.60
	Act.D	<b>3.92*</b>	<b>78.50*</b>	12.00	9.50
	Control	0.41	66.20	18.10	15.60

+ DNA content was analysed after staining with PI/RNase solution. The data represent the mean percentage of cells of three independent experiments in each phase of the cell cycle. \* statistical significance in all three independent experiments relative to the proportion of cells in the specific phase of the cell cycle relative to DMSO.



**Table 4.5** Representation of the number of gated CCL-228 cells in each phase of the cell cycle per experiment. Relative ratios were calculated by dividing cell numbers in each phase by total number of cells. If this ratio was greater than that of vehicle cells, a chi-squared contingency test was carried out per experiment to calculate the significance of treatments per phase of the cell cycle relative to control untreated.

		NUMBER OF GATED CELLS PER EXPERIMENT						
		CONTROL	RV	RV3G	RV4'G	RV3S	ACT.D	DMSO
1 <sup>st</sup> experiment	G0/G1	5401	4677	6702	6821	6095	6460	4725
2 <sup>nd</sup> experiment	G0/G1	5796	4232	6645	6473	5532	6889	5998
3 <sup>rd</sup> experiment	G0/G1	5552	3233	6890	5558	6275	6746	5688
1 <sup>st</sup> experiment	S	1709	2774	858	882	1244	1260	2376
2 <sup>nd</sup> experiment	S	1577	847	1235	1270	1684	1101	763
3 <sup>rd</sup> experiment	S	1303	2930	822	1353	1039	721	1411
1 <sup>st</sup> experiment	G2/M	1126	765	1157	1070	1273	818	1534
2 <sup>nd</sup> experiment	G2/M	1531	727	1293	1299	1398	998	714
3 <sup>rd</sup> experiment	G2/M	1296	1661	1322	1604	1372	611	923

#### 4.4.3 HCT-116

Depicted in Figure 4.19 are the images for HCT-116 cells prior to cell cycle distribution analysis. The morphology of cells after treatment with actinomycin D was completely altered and appeared that the cells were not capable of dividing, primarily due to the fact that the majority of the cells detached from the flask and remained floating. When comparing this to untreated cells and those treated with the vehicle control, the scenario is different where almost complete confluence was seen (Figure 4.19 B&D). As for resveratrol treatment, despite the fact that cells were capable of multiplying, they appeared morphologically different and slightly larger. In the case of the resveratrol

metabolites the cell morphology appeared to be similar to the untreated cells (Figure 4.19 E-G).

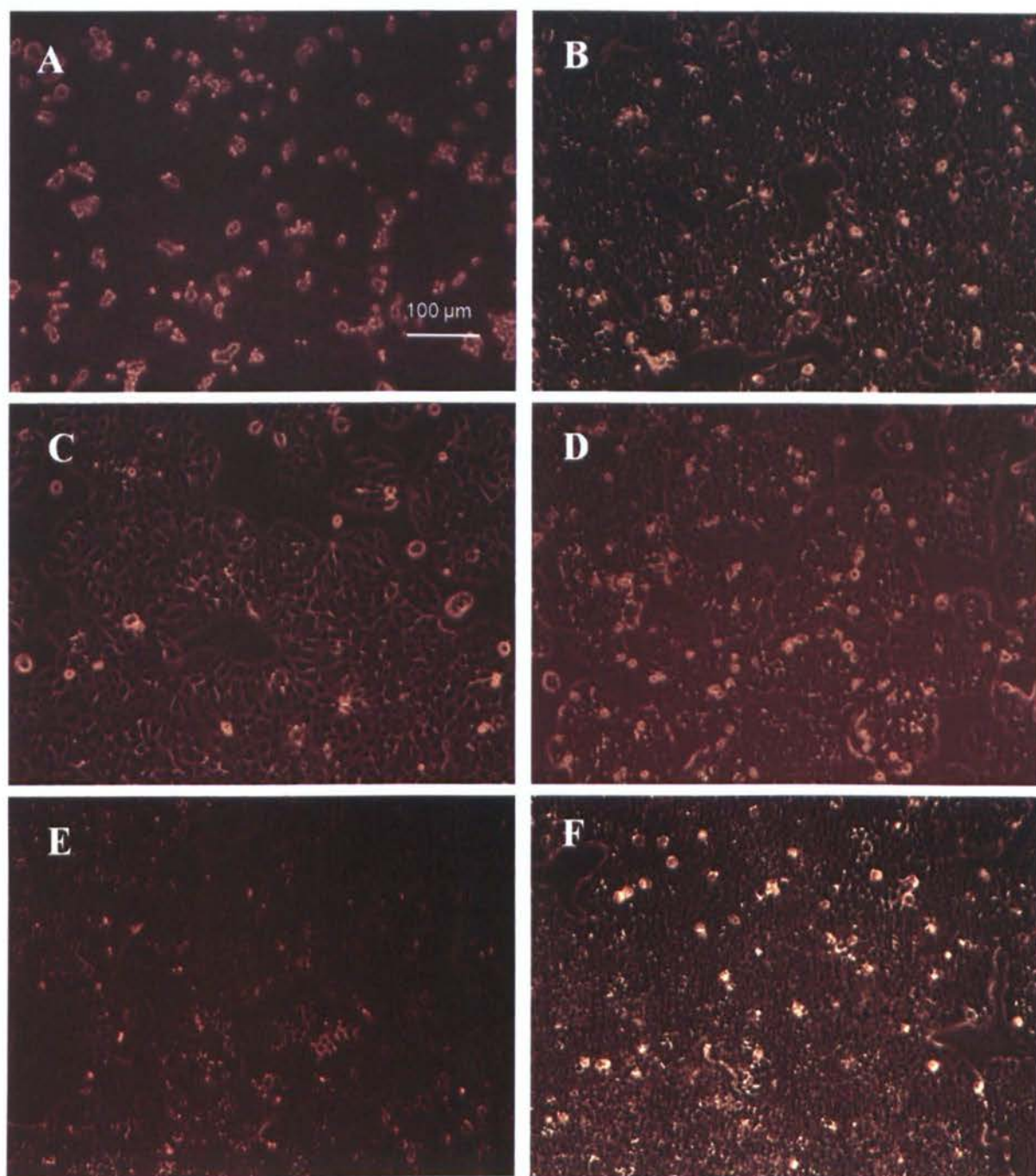


**Figure 4.19** Photomicrographs of HCT-116 cells after treatment with 10μg/ml actinomycin D (A); control untreated (B); 30μM resveratrol (C);30μM resveratrol-4'-O-D-glucuronide (D); 30μM resveratrol-3-O-D-glucuronide (E); and, 30μM resveratrol-3-O-D-sulphate (F) for 48 hours. Magnification X100.

As shown in Figure 4.20D, in untreated cells the majority of cells were normally distributed in G0/G1 and smaller populations in S and G2/M. In the case of resveratrol, an increase of cells in S phase was observed, whilst RV-3-G treatment led to a decrease in S phase with a constant proportion in G0/G1 (Figure 4.21 A&B). The histogram illustration of the distribution of cells after treatment with RV-4'-G was found to be similar to that of untreated cells whilst for RV-3-S, a decrease in S phase was evident. As for actinomycin D, there was a steep increase in G0/G1 followed by almost complete absence of cells in S phase, a decrease in G2/M and some degree of apoptosis evident by the cell population in sub-G1. The distribution of cells in the case of the vehicle control was similar to the untreated group (Figure 4.21).

HCT-116 cells did not seem to be arrested in any phase of the cell cycle by the resveratrol metabolites. Unlike the other two cell lines, there is no evidence of arrest in G0/G1 with the percentage of cells being comparable to untreated cells and to the vehicle control accordingly. More specifically, the normal distribution of untreated cells in G0/G1 was found to be 65.67% and after treatment with the metabolites, this changed to 63.73%, 62.35% and 62.79% for RV-3-G, RV-4'-G and RV-3-S respectively (Table 4.6). Treatment with resveratrol, however, appears to be consistent with the previously mentioned results. There was a profound increase in cells in S phase consistent with inhibition of DNA synthesis (from 13.3% to 25%) ( $p < 0.001$  for 3/3 independent experiments comparing cells in S phase against non-S phase) (Table 4.6). The only significant treatment in the case of HCT-116 cells was actinomycin D with G0/G1 arrest and the percentage of cells reaching 76.23% ( $p < 0.05$ ).

The sub-G1 peaks for all treatments appear to be greater in HCT-116 cells as compared to Caco-2 and CCL-228 but due to the large variation in error these were not statistically significant (Table 4.6). It is also apparent that the mean values for the



percentage of cells in sub-G1 in the untreated and vehicle control groups are quite high ( $7.87\% \pm 4.42\%$  and  $7.08\% \pm 5.98\%$  respectively). Overall however, there was no evidence of apoptosis after treatment with resveratrol or its metabolites.

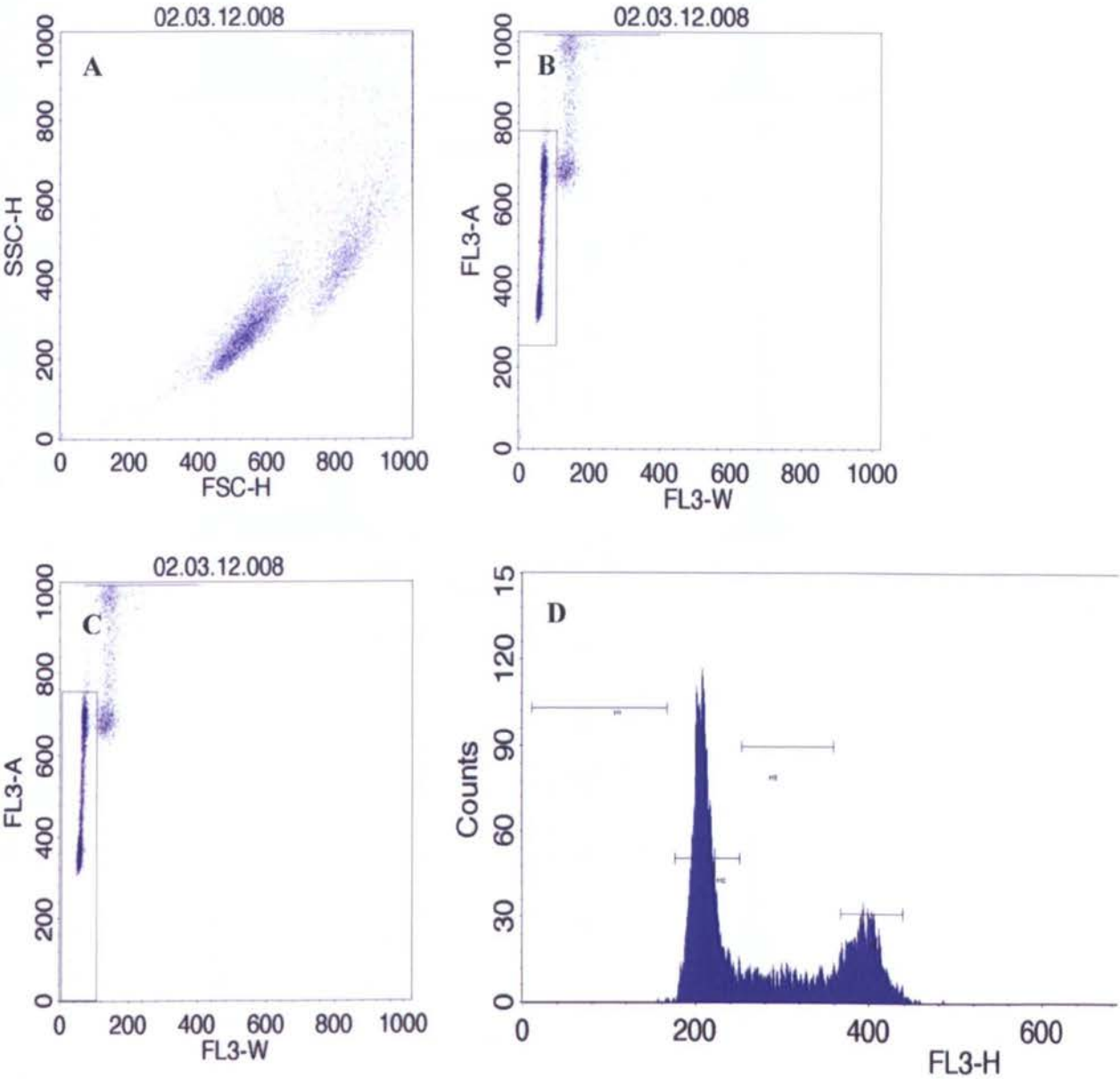


**Figure 4.20** Cell cycle analysis of untreated HCT-116 cells. After 48 hours of incubation, cells were labelled with PI/RNase solution and analysed by flow cytometry. Forward scatter versus side scatter dot plot (A); dot plot of gated cells excluding sub-G1 (B); dot plot illustrating gated cells including dead cells (C); and, histogram representing cell cycle analysis (D). All four figures are given as reference and therefore only histograms are shown for each treatment below.

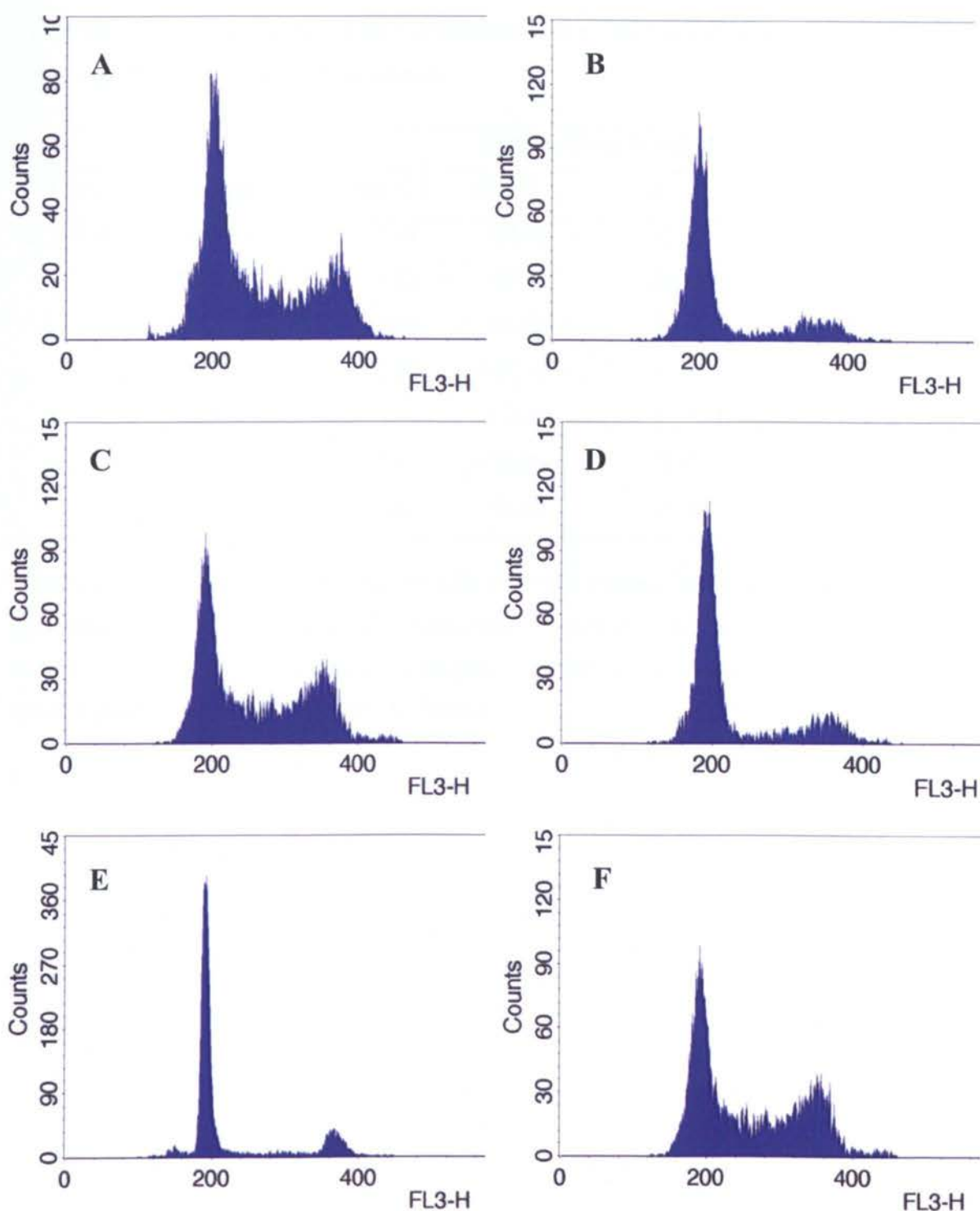


**Figure 4.21** Histogram representing cell cycle analysis of HCT-116 cells. After 48 hours of incubation, cells were labelled with PI/RNase solution and analysed by flow cytometry. Resveratrol (A); resveratrol-3-O-D-glucuronide (B); resveratrol-4'-O-D-glucuronide (C); resveratrol-3-O-D-sulphate (D); Actinomycin D (E); and, DMSO (F). All experiments were performed in triplicate and independent experiments gave similar results. Chi-squared contingency statistical analysis was carried out using GraphPad Prism.

**Table 4.6** Cell cycle distribution of HCT-116 human cancer cell line after treatment for 48 hours with DMSO or compounds of interest.

Cell line	Treatment	Distribution (% cells) <sup>+</sup>			
		Sub-G1	G0/G1	S	G2/M
HCT-116	DMSO	7.08	64.23	15.50	10.16
	RV	3.52	50.24	<b>24.98*</b>	18.70
	RV3G	9.96	63.73	13.55	11.93
	RV4'G	2.27	62.35	15.60	18.31
	RVS	7.70	62.79	15.88	11.16
	Act.D	2.32	<b>76.23*</b>	6.07	13.96
	Control	7.87	65.67	13.33	11.23

+ DNA content was analysed after staining with PI/RNase solution. The data represent the mean percentage of cells of three independent experiments in each phase of the cell cycle.\* statistical significance in all three independent experiments relative to the proportion of cells in the specific phase of the cell cycle relative to DMSO.

**Table 4.7** Representation of the number of gated HCT-116 cells in each phase of the cell cycle per experiment. Relative ratios were calculated by dividing cell numbers in each phase by total number of cells. If this ratio was greater than that of untreated cells, a chi-squared contingency test was carried out per experiment to calculate the significance of treatments per phase of the cell cycle relative to control untreated.

NUMBER OF GATED CELLS PER EXPERIMENT								
		CONTROL	RV	RV3G	RV4'G	RV3S	ACT.D	DMSO
1 <sup>st</sup> experiment	G0/G1	2981	3074	2554	2559	2467	6059	2944
2 <sup>nd</sup> experiment	G0/G1	1270	2644	1507	2711	1561	5396	1420
3 <sup>rd</sup> experiment	G0/G1	3575	2607	2838	2178	2911	ND	3443
1 <sup>st</sup> experiment	S	852	1028	803	555	1165	432	1467
2 <sup>nd</sup> experiment	S	267	1563	323	1078	333	385	313
3 <sup>rd</sup> experiment	S	474	1479	315	351	384	ND	313
1 <sup>st</sup> experiment	G2/M	1232	1712	965	1034	922	1062	1100
2 <sup>nd</sup> experiment	G2/M	65	598	74	828	76	807	63
3 <sup>rd</sup> experiment	G2/M	317	925	425	413	441	ND	379

\* ND- not determined

**4.4 Cell cycle distribution analysis (concentration-dependent effects using resveratrol and RV-3-G and CCL-228 cells)**

We further selected to compare the effects of increasing concentrations of resveratrol and one of its metabolites, RV-3-G on the CCL-228 cells which gave the most consistent results. Preliminary experiments were therefore carried out as previously but, CCL-228 cells were treated with 1µM, 3µM, 10µM and 30µM of either resveratrol or RV-3-G.

**Table 4.8** Cell cycle distribution analysis of CCL-228 cells treated with varying concentrations of resveratrol and resveratrol-3-O-D-glucuronide for 48 hours.

		Distribution (% cells)*			
Cell line	Treatment	Sub-G1	G0/G1	S	G2/M
CCL-228					
RV	DMSO	1.79	71.91	12.39	11.76
	Control	2.71	71.02	13.60	11.19
	1µM	2.26	73.14	12.45	11.35
	3µM	1.59	69.50	14.62	11.82
	10µM	1.53	62.31	19.99*	12.47
	30µM	9.64*	45.29	29.03*	14.84
RV-3-G	1µM	1.63	70.88	13.83	11.29
	3µM	1.53	71.24	13.51	11.47
	10µM	1.11	73.33	12.18	11.19
	30µM	0.87	73.84*	12.14	11.70
	Act.D	3.56	72.58	11.89	8.71

\* p<0.05 by  $\chi^2$  analysis of independent experiments.

It is evident from Table 4.8 that S phase arrest after treatment with resveratrol was dose-dependent and the effect became more profound at 30 $\mu$ M. More specifically, with 1 $\mu$ M and 3 $\mu$ M resveratrol treatments, the distribution of cells was comparable to the control and vehicle control ( $p>0.05$ ). Only at 10 $\mu$ M a significant difference occurred ( $p<0.05$ ) becoming even more profound at 30 $\mu$ M with the percentage of cells in the S phase reaching 19.99% and 29.03% respectively (control 13.6%). In the case of cells in sub-G1, no apoptosis was evident at concentrations below 30 $\mu$ M with values comparable to untreated cells. At 30 $\mu$ M however, the percent apoptosis was 9.64% $\pm$ 0.11% (Table 4.8).

In the case of RV-3-G where G0/G1 arrest was evident at 30 $\mu$ M from the previous experiment, it was clear that significant arrest was initiated from 30 $\mu$ M (73.84%) with no significant difference relative to the control at the lower concentrations of 1 $\mu$ M (70.88%  $\pm$  8.07%) and 3 $\mu$ M (71.24% $\pm$ 7.86%) for example (Table 4.8). The results from the dose-response experiment were in agreement with the cell cycle distribution analysis at 30 $\mu$ M from Section 4.3. More specifically, the mean percentages of cells in sub-G1 for all four concentrations of interest were not significantly different to either the control or vehicle control.

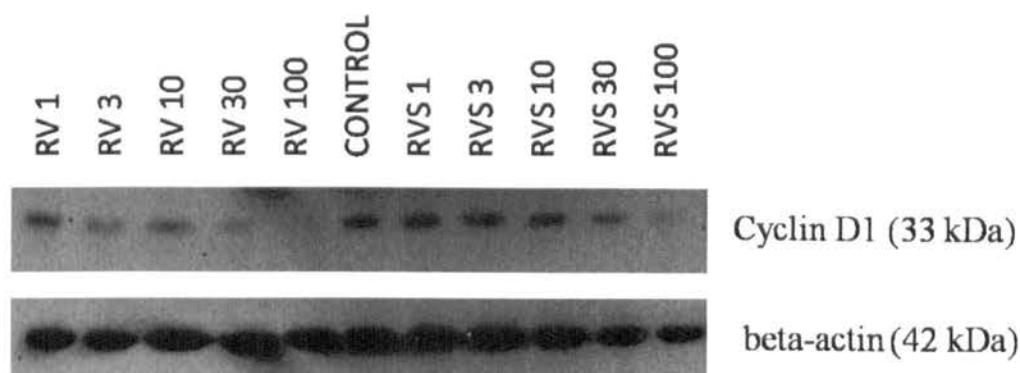
#### **4.4 Effects of resveratrol and metabolite treatments on cyclin D1 levels**

The results from the flow cytometry analysis on the cell cycle distribution suggested a G0/G1 arrest after treatment with 30 $\mu$ M of RV-3G and RV-4'-G. It therefore decided to investigate the effect of various concentrations (same used for the growth studies in Chapter 2) on the expression of cyclin D1 by western blot.

The results from the cyclin D1 blots after treatment with resveratrol and resveratrol-3-O-D-sulphate at 1 $\mu$ M, 3 $\mu$ M, 10 $\mu$ M, 30 $\mu$ M and 100 $\mu$ M concentrations are presented in Figure 4.22. Results showed that the levels of cyclinD1 normalised to beta-actin decreased at 30 $\mu$ M and 100 $\mu$ M resveratrol ( $p<0.01$  and  $p<0.001$  respectively) with no significant effect of treatment at lower concentrations. In the case of resveratrol-3-O-D-sulphate, concentrations up to 30 $\mu$ M were not sufficient to block the expression of cyclin D1 ( $p>0.05$ ) and a significant effect was only evident at 100 $\mu$ M ( $p<0.05$ ). Similar to untreated cells, there was no effect of treatment with 0.1% DMSO on the levels of cyclin D1 unlike actinomycin D (10 $\mu$ g/ml) where it was clearly evident that cyclin D1 was completely inhibited (data not shown).

It is apparent from Figure 4.23 that with increasing concentrations of RV-3-G and RV-4'-G, the cyclin D1 levels decreased and were almost completely diminished at 100 $\mu$ M in a dose-dependent manner. This however was only significant with 100 $\mu$ M RV-3-G treatment ( $p<0.05$ ) and not RV-4'-G ( $p>0.05$ ). After treatment with lower concentrations (up to 30 $\mu$ M), there was no significant difference relative to the untreated group. The expression levels of cyclin D1 did not seem to be affected after treatment with the vehicle control suggesting no effect of DMSO (data not shown).

A



B

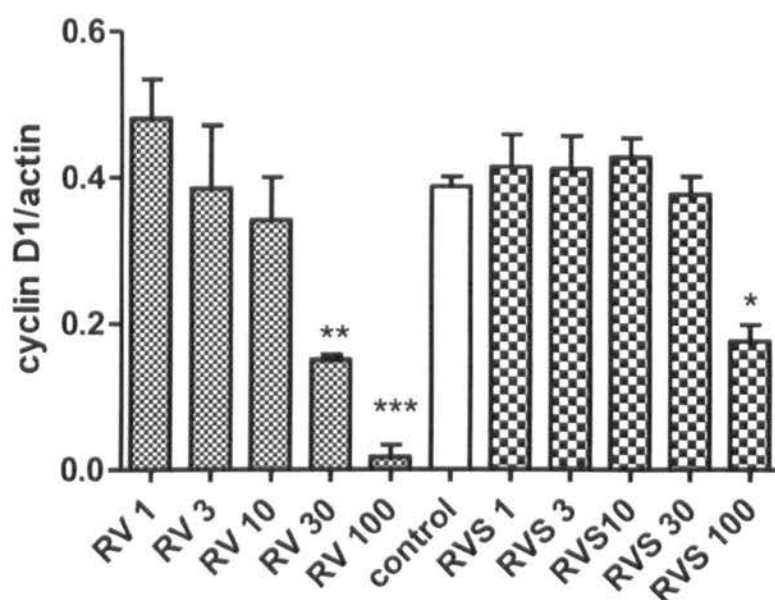
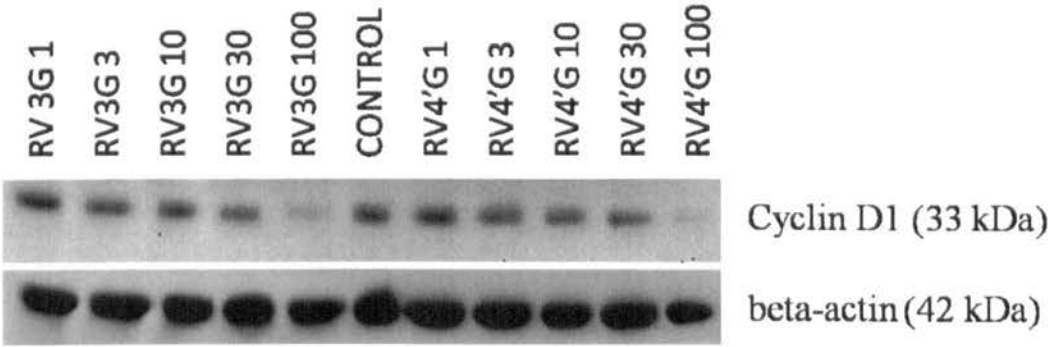


**Figure 4.22** Effect of 1 $\mu$ M, 3 $\mu$ M, 10 $\mu$ M, 30 $\mu$ M and 100 $\mu$ M resveratrol and resveratrol-3-sulphate treatments on the cyclin D1 levels of Caco-2 cells. (A) Western blot of cyclin D1 and beta-actin. Blot is representative of three independent experiments. (B) ImageJ analysis of the cyclin D1 levels normalised to beta-actin. Values represent means of three independent experiments  $\pm$ SEM. \*  $p < 0.05$ , \*\*  $p < 0.01$  and \*\*\*  $p < 0.001$  by repeated measures ANOVA and Dunnett's test relative to the untreated group.



A



B

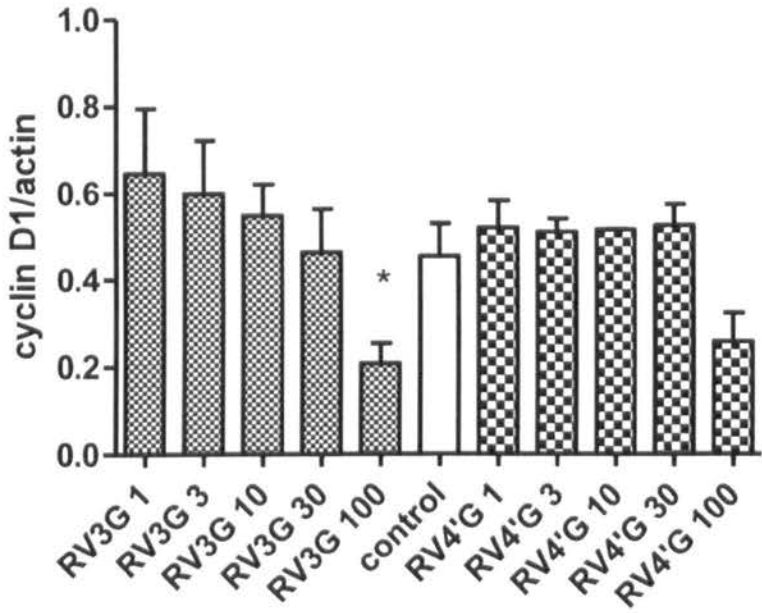
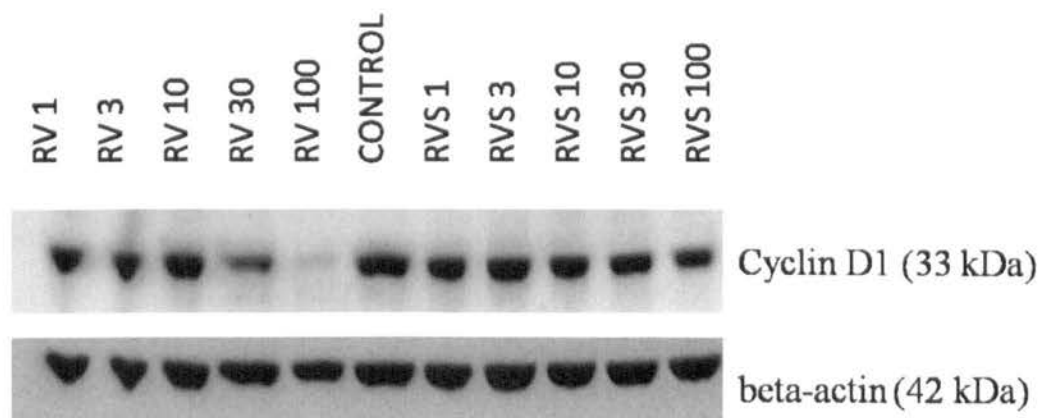


**Figure 4.23** Effect of 1µM, 3µM, 10µM, 30µM and 100µM resveratrol-3-glucuronide and resveratrol-4'-glucuronide treatments on the cyclin D1 levels of Caco-2 cells. (A) Western blot of cyclin D1 and beta-actin. Blot is representative of three independent experiments. (B) ImageJ analysis of the cyclin D1 levels normalised to beta-actin. Values represent means of three independent experiments  $\pm$ SEM. \*  $p < 0.05$  by repeated measures ANOVA and Dunnett's test relative to the untreated group.

The effect of treatment on the levels of cyclin D1 using CCL-228 cells was also investigated (Figure 4.24). Resveratrol concentrations reaching 10 $\mu$ M were not capable of causing an effect on the cyclin D1 levels. At 30 $\mu$ M and 100 $\mu$ M resveratrol a significant inhibition was noted ( $p < 0.001$ ). In the case of RV-3-S, there was no evidence of cyclin D1 inhibition at concentrations reaching 30 $\mu$ M except at 100 $\mu$ M where this was decreased significantly ( $p < 0.05$ ). The results after treatment with actinomycin D were consistent with those for Caco-2 where the cyclin D1 levels were blocked (data not shown).

CCL-228 cells were also treated with a range of RV-3-G and RV-4'-G concentrations (1 $\mu$ M-100 $\mu$ M) (Figure 4.25). Despite the gradual decrease in cyclin D1 levels with increasing RV-3-G concentrations, only at 100 $\mu$ M was this significant ( $p < 0.05$ ) (Figure 4.25 A&B). In the case of the second glucuronide metabolite, RV-4'-G, the effects were not so profound with minimal reduction at even the highest concentration of 100 $\mu$ M ( $p > 0.05$ ) and no effect at concentrations 1 $\mu$ M-30 $\mu$ M (Figure 4.25).

A



B

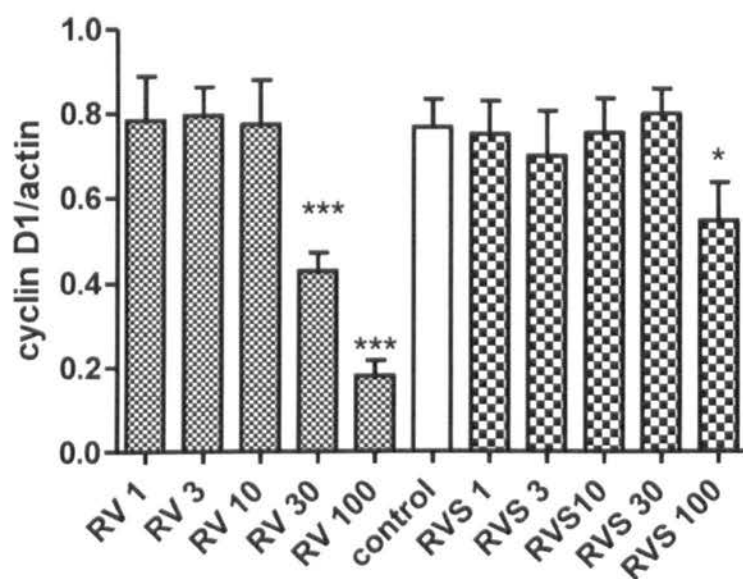
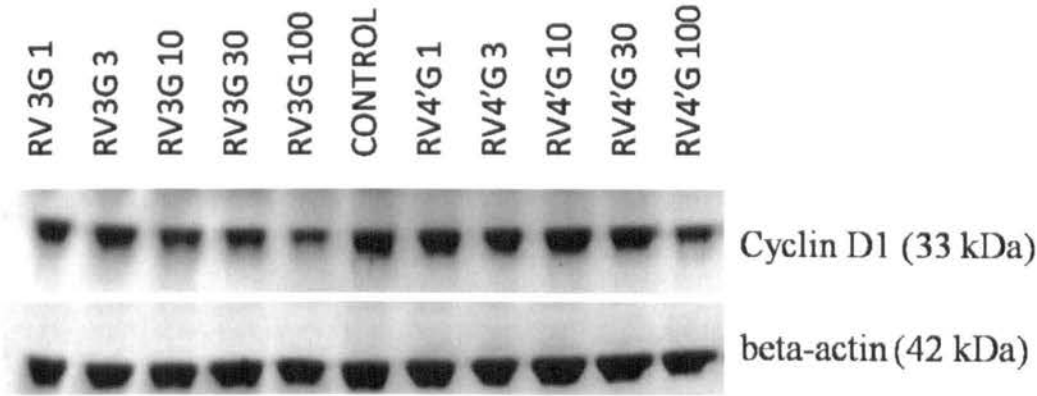


**Figure 4.24** Effect of 1μM, 3μM, 10μM, 30μM and 100μM resveratrol and resveratrol-3-sulphate treatments on the cyclin D1 levels of CCL-228 cells. (A) Western blot of cyclin D1 and beta-actin. Blot is representative of three independent experiments. (B) ImageJ analysis of the cyclin D1 levels normalised to beta-actin. Values represent means of three independent experiments ±SEM. \* p<0.05 and \*\*\* p<0.001 by repeated measures ANOVA and Dunnett's test relative to the untreated group.

A



B

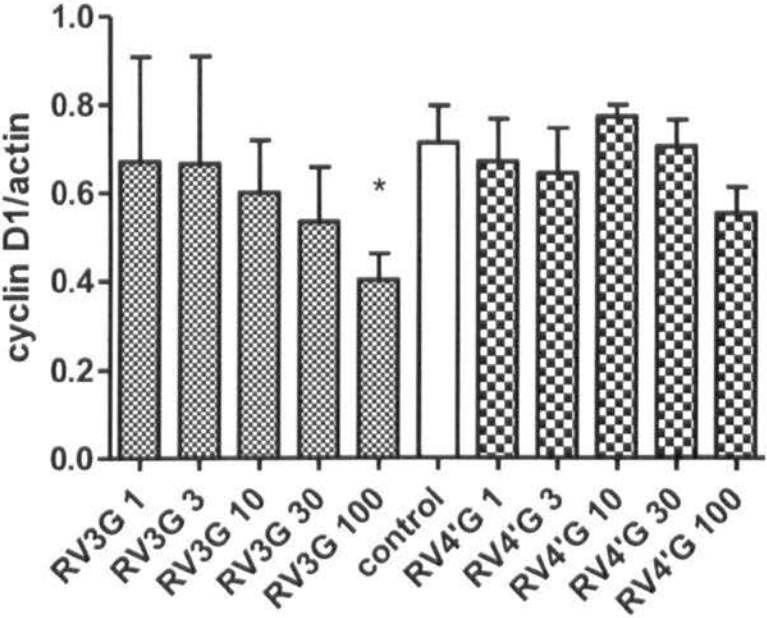
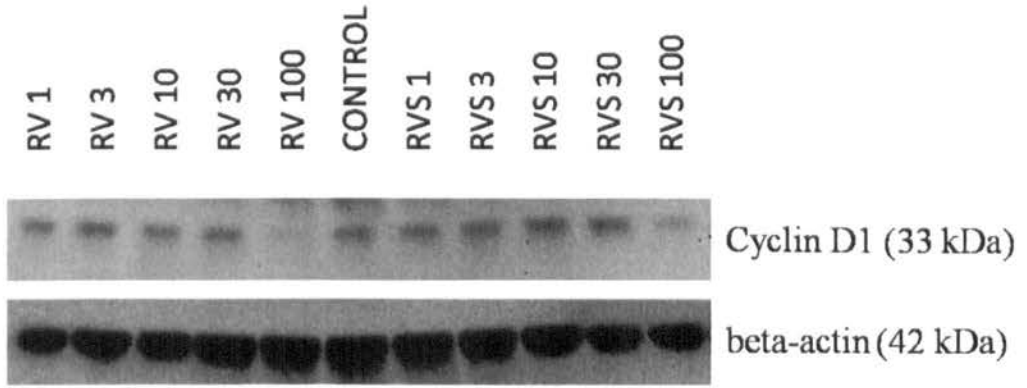


**Figure 4.25** Effect of 1 $\mu$ M, 3 $\mu$ M, 10 $\mu$ M, 30 $\mu$ M and 100 $\mu$ M resveratrol-3-glucuronide and resveratrol-4'-glucuronide treatments on the cyclin D1 levels of CCL-228 cells. (A) Western blot of cyclin D1 and beta-actin. Blot is representative of three independent experiments. (B) ImageJ analysis of the cyclin D1 levels normalised to beta-actin. Values represent means of three independent experiments  $\pm$ SEM. \*  $p < 0.05$  by repeated measures ANOVA and Dunnett's test relative to the untreated group.

The expression levels of cyclin D1 in HCT-116 cells after treatment with resveratrol and its three metabolites was also investigated. The analysis in Figure 4.26B for resveratrol shows that cyclin D1 levels actually increased above those for the control after treatment of 3-30 $\mu$ M but this was not significant. This however was not the case for 1 $\mu$ M resveratrol where levels remained comparable to the untreated group. Treatment with 100 $\mu$ M resveratrol was capable of reducing the levels of cyclin D1 however, after ANOVA analysis of three experiments, these effects were not significant ( $p>0.05$ ). HCT-116 cells treated with a range of RV-3-S concentrations gave variable results. It is evident from Figure 4.26A below that at the lower concentrations, cyclin D1 was not affected by treatment ( $p>0.05$ ). At 100 $\mu$ M however, it is clear that cyclin D1 levels were reduced relative to the control untreated group. Following ImageJ analysis of normalised cyclin D1 levels relative to beta-actin compared to the control the values were not found to be significant ( $p>0.05$ ) (Figure 4.26B).

HCT-116 cells were further treated with RV-3-G and RV-4'-G (Figure 4.27). Similar to treatment with resveratrol, at concentrations up to 30 $\mu$ M there was no evident effect on the levels of cyclin D1 for both RV-3-G and RV-4'-G. The scenario seemed to be different at 100 $\mu$ M where there was a significant reduction in cyclin D1 levels ( $p<0.01$  and  $p<0.05$  for RV-3-G and RV-4'-G respectively). In the case of actinomycin D, cyclin D1 levels were completely diminished 48 hours after treatment and as for the vehicle control, the levels were comparable to the untreated group (data not shown).

A



B

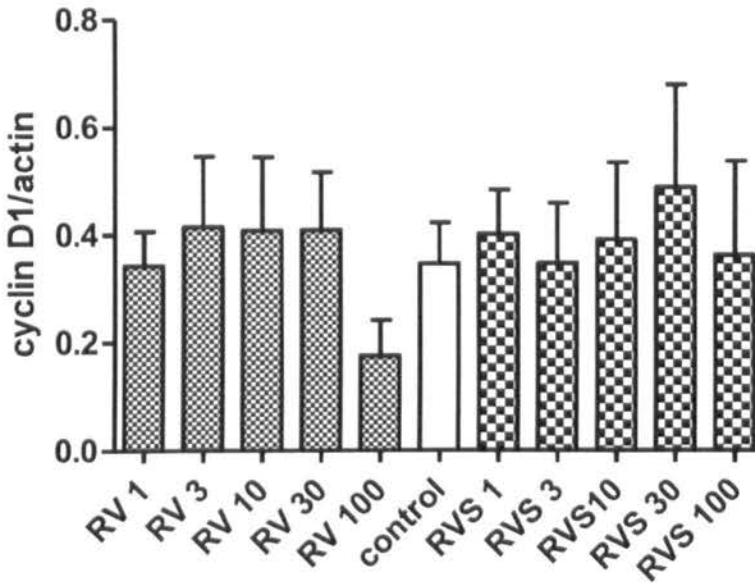
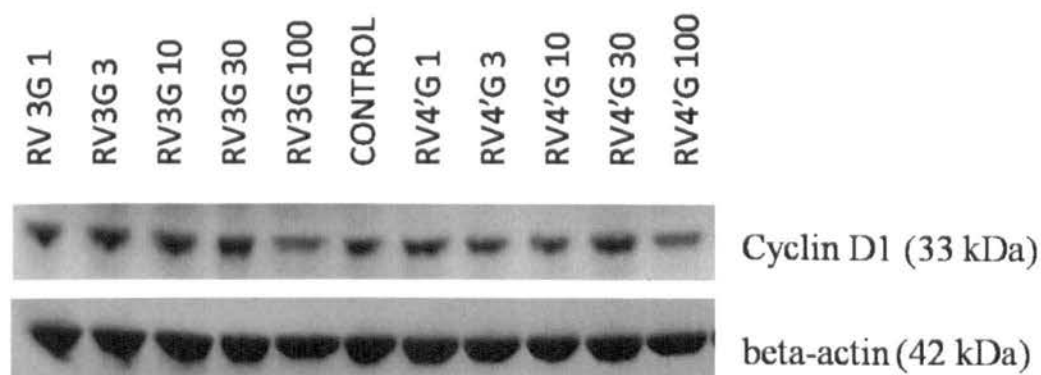


**Figure 4.26** Effect of 1 $\mu$ M, 3 $\mu$ M, 10 $\mu$ M, 30 $\mu$ M and 100 $\mu$ M resveratrol and resveratrol-3-sulphate treatments on the cyclin D1 levels of HCT-116 cells. (A) Western blot of cyclin D1 and beta-actin. Blot is representative of three independent experiments. (B) ImageJ analysis of the cyclin D1 levels normalised to beta-actin. Values represent means of three independent experiments  $\pm$ SEM.  $p > 0.05$  by repeated measures ANOVA and Dunnett's test relative to the untreated group.

A



B

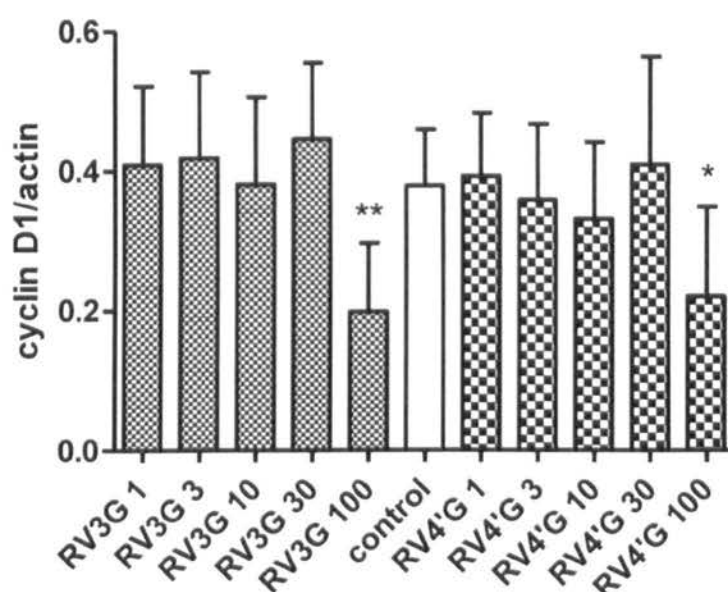


**Figure 4.27** Effect of 1μM, 3μM, 10μM, 30μM and 100μM resveratrol-3-glucuronide and resveratrol-4'-glucuronide treatments on the cyclin D1 levels of HCT-116 cells. (A) Western blot of cyclin D1 and beta-actin. Blot is representative of three independent experiments. (B) ImageJ analysis of the cyclin D1 levels normalised to beta-actin. Values represent means of three independent experiments  $\pm$ SEM. \*  $p < 0.05$  and \*\*  $p < 0.01$  by repeated measures ANOVA and Dunnett's test relative to the untreated group.

## **4.5 Discussion**

Resveratrol has been shown to exhibit both anti-proliferative and apoptotic effects in a range of cell lines, ranging from prostate to colon cancer (Roemer and Mahyar-Roemer, 2002). In this chapter we aimed to further investigate the effects seen in chapter 3 after treatment with resveratrol and its three metabolites, resveratrol-3-O-D-glucuronide (RV-3-G), resveratrol-4'-O-D-glucuronide (RV-4'-G) and resveratrol-3-O-D-sulphate (RV-3-S) on colon cancer cell lines and elucidate their mechanism of action.

### **No evidence of apoptosis in DAPI-stained cells**

The first experiment conducted was the fluorescent microscopic evaluation of cell nuclei using DAPI stained mounting medium. It was clear that cell treatment with the metabolites did not exhibit a morphology characteristic with apoptosis. More specifically, Caco-2, CCL-228 and HCT-116 cells responded to 30µM resveratrol and metabolites, concentrations capable of reducing growth by approximately 50% but there was no evidence of apoptosis (cytoplasmic condensation, nuclear fragmentation, or blebbing) (Kroemer *et al.*, 2005). It has been shown that DAPI-nuclear staining following treatment with resveratrol and its metabolites to detect apoptosis was not the ideal technique. One issue arose from the fact that treatment with the positive control, actinomycin D, resulted in very low number of cells making it unlikely that any apoptotic events would appear. Therefore, despite the fact that actinomycin D is known to cause apoptosis in colorectal cancer cells, this was not clearly exemplified when using DAPI nuclear staining (Choong *et al.*, 2009).



### **No evidence for caspase-dependent apoptosis**

In order to confirm these findings, cells were pre-treated with a pan-caspase inhibitor, Z-VAD-FMK. This confirmed the results from the DAPI images for the three cell lines used (Caco-2, CCL-228 and HCT-116) since addition of Z-VAD-FMK did not reverse the effects after treatment. The results from this study are in tight accordance with a recent study where reversal of effects was not evident at 50 $\mu$ M and 100 $\mu$ M concentrations of resveratrol but only at higher concentrations (150 $\mu$ M and 200 $\mu$ M) using MCF-7 (breast cancer cells) and H1299 (non-small lung carcinoma cells) (Ferraz da Costa *et al.*, 2012). Other studies, however, have demonstrated that resveratrol induced DNA-fragmentation which was completely blocked by addition of 100 $\mu$ M Z-VAD-FMK in U251glioma cells (Jiang *et al.*, 2005, Li *et al.*, 2009), NB4 acute promyelocytic leukaemia cells (Cao *et al.*, 2005), MDA-MD231 cells (Nguyen *et al.*, 2009) and SW-480 colon cancer cells (Delmas *et al.*, 2003). In the cell cycle distribution analysis experiments however, there was some evidence of apoptosis following resveratrol treatment in CCL-228 cells and with actinomycin D in Caco-2 cells. The three resveratrol metabolites however, did not seem to alter the proportion of cells in sub-G1 as compared to the untreated and vehicle control groups. In addition, we found no evidence of apoptosis induced by the resveratrol metabolites after 30 $\mu$ M so it would be interesting to investigate higher concentrations since concentrations below 100 $\mu$ M are considered as cytostatic (Joe *et al.*, 2002). Furthermore, western blot analysis investigating PARP cleavage and caspase-3 activation did not provide evidence of apoptosis (data not shown).

### **p53 involvement**

Alterations of tumour suppressor genes and proto-oncogenes in various signalling pathways are considered to be important in the carcinogenesis process (Chow et al., 2010b). p53 gene mutations have been detected in more than 50% tumours (Rivlin *et al.*, 2011, Liu and Bodmer, 2006). Inactivation and mutated p53 expression allow cells to proliferate further, evade apoptosis and cause resistance to chemotherapy (Sigal and Rotter, 2000, Brosh and Rotter, 2009). Activation of p53 aids in the repair of DNA whilst also inhibiting the proliferation of cancer cells mainly through the initiation of cell cycle arrest, senescence or programmed cell death (apoptosis) (Aylon and Oren, 2011).

Western blot analysis on the expression levels of p53 using HCT-116 cells (wild-type p53) revealed that resveratrol markedly increased the p53 levels at low micromolar concentrations (1 $\mu$ M) and less so at 10 $\mu$ M. In the case of the two glucuronidated metabolites, the effects were less profound. The findings were further confirmed by immunofluorescence where nuclear localisation occurred but whether p53 is responsible for the growth inhibition effects warrants further studies mainly due to the fact that the other two cell lines possess a mutated p53 yet growth was blocked to a similar extent as in HCT-116 cells. The higher p53 protein levels in the presence of resveratrol are in agreement with other reports (Ferraz da Costa *et al.*, 2012, Pozo-Guisado *et al.*, 2005). Resveratrol has been shown to induce apoptosis in a p53-dependent or –independent manner (Lin *et al.*, 2011) but no work so far has investigated the involvement of p53 after treatment with the metabolites. This and the strong growth inhibitory effect presented in the previous chapter led us to investigate the effects of resveratrol and its metabolites on the cell cycle.

## **Cell cycle distribution**

Cell cycle distribution was analysed by flow cytometry. Thirty micromolar of resveratrol caused S phase cell cycle arrest in all three cell lines which confirms the results from the growth studies where a dose-dependent inhibition was evident. There is a large line of evidence showing that resveratrol interferes with the cell cycle in cancer cells (Gatouillat *et al.*, 2010). Results from this study are in tight agreement with those by Joe *et al.* (2002), who illustrated that SW480 cells (CCL-228) underwent accumulation in the S phase (37% after DMSO treatment against 50% after 300 $\mu$ M RV treatment) (Joe *et al.*, 2002) and with other studies reporting an accumulation of Caco-2 cells in the S phase of the cell cycle without any signs of apoptosis (Wolter *et al.*, 2001, Schneider *et al.*, 2000).

A few studies have demonstrated that depending on the cell type, resveratrol is able to block the cell cycle progression at G0/G1, S or G2/M phases (Kuo *et al.*, 2002, Ahmad *et al.*, 2001, Larrosa *et al.*, 2003, Bai *et al.*, 2010). From the results of this study however, it is clear that resveratrol was only capable of blocking the cells at S phase. The resveratrol-mediated cell cycle arrest identified, seems to be p53 independent since Caco-2 and CCL-228 possess mutated p53 (Rochette *et al.*, 2005, Gartel *et al.*, 2003). In the designed experiment to measure the viability of cells using flow cytometry an unexpected and significant shift appeared in the side scatter parameter of Caco-2 and HCT-116 cells and in both the side and forward scatter for CCL-228 cells following resveratrol treatment but not with the metabolites. This suggests that treatment caused Caco-2 and HCT-116 cells to become more complex whilst in the case of the CCL-228 cells, to become larger in size and more complex. In fact, the images of cells in culture appeared bigger when treated with resveratrol. Similar findings were reported in another study using A2780 and CaOV3 ovarian cancer cells which further extended their

experiments using TEM microscopy to identify the presence of autophagocytic granules following resveratrol treatment at 24 hours and an intact nucleus and the absence of chromatin condensation at 48 hours (Opipari, 2004). It was also shown that these autophagocytic granules contained degraded organelles. These results further suggest the absence of apoptosis since apoptotic cell death is typically characterised by cell shrinkage.

In this study, for the first time, it was shown that resveratrol metabolites possess an anti-tumour effect (see previous chapter for growth inhibition studies). Whether they are the active form of resveratrol and act as a pool or whether they become de-conjugated back to resveratrol to exert their effects is still unknown. It is clear that from the cell cycle distribution analysis that the metabolites act differently compared to the parent compound. For example, RV-3-G and RV-4'-G caused a significant accumulation of cells in G0/G1 in Caco-2 cells and CCL-228 cells. The results with HCT-116 seem to be more variable with significant G0/G1 arrest after treatment with RV-4'-G for example in only one experiment. It is of interest that treatment with RV-3-G caused S phase arrest in one experiment with HCT-116 cells. As for the resveratrol metabolites, a recent study confirmed these findings suggesting a different mechanism of the metabolites and arrest at G0/G1 rather than S phase in the case of the parent compound (Storniolo and Moreno, 2012). Another interesting finding regarding metabolites comes from a study by Yang and colleagues (2006) where they treated NCI-H209 lung cancer cells with a range of quercetin glucuronide concentrations and found that they arrested cells at G2/M and caused apoptosis (Yang *et al.*, 2006). This emphasises the possible anti-tumour activity of natural product metabolites. Unlike resveratrol, however, there was no observed shift in either the size or complexity of the membrane of cells following treatments with the metabolites. Rather, the dot plot distribution appeared to

be similar to control untreated and vehicle control treated cells. These findings further highlight differences between resveratrol and its metabolites.

### **Involvement of cyclin D1**

The results from the cell cycle distribution led us to investigate the effect of treatment with resveratrol and its metabolites at a range of concentrations on the levels of cyclin D1. Western blot analysis on Caco-2 and CCL-228 cells revealed that cyclin D1 levels were inhibited at the highest resveratrol concentrations (30 $\mu$ M and 100 $\mu$ M) despite the fact that cell cycle arrest took place in the S phase and not G0/G1 at 30 $\mu$ M. One possibility for the inhibition of cyclin D1 at 100 $\mu$ M could be that with increasing concentrations, the arrest is shifted. A study by Liontas & Yeger (2004) found that resveratrol induced a significant S phase arrest in NUB-7 and LAN-5 neuroblastoma cells at 25-50 $\mu$ M but at 100 $\mu$ M this caused G0/G1 arrest after 48 hours (Liontas and Yeger, 2004). These findings were further substantiated by reports stating that 50 $\mu$ M resveratrol treatment for 24 hours caused S phase arrest but 100 $\mu$ M treatments caused an arrest in G0/G1 phase (Opipari, 2004). This therefore suggests that the effects of resveratrol on the cell cycle could be concentration-dependent and explains the inhibition of cyclin D1 by resveratrol at 100 $\mu$ M by western blot.

The results for HCT-116 cells treated with resveratrol are in accordance with the cell cycle distribution analysis results where no arrest was observed at any phase of the cell cycle. The cyclin D1 protein expression levels after treatment with the metabolites remained unaffected at the lower concentrations. In the case of 30 $\mu$ M which was used for the cell cycle analysis, the protein levels did not seem to be significantly reduced, but at 100 $\mu$ M these were markedly reduced in Caco-2 and CCL-228 cells. As for HCT-116 cells, a significant reduction in cyclin D1 levels was evident after treatment with

100 $\mu$ M RV-3-G and RV-4'-G alone. The results at 30 $\mu$ M treatments in HCT-116 cells are in close agreement with those from the cell cycle distribution analysis where no significant effect was apparent. No studies to date have investigated the effect of treatment with the metabolites on cyclin D1 protein levels so further studies are warranted to validate these results. Whether 100 $\mu$ M concentrations would be plausible in the *in vivo* scenario is an important factor to consider due to the poor bioavailability of resveratrol (Walle, 2011).

## **Conclusion**

Resveratrol and its metabolites are capable of inhibiting the growth of Caco-2, CCL-228 and HCT-116 colon cancer cell lines yet, the findings from this chapter only provide evidence of cell cycle arrest and no signs of apoptosis (except in the case of CCL-228 cells and resveratrol treatment). One possible explanation could be that resveratrol and its metabolites are capable of killing cells in a non-apoptotic manner by inducing autophagocytosis (type II programmed cell death) i.e autophagy.

In fact, a study using ovarian cancer cells and resveratrol, revealed the morphological presence of autophagocytic death instead of apoptotic-induced death despite the major characteristics of apoptosis, namely, cytochrome c release from the mitochondria, apoptosome complex formation and activation of the caspases (Opipari, 2004). However, this has not been investigated in this study and future studies are therefore necessary to elucidate the mechanism of cell death induction.

The observations in this chapter provide an insight on the effects of the three main resveratrol metabolites, namely, resveratrol-3-O-D-glucuronide, resveratrol-4'-O-D-glucuronide and resveratrol-3-O-D-sulphate on the growth of colon cancer cell lines. The metabolites appear to act in a distinct manner as compared to the parent compound

suggesting they have an anti-tumour effect. Further studies on their effects on key signalling pathways were designed to elucidate the molecular targets.

In the chapter that follows, an attempt was made to elucidate possible molecular targets following treatment with the metabolites. A simple pharmacological approach was employed using known inhibitors of key signalling pathways including AMPK, PI3K, MAPK and the adenosine A<sub>3</sub> receptor to identify any involvement.

## Chapter 5. Mechanism of action of resveratrol metabolites

The results from chapters three and four demonstrated that resveratrol and its metabolites are capable of reducing cell proliferation in three colorectal cancer cell lines (Caco-2, CCL-228 and HCT-116). In addition, studies aiming to identify whether cells undergo apoptosis or cell cycle arrest identified that the metabolites act in a different manner as compared to the parent compound. More specifically, resveratrol-3-O-D-glucuronide and resveratrol-4'-O-D-glucuronide were shown to induce G0/G1 arrest whilst resveratrol induced S phase arrest in both Caco-2 and CCL-228 cells. In the case of the third metabolite, resveratrol-3-O-D-sulphate, no significant effect was observed in either cell line. This suggests that the metabolites act in a distinct manner and any observed effects were cell-specific. It is noteworthy to point that all four compounds had no significant effect on the cell cycle distribution of HCT-116 cells. These observations indicate how different polyphenols work *via* different mechanisms.

These findings led us to further investigate the mechanism of action of resveratrol and its metabolites and their effects, if any, on key signalling pathways including AMPK, PI3K, MAPK and on the adenosine A<sub>3</sub> receptor. The PI3K/Akt signalling cascade is vital for cell growth, cellular transformation and survival. Previous studies have shown that resveratrol down-regulated the PI3K/Akt/mTOR signalling pathway by decreasing the expression and phosphorylation of Akt in U251 glioma cells (Jiang *et al.*, 2009) and by inhibition of the phosphorylated levels of PI3K, Akt and mTOR in LNCaP prostate cancer cells (Chen *et al.*, 2010). Resveratrol-induced apoptotic effects were further potentiated by co-treatment with the PI3K inhibitor, LY294002 (Chen *et al.*, 2010).

Similar to the PI3K pathway, the mitogen-activated protein kinases (MAPK) are responsible for transducing cell-proliferation signalling pathways (Fang and



Richardson, 2005). Of the three MAPK sub-families, the ERK/MAPK pathway was shown to be the most significant for cellular proliferation (Troppmair *et al.*, 1994). A study by Nam and colleagues (2008) illustrated that cell death induced by quercetin (a natural product) was reversed by addition of the ERK inhibitor, PD98059, stipulating the involvement of ERK activation (Nam *et al.*, 2008). Another study, however, showed the opposite effect; i.e. resveratrol-induced cell death was further potentiated by addition of PD98059, suggesting that suppression of tumour growth was associated with inhibition of ERK phosphorylation and thus apoptosis (Roy *et al.*, 2011). These results show how variable the effects of these inhibitors can be.

Multiple studies have implicated the AMPK pathway in the growth and proliferation of tumours via the regulation of an enzyme called the mammalian target of rapamycin (mTOR). It has also been shown that resveratrol up-regulated AMPK activity by increasing its phosphorylation (Lin *et al.*, 2010, Hwang *et al.*, 2007, Rashid *et al.*, 2011). Treatment with compound C in the presence of resveratrol inhibited AMPK activation (Lin *et al.*, 2010, Hwang *et al.*, 2007).

To date, four adenosine receptor subtypes have been identified, A<sub>1</sub>, A<sub>2A</sub>, A<sub>2B</sub> and A<sub>3</sub> in various tissues and these bind to specific G protein-coupled receptors in order to activate their associated downstream molecules (Gessi *et al.*, 2007). Activation of the A<sub>3</sub>R by the binding of a selective ligand was shown to inhibit cell proliferation and cause apoptosis in several cancer cell lines (Kamiya *et al.*, 2012). Studies have shown that adenosine A<sub>3</sub> receptors are expressed at considerable levels on the cell surface of cancer cells and colon tumour tissues and activation of all receptor subtypes leads to the phosphorylation of extracellular regulated kinase 1/2 (ERK 1/2) (Gessi *et al.*, 2007).

A pharmacological screening approach was taken first by co-treating cells with resveratrol and its metabolites (all at 30 $\mu$ M, so high end of IC<sub>50</sub> range) with: a) 10 $\mu$ M LY294002, a PI3K inhibitor, b) 10 $\mu$ M PD98059, a MAPK inhibitor, c) 10 $\mu$ M MRS-1191, a selective adenosine A<sub>3</sub> receptor antagonist and d) 12.5 $\mu$ M compound C, an AMPK inhibitor (Figure 5.1). Cell growth was assessed after 48 hours using the neutral red uptake assay (see Section 2.2.1). PI3K and MAPK are known to drive cell proliferation and the use of the inhibitors PD98059 and LY294002, was a positive control to test this assumption. Briefly, addition of MRS-1191 will block the activation of the adenosine A<sub>3</sub> receptor and therefore cause cell proliferation. Addition of compound C however, will activate AMPK thus causing a decrease in growth. Lastly, addition of the PI3K and MAPK inhibitors, LY294002 and PD98059 will cause inhibition of the pro-survival signalling pathways and subsequently lead to decreased cell proliferation (Figure 5.1). Further experiments included the investigation on the cell cycle distribution with MRS-1191 and compound C being co-treated with resveratrol and its metabolites using the same previously mentioned concentrations. Western blotting was incorporated into this study to further show the presence of the adenosine A<sub>3</sub> receptor followed by growth studies treating cells with 2CI-IB-MECA (a highly selective A<sub>3</sub> agonist) to demonstrate the involvement of A<sub>3</sub>R. In addition, cells were co-treated with 2CI-IB-MECA (30 $\mu$ M) and MRS-1191(10 $\mu$ M) to elucidate whether the growth-inhibitory effects seen with 2CI-IB-MECA could be reversed. Lastly, the total and phosphorylated levels of AMPK after 48 hour treatment with a range of concentrations (1 $\mu$ M, 3 $\mu$ M, 10 $\mu$ M, 30 $\mu$ M and 100 $\mu$ M) were assessed by western blot and band intensity analysed using ImageJ.

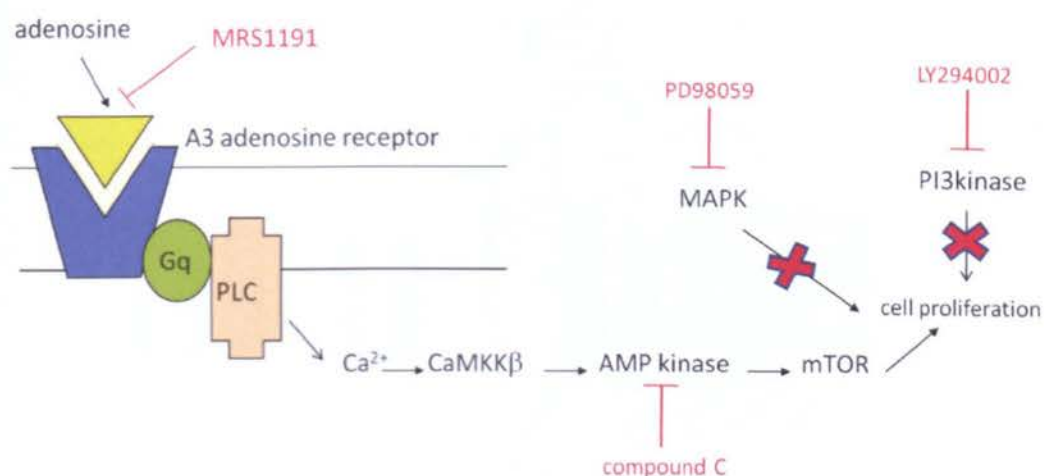


**Figure 5.1** Schematic representation of key signalling pathways and their possible implication in the effects exerted by resveratrol metabolites. Red crosses represent an inhibition of cell proliferation following inhibition of the MAPK and PI3K pathways with PD98059 and LY294002 respectively.

### 5.1 Probing key signalling pathways for a role in the effects of resveratrol and its metabolites

In order to gain a further insight into the molecular effects of resveratrol, we screened a range of inhibitors of key signalling pathways by co-treatment of Caco-2, CCL-228 and HCT-116 colorectal cancer cells. Cells were seeded as previously mentioned and treated with 30µM resveratrol and metabolites in the presence of either: a) Compound C – AMP kinase inhibitor (12.5µM), b) LY294002 – PI-3-kinase inhibitor (10µM), c) PD98059 – MAPK inhibitor (10µM) and d) MRS1191 – adenosine A<sub>3</sub> receptor antagonist (10µM) for 48 hours. Cell growth was then measured using the neutral red assay (see Section 2.2.1). The concentrations of the inhibitors used in this study were chosen based on published studies that had shown effectiveness (Das *et al.*, 2005, Jiang *et al.*, 2010, Nam *et al.*, 2008, Lee *et al.*, 2009, Lin *et al.*, 2010, Nakamura *et al.*, 2006, Kamiya *et al.*, 2012).

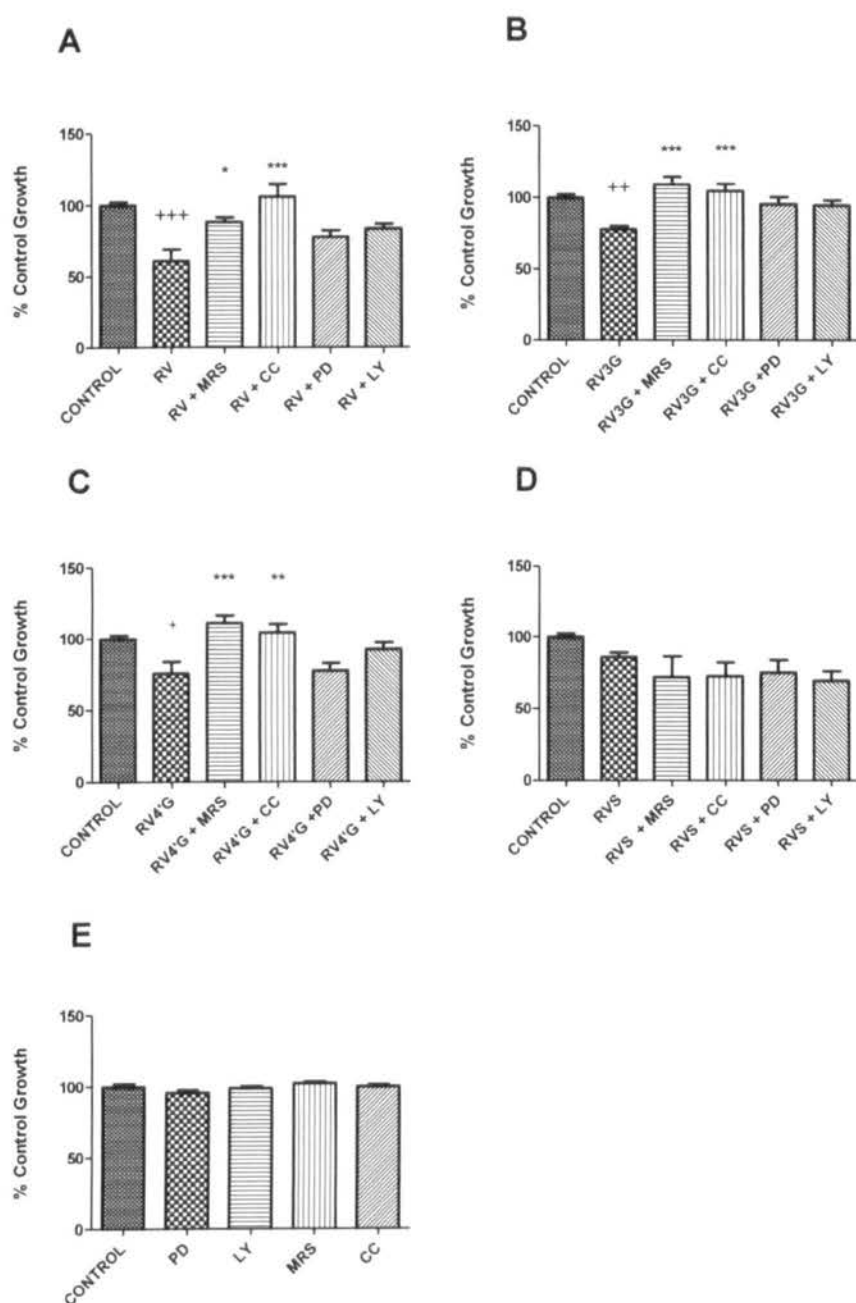


**Figure 5.2** Effect of MRS-1191, compound C, LY294002 and PD98059 on the growth inhibition after treatment with resveratrol and its metabolites in CCL-228 cells. Cells were treated with resveratrol (A), resveratrol-3-O-D-glucuronide (B), resveratrol-4'-O-D-glucuronide (C) and resveratrol-3-O-D-sulphate (D), all at 30  $\mu$ M, and either MRS-1191 (MRS, 10 $\mu$ M), compound C (CC, 12.5 $\mu$ M), LY294002 (LY, 10 $\mu$ M) and PD98059 (PD, 10 $\mu$ M) or treatment with inhibitors alone (E). Cell viability was measured 48 hours later using the neutral red uptake assay. Values represent the means (n=9) from 3 independent experiments. \*p<0.05, \*\*p<0.01 and \*\*\*p<0.001 relative to resveratrol or resveratrol metabolites and +p<0.05, ++p<0.01 and +++p<0.001 relative to untreated by repeated measures ANOVA and Dunnett's test.

The effects of treatment of resveratrol and its metabolites in the presence of either MRS-1191, compound C, LY294002 or PD98059 are shown in Figure 5.2. It is evident that co-treatment of resveratrol with MRS-1191 and compound C was sufficient to reverse the effects after treatment with resveratrol alone ( $p < 0.05$  and  $p < 0.001$  respectively). In contrast, the results for LY29002 and PD98059 showed no significant recovery of cell growth. Cells were treated with RV-3-G in the presence of the four inhibitors (Figure 5.2B and Table 5.1). Similar findings to resveratrol were seen with RV-3-G, where only MRS-1191 and compound C were capable of reversing the growth inhibition caused after treatment with RV-3-G alone. Again, LY294002 and PD98059 caused no significant difference. In agreement with the effects seen by the first glucuronide metabolite are the results using RV-4'-G (Figure 5.2C). More specifically, only MRS-1191 and compound C caused sufficient reversal of growth inhibition ( $p < 0.001$  and  $p < 0.01$  respectively) with no effect of LY294002 and PD98059 ( $p > 0.05$ ). Furthermore, the sulphated metabolite, RV-3-S as in the case of Caco-2 cells, did not show any significant activity on cells (Figure 5.2D); a further example of an unexpected loss in activity of the metabolites, as mentioned before. Treatment with the inhibitors alone did not exert any significant effect relative to the untreated group (Figure 5.2E).

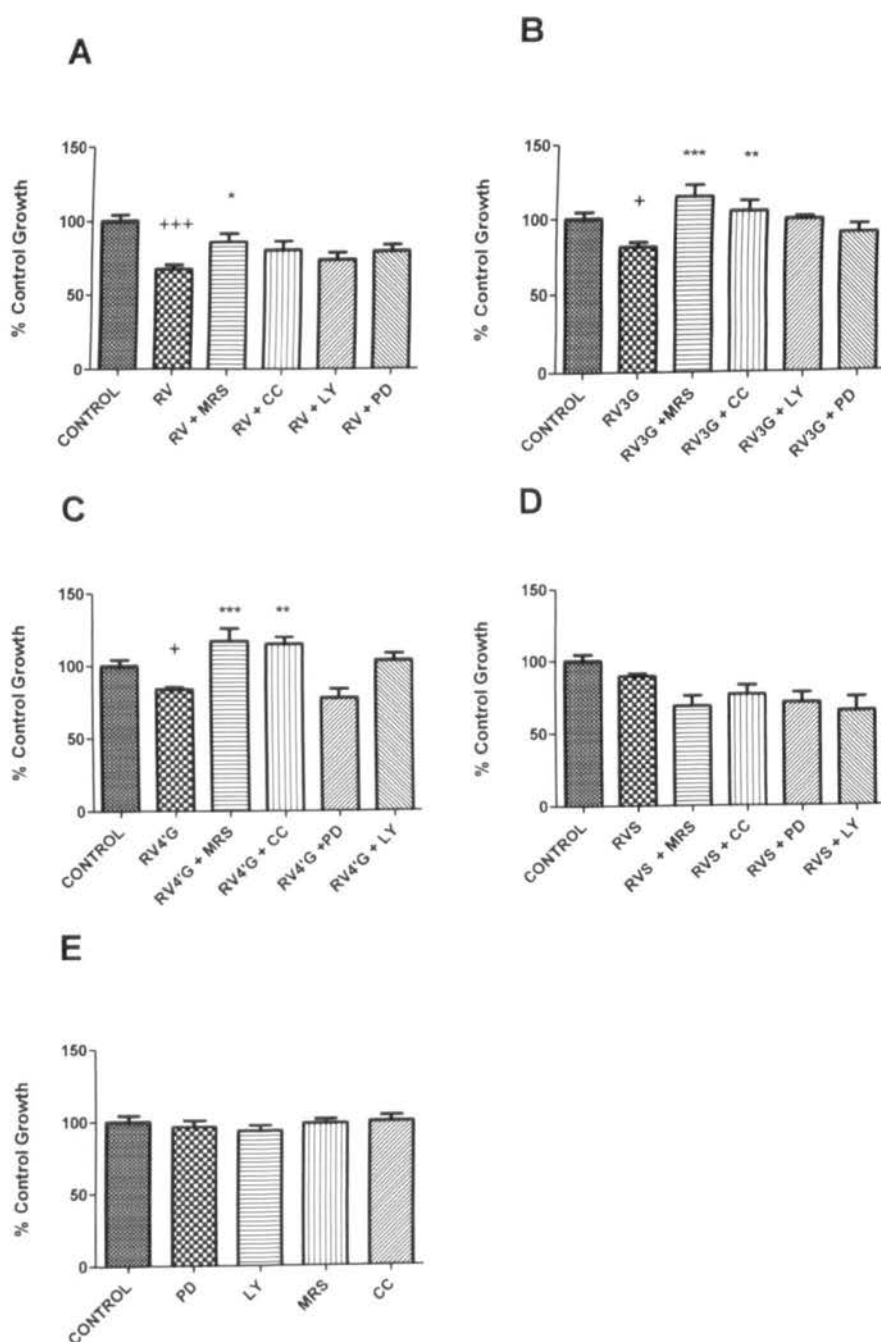


**Figure 5.3** Effect of MRS-1191, compound C, LY294002 and PD98059 on the growth inhibition after treatment with resveratrol and its metabolites in Caco-2 cells. Cells were treated with resveratrol (A), resveratrol-3-O-D-glucuronide (B), resveratrol-4'-O-D-glucuronide (C) and resveratrol-3-O-D-sulphate (D), all at 30  $\mu$ M and either MRS-1191 (MRS, 10 $\mu$ M), compound C (CC, 12.5 $\mu$ M), LY294002 (LY, 10 $\mu$ M) and PD98059 (PD, 10 $\mu$ M) or treatment with inhibitors alone (E). Cell viability was measured 48 hours later using the neutral red uptake assay. Values represent the means (n=9) from 3 independent experiments. \* $p$ <0.05, \*\* $p$ <0.01 and \*\*\* $p$ <0.001 relative to resveratrol or resveratrol metabolites and + $p$ <0.05 and +++ $p$ <0.001 relative to untreated by repeated measures ANOVA and Dunnett's test.

Co-treatment of Caco-2 cells with the three inhibitors, compound C, LY294002 and PD98059 was not sufficient to reverse the effects seen with resveratrol. The only inhibitor capable of reversing these effects was MRS-1191 ( $p < 0.05$ ) (Figure 5.3A). Similar to CCL-228 cells, only MRS-1191 and compound C were capable of causing a significant reversal of inhibition following treatment with RV-3-G ( $p < 0.001$  and  $p < 0.01$  respectively) (Figure 5.3B and Table 5.1). MRS-1191 and compound C were sufficient to reverse the effects of RV-4'-G. In the case of RV-3-S, it was evident that growth was reduced, but addition of the inhibitors did not significantly alter this effect (Figure 5.3D). Again, there was no significant difference between the untreated group and of inhibitors alone ( $p > 0.05$ ) (Figure 5.3E).

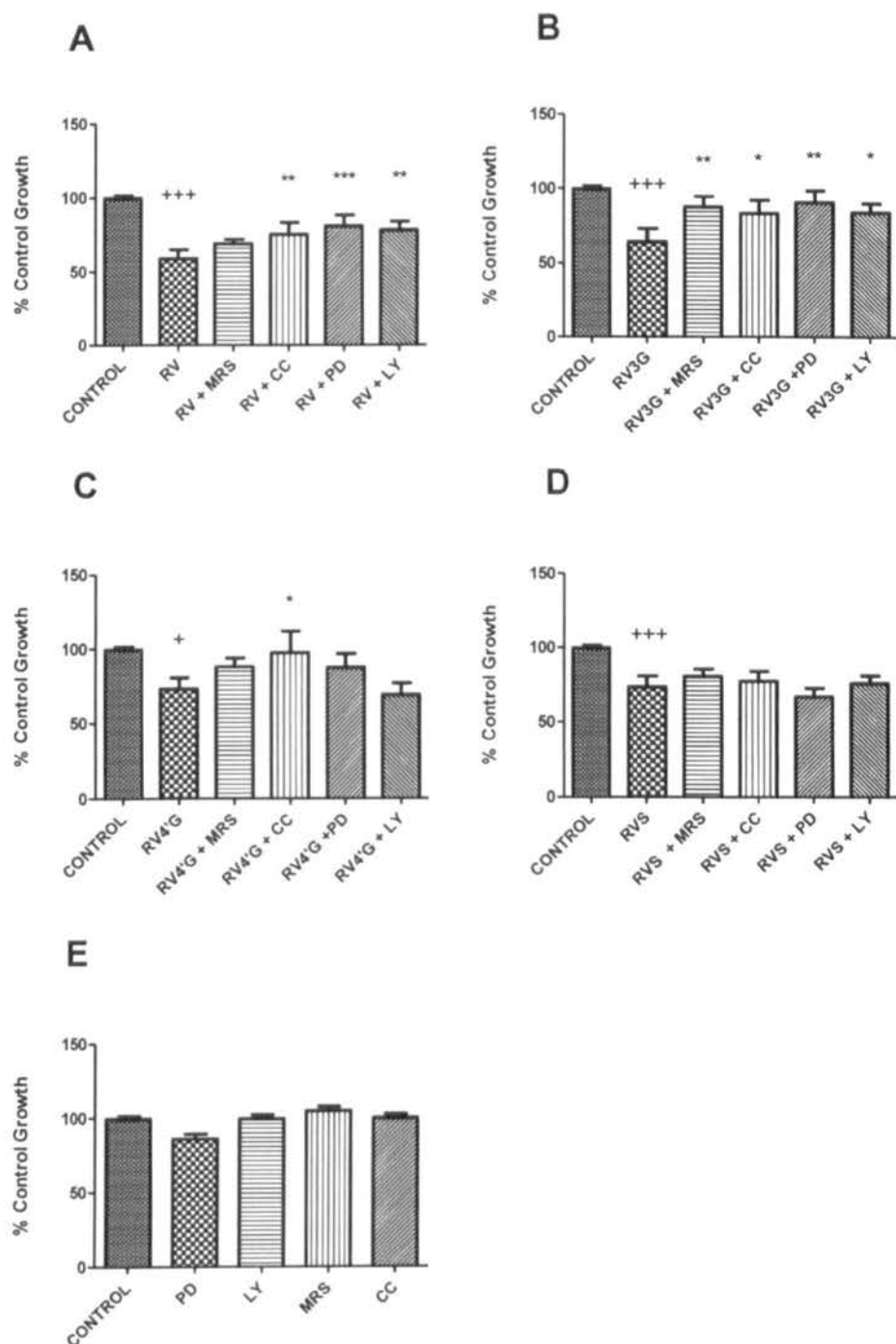


**Figure 5.4** Effect of MRS-1191, compound C, LY294002 and PD98059 on the growth inhibition after treatment with resveratrol and its metabolites in HCT-116 cells. Cells were treated with resveratrol (A), resveratrol-3-O-D-glucuronide (B), resveratrol-4'-O-D-glucuronide (C) and resveratrol-3-O-D-sulphate (D), all at 30  $\mu$ M and either MRS-1191 (MRS, 10 $\mu$ M), compound C (CC, 12.5 $\mu$ M), LY294002 (LY, 10 $\mu$ M) and PD98059 (PD, 10 $\mu$ M) or treatment with inhibitors alone (E). Cell viability was measured 48 hours later using the neutral red uptake assay. Values represent the means (n=9) from 3 independent experiments. \*p<0.05, \*\*p<0.01 and \*\*\*p<0.001 relative to resveratrol or resveratrol metabolites and +p<0.05 and +++p<0.001 relative to untreated by repeated measures ANOVA and Dunnett's test.



Experiments with HCT-116 cells showed increased growth in the presence of compound C, LY294002 and PD98059 following co-treatment with resveratrol ( $p<0.01$ ,  $p<0.01$  and  $p<0.001$  respectively) (Figure 5.4A). The same situation was seen with RV-3-G but also including MRS-1191 (Figure 5.4B). For both resveratrol and RV-3-G, the growth inhibition was not reversed when the inhibitors were applied. Only compound C reversed the growth inhibition by RV-4'-G (Figure 5.4C). Interestingly, none of the inhibitors reversed the growth inhibitory effects of RV-3-S (Figure 5.4D). Cell growth was unaffected by any of the inhibitors on their own (Figure 5.4E). The results for the effect of the inhibitors when used in combination are summarised in Table 5.1.

**Table 5.1** Summary of significant effects of the inhibitors and their ability to reverse the effects of resveratrol, resveratrol-3-O-D-glucuronide, resveratrol-4'-O-D-glucuronide and resveratrol-3-O-D-sulphate.

Cell Line	Combination treatments that significantly reversed the growth inhibition			
	RV	RV-3-G	RV-4'-G	RV-3-S
CCL-228	MRS-1191 Compound C	MRS-1191 Compound C	MRS-1191 Compound C	No activity of RV-3-S
Caco-2	MRS-1191	MRS-1191 Compound C	MRS-1191 Compound C	No activity of RV-3-S
HCT-116	Compound C PD98059 LY294002	MRS-1191 Compound C PD98059 LY294002	Compound C	-

## **5.2 Investigation of cell cycle analysis with MRS-1191 co-treatment**

The most consistent results from the pharmacological approach in Section 5.1 were in the case of CCL-228 cells. The presence of the adenosine A<sub>3</sub> receptor antagonist (MRS-1191) and the AMPK inhibitor (compound C) were both sufficient to reverse the effects of resveratrol, RV-3-G and RV-4'-G. We therefore decided to investigate the effect of resveratrol, RV-3-G, RV-4'-G and RV-3-S treatments (all at 30µM) in the presence of MRS-1191 (10µM) and whether the reversal of growth inhibition observed previously was associated with changes in the cell cycle distribution. CCL-228 cells were therefore simultaneously treated with resveratrol and the metabolites in the presence and absence of MRS-1191 for 48 hours. They were subsequently harvested and stained with PI/RNase solution as previously described (see Section 2.5.1).

**Table 5.2** Cell cycle distribution of the CCL-228 human cancer cell line after treatment for 48 hours with resveratrol or metabolites (all at 30µM) in the presence and absence of the adenosine A<sub>3</sub> receptor antagonist, MRS-1191 (10µM).

Distribution (% cells)*					
Cell Line	Treatment	Sub-G1	G0/G1	S	G2/M
CCL-228	Control	0.785	67.44	15.03	13.38
	MRS-1191	0.635	66.60	15.68	12.94
	RV	1.92	57.25	<b>20.98*</b>	15.63
	RV+MRS-1191	2.045	56.12	19.17	18.28
	RV-3-G	0.810	<b>69.42*</b>	13.89	13.09
	RV-3-G + MRS	0.875	69.84	14.30	12.49
	RV-4'-G	0.82	<b>74.56*</b>	11.21	11.78
	RV-4'G + MRS	1.16	73.97	11.87	11.80
	RV-3-S	0.89	69.22	14.18	11.52
	RV-3-S + MRS	0.66	67.98	14.26	13.92
	ACT.D	1.52	66.10	18.84	9.74
	ACT.D + MRS	5.91	61.85	16.55	10.01
	DMSO	0.66	65.68	16.58	13.55
	DMSO + MRS	0.85	66.33	16.06	12.88

\*DNA content was analysed after staining with PI/RNase solution. The data represent the mean percentage of gated cells of three independent experiments in each phase of the cell cycle. There was no significant difference when comparing treatment alone or in the presence of MRS-1191 by  $\chi^2$  contingency analysis. \*p<0.05 if resveratrol or its metabolites were active compared to DMSO.

Treatment of CCL-228 cells with MRS-1191 alone did not lead to any differences in the distribution of cells. In fact, these were comparable to the untreated cells (percentage of cells in G0/G1 was 67.44% and 66.60% in untreated and MRS-1191 respectively). The S- and G2/M- phases were also similar in the two groups. Resveratrol treatment alone decreased the G0/G1 population to 57.25% but simultaneously increased the population of cells in both S (15.03% to 20.98%) and G2/M (13.38% to 15.63%) phases. Even though MRS-1191 co-treatment with resveratrol changed the proportion of cells in G0/G1 from 57.25% to 56.12% compared to resveratrol alone, this was not sufficient to completely reverse the effects back to the levels seen with the control (Table 5.2). In the case of RV-3-G, the proportion of cells in each phase of the cell cycle was not affected by the presence of MRS-1191. For example, the proportion of cells in G0/G1 with RV-3-G alone was 69.42% and with addition of MRS-1191, 69.84% (Table 5.2). Addition of MRS-1191 to cells treated with RV-4'-G further reduced the proportion of cells in G0/G1 (75.56% to 73.97%) and slightly increased those in S phase (11.21% to 11.87%), with no effect in G2/M. Resveratrol-3-O-D-sulphate alone had no significant effect on the cell cycle. More specifically, co-treatment increased the cells in G0/G1 from 69.22% to 67.98%, decreased those in S phase (14.18% to 14.26%) and finally, decreased the proportion in G2/M (11.52% to 13.92%). Similar to the untreated group, the vehicle control (0.1% DMSO) in the presence and absence of MRS-1191 did not affect the distribution of cells (Table 5.2). Actinomycin D did not cause arrest when added alone to CCL-228 cells with the proportion of cells in G0/G1 reaching 66.10%.

Contingency analysis of independent experiments (as mentioned in Chapter 2) investigating the differences in the presence and absence of the antagonist did not exhibit significance in all three experiments. Therefore, despite the fact that MRS-1191 was capable of reversing the effects of resveratrol and its two glucuronides on growth, it

does not seem likely that the distribution of cells in the various phases of the cell cycle is affected. It is evident from Table 5.1 that the proportion of cells in sub-G1 in the presence of absence of MRS-1191 is not significantly different in any group (Figure 5.4).

### **5.3 Investigation of cell cycle analysis with compound C co-treatment**

As mentioned previously, the findings from Section 5.2 involving the reversal of effects of resveratrol and its two glucuronides on the growth of CCL-228 following co-treatment with the AMPK inhibitor, compound C, led us to investigate the possible effect on the cell cycle. If compound C is capable of indirectly acting on the cell cycle, co-treatment will cause re-distribution of cells and the percentage of gated cells within each phase will reach the levels found in the untreated and vehicle control (0.1% DMSO) groups.

**Table 5.3** Cell cycle distribution of the CCL-228 human cancer cell line after treatment for 48 hours with resveratrol or metabolites (all at 30µM) in the presence and absence of the AMPK inhibitor, compound C (12.5µM).

Distribution (% cells)*					
Cell Line	Treatment	Sub-G1	G0/G1	S	G2/M
CCL-228	Control	0.785	58.01	20.60	18.63
	Compound C	1.92	63.00	19.04	14.90
	RV	1.92	56.53	20.98	17.00
	RV+ CC	5.12	<b>68.49</b>	14.44	12.47
	RV-3-G	0.81	<b>65.40*</b>	15.36	16.37
	RV-3-G + CC	1.24	64.49	16.68	15.68
	RV-4'-G	0.82	<b>65.74*</b>	15.11	16.21
	RV-4'G + CC	1.84	62.42	18.75	15.93
	RV-3-S	0.89	61.71	17.88	17.18
	RV-3-S + CC	3.76	60.11	20.87	15.17
	ACT.D	1.52	<b>65.68*</b>	18.68	11.27
	ACT.D + CC	6.92	<b>60.89</b>	18.41	11.35
	DMSO	0.66	57.87	21.17	17.23
	DMSO + CC	1.70	57.61	22.77	15.14

\*DNA content was analysed after staining with PI/RNase solution. The data represent the mean percentage of gated cells of three independent experiments in each phase of the cell cycle. There was no significant difference when comparing treatment alone or in the presence of compound C by X<sup>2</sup> contingency analysis. \*p<0.05 if resveratrol or its metabolites were active.

It is apparent from Table 5.3 above, that the cell distribution following treatment with the vehicle control is not significantly different to the untreated group (57.87% and 58.01% respectively). Addition of compound C alone increased the percentage of cells in G0/G1 as compared to both the vehicle and untreated groups but, following analysis this was not found to be significant. The combination of 0.1% DMSO with compound C did not alter the cell cycle when compared to treatment alone. Co-treatment of the parent compound, resveratrol with compound C not only decreased the percentage of cells in S phase, but actually arrested the cells in G0/G1 to levels greater than those seen with the two glucuronides. Resveratrol alone however, did not significantly arrest cells in S phase for all three experiments. More specifically, resveratrol with compound C caused a shift in the distribution from 56.53% (resveratrol alone) to 68.49% with a concomitant decrease in S phase from 20.98% to 14.44%.

In the case of RV-3-G, the observed G0/G1 arrest was not altered following combination treatment with compound C. For example, cells in G0/G1 in the presence of RV-3-G reached 65.40% and this was slightly, but not significantly, reduced to 64.49% following combination treatment by  $\chi^2$  analysis. The effect of RV-4'-G was more profound with a reduction in the cells present in G0/G1 from 65.74% to 62.42% and those in S phase increasing from 15.11% to 18.75% followed by a slight decrease in G2/M (16.21% to 15.93%). The scenario for RV-3-S was slightly different however; as exemplified previously, 30 $\mu$ M of RV-3-S alone was not sufficient to cause G0/G1 arrest (61.71%) unlike the other two metabolites. Administration of cells with compound C decreased the percentage of cells to 60.11% in G0/G1 followed by an increase in S phase from 17.88% to 20.87%. In fact, this value reached the levels for the control group (20.60%), and was followed by a slight decrease in the proportion of cells in G2/M (17.18% to 15.17%).

The scenario with the positive control, actinomycin D, was more profound. Co-administration with compound C was capable of reducing the percentage of cells in G0/G1 from 65.68% to 60.89% with a very surprising increase in sub-G1 to 6.92% ( $p>0.05$ ). The S- and G2/M phases were not affected however, when comparing the two groups. As in the previous section with MRS-1191 co-treatment, there was no significant effect in the number of cells in sub-G1 in the presence or absence compound C (Table 5.3). Based on these findings with compound C, it seems that actinomycin D causes AMPK activation.

**5.5 Western blot on the presence of Adenosine A3 receptor**

In order to confirm the presence of the adenosine A<sub>3</sub>receptor in Caco-2, CCL-228 and HCT-116 cells, western blot analysis was performed on untreated lysates. The blot in Figure 5.5 clearly confirms the presence of the A<sub>3</sub> receptor with comparable levels of protein in all three cell lines.

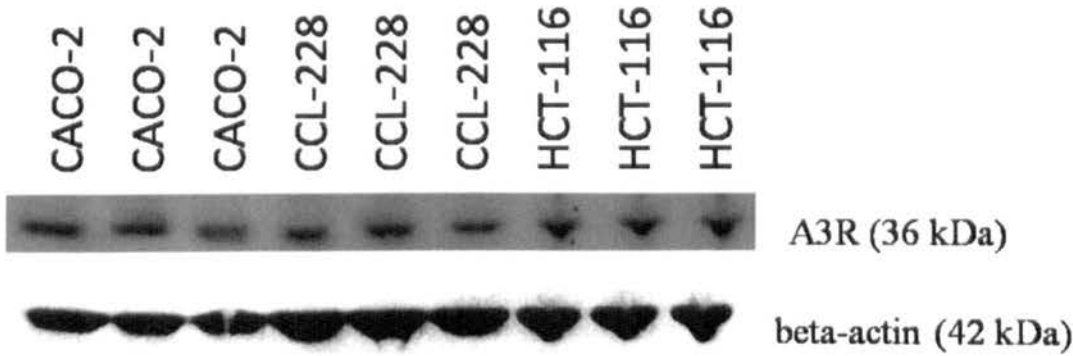


**Figure 5.5** Western blot analysis of untreated Caco-2, CCL-228 and HCT-116 cells to determine the presence of the adenosine A<sub>3</sub> receptor. Each cell line is blotted in triplicate and the image is representative of three independent experiments.



## 5.6 Adenosine A<sub>3</sub> receptor stimulation by 2CI-IB-MECA

The western blot results from section 5.5 confirmed the presence of the adenosine A<sub>3</sub> receptor. The highly selective A<sub>3</sub> receptor agonist, 2CI-IB-MECA was therefore added at a range of concentrations (1μM, 3μM, 10μM, 30μM and 100μM) to Caco-2, CCL-228 and HCT-116 cells for 48 hours and the viability was measured using the neutral red assay as mentioned previously in order to confirm the receptor activation.

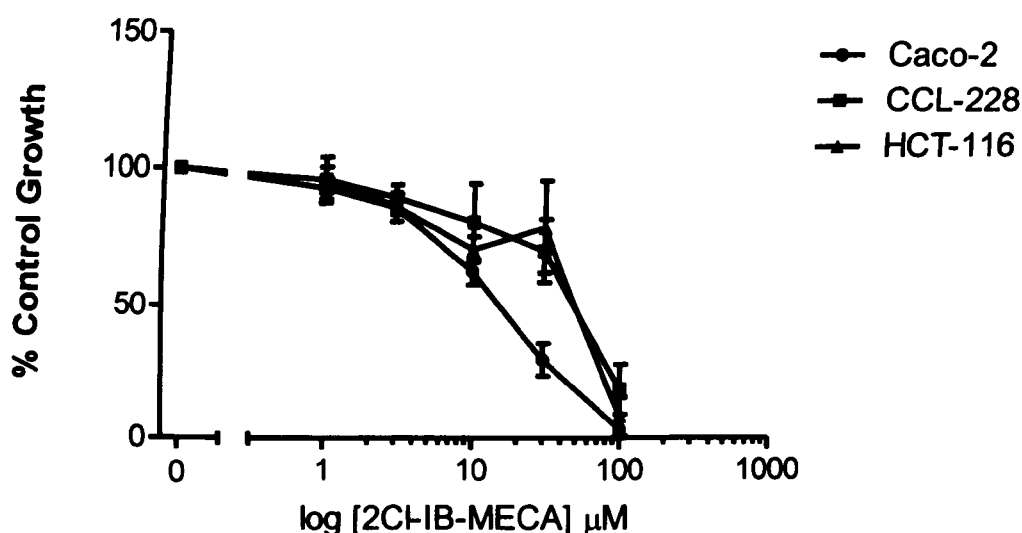


**Figure 5.6** Effect of the highly selective adenosine A<sub>3</sub> receptor agonist, 2CI-IB-MECA on the growth of Caco-2, CCL-228 and HCT-116 cells. Briefly, cells were treated at a range of concentrations for 48 hours and the neutral red viability assay was employed. Values represent the means (n=18) from three independent experiments ±SEM. Analysed by repeated measures ANOVA and Dunnett's test.

Treatment of Caco-2 cells with a range of 2CI-IB-MECA concentrations for 48 hours was capable of reducing the growth of cells. More specifically, a significant effect was seen at 10μM treatment with growth being reduced to 62.7±4.7% (p<0.05). This was greater at 30μM and even more so at 100μM where almost complete inhibition was achieved. The percentage of viable cells after 30μM treatment reached 29.9±6.2% whilst at 100μM, 3.7±1.8% (p<0.05 in both cases) (Figure 5.6). At lower concentrations

however, there was no significant reduction in growth with a mere inhibition of 15% after 3 $\mu$ M treatment and less so at 1 $\mu$ M ( $p \geq 0.05$ ). The  $IC_{50}$  in the case of Caco-2 was 14.3 $\mu$ M $\pm$ 3.0.

CCL-228 cells were also treated with 2CI-IB-MECA for 48 hours and the percent of control growth calculated relative to the absorbance of the untreated group. The effects of treatment exemplified in Figure 5.6 above seem less profound as compared to those seen with Caco-2 cells. More specifically, the only significant effect was apparent at 100 $\mu$ M treatment with growth being reduced to 18.7 $\pm$ 9.6% ( $p < 0.05$ ). In addition, the growth of CCL-228 cells was reduced by 30% at 30 $\mu$ M treatment but this was not significant ( $p > 0.05$ ) whilst at the lower concentrations of 1 $\mu$ M, 3 $\mu$ M and 10 $\mu$ M the effects were even less profound (95.8 $\pm$ 4.5%, 89.3 $\pm$ 4.4% and 80.4 $\pm$ 13.4% respectively). The  $IC_{50}$  value in the case of CCL-228 cells was found to be 42.5 $\mu$ M.

Treatment of HCT-116 cells with 2CI-IB-MECA for 48 hours produced similar results as in the case of CCL-228. More specifically, treatment at concentrations reaching 30 $\mu$ M had no significant effect on the growth of HCT-116 cells and thus no activation of the adenosine  $A_3$  receptor. For example 1 $\mu$ M treatment was sufficient to inhibit the growth of cells by 4.3% whilst at 10 $\mu$ M this was increased to 13.8% but overall the effects were not significantly different to the untreated group. At 30 $\mu$ M, this was potentiated further to 29.3% but this was not significant ( $p > 0.05$ ) (Figure 5.6). Similar to CCL-228, at 100 $\mu$ M, the growth of HCT-116 cells was significantly reduced indicating the activation of the receptor by the agonist with growth being 8.3 $\pm$ 7.3%. The  $IC_{50}$  value was 40.2 $\mu$ M, more comparable to CCL-288 cells rather than Caco-2.

**5.7 Co-treatment of cells with 2CI-IB-MECA and MRS-1191**

The adenosine A<sub>3</sub> receptor antagonist, MRS-1191 at a concentration of 10μM was added in the presence of 30μM 2CI-IB-MECA in order to investigate whether the observed effects of the agonist were reversed. The results from the neutral red assay were converted to percentage of control growth and presented in the figures below.

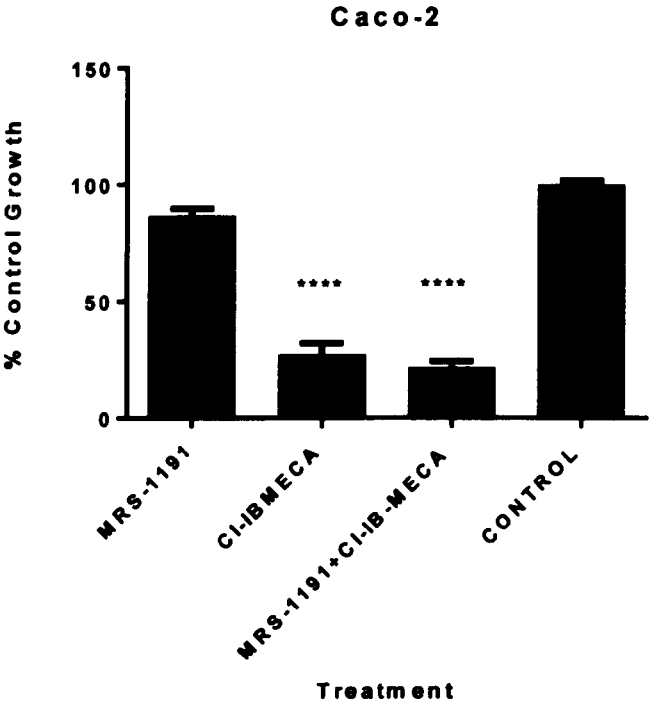


**Figure 5.7** Evaluation of the effects of MRS-1191 and 2CI-IB-MECA co-treatment in Caco-2 cells. Briefly 10μM MRS-1191 was added in the presence of 30μM 2CI-IB-MECA for 48 hours and the neutral red assay employed as previously described. Values represent mean (n=18) from three independent experiments. \*\*\*\* p<0.0001 relative to control by repeated measures ANOVA and Tukey’s test.

The results from co-treatment of MRS-1191 and 2CI-IB-MECA in Caco-2 cells are presented in Figure 5.7 above. It is apparent that treatment with 2CI-IB-MECA alone significantly inhibited the growth of cells to 27.4±4.8% (p<0.0001). Addition of MRS-1191 however was not sufficient to reverse the inhibitory effects of the adenosine A<sub>3</sub>

receptor agonist and remained significantly different to the untreated group with growth reaching even lower levels of  $21.8 \pm 2.8\%$  ( $p < 0.0001$ ). The effects of MRS-1191 alone were similar to the effects seen in the untreated group ( $p > 0.05$ ).

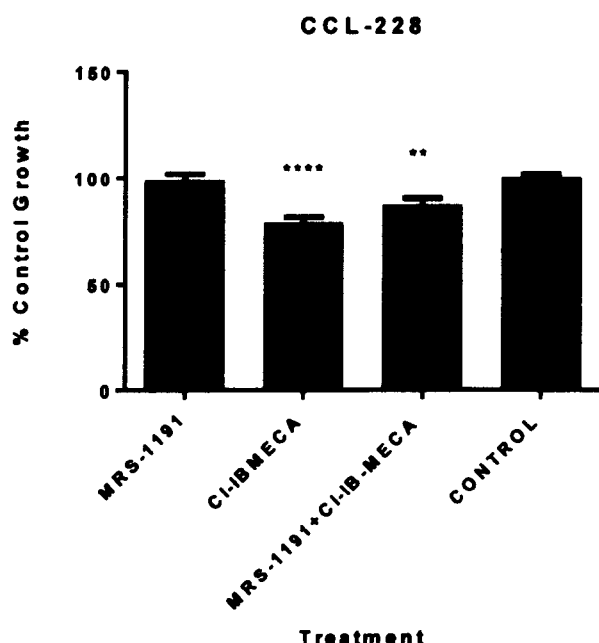


**Figure 5.8** Evaluation of the effects of MRS-1191 and 2CI-IB-MECA co-treatment in CCL-228 cells. Briefly  $10\mu\text{M}$  MRS-1191 was added in the presence of  $30\mu\text{M}$  2CI-IB-MECA for 48 hours and the neutral red assay employed as previously described. Values represent mean ( $n=18$ ) from three independent experiments. \*\* $p < 0.01$  and \*\*\*\* $p < 0.0001$  relative to control by repeated measures ANOVA and Tukey's test.

The possible reversal of growth inhibition was further investigated in CCL-228 cells. It is evident from Figure 5.8 above that addition of  $30\mu\text{M}$  2CI-IB-MECA in the absence of MRS-1191 significantly reduced the growth of CCL-228 cells to  $79.1 \pm 2.8\%$  relative to the control ( $p < 0.0001$ ). Despite the fact that addition of MRS-1191 slightly reversed the effects of the agonist to  $87.5 \pm 3.2\%$  this was not significant relative to 2CI-IB-MECA alone but to the control ( $p < 0.01$ ). MRS-1191 alone had no effect on growth ( $98.9 \pm 3.0\%$ ).

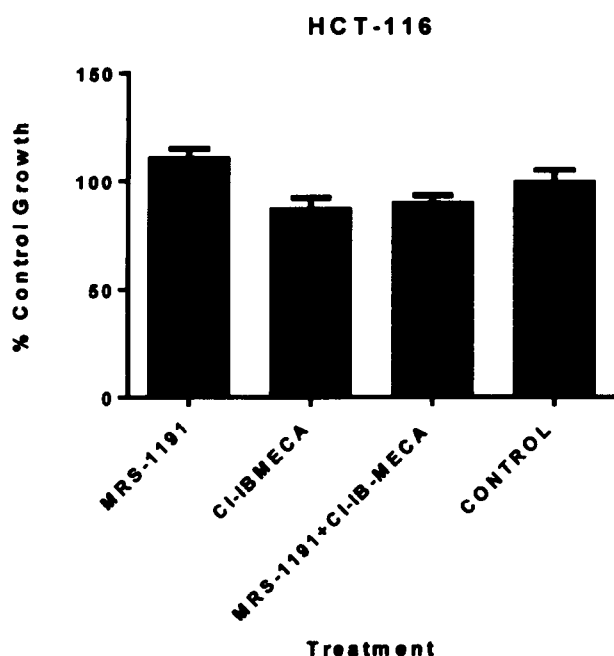


**Figure 5.9** Evaluation of the effects of MRS-1191 and 2CI-IB-MECA co-treatment in HCT-116 cells. Briefly 10 $\mu$ M MRS-1191 was added in the presence of 30 $\mu$ M 2CI-IB-MECA for 48 hours and the neutral red assay employed as previously described. Values represent mean (n=18) from three independent experiments.  $p>0.05$  relative to control by repeated measures ANOVA and Tukey's test.

Treatment of 2CI-IB-MECA in the presence and absence of MRS-1191 was further extended to HCT-116 cells. It is clear from Figure 5.9 that 30 $\mu$ M 2CI-IB-MECA treatment reduced the growth of HCT-116 cells to 88 $\pm$ 4.4% but this was not significantly different to the control group as expected ( $p>0.05$ ). Addition of the antagonist slightly reduced this inhibition and growth increased to 90.6 $\pm$ 2.8% but once again was found to be non-significant ( $p>0.05$ ). Similar to the results with the two other cell lines, MRS-1191 treatment alone had no effect on the growth of the cells as compared to the control with growth reaching 111.3 $\pm$ 3.6%. The results of the effect of 30 $\mu$ M 2CI-IB-MECA on the growth of the three cell lines are in agreement with the previous experiment (Section 5.6).

## 5.8 Western blots for AMPK and p-AMPK

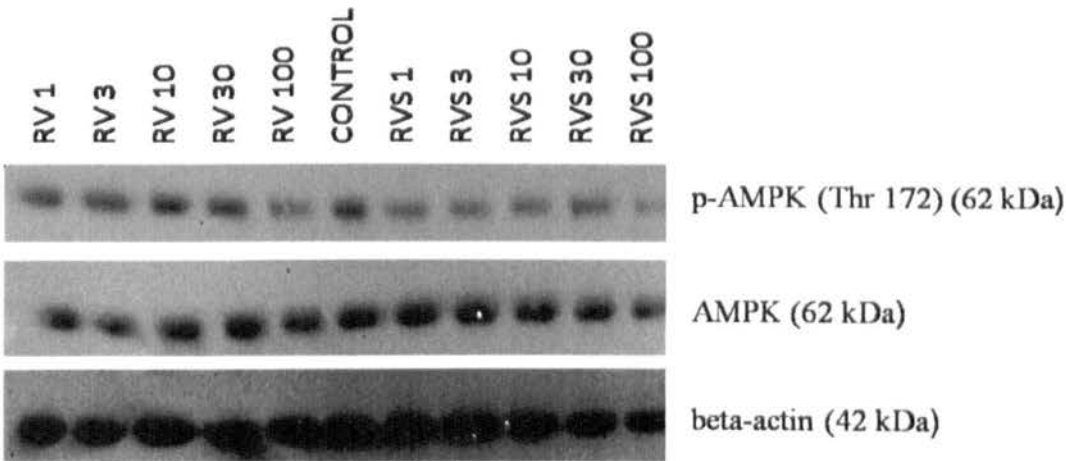
The results from the screening experiment with four known inhibitors identified two promising targets for resveratrol and its metabolites. We therefore decided to assess the phosphorylation levels of AMPK in the three cell lines at a range of concentrations after 48 hour treatment.

Caco-2 cells were treated with resveratrol and its metabolites, RV-3-G, RV-4'-G and RV-3-S at a range of concentrations (1 $\mu$ M, 3 $\mu$ M, 10 $\mu$ M, 30 $\mu$ M and 100 $\mu$ M) for 48 hours and western blot analysis performed in order to assess the total and phosphorylated levels of AMPK. Following density analysis by the ImageJ software it is evident that the relative ratios of phosphorylated AMPK to total AMPK were greater in the treated groups as compared to the control but the difference was not found to be significant (Figure 5.10B). For example 3 $\mu$ M resveratrol gave a greater relative density as compared to the control, but, this was not significant. The results from cells treated with RV-3-S appear in Figure 5.10 where activation of AMPK via phosphorylation does not take place at any concentration. Density analysis of the bands for each concentration appears to be comparable to the relative levels of the control with no significant difference ( $p>0.05$ ) (Figure 5.10B).

The representation in Figure 5.11 illustrates the phosphorylated and total AMPK levels in Caco-2 cells following treatment with the two glucuronide metabolites, RV-3-G and RV-4'-G. Similar to the results from the sulphated metabolite, it seems that AMPK did not become activated (phosphorylated) at a higher degree than the basal levels. Again, increasing concentrations do not appear to affect the level of activation. This appeared to be consistent in the case of both RV-3-G and RV-4'-G. Analysis of the relative levels of p-AMPK/AMPK shown in Figure 5.11 further exemplified these findings. The only

exception was in the case of 100μM RV-4'-G where an increase in the relative value was seen after three experiments but this was not found to be a significant difference.

A



B

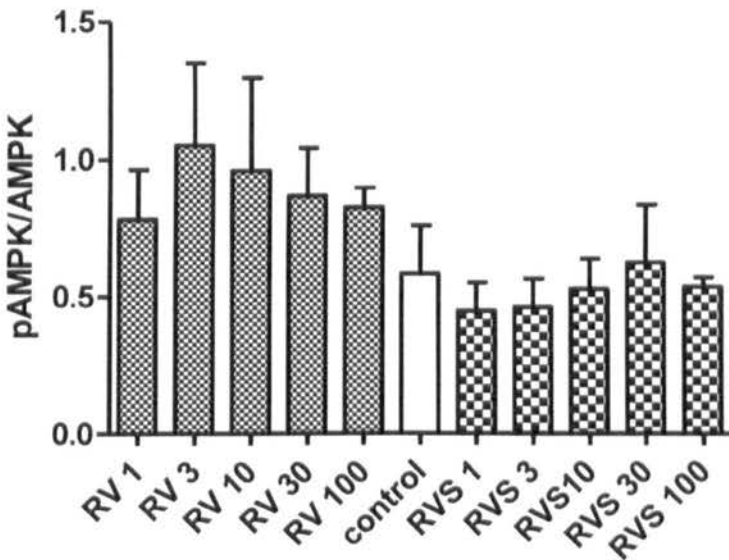
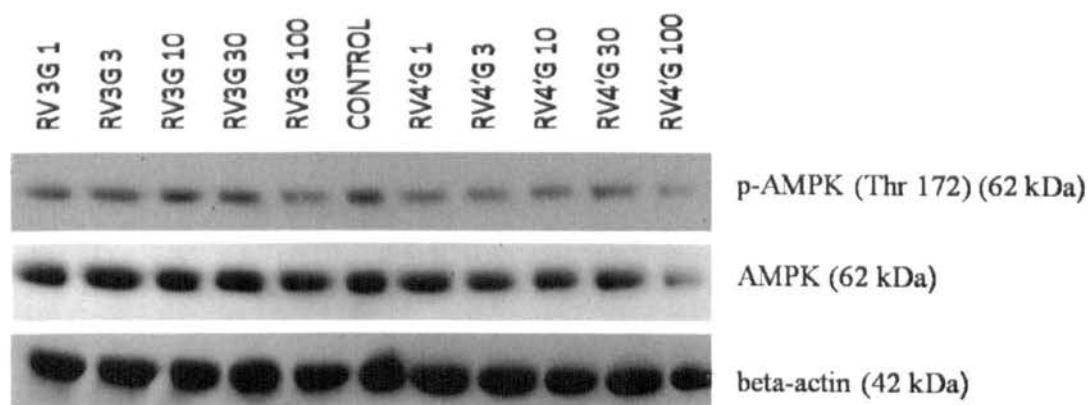


**Figure 5.10** Western blot analysis of total and phosphorylated AMPK levels after treatment with resveratrol and RV-3-S in Caco-2 cells. Representative blot (A) and density analysis by ImageJ of p-AMPK/AMPK relative levels. Levels are the means of three independent experiments±SEM.  $p>0.05$  by repeated measures ANOVA and Dunnett's test relative to the control group.

A



B

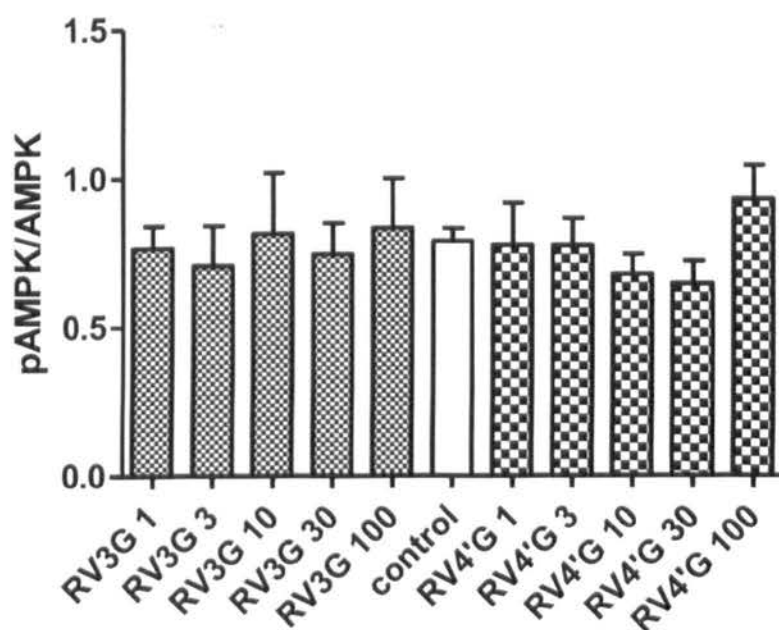


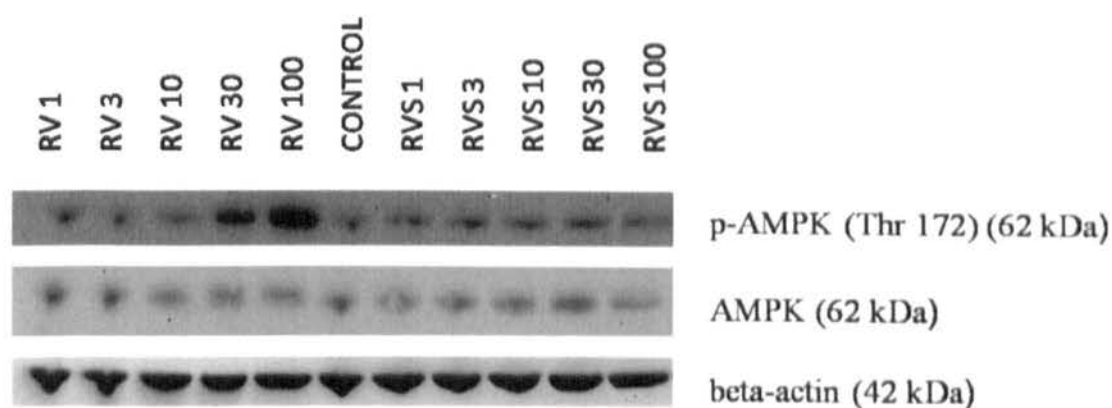
**Figure 5.11** Western blot analysis of total and phosphorylated AMPK levels after treatment with RV-3-G and RV-4'-G in Caco-2 cells. Representative blot (A) and density analysis by ImageJ of p-AMPK/AMPK relative levels. Levels are the means of three independent experiments  $\pm$  SEM.  $p > 0.05$  by repeated measures ANOVA and Dunnett's test relative to the control group.



Unlike in the case of Caco-2 cells, treatment of CCL-228 cells with increasing concentrations of resveratrol significantly increased the phosphorylation levels of AMPK (Figure 5.12). This was found to be significant at 30 $\mu$ M and 100 $\mu$ M ( $p < 0.01$  and  $p < 0.001$  respectively) (Figure 5.12B). Similar to the effects of RV-3-S treatment on Caco-2 cells were those on CCL-228. More specifically, 48 hour treatment with a range of RV-3-S concentrations was not sufficient to activate AMPK and the relative levels following three experiments remained constant and at the same levels as the untreated group.

Seen in Figure 5.13 below is the representative blot of CCL-228 cells after treatment with the two glucuronide metabolites. It appears that with increasing concentrations of RV-3-G, the total AMPK levels remained unaffected as did the phosphorylated levels (Figure 5.13A). Density analysis further confirmed this with p-AMPK/AMPK relative levels not appearing any significantly different to the control group (Figure 5.13B). The scenario in the case of RV-4'-G appears slightly different. More specifically, the p-AMPK levels were increased at 30 $\mu$ M and 100 $\mu$ M but not at 1 $\mu$ M, 3 $\mu$ M and 10 $\mu$ M. The total AMPK protein levels remained fairly constant independent of concentration. Further analysis of the relative levels has identified a slight increase at 10 $\mu$ M but this were not significantly different. The greatest effect was seen at 30 $\mu$ M where the relative levels increased significantly ( $p < 0.01$ ) (Figure 5.13B).

A



B

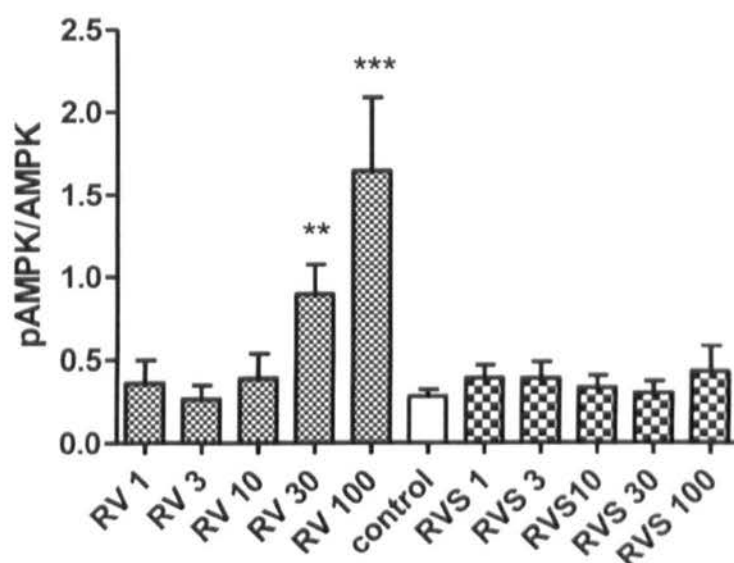
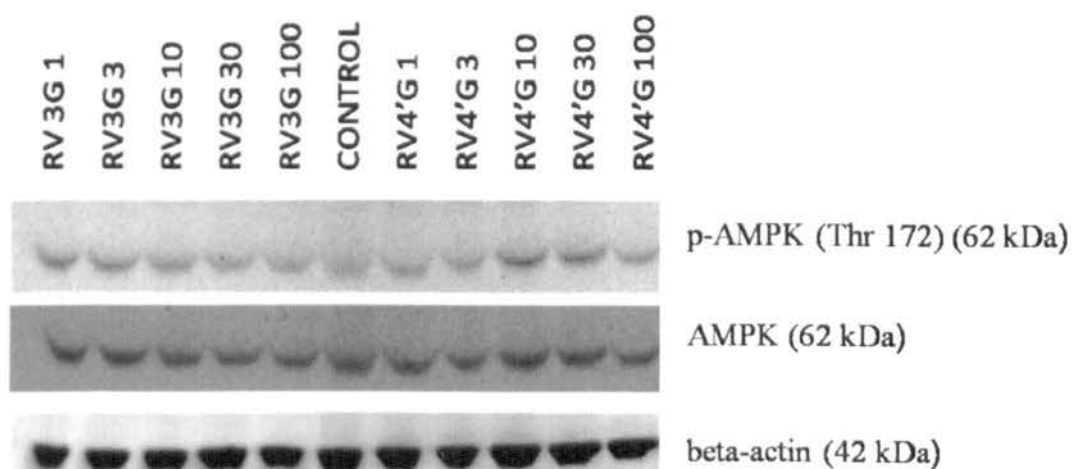


**Figure 5.12** Western blot analysis of total and phosphorylated AMPK levels after treatment with resveratrol and RV-3-S in CCL-228 cells. Representative blot (A) and density analysis by ImageJ of p-AMPK/AMPK relative levels. Levels are the means of three independent experiments $\pm$ SEM. \*\*  $p < 0.01$  and \*\*\*  $p < 0.001$  by repeated measures ANOVA and Dunnett's test relative to the control group.

A



B

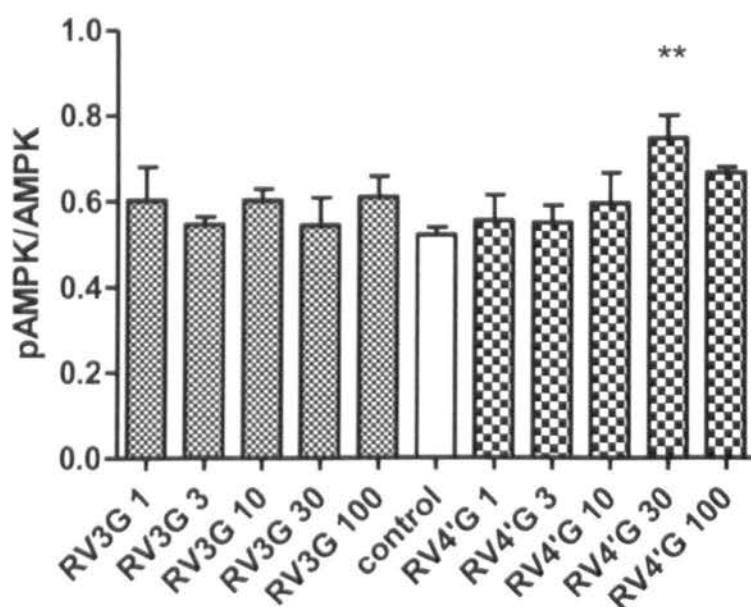
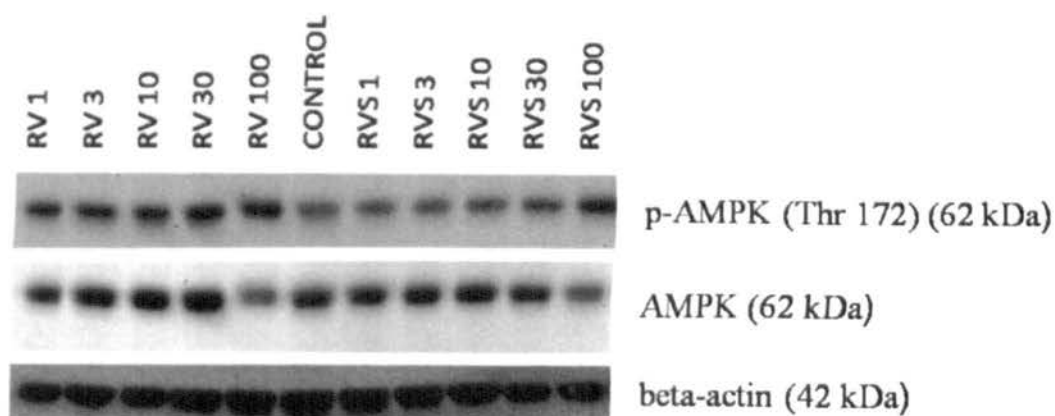


**Figure 5.13** Western blot analysis of total and phosphorylated AMPK levels after treatment with RV-3-G and RV-4'-G in CCL-228 cells. Representative blot (A) and density analysis by ImageJ of p-AMPK/AMPK relative levels. Levels are the means of three independent experiments $\pm$ SEM. \*\*  $p < 0.01$  by repeated measures ANOVA and Dunnett's test relative to the control group.

Western blot analysis was further performed on HCT-116 treated cells with resveratrol and resveratrol-3-O-D-sulphate. It is evident that with increasing resveratrol concentrations the phosphorylation levels increased whilst total AMPK levels remain constant except in the case of 100 $\mu$ M where total AMPK was reduced (Figure 5.14). Density analysis further illustrated this with a significant difference in the relative levels of p-AMPK/AMPK at 100 $\mu$ M resveratrol treatment ( $p<0.001$ ) (Figure 5.14). The levels of the phosphorylated protein of the control group remained low. In the case of RV-3-S, the levels of total AMPK reduced with increasing concentrations followed by a concomitant increase in p-AMPK which was more evident at 100 $\mu$ M. Further analysis demonstrated this activation of AMPK at 100 $\mu$ M but this was not found to be significant.

Exemplified in Figure 5.15 below are the results following RV-3-G and RV-4'-G treatment in HCT-116 cells. It can be clearly seen from the image of the blot that total AMPK levels remained constant at concentrations up to 30 $\mu$ M and these drop at 100 $\mu$ M (Figure 5.15). With regards to p-AMPK expression and RV-3-G treatment, levels appeared the same to the untreated samples except in the case of 100 $\mu$ M where the levels increased but not significantly. In addition, treatment with RV-4'-G expressed lower levels of total AMPK as compared to RV-3-G treatment and were decreased significantly at 100 $\mu$ M. Regarding p-AMPK levels, these were gradually increased with increasing concentrations. Analysis using ImageJ clearly identified a significant activation of AMPK at 100 $\mu$ M RV-4'-G treatment ( $p<0.01$ ) (Figure 5.15).

A



B

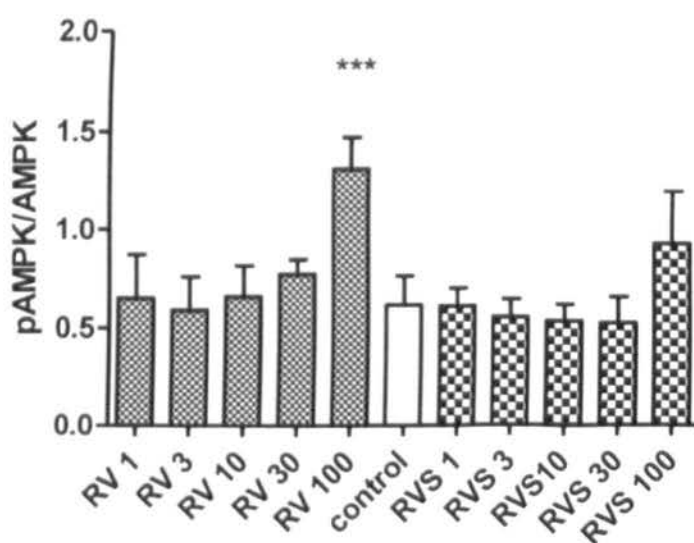
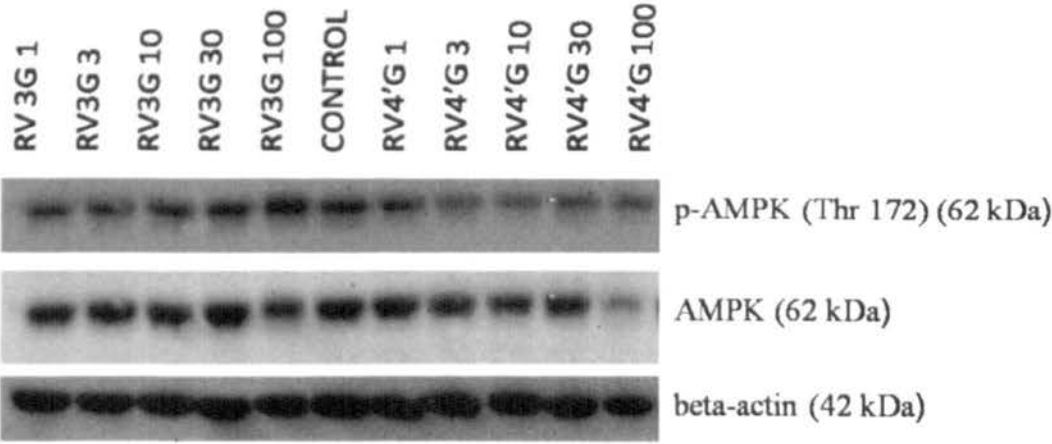


**Figure 5.14** Western blot analysis of total and phosphorylated AMPK levels after treatment with resveratrol and RV-3-S in HCT-116 cells. Representative blot (A) and density analysis by ImageJ of p-AMPK/AMPK relative levels. Levels are the means of three independent experiments  $\pm$  SEM. \*\*\*  $p < 0.001$  by repeated measures ANOVA and Dunnett's test relative to the control group.

A



B

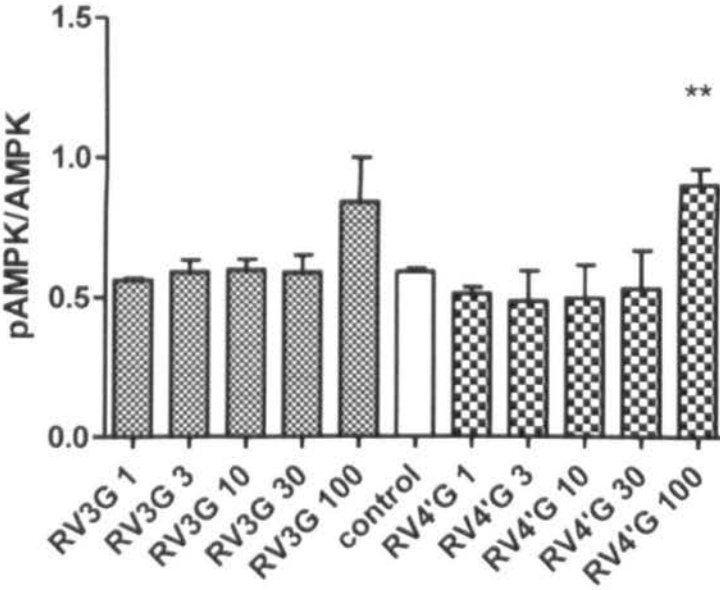


**Figure 5.15** Western blot analysis of total and phosphorylated AMPK levels after treatment with RV-3-G and RV-4'-G in HCT-116 cells. Representative blot (A) and density analysis by ImageJ of p-AMPK/AMPK relative levels. Levels are the means of three independent experiments $\pm$ SEM. \*\*  $p < 0.01$  by repeated measures ANOVA and Dunnett's test relative to the control group.

## 5.9 Discussion

The aim of this chapter was to gain a further insight into the mechanism of action of resveratrol metabolites and to further elucidate the growth arrest effects seen in the previous chapters. The results from the initial screening with four known inhibitors (MRS-1191, compound C, LY294002 and PD98059) provided us with some indication of possible targets being affected by treatment. MRS-1191 was effective in seven out of nine experiments where resveratrol, RV-3-G and RV-4'-G inhibited growth in the three cell lines. Compound C was effective in eight out of nine experiments. PD98059 and LY294002 were positive in the case of HCT-116 and only resveratrol and RV-3-G. RV-3-S suppressed growth inefficiently and inhibitors had no reversing effect (Table 5.1).

### **Adenosine A<sub>3</sub> receptors**

Adenosine A<sub>3</sub> receptors have been widely studied and suggested to be involved in the protective effects exerted by resveratrol on ischaemia in the heart (Das *et al.*, 2005). These findings led to suggest their involvement in cancer cell growth. It has been shown that adenosine A<sub>3</sub> receptor expression is up-regulated in tumour cells and tissues with variable expression levels in different cell lines (Gessi *et al.*, 2007). Western blot results from this study on untreated Caco-2, CCL-228 and HCT-116 cells have confirmed the presence of the A<sub>3</sub> receptor. These findings were further substantiated by demonstrating that activation of A<sub>3</sub> using a selective agonist, 2CI-IB-MECA caused growth inhibition in all three cell lines in a dose-dependent manner. It is also possible that adenosine A<sub>3</sub> receptors are expressed on the apical side of Caco-2 monolayers therefore explaining some of the effects of resveratrol and the metabolites at 30 µM treatments on the apical side (see Chapter 3). In fact, unpublished data from our laboratory (Dr. Mark Carew)

has identified that 2CI-IB-MECA is active on the apical side of Caco-2 monolayers and stimulates the short circuit current ( $I_{SC}$ ) (a measure of net ion transport) suggesting expression of apical  $A_3$  receptors.

Presumed activation of the adenosine  $A_3$  receptor resulted in marked impairment in cell growth therefore suggesting a vital role of this receptor in the control of the cell cycle. In fact, these findings seem to correlate with the results from the previous chapters where growth inhibition and cell cycle arrest were evident. The selective adenosine  $A_3$  receptor antagonist, MRS-1191 at  $10\mu\text{M}$  however, was not capable of preventing the effects of 2CI-IB-MECA. Several possibilities could be the higher 2CI-IB-MECA concentration used in this study ( $30\mu\text{M}$ ) as compared to other studies ( $10\mu\text{M}$  and  $20\mu\text{M}$  for 24 and 48 hours) (Kim *et al.*, 2012), insufficient MRS-1191 leading to non-reversal of effects or this could be overall attributed to cell variability. For example, Kim and colleagues (2012) showed that the reduction of ERK and Akt phosphorylation induced by  $20\mu\text{M}$  2CI-IB-MECA was prevented by  $10\mu\text{M}$  MRS-1191 therefore suggesting that 2CI-IB-MECA-induced ERK and Akt down-regulation was through the activation of the  $A_3$  receptor. Another study however, showed that 2CI-IB-MECA at concentrations greater than  $10\mu\text{M}$  was capable of inhibiting the growth of human thyroid cancer cells (NPA), independently of adenosine  $A_3$  receptor activation which could explain the inability of MRS-1191 of reversing the effects in the experiments of this study (Morello *et al.*, 2008). In fact the same group also used varying concentrations of additional selective  $A_3$  receptor antagonists including MRS-1523 ( $0.03\text{--}10\mu\text{M}$ ) and FA385 ( $0.5\text{--}5\mu\text{M}$ ) that were not able to counteract the inhibitory effect of 2CI-IB-MECA after 24 hour incubation. This suggests that 2CI-IB-MECA might interact with various intracellular targets following entry into the cell. Morello and colleagues tested the likelihood that 2CI-IB-MECA acts in an intracellular manner as a second messenger



following transport into the cells. Addition of the nucleoside transport inhibitor NBTI or dipyridamole (both at 10 $\mu$ M) did not reverse the effects of 2CI-IB-MECA and suggested that 2CI-IB-MECA could act directly with an intracellular target following cell entry by a nucleoside transporter-independent mechanism. A further group also identified that 2CI-IB-MECA causes apoptosis in two leukaemic cell lines through an adenosine A<sub>3</sub>-independent mechanism (Kim *et al.*, 2002).

An important finding in this study was the prevention of growth inhibitory effects of resveratrol and its glucuronides in the presence of the adenosine A<sub>3</sub> receptor antagonist, MRS-1191. These results therefore suggest the involvement, though not exclusive, of A<sub>3</sub> receptors in the effects of resveratrol and its glucuronides on growth. However, cell cycle distribution analysis using CCL-228 cells in the presence of resveratrol and its metabolites found that MRS-1191 caused no significant shift in the redistribution of cells in each phase of the cell cycle. In addition, despite the fact that the growth of HCT-116 cells was halted at the highest 2CI-IB-MECA concentrations, addition of MRS-1191 was not sufficient to reverse the effects of resveratrol or its metabolites. These findings imply that the A<sub>3</sub> receptor signalling pathway is dependent on the cell-specific characteristics and the type of treatment (Merighi *et al.*, 2006).

A study using selective A<sub>1</sub> (DPCPX), A<sub>2A</sub> (2M 241385) and A<sub>2B</sub> (PSB1115) antagonists on the cell proliferation of NPA thyroid cancer cells in the presence of 2CI-IB-MECA have demonstrated the inability to block this effect or to prevent ERK1/2 dephosphorylation (Morello *et al.*, 2008).

The adenosine A<sub>3</sub> receptor is linked to phospholipase C (PLC) and its activation is expected to increase calcium levels. Activation is also associated with a decrease in adenylyl cyclase and cAMP levels but these were not measured. In order to further

implicate the involvement of the adenosine A<sub>3</sub> receptor pathway and its downstream molecules we designed a study where the phospholipase C (PLC) inhibitor, U73122 and the selective chelator of intracellular Ca<sup>2+</sup> stores, BAPTA-AM were added in the presence of 30µM treatments of resveratrol and its metabolites for 48 hours. Unfortunately however, the concentrations of U73122 and BAPTA-AM when used alone had detrimental effects on the cells and these experiments were not pursued (data not shown).

### **AMPK**

The implication of AMPK in the effects presented in the previous chapters arose from the results after addition of compound C where reversal of growth inhibition was evident for resveratrol and the glucuronides in Caco-2 and CCL-228 cells. Protein expressions levels of p-AMPK (Thr172) (activated AMPK) following resveratrol treatment at 30µM and 100µM clearly showed this activation which was in tight agreement with the results of co-treatment with compound C. The increase in the proportion of cells in G0/G1 due to the drop in S phase during combination of resveratrol with compound C and the subsequent decrease in the expression levels of cyclin D1 at both concentrations further involve the AMPK pathway. A noteworthy point to make at this stage is the absence of resveratrol-induced activation of AMPK in Caco-2 cells and the weak activation in HCT-116 (only at 100µM) further illustrating the differences between cell lines. This either suggests that cell lines are not reliable, or the AMPK is not always activated. Thirty micromolar concentrations of resveratrol-4'-O-D-glucuronide were sufficient to increase the phosphorylation levels of AMPK in CCL-228, in agreement with the growth studies in the presence of compound C and those of the cell cycle distribution. Additionally, 100µM treatment was sufficient to increase the protein expression levels but not to significant levels suggesting a dose-

dependent effect. This suggests that AMPK activation is weakly stimulated by the resveratrol glucuronides. The results of AMPK activation are in agreement with the study by Hwang and colleagues (2007) where it was suggested that AMPK activation seemed to be involved in the control of cell proliferation in resveratrol-treated HT-29 colorectal cancer cells (Hwang *et al.*, 2007). In addition, a further study reported similar findings in MDA-MB-231 and MCF-7 breast cancer cells where resveratrol caused an increase of AMPK phosphorylation at 10 $\mu$ M, 20 $\mu$ M, 40 $\mu$ M and 80 $\mu$ M treatments in a dose-dependent manner (Lin *et al.*, 2010). The results in the presence of compound C further indicated that AMPK was vital for growth inhibition of cancer cells treated with resveratrol and the glucuronide metabolites.

### **PI3K and MAPK**

Any possible involvement of the PI3K and MAPK pathways with resveratrol metabolites treatment was investigated to a small extent in this study. More specifically, by using the inhibitors LY294002 (PI3K inhibitor) and PD98059 (MAPK inhibitor) we aimed to identify whether the effects of the metabolites were reversed. These experiments showed several inconsistencies exemplified by the variable effects of these compounds on the different cell lines. For example, PD98059 was able to sufficiently halt the growth inhibition caused by resveratrol and resveratrol-3-O-D-glucuronide in HCT-116 cells only. In the case of LY294002, significant effects were only evident after resveratrol and RV-3-G treatments in HCT-116 cells. In fact a study by Chen *et al.* (2010) showed that treatment of LNCaP cells with LY294002 in the presence of resveratrol further potentiated the effects and caused inhibition of cyclin D1 and induction of Bim, p27<sup>Kip1</sup>, TRAIL, DR4 and DR5 (Chen *et al.*, 2010). Furthermore, addition of LY294002 significantly decreased cell proliferation in a dose-dependent manner at 24 and 48 hour exposure times in NPC cells with a concomitant increase in

apoptotic cells (Jiang *et al.*, 2010). PD98059 was also employed in a study investigating the effect of the flavonoid quercetin on the role of MAPK signalling in osteoblast growth. Results showed that cell death caused by quercetin was significantly reversed by the MEK/ERK inhibitor but not SB203580 (p38 inhibitor) and SP600125 (JNK inhibitor) (Nam *et al.*, 2008).

## **Conclusion**

The experiments in this chapter have provided evidence for the involvement of the adenosine A<sub>3</sub> receptor and its activation leading to growth inhibition of Caco-2 and CCL-228 cells. Additionally, activation of AMPK *via* phosphorylation at threonine 172 at moderate but achievable resveratrol and glucuronide metabolites concentrations was shown in CCL-228 and HCT-116 cells. These findings further suggest that any observed effects are cell-dependent with variability arising from cell type and response to agonists/activators (resveratrol and its metabolites) and inhibitors. Also, treatment of cells with 2CI-IB-MECA gave different IC<sub>50</sub> values which, further supports the idea of cell-dependent effects. The variable results seen in this chapter could be accounted for by cell variability and overall biological differences *in vitro*. This in turn illustrates the importance of conducting *in vivo* experiments to identify the effects of the metabolites as will be discussed in the next chapter.

## Chapter 6. Discussion

### 6.1 Overview

In this study, the identification of the growth inhibitory effect of three resveratrol metabolites (resveratrol-3-O-D-glucuronide, resveratrol-4'-O-D-glucuronide and resveratrol-3-O-D-sulphate) was evaluated using two widely known viability assays, the neutral red and MTT assays. It appears that the neutral red uptake assay, which is based on the incorporation of the dye in the lysosomes of viable cells, conferred greater sensitivity as compared to the MTT assay, which is a mitochondrial based assays. The main aim of this study was to investigate the effect of resveratrol metabolites therefore, despite the promising results of piceatannol and pterostilbene, these were not pursued further. Future studies discussed later however, will incorporate the two analogues.

Since this is one of the first studies investigating the effect of the metabolites on the growth of colorectal cancer cells it was vital to identify whether these compounds exerted any cytotoxic effects on normal cells. For this reason, sheep red blood cells were employed and high concentrations of drugs used. We found no evidence for necrosis, apoptosis, either caspase-dependent or -independent. However, these agents were capable of inducing cell cycle arrest. The effects of the metabolites on Caco-2 cells have since been shown in another study with inhibition of cell growth in a concentration-dependent manner ( $IC_{50} \sim 10\mu M$ ) and cell cycle arrest in G0/G1, contrary to resveratrol that caused S phase arrest (Storniolo & Moreno, 2012). The results depicted in this study however are not in agreement with a more recent study by Aires and colleagues (2013) which have reported an S phase arrest with all three metabolites ( $30\mu M$ ) in SW620 (metastatic colorectal cancer cell line).

The results obtained with resveratrol in this study are consistent with previous studies (Delmas *et al.*, 2003, Walle *et al.*, 2004, Rimando & Suh, 2008).

In order to mimic the intestinal epithelium, polarised cells were used and treated for a longer period of time at lower and more feasible concentrations. Results, however, showed that polarised, differentiated cells were not affected by these drugs at low micromolar concentrations. Growth was slightly affected at 30 $\mu$ M, when drugs were delivered from the apical side (Table 6.1). This suggested a possible receptor-mediated event. Another explanation for the differential effect could lie between the differences in the polarised cells (differentiated) as compared to growing cells (on 96-well plates).

There still remains insufficient evidence for a cytostatic action of the drugs at 30 $\mu$ M following drug removal and addition of fresh media for 48 hours using the three colorectal cancer cell lines (Figures 3.11-3.13). In fact, various experiments investigating the degree of apoptosis yielded negative results, concluding that these compounds do not induce apoptosis. It seems possible that due to the very low half-life of resveratrol (~8-14 minutes), drug removal removes the inhibition and causes arrest. If the growth inhibition relied solely on receptor activation, then removal of the drug would not cause or sustain this activation. Whether the metabolites actually get internalised into the cell would be an interesting possibility to investigate.

Cell cycle distribution analysis identified cell cycle arrest at G0/G1 for the two glucuronides in Caco-2 and CCL-228 cells but not HCT-116 indicating that the observed effects are cell type specific (Figures 4.2, 4.4 and 4.6). The sulphated metabolite showed no significant effect in the distribution of cells relative to untreated cells. The parent compound on the other hand caused S phase arrest in all three cell

lines, again illustrating the differential effect of the metabolites compared to resveratrol (Table 6.1).

As shown in Figures 5.2 and 5.3, a similar response of CCL-228 and Caco-2 cells to resveratrol, RV-3-G and RV-4'-G when used in combination with MRS-1191 and compound C, was observed causing reversal of growth inhibition. In HCT-116 cells the responses were more complicated. Indeed, in an initial analysis we found no effect of inhibitors (n=1). Further analysis of three experiments showed the involvement of AMPK (compound C) following treatment with resveratrol, RV-3-G and RV-4'-G. MRS-1191 was effective at reversing the inhibition observed with RV-3-G. For the first time, effects were observed with PD98059 and LY294002 in response to resveratrol and RV-3-G. The lack of any effects of LY294002 and PD98059 on the Caco-2 and CCL-228 cell lines was surprising since the MAPK and PI3K pathways are implicated and known to be important in colorectal cancer. One possibility explaining this lack of effect could be the concentrations used in this study and therefore further experiments are required for elucidation.

The involvement of A<sub>3</sub> receptors and AMPK were investigated in further detail, because the most commonly observed reversal effects were in the case of MRS-1191 and compound C. A pathway was therefore hypothesised leading from the activation of the adenosine A<sub>3</sub> receptor to inhibition of cell proliferation via effects on AMPK (Figure 6.1).

The presence of the A<sub>3</sub> receptor was confirmed by western blot and the stimulation of the receptor by addition of the highly selective agonist, 2CI-IB-MECA respectively. The involvement of the A<sub>3</sub> receptor was further shown following co-treatment of MRS-1191 (antagonist) in the presence of resveratrol and its glucuronide metabolites in

CCL-228 and Caco-2 cells with the evidence of reversal of growth inhibition. It has been previously shown that the adenosine A<sub>3</sub> receptor is highly expressed in cancer cells whilst the expression in normal cells is low. The expression of this receptor in tumour tissues was linked to disease severity (Fishman *et al.*, 2009). Previous studies have shown that targeting the A<sub>3</sub> receptor with specific agonists will lead to inhibition of tumour growth *via* controlling the Wnt and the NF-κB signalling pathways (Fishman *et al.*, 2009).

Measurement of the protein levels of total AMPK and phosphorylated AMPK as measured by western blot revealed its activation following treatment with resveratrol-4'-O-D-glucuronide in CCL-228 and HCT-116 at 30μM and 100μM respectively (Figures 5.13 and 5.15). Resveratrol-3-O-D-glucuronide, however, despite prior indications of the involvement of AMPK was not capable of significant activation of AMPK. AMPK activation by resveratrol on Caco-2 cells was not reliable and despite the fact that AMPK is a major target, it was not so easy to activate it consistently in this cell line. In the case of CCL-228 cells however, activation was clear at 30μM and 100μM but only significant at 30μM (Figure 5.12).



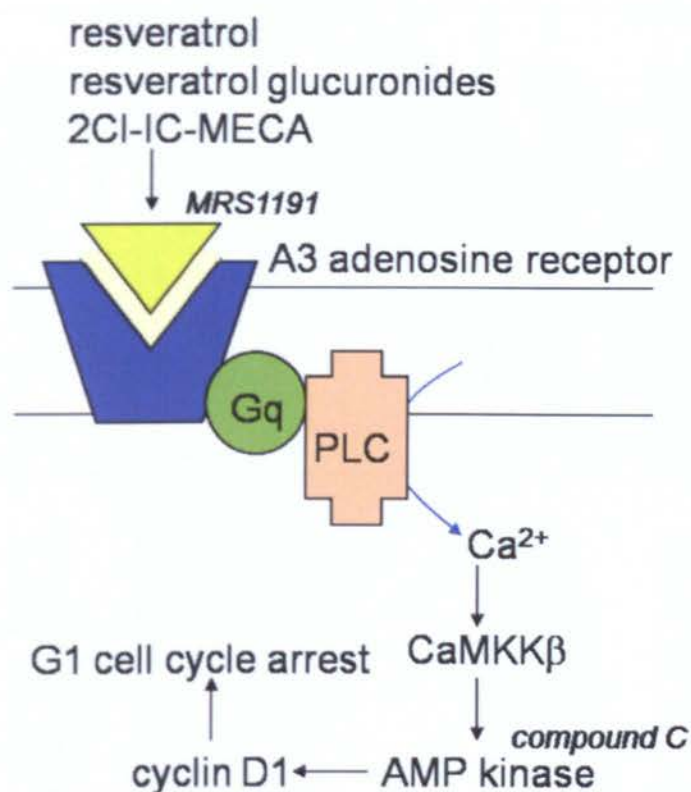


**Figure 6.1** Proposed signalling pathways in the action of resveratrol and its glucuronides on cell growth. The A<sub>3</sub> adenosine receptor is coupled via G<sub>q</sub> to phospholipase C (PLC) and an increase in intracellular calcium concentration (the receptor is also negatively coupled to G<sub>i</sub> and a decrease in cAMP, not shown). MRS-1191 is an adenosine A<sub>3</sub> receptor antagonist. Subsequent activation of calmodulin-dependent kinase kinase beta stimulates AMP-activated kinase (compound C is an inhibitor of this enzyme), leading to cyclin D1 depletion and cell cycle arrest.

**Table 6.1** Summary of the main findings of this study.

Experiment	Cell Line		
	Caco-2	CCL-228	HCT-116
Growth inhibition (NRU)	Dose-dependent response for all drugs with almost complete inhibition at 100µM (Table 3.1). IC <sub>50</sub> values: RV 23.8µM, RV-3-G 16.5µM, RV-4'-G 18.6µM, RV-3-S 11.2µM, PI 21.65µM, PS 4.98µM.	Dose-dependent response for all drugs with almost complete inhibition at 100µM (Table 3.1). IC <sub>50</sub> values: RV 9.8µM, RV-3-G 15.75µM, RV-4'-G 12.87µM, RV-3-S 21µM, PI 29.62µM, PS 35.76µM.	Dose-dependent response for all drugs with almost complete inhibition at 100µM (Table 3.1). IC <sub>50</sub> values: RV 15.1µM, RV-3-G 10.14µM, RV-4'-G 24.43µM, RV-3-S 31.03µM, PI 28.01µM, PS 18.25µM.
Growth inhibition (MTT)	Less sensitive as compared to the NRU. IC <sub>50</sub> values: RV 47.74µM, RV-3-G 28.94µM, RV-4'-G 15.40µM, RV-3-S 33.61µM.	Less sensitive as compared to the NRU. IC <sub>50</sub> values not possible to calculate.	Less sensitive as compared to the NRU. IC <sub>50</sub> values: RV 34.60µM, RV-3-G 40.63µM, RV-4'-G 42.57µM, RV-3-S 57.01µM.
11-day treatment on monolayers	No effect at 1µM apical or basolateral (except for Act.D) Significant effect with 30µM apical RV(50% reduction in growth) and less so with metabolites (20% reduction) (Figure 3.10).	N/A	N/A
Cytostatic experiment	No significant difference with RV; little activity of metabolites; no recovery with Act.D (Figure 3.11).	No activity with RV, RV-3-G and RV-4'-G; RV-3-S active but effect not reversed; no recovery with Act.D (Figure 3.12).	All compounds active; no significant reversal for RV and RV-3-G; RV-4'-G and RV-3-S effects not reversed; no recovery with Act.D (Figure 3.13).
Pre-treatment with Z-VAD-FMK	No significant effect (Figure 4.1).	No significant effect (Figure 4.2).	No significant effect (Figure 4.3).
DAPI-stained nuclei	No signs of apoptosis (Figure 4.4).	No signs of apoptosis (Figure 4.5).	No signs of apoptosis (Figure 4.6).
Expression levels of p53 (western blot)	N/A	N/A	Significant effect with 1µM RV and 4µM Act.D; no significant difference with the metabolites (Figure 4.7).

Table 6.1 continuation

	<b>Caco-2</b>	<b>CCL-228</b>	<b>HCT-116</b>
Expression levels of p53 (immunofluorescence)	N/A	N/A	Biphasic effect- higher levels at lower concentrations; decreased or no expression at 30μM and 100μM (Figures 4.8-4.12).
Cell cycle distribution analysis	S phase arrest with RV; G0/G1 with RV-3-G and RV-4'-G; no effect with RV-3-S; G0/G1 arrest with Act.D; no apoptosis (Table 4.2).	S phase arrest with RV; G0/G1 with RV-3-G and RV-4'-G; no effect with RV-3-S; G0/G1 arrest with Act.D; apoptosis only with RV (Table 4.4).	S phase arrest with RV; G0/G1 arrest with Act.D; no apoptosis (Table 4.6).
Expression levels of cyclin D1 (western blot)	Decreased levels with RV at 30μM and 100μM; RV-3-G and RV-3-S at 100μM (Figures 4.22 and 4.23).	Decreased levels with RV at 30μM and 100μM; RV-3-G and RV-3-S at 100μM (Figures 4.24 and 4.25).	RV-3-G and RV-4'-G at 100μM caused reduction in cyclin D1 (Figures 4.26 and 4.27).
Presence of inhibitors	Reversal of inhibition with: RV, RV-3-G and RV-4'-G with MRS-1191 and compound C except RV and compound C (Figure 5.3).	Reversal of inhibition with: RV, RV-3-G and RV-4'-G with MRS-1191 and compound C (Figure 5.2).	Reversal of inhibition with: RV with compound C, LY294002 and PD98059; RV-3-G with MRS-1191, compound C, LY294002 and PD98059; RV-4'-G with compound C (Figure 5.4).
Cell cycle distribution in the presence of MRS-1191	N/A	No significant difference in the presence of MRS-1191 (Table 5.2).	N/A
Cell cycle distribution in the presence of compound C	N/A	Change of S phase arrest to G0/G1 arrest with RV (Table 5.3).	N/A
Expression of the A <sub>3</sub> receptor	Present (Figure 5.7).	Present (Figure 5.7).	Present (Figure 5.7).
Effect of 2CI-IB-MECA	Dose-dependent effect (IC <sub>50</sub> 14.32μM) (Figure 5.8).	Dose-dependent effect (IC <sub>50</sub> 42.50μM) (Figure 5.8).	Dose-dependent effect (IC <sub>50</sub> 40.19μM) (Figure 5.8).
Co-treatment of 2CI-IB-MECA with MRS-1191	No reversal (Figure 5.9).	No reversal (Figure 5.10).	No reversal (Figure 5.11).
Expression levels of p-AMPK (Thr172) (western blot)	No significant effect (Figures 5.12 and 5.13).	Significant increase with 30μM and 100μM RV and 30μM RV-4'-G (Figures 5.14 and 5.15).	Significant increase with 100μM RV and 100μM RV-4'-G (Figures 5.16 and 5.17).

## **6.2 Future directions**

The incorporation of three colorectal cancer cell lines in this study and treatment with resveratrol and its metabolites returned variable results. One of the main points to emphasise is the variable action of drugs on different cell lines. Future drug studies on growth should, therefore also be employed on synchronised cells in specific phases of the cell cycle. Additional future considerations are presented below.

### **6.2.1 Effect of combination studies**

This is the first study investigating the mechanistic effects of the resveratrol metabolites and has provided some insight into certain molecular targets. As far as growth studies are involved it would be interesting to investigate the combinatorial effect of resveratrol, with its metabolites as well as piceatannol and pterostilbene and whether an additive, synergistic or antagonistic effect is observed. In fact, one of the recommendations of the Resveratrol 2012 Scientific Committee was to address the combination of resveratrol with other compounds ([www.resveratrol2012.eu](http://www.resveratrol2012.eu)). Also investigation of the effect of combination treatment on the cell cycle would be a logical next step. Moreover, studies investigating changes in the levels of other important cyclins involved in the cell cycle including cyclin E (late G1), cyclin A (S phase) and cyclin B1 (G2/M phase) are warranted for providing a greater insight in the actual involvement of these compounds in the cell cycle. Whether the metabolites directly target the cyclins or affect the cell cycle checkpoint inhibitors including p21 and p27 is another question that needs to be answered.

### 6.2.2 Autophagy

Since, for example, the growth inhibitory effects seen after treatment of Caco-2, CCL-228 and HCT-116 cells with resveratrol and its metabolites alone were not due to induction of apoptosis, it would be interesting to test the hypothesis of autophagy at concentrations less than 30 $\mu$ M. In fact, several studies have implicated resveratrol to cause death by autophagy (Opipari, 2004, Morselli *et al.*, 2011). The simplest experiment to conduct would be the measurement of LC3-GFP. LC3 stands for autophagosome-associated protein microtubule-associated protein 1 light chain and is being used as a marker of autophagy. In the absence of autophagy activation, LC3 is localised in the cytoplasm whilst following activation, it interacts with the isolation membrane and stays associated with the autophagosome membrane subsequent to vacuole formation (Kondo and Kondo, 2006). For this reason, transfection with the green fluorescent protein-linked LC3 chimeric plasmid is very helpful. Autophagic cells can therefore be identified using a fluorescent microscope by the presence of GFP-LC3 dots due to the fact that GFP-LC3 is restricted to autophagosomes. LC3 consists of two forms, type I and type II. Type I is present in the cytoplasm whilst type II is bound to the membrane. During the process of autophagy, the levels of type II increase due to the conversion of type I into type II (Kabeya *et al.*, 2000). The increased expression of LC3 type II can ultimately be detected by western blot due to the different molecular weights of the two forms, as can Beclin-1 which is an autophagy related protein. A study by Opipari *et al.* (2004) for example, showed that resveratrol caused S-phase arrest at 50 $\mu$ M after 24 hours and this accumulation was shifted into G0/G1 at 100 $\mu$ M with no increase in cells with hypodiploid DNA content therefore suggesting that cell death was not induced. Additionally, cells responding to 50 $\mu$ M resveratrol did not display the typical features of apoptosis including cytoplasmic condensation, nuclear fragmentation

or blebbing. In addition to the quantification of the marker of autophagy, transmission electron microscopy for the detection of autophagosomes would be an ideal way to confirm autophagy.

### **6.2.3 Involvement of p53 on growth**

The results from this current study showed that resveratrol and its metabolites are capable of inhibiting the growth of the three cell lines irrespective of p53 status suggesting that inhibition is not solely dependent on p53. The protein expression levels of p53 in HCT-116 cells were investigated by western blot and immunofluorescence. It was evident that resveratrol was capable of inducing the expression of total p53 whilst the effect was less profound with the metabolites by western blot. It would be noteworthy to quantify the levels of phosphorylated p53 (Serine 15) consequent to treatment in order to identify any differences. A time-dependent measurement of p53 is another possibility since a study by Lontas & Yeger (2004) for example, noted a progressive response in p53 with an apparent increase in cytoplasmic p53 by three hours, nuclear accumulation by six hours and apoptotic nuclei by twenty-four hours. Since the p53 experiments were conducted using the HCT-116 cells that possess wild-type p53, future work could involve using additional wild-type p53 cell types and also identification of any changes in the p53 status of Caco-2 and CCL-228 cell lines. *TP53* gene knockout experiments could also be conducted to identify whether cell growth is affected i.e. evidence of decreased growth inhibition.

Western blot and immunofluorescence analysis of treated HCT-116 cells with resveratrol and its metabolites identified a biphasic effect of treatment. For example, the protein levels of p53 were significantly increased following 1 $\mu$ M treatment of resveratrol but this decreased at higher concentrations. This suggests that hormesis

occurs and very low concentrations of resveratrol should be employed. Hormesis is characterised as a biphasic dose-response where low doses of a drug produce a given effect and higher doses result in the opposite effect (Vargas and Burd, 2010).

Studies investigating the effect of the flavonoid quercetin, in the absence of p53, have identified that mitochondria-mediated cell death occurs through the presence of p63 and p73 (Zhang *et al.*, 2009). p63 and p73 possess more than 60% homology within the DNA binding region of p53. This leads to transactivation of several p53 target genes by p63 and p73 including Bax. It would be interesting to investigate the possibility that both p63 and p73 are involved in or even replace the functions of p53 in cell lines with mutations in the tumour suppressor protein. The same group has identified a mechanism by which flavones and flavonols induce G2/M arrest and apoptosis in KYSE-510 oesophageal squamous cell carcinoma cells. This includes an increase in the expression levels of p63 and p73, leading to an increase in p21 that causes cell cycle arrest in G2/M phases followed by a reduction in cyclin B1 levels. These proteins also induced mitochondrial-dependent apoptosis via up-regulation of PIG3 (p53-inducible gene 3) and consequent caspase-9 and caspase-3 cleavage.

#### **6.2.4 Further investigation on the effect of resveratrol and its metabolites on signalling pathways**

The findings from the pharmacological approach using four known inhibitors have raised certain questions. Firstly, will lower concentrations of either the drugs of interest or of the inhibitors have the same effect as already seen? Are the effects cell type or tumour-type dependent? In fact, of the three cell lines used, it is already clearly evident that depending on the cell line, different targets are affected. Further studies are warranted however in order to substantiate the findings of this study and more

specifically probing for the involvement of the adenosine A<sub>3</sub> receptor. It is vital to elucidate whether the metabolites remain outside the cell to exert their effects or if they are capable of entering the cell. In addition, analysis by western blot using co-treated cells with these inhibitors and probing for the expression of total and phosphorylated levels of AMPK, PI3K and MAPK would be a logical next step. A further interesting experiment to perform would be the knockdown of the genes coding for these proteins or their over-expression and identify how the cells responded to treatment.

#### **6.2.4.1 AMPK**

In the case of quantifying the protein levels of AMPK, p-AMPK and cyclin D, further investigation is warranted to compare differences with either lower or greater exposure time to the drugs as well as using serum-free conditions. Additionally, the total and phosphorylated levels upon compound C co-treatment should be assessed by western blot. The implications that treatment has on upstream and downstream proteins in the AMPK pathway including LKB1 and mTOR would provide further insight into whether AMPK is a direct target of resveratrol and its metabolites. The levels of mTOR should therefore be measured in the future following treatment or identify the effects by blocking this with rapamycin.

#### **6.2.4.2 Adenosine A<sub>3</sub> receptor**

In the case of the possible involvement of the adenosine A<sub>3</sub> receptor as a target of resveratrol metabolites, this study has only provided some insight. It is vital to investigate each step downstream of the A<sub>3</sub> receptor (Figure 6.1). The results from this study have provided a mechanistic hypothesis and more specifically that resveratrol and the glucuronide metabolites bind to the adenosine A<sub>3</sub> receptor, and through activation of AMPK, cancer cell growth is inhibited. Future studies are therefore warranted to



provide direct evidence, including looking at the binding capability of the metabolites to the receptor in order to induce further downstream effects.

Furthermore, the effects of treatment on cells expressing high levels of the adenosine A<sub>3</sub> receptor compared to those with the gene knockdown of this receptor would be of great significance to identify possible differences and just how vital the A<sub>3</sub> receptor is. Additionally, upregulation of the A<sub>3</sub> receptor expression in cell lines followed by treatment with resveratrol and its metabolites would further substantiate its involvement. Since only 10µM MRS-1191 concentrations were used in the presence of resveratrol and metabolites (all at 30µM), further examination using a dose response of MRS-1191 on various other drug concentrations is required to identify the optimum concentrations. The specific MRS-1191 concentration was not sufficient to reverse the growth inhibitory effects of 2CI-IB-MECA for possible reasons explained previously so, again this emphasises the need for different concentrations. Protein levels of the A<sub>3</sub> receptor following treatment alone or in combination with MRS-1191 and other selective antagonists including MRE3008F20 and MRS1523 (A<sub>3</sub> antagonists), DPCPX (A<sub>1</sub> antagonist), ZM 241385 (A<sub>2</sub> antagonist) and PSB1115 (A<sub>2B</sub> antagonist) should be measured. In addition, the adenosine A<sub>3</sub> receptor levels should be assessed prior to and following treatment with resveratrol and its metabolites in order to make sure that the growth of these cells is not affected.

The experiments aimed to measure the changes in the intracellular Ca<sup>2+</sup> levels by co-treating cells with BAPTA-AM could not be presented due to the detrimental effect of BAPTA-AM alone on cells. Therefore, another experiment intended to measuring these levels using a fluorescent Ca<sup>2+</sup> indicator, Fura-2/AM in the presence and absence of the test compounds could be used and the fluorescent intensity ratio values recorded.

In addition to the *in vitro* based experiments, *in vivo* experiments investigating the various scenarios mentioned above are vital. This is due to the reason that in some occasions, the results from *in vitro* studies cannot be extrapolated or even reproduced *in vivo*. If the A<sub>3</sub> receptor is actually involved, MRS-1191 perfusion could be performed in animal studies to gain further insight. For example, this would involve dosing rats with AOM-induced cancers (azoxymethane), or APC<sup>Min</sup> mice for example, with resveratrol or metabolites and co-administer MRS-1191. It would also be interesting to look for signs of A<sub>3</sub> receptor activation e.g an increase in AMID in the nucleus. AMID is a marker protein, known as apoptosis-inducing factor (AIF)-homologous and mitochondria-associated protein that has been shown to be involved in caspase-independent apoptosis. It has been shown recently that adenosine causes caspase-independent apoptosis in SBC-3 lung cancer cells by upregulating AMID expression and promoting its translocation into the nucleus through the adenosine A<sub>3</sub> receptor (Kanno *et al.*, 2012). Therefore, it would be interesting to investigate the upregulation of AMID after growth inhibition by A<sub>3</sub> receptor stimulation.

### **6.3 Concluding remarks**

In conclusion, resveratrol still remains a very interesting drug with multiple effects and targets. The studies presented here show that the glucuronide and sulphate metabolites are active, which is a major step forward and that the mechanism may involve the A<sub>3</sub> receptor in some cell lines. These findings suggest a new hypothesis concerning the action of resveratrol that is readily testable. Possible intracellular targets have been identified in this study and further studies will aim to confirm and extend these results.

## Chapter 7. References

- ABBRACCHIO, M. P., BRAMBILLA, R., CERUTI, S., KIM, H. O., VON LUBITZ, D., JACOBSON, K. A. & CATTABENI, F. 1995. G protein-dependent activation of phospholipase C by adenosine A3 receptors in rat brain. *Molecular pharmacology*, 48, 1038-1045.
- AGGARWAL, B. B., BHARDWAJ, A., AGGARWAL, R. S., SEERAM, N. P., SHISHODIA, S. & TAKADA, Y. 2004. Role of Resveratrol in Prevention and Therapy of Cancer: Preclinical and Clinical Studies. *Anticancer research*, 24, 2783-2840.
- AGO, T., KURODA, J., PAIN, J., FU, C., LI, H. & SADOSHIMA, J. 2010. Upregulation of Nox4 by Hypertrophic Stimuli Promotes Apoptosis and Mitochondrial Dysfunction in Cardiac Myocytes. *Circulation Research*, 106, 1253-1264.
- AHMAD, N., ADHAMI, V. M., AFAQ, F., FEYES, D. K. & MUKHTAR, H. 2001. Resveratrol causes WAF-1/p21-mediated G1-phase arrest of cell cycle and induction of apoptosis in human epidermoid carcinoma A431 cells. *Clinical Cancer Research*, 7, 1466-1473.
- AIRES, V., LIMAGNE, E., COTTE, A. K., LATRUFFE, N., GHIRINGHELLI, F. & DELMAS, D. 2013. Resveratrol metabolites inhibit human metastatic colon cancer cells progression and synergize with chemotherapeutic drugs to induce cell death. *Molecular nutrition & food research*.
- ALESSI, D. R., ANDJELKOVIC, M., CAUDWELL, B., CRON, P., MORRICE, N., COHEN, P. & HEMMINGS, B. 1996. Mechanism of activation of protein kinase B by insulin and IGF-1. *The EMBO journal*, 15, 6541.
- ALMEIDA, L., VAZ-DA-SILVA, M., FALCÃO, A., SOARES, E., COSTA, R., LOUREIRO, A. I., FERNANDES-LOPES, C., ROCHA, J. F., NUNES, T. & WRIGHT, L. 2009. Pharmacokinetic and safety profile of trans-resveratrol in a rising multiple-dose study in healthy volunteers. *Molecular nutrition & food research*, 53, S7-S15.

ANDRÉ, T., BONI, C., MOUNEDJI-BOUDIAF, L., NAVARRO, M., TABERNERO, J., HICKISH, T., TOPHAM, C., ZANINELLI, M., CLINGAN, P. & BRIDGEWATER, J. 2004. Oxaliplatin, fluorouracil, and leucovorin as adjuvant treatment for colon cancer. *New England Journal of Medicine*, 350, 2343-2351.

ANDREADI, C., PATEL, K., BRITTON, R., SALE, S., HORNER-GLISTER, E., BROWN, V., BRENNER, D., SINGH, R., STEWARD, W., GESCHER, A., BROWN, K. Resveratrol sulfates provide an intracellular reservoir for generation of parent resveratrol and induce autophagy together with senescence in human colorectal cancer cells. Proceedings 8th NCRI Cancer Conference 2012, 2012 2012 Liverpool, UK.

ARIAS, M., QUIJANO, J. C., HARIDAS, V., GUTTERMAN, J. U. & LEMESHKO, V. V. 2010. Red blood cell permeabilization by hypotonic treatments, saponin, and anticancer avicins. *Biochimica et Biophysica Acta (BBA)-Biomembranes*, 1798, 1189-1196.

ATHAR, M., BACK, J. H., TANG, X., KIM, K. H., KOPELOVICH, L., BICKERS, D. R. & KIM, A. L. 2007. Resveratrol: A review of preclinical studies for human cancer prevention. *Toxicology and applied pharmacology*, 224, 274-283.

AVERY-KIEJDA, K., BOWDEN, N., CROFT, A., SCURR, L., KAIRUPAN, C., ASHTON, K., TALSETH-PALMER, B., RIZOS, H., ZHANG, X. & SCOTT, R. 2011. P53 in human melanoma fails to regulate target genes associated with apoptosis and the cell cycle and may contribute to proliferation. *BMC cancer*, 11, 203.

AYLON, Y. & OREN, M. 2011. New plays in the p53 theater. *Current opinion in genetics & development*, 21, 86-92.

AZIZ, M. H., AFAQ, F. & AHMAD, N. 2005. Prevention of Ultraviolet-B Radiation Damage by Resveratrol in Mouse Skin Is Mediated via Modulation in Survivin<sup>¶</sup>. *Photochemistry and photobiology*, 81, 25-31.

BAI, L. & ZHU, W. G. 2006. p53: structure, function and therapeutic applications. *J Cancer Mol*, 2, 141-153.

- BAI, Y., MAO, Q. Q., QIN, J., ZHENG, X. Y., WANG, Y. B., YANG, K., SHEN, H. F. & XIE, L. P. 2010. Resveratrol induces apoptosis and cell cycle arrest of human T24 bladder cancer cells in vitro and inhibits tumor growth in vivo. *Cancer science*, 101, 488-493.
- BALMAIN, A., BARRETT, J. C., MOSES, H. & RENAN, M. J. 1993. How many mutations are required for tumorigenesis? implications from human cancer data. *Molecular carcinogenesis*, 7, 139-146.
- BAR-YEHUDA, S., BARER, F., VOLFFSSON, L. & FISHMAN, P. 2001. Resistance of muscle to tumor metastases: a role for A3 adenosine receptor agonists. *Neoplasia (New York, NY)*, 3, 125.
- BAUR, J. A., PEARSON, K. J., PRICE, N. L., JAMIESON, H. A., LERIN, C., KALRA, A., PRABHU, V. V., ALLARD, J. S., LOPEZ-LLUCH, G. & LEWIS, K. 2006. Resveratrol improves health and survival of mice on a high-calorie diet. *Nature*, 444, 337-342.
- BAUR, J. A. & SINCLAIR, D. A. 2006. Therapeutic potential of resveratrol: the in vivo evidence. *Nature reviews. Drug discovery*, 5, 493-506.
- BISHAYEE, A. 2009. Cancer prevention and treatment with resveratrol: from rodent studies to clinical trials. *Cancer prevention research*, 2, 409-18.
- BISHOP, J. M. & WEINBERG, R. A. 1996. *Scientific American molecular oncology*, Scientific American.
- BOOCOCK, D. J., FAUST, G. E., PATEL, K. R., SCHINAS, A. M., BROWN, V. A., DUCHARME, M. P., BOOTH, T. D., CROWELL, J. A., PERLOFF, M., GESCHER, A. J., STEWARD, W. P. & BRENNER, D. E. 2007a. Phase I dose escalation pharmacokinetic study in healthy volunteers of resveratrol, a potential cancer chemopreventive agent. *Cancer epidemiology, biomarkers & prevention : a publication of the American Association for Cancer Research, cosponsored by the American Society of Preventive Oncology*, 16, 1246-52.

- BOOCOCK, D. J., FAUST, G. E. S., PATEL, K. R., SCHINAS, A. M., BROWN, V. A., DUCHARME, M. P., BOOTH, T. D., CROWELL, J. A., PERLOFF, M., GESCHER, A. J., STEWARD, W. P. & BRENNER, D. E. 2007b. Phase I Dose Escalation Pharmacokinetic Study in Healthy Volunteers of Resveratrol, a Potential Cancer Chemopreventive Agent. *Cancer Epidemiology Biomarkers & Prevention*, 16, 1246-1252.
- BRADAMANTE, S., BARENGHI, L. & VILLA, A. 2004. Cardiovascular protective effects of resveratrol. *Cardiovascular drug reviews*, 22, 169-188.
- BROSH, R. & ROTTER, V. 2009. When mutants gain new powers: news from the mutant p53 field. *Nature reviews. Cancer*, 9, 701-13.
- BROWN, V. A., PATEL, K. R., VISKADURAKI, M., CROWELL, J. A., PERLOFF, M., BOOTH, T. D., VASILININ, G., SEN, A., SCHINAS, A. M. & PICCIRILLI, G. 2010. Repeat dose study of the cancer chemopreventive agent resveratrol in healthy volunteers: safety, pharmacokinetics, and effect on the insulin-like growth factor axis. *Cancer research*, 70, 9003-9011.
- CALAMINI, B., RATIA, K., MALKOWSKI, M. G., CUENDET, M., PEZZUTO, J. M., SANTARSIERO, B. D. & MESECAR, A. D. 2010. Pleiotropic mechanisms facilitated by resveratrol and its metabolites. *The Biochemical journal*, 429, 273-82.
- CANTLEY, L. C. 2002. The phosphoinositide 3-kinase pathway. *Science Signalling*, 296, 1655.
- CAO, Y., WANG, F., LIU, H. Y., FU, Z. D. & HAN, R. 2005. Resveratrol induces apoptosis and differentiation in acute promyelocytic leukemia (NB4) cells. *Journal of Asian natural products research*, 7, 633-41.
- CATALGOL, B., BATIREL, S., TAGA, Y. & OZER, N. K. 2012. Resveratrol: French paradox revisited. *Frontiers in pharmacology*, 3, 141.
- CHAN, A. T. & GIOVANNUCCI, E. L. 2010. Primary prevention of colorectal cancer. *Gastroenterology*, 138, 2029-2043 e10.

- CHEN, Q., GANAPATHY, S., SINGH, K. P., SHANKAR, S. & SRIVASTAVA, R. K. 2010. Resveratrol induces growth arrest and apoptosis through activation of FOXO transcription factors in prostate cancer cells. *PloS one*, 5, e15288.
- CHOONG, M. L., YANG, H., LEE, M. A. & LANE, D. P. 2009. Specific activation of the p53 pathway by low dose actinomycin D: a new route to p53 based cyclotherapy. *Cell Cycle*, 8, 2810-2818.
- CHOW, H.-H. S., GARLAND, L. L., HSU, C.-H., VINING, D. R., CHEW, W. M., MILLER, J. A., PERLOFF, M., CROWELL, J. A. & ALBERTS, D. S. 2010a. Resveratrol Modulates Drug- and Carcinogen-Metabolizing Enzymes in a Healthy Volunteer Study. *Cancer prevention research*, 3, 1168-1175.
- CHOW, W.-H., DONG, L. M. & DEVESA, S. S. 2010b. Epidemiology and risk factors for kidney cancer. *Nature Reviews Urology*, 7, 245-257.
- CICHEWICZ, R. H. & KOUZI, S. A. 2002. Resveratrol oligomers: structure, chemistry, and biological activity. *Studies in natural products chemistry*, 26, 507-579.
- CLÉMENT, M.-V., HIRPARA, J. L., CHAUDHURY, S.-H. & PERVAIZ, S. 1998. Chemopreventive Agent Resveratrol, a Natural Product Derived From Grapes, Triggers CD95 Signaling-Dependent Apoptosis in Human Tumor Cells. *Blood*, 92, 996-1002.
- DAHLIN, A. M., VAN GUELPE, B., HULTDIN, J., JOHANSSON, I., HALLMANS, G. & PALMQVIST, R. 2008. Plasma vitamin B12 concentrations and the risk of colorectal cancer: a nested case-referent study. *International journal of cancer. Journal international du cancer*, 122, 2057-61.
- DAS, S., TOSAKI, A., BAGCHI, D., MAULIK, N. & DAS, D. K. 2005. Resveratrol-mediated activation of cAMP response element-binding protein through adenosine A3 receptor by Akt-dependent and -independent pathways. *The Journal of pharmacology and experimental therapeutics*, 314, 762-9.
- DEBNATH, J., BAEHRECKE, E. H. & KROEMER, G. 2005. Does autophagy contribute to cell death? *Autophagy*, 1, 66-74.

- DEFAZIO, A., CHIEW, Y. E., SINI, R. L., JANES, P. W. & SUTHERLAND, R. L. 2000. Expression of c-erbB receptors, heregulin and oestrogen receptor in human breast cell lines. *International Journal of Cancer*, 87, 487-498.
- DELMAS, D., AIRES, V., LIMAGNE, E., DUTARTRE, P., MAZUE, F., GHIRINGHELLI, F. & LATRUFFE, N. 2011. Transport, stability, and biological activity of resveratrol. *Annals of the New York Academy of Sciences*, 1215, 48-59.
- DELMAS, D., JANNIN, B., CHERKAOU, M. M. & LATRUFFE, N. 2000. Inhibitory effect of resveratrol on the proliferation of human and rat hepatic derived cell lines. *Oncology reports*, 7, 847.
- DELMAS, D., REBE, C., LACOUR, S., FILOMENKO, R., ATHIAS, A., GAMBERT, P., CHERKAOU-MALKI, M., JANNIN, B., DUBREZ-DALLOZ, L., LATRUFFE, N. & SOLARY, E. 2003. Resveratrol-induced apoptosis is associated with Fas redistribution in the rafts and the formation of a death-inducing signaling complex in colon cancer cells. *The Journal of biological chemistry*, 278, 41482-90.
- DO, G. M., KWON, E. Y., KIM, H. J., JEON, S. M., HA, T. Y., PARK, T. & CHOI, M. S. 2008. Long-term effects of resveratrol supplementation on suppression of atherogenic lesion formation and cholesterol synthesis in apo E-deficient mice. *Biochemical and biophysical research communications*, 374, 55-59.
- DONG, C., DAVIS, R. J. & FLAVELL, R. A. 2002. MAP kinases in the immune response. *Annual review of immunology*, 20, 55-72.
- DONG, Z. 2003. Molecular mechanism of the chemopreventive effect of resveratrol. *Mutation Research/Fundamental and Molecular Mechanisms of Mutagenesis*, 523-524, 145-150.
- DOUILLARD, J.-Y., HOFF, P. M., SKILLINGS, J. R., EISENBERG, P., DAVIDSON, N., HARPER, P., VINCENT, M. D., LEMBERSKY, B. C., THOMPSON, S. & MANIERO, A. 2002. Multicenter phase III study of uracil/tegafur and oral leucovorin versus fluorouracil and leucovorin in patients with previously untreated metastatic colorectal cancer. *Journal of clinical oncology*, 20, 3605-3616.



EASTON, J., WEI, T., LAHTI, J. M. & KIDD, V. J. 1998. Disruption of the cyclin D/cyclin-dependent kinase/INK4/retinoblastoma protein regulatory pathway in human neuroblastoma. *Cancer research*, 58, 2624-2632.

ELMORE, S. 2007. Apoptosis: a review of programmed cell death. *Toxicologic pathology*, 35, 495-516.

EUSSEN, S. J., VOLLSET, S. E., HUSTAD, S., MIDTTUN, O., MEYER, K., FREDRIKSEN, A., UELAND, P. M., JENAB, M., SLIMANI, N., BOFFETTA, P., OVERVAD, K., THORLACIUS-USSING, O., TJONNELAND, A., OLSEN, A., CLAVEL-CHAPELON, F., BOUTRON-RUAULT, M. C., MOROIS, S., WEIKERT, C., PISCHON, T., LINSEISEN, J., KAAKS, R., TRICHOPOULOU, A., ZILIS, D., KATSOULIS, M., PALLI, D., PALA, V., VINEIS, P., TUMINO, R., PANICO, S., PEETERS, P. H., BUENO-DE-MESQUITA, H. B., VAN DUINHOFEN, F. J., SKEIE, G., MUNOZ, X., MARTINEZ, C., DORRONSORO, M., ARDANAZ, E., NAVARRO, C., RODRIGUEZ, L., VANGUELLEN, B., PALMQVIST, R., MANJER, J., ERICSON, U., BINGHAM, S., KHAW, K. T., NORAT, T. & RIBOLI, E. 2010. Plasma vitamins B2, B6, and B12, and related genetic variants as predictors of colorectal cancer risk. *Cancer epidemiology, biomarkers & prevention : a publication of the American Association for Cancer Research, cosponsored by the American Society of Preventive Oncology*, 19, 2549-61.

FANG, J. Y. & RICHARDSON, B. C. 2005. The MAPK signalling pathways and colorectal cancer. *The Lancet Oncology*, 6, 322-327.

FARBER, E. 1984. Cellular biochemistry of the stepwise development of cancer with chemicals: GHA Clowes memorial lecture. *Cancer research*, 44, 5463-5474.

FEARNHEAD, N. S., WILDING, J. L. & BODMER, W. F. 2002. Genetics of colorectal cancer: hereditary aspects and overview of colorectal tumorigenesis. *British medical bulletin*, 64, 27-43.

FERRAZ DA COSTA, D. C., CASANOVA, F. A., QUARTI, J., MALHEIROS, M. S., SANCHES, D., DOS SANTOS, P. S., FIALHO, E. & SILVA, J. L. 2012. Transient Transfection of a Wild-Type p53 Gene Triggers Resveratrol-Induced Apoptosis in Cancer Cells. *PloS one*, 7, e48746.

- FISHMAN, P., BAR-YEHUDA, S., OHANA, G., PATHAK, S., WASSERMAN, L., BARER, F. & MULTANI, A. 2000. Adenosine acts as an inhibitor of lymphoma cell growth: a major role for the A3 adenosine receptor. *European journal of cancer*, 36, 1452-1458.
- FISHMAN, P., BAR-YEHUDA, S., SYNOWITZ, M., POWELL, J., KLOTZ, K., GESSI, S. & BOREA, P. 2009. Adenosine receptors and cancer. *Adenosine Receptors in Health and Disease*. Springer.
- FREDHOLM, B. B. 2003. Adenosine receptors as targets for drug development. *Drug News Perspect*, 16, 283-289.
- FREDHOLM, B. B., IJZERMAN, A. P., JACOBSON, K. A., KLOTZ, K. N. & LINDEN, J. 2001. International Union of Pharmacology. XXV. Nomenclature and classification of adenosine receptors. *Pharmacological reviews*, 53, 527-552.
- GARTEL, A. L., FELICIANO, C. & TYNER, A. L. 2003. A new method for determining the status of p53 in tumor cell lines of different origin. *Oncology Research Featuring Preclinical and Clinical Cancer Therapeutics*, 13, 6, 405-408.
- GATOULLAT, G., BALASSE, E., JOSEPH-PIETRAS, D., MORJANI, H. & MADOULET, C. 2010. Resveratrol induces cell-cycle disruption and apoptosis in chemoresistant B16 melanoma. *Journal of Cellular Biochemistry*, 110, 893-902.
- GESCHER, A. J. & STEWARD, W. P. 2003. Relationship between Mechanisms, Bioavailability, and Preclinical Chemopreventive Efficacy of Resveratrol: A Conundrum. *Cancer Epidemiology Biomarkers & Prevention*, 12, 953-957.
- GESSI, S., CATTABRIGA, E., AVITABILE, A., LANZA, G., CAVAZZINI, L., BIANCHI, N., GAMBARI, R., FEO, C., LIBONI, A. & GULLINI, S. 2004. Elevated expression of A3 adenosine receptors in human colorectal cancer is reflected in peripheral blood cells. *Clinical Cancer Research*, 10, 5895-5901.
- GESSI, S., MERIGHI, S., VARANI, K., CATTABRIGA, E., BENINI, A., MIRANDOLA, P., LEUNG, E., MAC LENNAN, S., FEO, C. & BARALDI, S. 2007. Adenosine receptors in colon carcinoma tissues and colon tumoral cell lines: focus on the A3 adenosine subtype. *Journal of cellular physiology*, 211, 826-836.

- GHOBRAL, I. M., WITZIG, T. E. & ADJEI, A. A. 2009. Targeting apoptosis pathways in cancer therapy. *CA: a cancer journal for clinicians*, 55, 178-194.
- GIUDICE, A. & MONTELLA, M. 2006. Activation of the Nrf2–ARE signaling pathway: a promising strategy in cancer prevention. *Bioessays*, 28, 169-181.
- GOLDBERG, D. M., YAN, J. & SOLEAS, G. J. 2003. Absorption of three wine-related polyphenols in three different matrices by healthy subjects. *Clinical Biochemistry*, 36, 79-87.
- GUERTIN, D. A. & SABATINI, D. M. 2007. Defining the role of mTOR in cancer. *Cancer cell*, 12, 9-22.
- GUSMAN, J., MALONNE, H. & ATASSI, G. 2001. A reappraisal of the potential chemopreventive and chemotherapeutic properties of resveratrol. *Carcinogenesis*, 22, 1111-1117.
- HAHNVAJANAWONG, C. 2011. Inhibition of cell cycle progression and apoptotic activity of resveratrol in human intrahepatic cholangiocarcinoma cell lines. *Asian Biomed*, 5, 775.
- HALLIWELL, B. 2008. Are polyphenols antioxidants or pro-oxidants? What do we learn from cell culture and in vivo studies? *Archives of Biochemistry and Biophysics*, 476, 107-112.
- HANAHAN, D. & WEINBERG, R. 2000. The Hallmarks of Cancer. *Cell*, 100, 57-70.
- HANAHAN, D. & WEINBERG, ROBERT A. 2011. Hallmarks of Cancer: The Next Generation. *Cell*, 144, 646-674.
- HARDIE, D. G. & CARLING, D. 1997. The AMP-Activated Protein Kinase. *European Journal of Biochemistry*, 246, 259-273.
- HARIKUMAR, K. B. & AGGARWAL, B. B. 2008. Resveratrol: A multitargeted agent for age-associated chronic diseases. *Cell Cycle*, 7, 1020-1035.

- HOSHINO, J., PARK, E. J., KONDRATYUK, T. P., MARLER, L., PEZZUTO, J. M., VAN BREEMEN, R. B., MO, S., LI, Y. & CUSHMAN, M. 2010. Selective synthesis and biological evaluation of sulfate-conjugated resveratrol metabolites. *Journal of medicinal chemistry*, 53, 5033-43.
- HOWITZ, K. T., BITTERMAN, K. J., COHEN, H. Y., LAMMING, D. W., LAVU, S., WOOD, J. G., ZIPKIN, R. E., CHUNG, P., KISIELEWSKI, A. & ZHANG, L.-L. 2003a. Small molecule activators of sirtuins extend *Saccharomyces cerevisiae* lifespan. *Nature*, 425, 191-196.
- HOWITZ, K. T., BITTERMAN, K. J., COHEN, H. Y., LAMMING, D. W., LAVU, S., WOOD, J. G., ZIPKIN, R. E., CHUNG, P., KISIELEWSKI, A. & ZHANG, L. L. 2003b. Small molecule activators of sirtuins extend *Saccharomyces cerevisiae* lifespan. *Nature*, 425, 191-196.
- HWANG, J. T., KWAK, D. W., LIN, S. K., KIM, H. M., KIM, Y. M. & PARK, O. J. 2007. Resveratrol induces apoptosis in chemoresistant cancer cells via modulation of AMPK signaling pathway. *Annals of the New York Academy of Sciences*, 1095, 441-8.
- IP, Y. T. & DAVIS, R. J. 1998. Signal transduction by the c-Jun N-terminal kinase (JNK)--from inflammation to development. *Current opinion in cell biology*, 10, 205.
- JANG, M. 1997. Cancer Chemopreventive Activity of Resveratrol, a Natural Product Derived from Grapes. *Science*, 275, 218-220.
- JANG, M., CAI, L., UDEANI, G. O., SLOWING, K. V., THOMAS, C. F., BEECHER, C. W. W., FONG, H. H. S., FARNSWORTH, N. R., KINGHORN, A. D. & MEHTA, R. G. 1997. Cancer chemopreventive activity of resveratrol, a natural product derived from grapes. *Science*, 275, 218-220.
- JIANG, H., FAN, D., ZHOU, G., LI, X. & DENG, H. 2010. Phosphatidylinositol 3-kinase inhibitor(LY294002) induces apoptosis of human nasopharyngeal carcinoma in vitro and in vivo. *Journal of experimental & clinical cancer research : CR*, 29, 34.
- JIANG, H., SHANG, X., WU, H., GAUTAM, S. C., AL-HOLOU, S., LI, C., KUO, J., ZHANG, L. & CHOPP, M. 2009. Resveratrol downregulates PI3K/Akt/mTOR signaling pathways in human U251 glioma cells. *Journal of experimental therapeutics & oncology*, 8, 25.

JIANG, H., ZHANG, L., KUO, J., KUO, K., GAUTAM, S. C., GROG, L., RODRIGUEZ, A. I., KOUBI, D., HUNTER, T. J., CORCORAN, G. B., SEIDMAN, M. D. & LEVINE, R. A. 2005. Resveratrol-induced apoptotic death in human U251 glioma cells. *Molecular cancer therapeutics*, 4, 554-61.

JOE, A. K., LIU, H., SUZUI, M., VURAL, M. E., XIAO, D. & WEINSTEIN, I. B. 2002. Resveratrol Induces Growth Inhibition, S-phase Arrest, Apoptosis, and Changes in Biomarker Expression in Several Human Cancer Cell Lines. *Clinical Cancer Research*, 8, 893-903.

JONES, R. G., PLAS, D. R., KUBEK, S., BUZZAI, M., MU, J., XU, Y., BIRNBAUM, M. J. & THOMPSON, C. B. 2005. AMP-activated protein kinase induces a p53-dependent metabolic checkpoint. *Molecular cell*, 18, 283-293.

JUAN, M. E., ALFARAS, I. & PLANAS, J. M. 2012. Colorectal cancer chemoprevention by trans-resveratrol. *Pharmacological research : the official journal of the Italian Pharmacological Society*, 65, 584-91.

JUNG, H. J., HWANG, I. A., SUNG, W. S., KANG, H., KANG, B. S., SEU, Y. B. & LEE, D. G. 2005. Fungicidal effect of resveratrol on human infectious fungi. *Archives of pharmacal research*, 28, 557-560.

KABEYA, Y., MIZUSHIMA, N., UENO, T., YAMAMOTO, A., KIRISAKO, T., NODA, T., KOMINAMI, E., OHSUMI, Y. & YOSHIMORI, T. 2000. LC3, a mammalian homologue of yeast Apg8p, is localized in autophagosome membranes after processing. *The EMBO journal*, 19, 5720-5728.

KAMIYA, H., KANNO, T., FUJITA, Y., GOTOH, A., NAKANO, T. & NISHIZAKI, T. 2012. Apoptosis-Related Gene Transcription in Human A549 Lung Cancer Cells via A<sub>3</sub> Adenosine Receptor. *Cellular Physiology and Biochemistry*, 29, 687-696.

KANNO, T., NAKANO, T., FUJITA, Y., GOTOH, A. & NISHIZAKI, T. 2012. Adenosine Induces Apoptosis in SBC-3 Human Lung Cancer Cells through A<sub>3</sub> Adenosine Receptor-Dependent AMID Upregulation. *Cellular Physiology and Biochemistry*, 30, 666-676.

- KENEALEY, J. D., SUBRAMANIAN, L., VAN GINKEL, P. R., DARJATMOKO, S., LINDSTROM, M. J., SOMOZA, V., GHOSH, S. K., SONG, Z., HSUNG, R. P., KWON, G. S., ELICEIRI, K. W., ALBERT, D. M. & POLANS, A. S. 2011. Resveratrol metabolites do not elicit early pro-apoptotic mechanisms in neuroblastoma cells. *Journal of agricultural and food chemistry*, 59, 4979-86.
- KEY, T. J., APPLEBY, P. N., MASSET, G., BRUNNER, E. J., CADE, J. E., GREENWOOD, D. C., STEPHEN, A. M., KUH, D., BHANIANI, A., POWELL, N. & KHAW, K. T. 2012. Vitamins, minerals, essential fatty acids and colorectal cancer risk in the United Kingdom Dietary Cohort Consortium. *International journal of cancer. Journal international du cancer*, 131, E320-5.
- KHANDUJA, K. L., BHARDWAJ, A. & KAUSHIK, G. 2004. Resveratrol inhibits N-nitrosodiethylamine-induced ornithine decarboxylase and cyclooxygenase in mice. *Journal of nutritional science and vitaminology*, 50, 61.
- KIM, K. H., YANG, S. S., YOON, Y. S., LIM, S. B., YU, C. S. & KIM, J. C. 2011. Validation of the seventh edition of the American Joint Committee on Cancer tumor-node-metastasis (AJCC TNM) staging in patients with stage II and stage III colorectal carcinoma: analysis of 2511 cases from a medical centre in Korea. *Colorectal disease : the official journal of the Association of Coloproctology of Great Britain and Ireland*, 13, e220-6.
- KIM, S. G., RAVI, G., HOFFMANN, C., JUNG, Y.-J., KIM, M., CHEN, A. & JACOBSON, K. A. 2002. p53-Independent induction of Fas and apoptosis in leukemic cells by an adenosine derivative, Cl-IB-MECA. *Biochemical pharmacology*, 63, 871-880.
- KIM, T. H., KIM, Y. K. & WOO, J. S. 2012. The Adenosine A3 Receptor Agonist Cl-IB-MECA Induces Cell Death Through Ca(2+)/ROS-Dependent Down Regulation of ERK and Akt in A172 Human Glioma Cells. *Neurochemical research*, 37, 2667-77.
- KING, D., PRINGLE, J., HUTCHINSON, M. & COHEN, G. 1998. Processing/activation of caspases,-3 and-7 and-8 but not caspase-2, in the induction of apoptosis in B-chronic lymphocytic leukemia cells. *Leukemia*, 12, 1553-1560.

- KING, R. E., BOMSER, J. A. & MIN, D. B. 2006. Bioactivity of Resveratrol. *Comprehensive Reviews in Food Science and Food Safety*, 5, 65-70.
- KONDO, Y. & KONDO, S. 2006. Autophagy and Cancer Therapy. *Autophagy*, 2, 85-90.
- KROEMER, G., EL-DEIRY, W., GOLSTEIN, P., PETER, M., VAUX, D., VANDENABEELE, P., ZHIVOTOVSKY, B., BLAGOSKLONNY, M., MALORNI, W. & KNIGHT, R. 2005. Classification of cell death: recommendations of the Nomenclature Committee on Cell Death. *Cell Death & Differentiation*, 12, 1463-1467.
- KROEMER, G., GALLUZZI, L., VANDENABEELE, P., ABRAMS, J., ALNEMRI, E. S., BAEHRECKE, E., BLAGOSKLONNY, M., EL-DEIRY, W., GOLSTEIN, P. & GREEN, D. 2008. Classification of cell death: recommendations of the Nomenclature Committee on Cell Death 2009. *Cell Death & Differentiation*, 16, 3-11.
- KUNDU, J. K. & SURH, Y. J. 2004. Molecular basis of chemoprevention by resveratrol: NF-kappaB and AP-1 as potential targets. *Mutation research*, 555, 65-80.
- KUNE, G. & WATSON, L. 2011. Lowering the Risk of Rectal Cancer among Habitual Beer Drinkers by Dietary Means. *Advances in preventive medicine*, 2011, 874048.
- KUO, P. L., CHIANG, L. C. & LIN, C. C. 2002. Resveratrol-induced apoptosis is mediated by p53-dependent pathway in Hep G2 cells. *Life sciences*, 72, 23-34.
- LAMONT, K. T., SOMERS, S., LACERDA, L., OPIE, L. H. & LECOUR, S. 2011. Is red wine a SAFE sip away from cardioprotection? Mechanisms involved in resveratrol-and melatonin-induced cardioprotection. *Journal of pineal research*, 50, 374-380.
- LANGCAKE, P. & PRYCE, R. 1976. The production of resveratrol by *Vitis vinifera* and other members of the Vitaceae as a response to infection or injury. *Physiological Plant Pathology*, 9, 77-86.
- LARROSA, M., TOMÁS-BARBERÁN, F. A. & ESPÍN, J. C. 2003. Grape polyphenol resveratrol and the related molecule 4-hydroxystilbene induce growth inhibition, apoptosis, S-phase arrest, and upregulation of cyclins A, E, and B1 in human SK-Mel-28 melanoma cells. *Journal of agricultural and food chemistry*, 51, 4576-4584.

- LAWRENCE, M. C., JIVAN, A., SHAO, C., DUAN, L., GOAD, D., ZAGANJOR, E., OSBORNE, J., MCGLYNN, K., STIPPEC, S. & EARNEST, S. 2008. The roles of MAPKs in disease. *Cell research*, 18, 436-442.
- LE MARCHAND, L., WANG, H., SELHUB, J., VOGT, T. M., YOKOCHI, L. & DECKER, R. 2011. Association of plasma vitamin B6 with risk of colorectal adenoma in a multiethnic case-control study. *Cancer causes & control : CCC*, 22, 929-36.
- LEE, S. K., MBWAMBO, Z., CHUNG, H., LUYENGI, L., GAMEZ, E., MEHTA, R., KINGHORN, A. & PEZZUTO, J. 1998. Evaluation of the antioxidant potential of natural products. *Combinatorial chemistry & high throughput screening*, 1, 35.
- LEE, Y. K., PARK, S. Y., KIM, Y. M., LEE, W. S. & PARK, O. J. 2009. AMP kinase/cyclooxygenase-2 pathway regulates proliferation and apoptosis of cancer cells treated with quercetin. *Experimental & molecular medicine*, 41, 201-7.
- LEONI, B. D., NATOLI, M., NARDELLA, M., BUCCI, B., ZUCCO, F., D'AGNANO, I. & FELSANI, A. 2012. Differentiation of Caco-2 cells requires both transcriptional and post-translational down-regulation of Myc. *Differentiation*, 83, 116-127.
- LEVINE, B. & KLIONSKY, D. J. 2004. Development by Self-Digestion: Molecular Mechanisms and Biological Functions of Autophagy. *Developmental Cell*, 6, 463-477.
- LEVINE, B. & KROEMER, G. 2008. Autophagy in the pathogenesis of disease. *Cell*, 132, 27-42.
- LEWIS, T. S., SHAPIRO, P. S. & AHN, N. G. 1998. Signal transduction through MAP kinase cascades. *Advances in cancer research*, 74, 49-139.
- LI, J., QIN, Z. & LIANG, Z. 2009. The prosurvival role of autophagy in Resveratrol-induced cytotoxicity in human U251 glioma cells. *BMC cancer*, 9, 215.
- LI, Z. G., HONG, T., SHIMADA, Y., KOMOTO, I., KAWABE, A., DING, Y., KAGANOI, J., HASHIMOTO, Y. & IMAMURA, M. 2002. Suppression of N-nitrosomethylbenzylamine (NMBA)-induced esophageal tumorigenesis in F344 rats by resveratrol. *Carcinogenesis*, 23, 1531-1536.



- LIAO, Y. & HUNG, M. C. 2003. Regulation of the activity of p38 mitogen-activated protein kinase by Akt in cancer and adenoviral protein E1A-mediated sensitization to apoptosis. *Molecular and cellular biology*, 23, 6836-6848.
- LIN, H.-Y., TANG, H.-Y., DAVIS, F. B. & DAVIS, P. J. 2011. Resveratrol and apoptosis. *Annals of the New York Academy of Sciences*, 1215, 79-88.
- LIN, J. N., LIN, V. C., RAU, K. M., SHIEH, P. C., KUO, D. H., SHIEH, J. C., CHEN, W. J., TSAI, S. C. & WAY, T. D. 2010. Resveratrol modulates tumor cell proliferation and protein translation via SIRT1-dependent AMPK activation. *Journal of agricultural and food chemistry*, 58, 1584-92.
- LIONTAS, A. & YEGER, H. 2004. Curcumin and resveratrol induce apoptosis and nuclear translocation and activation of p53 in human neuroblastoma. *ANTICANCER RESEARCH*, 24, 987-998.
- LIU, Y. & BODMER, W. F. 2006. Analysis of P53 mutations and their expression in 56 colorectal cancer cell lines. *Proceedings of the National Academy of Sciences of the United States of America*, 103, 976-81.
- LOHNER, K., SCHNABELE, K., DANIEL, H., OESTERLE, D., RECHKEMMER, G., GOTTLICHER, M. & WENZEL, U. 2007. Flavonoids alter P-gp expression in intestinal epithelial cells in vitro and in vivo. *Molecular nutrition & food research*, 51, 293-300.
- LOSA, G. 2003. Resveratrol modulates apoptosis and oxidation in human blood mononuclear cells. *European journal of clinical investigation*, 33, 818-823.
- LOWRY, O. H., ROSEBROUGH, N. J., FARR, A. L. & RANDALL, R. J. 1951. Protein measurement with the Folin phenol reagent. *The Journal of biological chemistry*, 193, 265-275.
- MAHYAR-ROEMER, M., KATSEN, A., MESTRES, P. & ROEMER, K. 2001. Resveratrol induces colon tumor cell apoptosis independently of p53 and precede by epithelial differentiation, mitochondrial proliferation and membrane potential collapse. *International Journal of Cancer*, 94, 615-622.

- MAIER-SALAMON, A., HAGENAUER, B., WIRTH, M., GABOR, F., SZEKERES, T. & JAGER, W. 2006. Increased transport of resveratrol across monolayers of the human intestinal Caco-2 cells is mediated by inhibition and saturation of metabolites. *Pharmaceutical research*, 23, 2107-15.
- MALUMBRES, M. & BARBACID, M. 2001. To cycle or not to cycle: a critical decision in cancer. *Nature reviews. Cancer*, 1, 222-231.
- MANACH, C., SCALBERT, A., MORAND, C., RÉMÉSY, C. & JIMÉNEZ, L. 2004. Polyphenols: food sources and bioavailability. *The American Journal of Clinical Nutrition*, 79, 727-747.
- MARTÍN, A. R., VILLEGAS, I., LA CASA, C. & DE LA LASTRA, C. A. 2004. Resveratrol, a polyphenol found in grapes, suppresses oxidative damage and stimulates apoptosis during early colonic inflammation in rats. *Biochemical pharmacology*, 67, 1399-1410.
- MCCORMACK, D. & MCFADDEN, D. 2012. Pterostilbene and Cancer: Current Review. *Journal of Surgical Research*, 173, e53-e61.
- MENG, X., MALIAKAL, P., LU, H., LEE, M.-J. & YANG, C. S. 2004. Urinary and Plasma Levels of Resveratrol and Quercetin in Humans, Mice, and Rats after Ingestion of Pure Compounds and Grape Juice. *Journal of agricultural and food chemistry*, 52, 935-942.
- MERIGHI, S., BENINI, A., MIRANDOLA, P., GESSI, S., VARANI, K., LEUNG, E., MACLENNAN, S., BARALDI, P. G. & BOREA, P. A. 2005. Adenosine Receptors Modulate Hypoxia-Inducible Factor-1 $\alpha$  Expression in Human A375 Melanoma Cells. *Neoplasia*, 7, 894-903.
- MERIGHI, S., BENINI, A., MIRANDOLA, P., GESSI, S., VARANI, K., LEUNG, E., MACLENNAN, S. & BOREA, P. A. 2006. Adenosine modulates vascular endothelial growth factor expression via hypoxia-inducible factor-1 in human glioblastoma cells. *Biochemical pharmacology*, 72, 19-31.

- MERIGHI, S., MIRANDOLA, P., MILANI, D., VARANI, K., GESSI, S., KLOTZ, K. N., LEUNG, E., BARALDI, P. G. & BOREA, P. A. 2002. Adenosine receptors as mediators of both cell proliferation and cell death of cultured human melanoma cells. *Journal of investigative dermatology*, 119, 923-933.
- MERIGHI, S., MIRANDOLA, P., VARANI, K., GESSI, S., LEUNG, E., BARALDI, P. G., TABRIZI, M. A. & BOREA, P. A. 2003. A glance at adenosine receptors: novel target for antitumor therapy. *Pharmacology & therapeutics*, 100, 31-48.
- MEYERHARDT, J. A. & MAYER, R. J. 2005. Systemic therapy for colorectal cancer. *New England Journal of Medicine*, 352, 476-487.
- MIKSITS, M., MAIER-SALAMON, A., AUST, S., THALHAMMER, T., REZNICEK, G., KUNERT, O., HASLINGER, E., SZEKERES, T. & JAEGER, W. 2005. Sulfation of resveratrol in human liver: evidence of a major role for the sulfotransferases SULT1A1 and SULT1E1. *Xenobiotica*, 35, 1101-1119.
- MIKSITS, M., WLCEK, K., SVOBODA, M., KUNERT, O., HASLINGER, E., THALHAMMER, T., SZEKERES, T. & JAGER, W. 2009. Antitumor activity of resveratrol and its sulfated metabolites against human breast cancer cells. *Planta medica*, 75, 1227.
- MILOSO, M., BERTELLI, A. A. E., NICOLINI, G. & TREDICI, G. 1999. Resveratrol-induced activation of the mitogen-activated protein kinases, ERK1 and ERK2, in human neuroblastoma SH-SY5Y cells. *Neuroscience letters*, 264, 141-144.
- MORELLO, S., PETRELLA, A., FESTA, M., POPOLO, A., MONACO, M., VUTTARIELLO, E., CHIAPPETTA, G., PARENTE, L. & PINTO, A. 2008. CI-IB-MECA inhibits human thyroid cancer cell proliferation independently of A3 adenosine receptor activation. *Cancer Biology & Therapy*, 7, 278-284.
- MORGAN, D. O. 1995. Principles of CDK regulation. *Nature*, 374, 131.
- MORSELLI, E., MARIÑO, G., BENNETZEN, M. V., EISENBERG, T., MEGALOU, E., SCHROEDER, S., CABRERA, S., BÉNIT, P., RUSTIN, P. & CRIOLLO, A. 2011. Spermidine and resveratrol induce autophagy by distinct pathways converging on the acetylproteome. *The Journal of cell biology*, 192, 615-629.

- MOSMANN, T. 1983. Rapid colorimetric assay for cellular growth and survival: application to proliferation and cytotoxicity assays. *J Immunol methods*, 65, 55-63.
- MUJOOMDAR, M., BENNETT, A., HOSKIN, D. & BLAY, J. 2004. Adenosine stimulation of proliferation of breast carcinoma cell lines: evaluation of the [3H] thymidine assay system and modulatory effects of the cellular microenvironment in vitro. *Journal of cellular physiology*, 201, 429-438.
- MURIAS, M., HANDLER, N., ERKER, T., PLEBAN, K., ECKER, G., SAIKO, P., SZEKERES, T. & JAGER, W. 2004. Resveratrol analogues as selective cyclooxygenase-2 inhibitors: synthesis and structure-activity relationship. *Bioorganic & medicinal chemistry*, 12, 5571-8.
- MURTHY, S., TOSOLINI, A., TAGUCHI, T. & TESTA, J. 2000. Mapping of AKT3, encoding a member of the Akt/protein kinase B family, to human and rodent chromosomes by fluorescence in situ hybridization. *Cytogenetic and Genome Research*, 88, 38-40.
- NAKAMURA, K., YOSHIKAWA, N., YAMAGUCHI, Y., KAGOTA, S., SHINOZUKA, K. & KUNITOMO, M. 2006. Antitumor effect of cordycepin (3'-deoxyadenosine) on mouse melanoma and lung carcinoma cells involves adenosine A3 receptor stimulation. *ANTICANCER RESEARCH*, 26, 43-47.
- NAM, K. A., KIM, S., HEO, Y. H. & LEE, S. K. 2001. Resveratrol analog, 3, 5, 2', 4'-tetramethoxy-trans-stilbene, potentiates the inhibition of cell growth and induces apoptosis in human cancer cells. *Archives of pharmacal research*, 24, 441-445.
- NAM, T. W., YOO, C. I., KIM, H. T., KWON, C. H., PARK, J. Y. & KIM, Y. K. 2008. The flavonoid quercetin induces apoptosis and inhibits migration through a MAPK-dependent mechanism in osteoblasts. *Journal of bone and mineral metabolism*, 26, 551-60.
- NGUYEN, A. V., MARTINEZ, M., STAMOS, M. J., MOYER, M. P., PLANUTIS, K., HOPE, C. & HOLCOMBE, R. F. 2009. Results of a phase I pilot clinical trial examining the effect of plant-derived resveratrol and grape powder on Wnt pathway target gene expression in colonic mucosa and colon cancer. *Cancer management and research*, 1, 25.

- NONOMURA, S., KANAGAWA, H. & MAKIMOTO, A. 1963. CHEMICAL CONSTITUENTS OF POLYGONACEOUS PLANTS. I. STUDIES ON THE COMPONENTS OF KO-J O-KON.(POLYGONUM CUSPIDATUM SIEB. ET ZUCC.)). *Yakugaku zasshi: Journal of the Pharmaceutical Society of Japan*, 83, 988.
- NORBURY, C. J. & HICKSON, I. D. 2001. Cellular responses to DNA damage. *Annual review of pharmacology and toxicology*, 41, 367-401.
- NUNES, T., ALMEIDA, L., ROCHA, J. F., FALCÃO, A., FERNANDES-LOPES, C., LOUREIRO, A. I., WRIGHT, L., VAZ-DA-SILVA, M. & SOARES-DA-SILVA, P. 2009. Pharmacokinetics of Trans-resveratrol Following Repeated Administration in Healthy Elderly and Young Subjects. *The Journal of Clinical Pharmacology*, 49, 1477-1482.
- NUNEZ, R. 2001a. DNA measurement and cell cycle analysis by flow cytometry. *Current issues in molecular biology*, 3, 67-70.
- NUNEZ, R. 2001b. Flow cytometry: principles and instrumentation. *Current issues in molecular biology*, 3, 39-45.
- NUTAKUL, W., SOBERS, H. S., QIU, P., DONG, P., DECKER, E. A., MCCLEMENTS, D. J. & XIAO, H. 2011. Inhibitory effects of resveratrol and pterostilbene on human colon cancer cells: a side-by-side comparison. *Journal of agricultural and food chemistry*, 59, 10964-70.
- OPIE, L., LAMONT, K. & LECOUR, S. 2011. Wine and heart health: learning from the French paradox. *SA Heart Journal*, 8, 172-177.
- OPIPARI, A. W. 2004. Resveratrol-induced Autophagocytosis in Ovarian Cancer Cells. *Cancer research*, 64, 696-703.
- OREN, M. & ROTTER, V. 1999. Introduction: p53—the first twenty years. *Cellular and molecular life sciences*, 55, 9-11.
- ORTUÑO, J., COVAS, M.-I., FARRE, M., PUJADAS, M., FITO, M., KHYMENETS, O., ANDRES-LACUEVA, C., ROSET, P., JOGLAR, J., LAMUELA-RAVENTÓS, R. M. & TORRE, R. D. L. 2010. Matrix effects on the bioavailability of resveratrol in humans. *Food Chemistry*, 120, 1123-1130.

PACHOLEC, M., BLEASDALE, J. E., CHRUNYK, B., CUNNINGHAM, D., FLYNN, D., GAROFALO, R. S., GRIFFITH, D., GRIFFOR, M., LOULAKIS, P., PABST, B., QIU, X., STOCKMAN, B., THANABAL, V., VARGHESE, A., WARD, J., WITHKA, J. & AHN, K. 2010. SRT1720, SRT2183, SRT1460, and resveratrol are not direct activators of SIRT1. *The Journal of biological chemistry*, 285, 8340-51.

PAN, M.-H., LAI, C.-S., WU, J.-C. & HO, C.-T. 2011. Molecular mechanisms for chemoprevention of colorectal cancer by natural dietary compounds. *Molecular nutrition & food research*, 55, 32-45.

PAN, M. H., CHIOU, Y. S., CHEN, W. J., WANG, J. M., BADMAEV, V. & HO, C. T. 2009. Pterostilbene inhibited tumor invasion via suppressing multiple signal transduction pathways in human hepatocellular carcinoma cells. *Carcinogenesis*, 30, 1234-42.

PAN, M. H., GAO, J. H., LAI, C. S., WANG, Y. J., CHEN, W. M., LO, C. Y., WANG, M., DUSHENKOV, S. & HO, C. T. 2007. Antitumor activity of 3, 5, 4'-trimethoxystilbene in COLO 205 cells and xenografts in SCID mice. *Molecular carcinogenesis*, 47, 184-196.

PAREKH, P., MOTIWALE, L., NAIK, N. & RAO, K. V. 2011. Downregulation of cyclin D1 is associated with decreased levels of p38 MAP kinases, Akt/PKB and Pak1 during chemopreventive effects of resveratrol in liver cancer cells. *Experimental and toxicologic pathology : official journal of the Gesellschaft fur Toxikologische Pathologie*, 63, 167-73.

PARKIN, D. M., BOYD, L. & WALKER, L. C. 2011. 16. The fraction of cancer attributable to lifestyle and environmental factors in the UK in 2010. *British journal of cancer*, 105 Suppl 2, S77-81.

PATEL, K. R., BROWN, V. A., JONES, D. J., BRITTON, R. G., HEMINGWAY, D., MILLER, A. S., WEST, K. P., BOOTH, T. D., PERLOFF, M., CROWELL, J. A., BRENNER, D. E., STEWARD, W. P., GESCHER, A. J. & BROWN, K. 2010. Clinical pharmacology of resveratrol and its metabolites in colorectal cancer patients. *Cancer research*, 70, 7392-9.

- PATEL, K. R., SCOTT, E., BROWN, V. A., GESCHER, A. J., STEWARD, W. P. & BROWN, K. 2011. Clinical trials of resveratrol. *Annals of the New York Academy of Sciences*, 1215, 161-9.
- PAUL, S., DECASTRO, A. J., LEE, H. J., SMOLAREK, A. K., SO, J. Y., SIMI, B., WANG, C. X., ZHOU, R., RIMANDO, A. M. & SUH, N. 2010. Dietary intake of pterostilbene, a constituent of blueberries, inhibits the beta-catenin/p65 downstream signaling pathway and colon carcinogenesis in rats. *Carcinogenesis*, 31, 1272-8.
- PEARSON, K. J., BAUR, J. A., LEWIS, K. N., PESHKIN, L., PRICE, N. L., LABINSKY, N., SWINDELL, W. R., KAMARA, D., MINOR, R. K. & PEREZ, E. 2008. Resveratrol delays age-related deterioration and mimics transcriptional aspects of dietary restriction without extending life span. *Cell metabolism*, 8, 157-168.
- PETERSON, G. L. 1979. Review of the Folin phenol protein quantitation method of Lowry, Rosebrough, Farr and Randall. *Analytical biochemistry*, 100, 201-220.
- PINES, J. 1995. Cyclins and cyclin-dependent kinases: a biochemical view. *Biochemical Journal*, 308, 697.
- POTTER, G., PATTERSON, L., WANOGHO, E., PERRY, P., BUTLER, P., IJAZ, T., RUPARELIA, K., LAMB, J., FARMER, P. & STANLEY, L. 2002. The cancer preventative agent resveratrol is converted to the anticancer agent piceatannol by the cytochrome P450 enzyme CYP1B1. *British journal of cancer*, 86, 774-778.
- POZO-GUISADO, E., MERINO, J. M., MULERO-NAVARRO, S., LORENZO-BENAYAS, M. J., CENTENO, F., ALVAREZ-BARRIENTOS, A. & SALGUERO, P. M. F. 2005. Resveratrol-induced apoptosis in MCF-7 human breast cancer cells involves a caspase-independent mechanism with downregulation of Bcl-2 and NF- $\kappa$ B. *International Journal of Cancer*, 115, 74-84.

PRICE, NATHAN L., GOMES, ANA P., LING, ALVIN J. Y., DUARTE, FILIPE V., MARTIN-MONTALVO, A., NORTH, BRIAN J., AGARWAL, B., YE, L., RAMADORI, G., TEODORO, JOAO S., HUBBARD, BASIL P., VARELA, ANA T., DAVIS, JAMES G., VARAMINI, B., HAFNER, A., MOADDEL, R., ROLO, ANABELA P., COPPARI, R., PALMEIRA, CARLOS M., DE CABO, R., BAUR, JOSEPH A. & SINCLAIR, DAVID A. 2012. SIRT1 Is Required for AMPK Activation and the Beneficial Effects of Resveratrol on Mitochondrial Function. *Cell metabolism*, 15, 675-690.

RASHID, A., LIU, C., SANLI, T., TSIANI, E., SINGH, G., BRISTOW, R. G., DAYES, I., LUKKA, H., WRIGHT, J. & TSAKIRIDIS, T. 2011. Resveratrol enhances prostate cancer cell response to ionizing radiation. Modulation of the AMPK, Akt and mTOR pathways. *Radiat Oncol*, 6, 144.

RENAUD, S. & DE LORGERIL, M. 1992. Wine, alcohol, platelets, and the French paradox for coronary heart disease. *The Lancet*, 339, 1523-1526.

REPETTO, G., DEL PESO, A. & ZURITA, J. L. 2008. Neutral red uptake assay for the estimation of cell viability/cytotoxicity. *Nature Protocols*, 3, 1125-1131.

RESEARCH, W. C. R. F. A. I. F. C. 2011. Continuous Update Project Report Summary. *Food, Nutrition, Physical Activity, and the Prevention of Colorectal Cancer*.

RIMANDO, A. M. & SUH, N. 2008. Biological/chemopreventive activity of stilbenes and their effect on colon cancer. *Planta medica*, 74, 1635-43.

RIVLIN, N., BROSH, R., OREN, M. & ROTTER, V. 2011. Mutations in the p53 Tumor Suppressor Gene: Important Milestones at the Various Steps of Tumorigenesis. *Genes & cancer*, 2, 466-74.

ROBICH, M. P., CHU, L. M., CHAUDRAY, M., NEZAFAT, R., HAN, Y., CLEMENTS, R. T., LAHAM, R. J., MANNING, W. J., COADY, M. A. & SELLKE, F. W. 2010. Anti-angiogenic effect of high-dose resveratrol in a swine model of metabolic syndrome. *Surgery*, 148, 453-462.

ROCHETTE, P. J., BASTIEN, N., LAVOIE, J., GUERIN, S. L. & DROUIN, R. 2005. SW480, a p53 double-mutant cell line retains proficiency for some p53 functions. *Journal of molecular biology*, 352, 44-57.



- ROEMER, K. & MAHYAR-ROEMER, M. 2002. The basis for the chemopreventive action of resveratrol. *Drugs Today*, 38, 571-580.
- ROY, S. K., CHEN, Q., FU, J., SHANKAR, S. & SRIVASTAVA, R. K. 2011. Resveratrol inhibits growth of orthotopic pancreatic tumors through activation of FOXO transcription factors. *PloS one*, 6, e25166.
- SACK, J. & ROTHMAN, J. M. 2000. Colorectal cancer: natural history and management. *Hospital Physician*, 65.
- SAIKO, P., SZAKMARY, A., JAEGER, W. & SZEKERES, T. 2008. Resveratrol and its analogs: defense against cancer, coronary disease and neurodegenerative maladies or just a fad? *Mutation research*, 658, 68-94.
- SALE, S., TUNSTALL, R. G., RUPARELIA, K. C., POTTER, G. A., STEWARD, W. P. & GESCHER, A. J. 2005. Comparison of the effects of the chemopreventive agent resveratrol and its synthetic analog trans 3, 4, 5, 4'-tetramethoxystilbene (DMU-212) on adenoma development in the ApcMin<sup>+</sup> mouse and cyclooxygenase-2 in human-derived colon cancer cells. *International Journal of Cancer*, 115, 194-201.
- SATO, S., FUJITA, N. & TSURUO, T. 2004. Involvement of 3-phosphoinositide-dependent protein kinase-1 in the MEK/MAPK signal transduction pathway. *Journal of Biological Chemistry*, 279, 33759-33767.
- SATOH, A., STEIN, L. & IMAI, S. 2011. The Role of Mammalian Sirtuins in the Regulation of Metabolism, Aging, and Longevity. In: YAO, T.-P. & SETO, E. (eds.) *Histone Deacetylases: the Biology and Clinical Implication*. Springer Berlin Heidelberg.
- SCHIFFRIN, E. L. 2010. Antioxidants in hypertension and cardiovascular disease. *Molecular interventions*, 10, 354-362.
- SCHLUMPBERGER, M., SCHAEFFELER, E., STRAUB, M., BREDSCHNEIDER, M., WOLF, D. H. & THUMM, M. 1997. AUT1, a gene essential for autophagocytosis in the yeast *Saccharomyces cerevisiae*. *Journal of bacteriology*, 179, 1068-1076.

- SCHNEIDER, Y., CHABERT, P., STUTZMANN, J., COELHO, D., FOUGEROUSSE, A., GOSSE, F., LAUNAY, J. F., BROUILLARD, R. & RAUL, F. 2003. Resveratrol analog (Z)-3,5,4'-trimethoxystilbene is a potent anti-mitotic drug inhibiting tubulin polymerization. *International journal of cancer. Journal international du cancer*, 107, 189-96.
- SCHNEIDER, Y., VINCENT, F., DURANTON, B. T., BADOLO, L., GOSSÉ, F., BERGMANN, C., SEILER, N. & RAUL, F. 2000. Anti-proliferative effect of resveratrol, a natural component of grapes and wine, on human colonic cancer cells. *Cancer letters*, 158, 85-91.
- SCHULTE, G. & FREDHOLM, B. B. 2000. Human adenosine A1, A2A, A2B, and A3 receptors expressed in Chinese hamster ovary cells all mediate the phosphorylation of extracellular-regulated kinase 1/2. *Molecular pharmacology*, 58, 477-482.
- SHACKELFORD, D. B. & SHAW, R. J. 2009. The LKB1–AMPK pathway: metabolism and growth control in tumour suppression. *Nature Reviews Cancer*, 9, 563-575.
- SHANKAR, S., SINGH, G. & SRIVASTAVA, R. K. 2007. Chemoprevention by resveratrol: molecular mechanisms and therapeutic potential. *Front Biosci*, 12, 4839-4854.
- SIEGEL, R., NAISHADHAM, D. & JEMAL, A. 2012. Cancer statistics, 2012. *CA: a cancer journal for clinicians*, 62, 10-29.
- SIEMANN, E. & CREASY, L. 1992. Concentration of the phytoalexin resveratrol in wine. *American Journal of Enology and Viticulture*, 43, 49-52.
- SIGAL, A. & ROTTER, V. 2000. Oncogenic mutations of the p53 tumor suppressor: the demons of the guardian of the genome. *Cancer research*, 60, 6788-6793.
- SINHA, K., CHAUDHARY, G. & KUMAR GUPTA, Y. 2002. Protective effect of resveratrol against oxidative stress in middle cerebral artery occlusion model of stroke in rats. *Life sciences*, 71, 655-665.

- SLEE, E. A., ZHU, H., CHOW, S. C., MACFARLANE, M., NICHOLSON, D. W. & COHEN, G. M. 1996. Benzyloxycarbonyl-Val-Ala-Asp (OMe) fluoromethylketone (Z-VAD. FMK) inhibits apoptosis by blocking the processing of CPP32. *Biochemical Journal*, 315, 21.
- SOH, J. W., MAO, Y., LIU, L., THOMPSON, W. J., PAMUKCU, R. & WEINSTEIN, I. B. 2001. Protein kinase G activates the JNK1 pathway via phosphorylation of MEKK1. *Journal of Biological Chemistry*, 276, 16406-16410.
- SOLEAS, G. J., DIAMANDIS, E. P. & GOLDBERG, D. M. 1997. Resveratrol: A molecule whose time has come? And gone? *Clinical Biochemistry*, 30, 91-113.
- STORNILO, C. E. & MORENO, J. J. 2012. Resveratrol metabolites have an antiproliferative effect on intestinal epithelial cancer cells. *Food Chemistry*, 134, 1385-1391.
- STRAUB, M., BREDSCHNEIDER, M. & THUMM, M. 1997. AUT3, a serine/threonine kinase gene, is essential for autophagocytosis in *Saccharomyces cerevisiae*. *Journal of bacteriology*, 179, 3875.
- SUBBARAMAIAH, K., CHUNG, W. J., MICHALUART, P., TELANG, N., TANABE, T., INOUE, H., JANG, M., PEZZUTO, J. M. & DANNENBERG, A. J. 1998. Resveratrol inhibits cyclooxygenase-2 transcription and activity in phorbol ester-treated human mammary epithelial cells. *Journal of Biological Chemistry*, 273, 21875-21882.
- SUN, L., WU, S., COLEMAN, K., FIELDS, K. C., HUMPHREY, L. E. & BRATTAIN, M. G. 1994. Autocrine Transforming Growth Factor- $\beta$ 1 and  $\beta$ 2 Expression Is Increased by Cell Crowding and Quiescence in Colon Carcinoma Cells. *Experimental Cell Research*, 214, 215-224.
- TAKAOKA, M. 1940. Of the phenolic substances of white hellebore (*Veratrum grandiflorum* Loes. fil.). *Journal of Faculty of Sciences Hokkaido Imperial University*, 3, 1-16.
- TESSITORE, L., DAVIT, A., SAROTTO, I. & CADERNI, G. 2000. Resveratrol depresses the growth of colorectal aberrant crypt foci by affecting bax and p21CIP expression. *Carcinogenesis*, 21, 1619-1622.

TESTA, J. R. & BELLACOSA, A. 2001. AKT plays a central role in tumorigenesis. *Science Signalling*, 98, 10983.

TORTORA, G. J. & DERRICKSON, B. H. 2008. *Principles of anatomy and physiology*, Wiley.

TRAINER, D. L., KLINE, T., MCCABE, F. L., FAUCETTE, L. F., FEILD, J., CHAIKIN, M., ANZANO, M., REIMAN, D., HOFFSTEIN, S. & LI, D. J. 2006. Biological characterization and oncogene expression in human colorectal carcinoma cell lines. *International Journal of Cancer*, 41, 287-296.

TREISMAN, R. 1994. Ternary complex factors: growth factor regulated transcriptional activators. *Current opinion in genetics & development*, 4, 96-101.

TROPPMAIR, J., BRUDER, J., MUNOZ, H., LLOYD, P. A., KYRIAKIS, J., BANERJEE, P., AVRUCH, J. & RAPP, U. 1994. Mitogen-activated protein kinase/extracellular signal-regulated protein kinase activation by oncogenes, serum, and 12-O-tetradecanoylphorbol-13-acetate requires Raf and is necessary for transformation. *Journal of Biological Chemistry*, 269, 7030-7035.

TSUKADA, M. & OHSUMI, Y. 1993. Isolation and characterization of autophagy-defective mutants of *Saccharomyces cerevisiae*. *FEBS letters*, 333, 169-174.

UNGVARI, Z., OROSZ, Z., RIVERA, A., LABINSKY, N., XIANGMIN, Z., OLSON, S., PODLUTSKY, A. & CSISZAR, A. 2007. Resveratrol increases vascular oxidative stress resistance. *American Journal of Physiology-Heart and Circulatory Physiology*, 292, H2417-H2424.

VALENZANO, D. R., TERZIBASI, E., GENADE, T., CATTANEO, A., DOMENICI, L. & CELLERINO, A. 2006. Resveratrol prolongs lifespan and retards the onset of age-related markers in a short-lived vertebrate. *Current Biology*, 16, 296-300.

VARA, J. Á. F., CASADO, E., DE CASTRO, J., CEJAS, P., BELDA-INIESTA, C. & GONZÁLEZ-BARÓN, M. 2004. PI3K/Akt signalling pathway and cancer. *Cancer Treatment Reviews*, 30, 193-204.

VARGAS, A. J. & BURD, R. 2010. Hormesis and synergy: pathways and mechanisms of quercetin in cancer prevention and management. *Nutrition reviews*, 68, 418-428.

- VASTANO, B. C., CHEN, Y., ZHU, N., HO, C.-T., ZHOU, Z. & ROSEN, R. T. 2000. Isolation and Identification of Stilbenes in Two Varieties of *Polygonum cuspidatum*. *Journal of agricultural and food chemistry*, 48, 253-256.
- VERMEULEN, K., VAN BOCKSTAELE, D. R. & BERNEMAN, Z. N. 2003. The cell cycle: a review of regulation, deregulation and therapeutic targets in cancer. *Cell proliferation*, 36, 131-149.
- WAHEED, A., BARKER, J., BARTON, S. J., KHAN, G.-M., NAJM-US-SAQIB, Q., HUSSAIN, M., AHMED, S., OWEN, C. & CAREW, M. A. 2011. Novel acylated steroidal glycosides from *Caralluma tuberculata* induce caspase-dependent apoptosis in cancer cells. *Journal of ethnopharmacology*, 137, 1189-1196.
- WAHEED, A., BARKER, J., BARTON, S. J., OWEN, C. P., AHMED, S. & CAREW, M. A. 2012. A novel steroidal saponin glycoside from *Fagonia indica* induces cell-selective apoptosis or necrosis in cancer cells. *European Journal of Pharmaceutical Sciences*, 47, 464-473.
- WALLE, T. 2011. Bioavailability of resveratrol. *Annals of the New York Academy of Sciences*, 1215, 9-15.
- WALLE, T., HSIEH, F., DELEGGE, M. H., OATIS, J. E., JR. & WALLE, U. K. 2004. High absorption but very low bioavailability of oral resveratrol in humans. *Drug metabolism and disposition: the biological fate of chemicals*, 32, 1377-82.
- WALLERATH, T., DECKERT, G., TERNES, T., ANDERSON, H., LI, H., WITTE, K. & FÖRSTERMANN, U. 2002. Resveratrol, a polyphenolic phytoalexin present in red wine, enhances expression and activity of endothelial nitric oxide synthase. *Circulation*, 106, 1652-1658.
- WANG, L. X., HEREDIA, A., SONG, H., ZHANG, Z., YU, B., DAVIS, C. & REDFIELD, R. 2004a. Resveratrol glucuronides as the metabolites of resveratrol in humans: characterization, synthesis, and anti-HIV activity. *Journal of pharmaceutical sciences*, 93, 2448-57.
- WANG, Q., XU, J., ROTTINGHAUS, G. E., SIMONYI, A., LUBAHN, D., SUN, G. Y. & SUN, A. Y. 2002. Resveratrol protects against global cerebral ischemic injury in gerbils. *Brain research*, 958, 439-447.

- WANG, X., WANG, Q., HU, W. & EVERS, B. M. 2004b. Regulation of phorbol ester-mediated TRAF1 induction in human colon cancer cells through a PKC/RAF/ERK/NF- $\kappa$ B-dependent pathway. *Oncogene*, 23, 1885-1895.
- WENZEL, E. & SOMOZA, V. 2005. Metabolism and bioavailability of trans-resveratrol. *Molecular nutrition & food research*, 49, 472-81.
- WÖLFEL, T., HAUER, M., SCHNEIDER, J., SERRANO, M., WÖLFEL, C., KLEHMANN-HIEB, E., DE PLAEN, E., HANKELN, T., MEYER, Z. B. K. & BEACH, D. 1995. A p16INK4a-insensitive CDK4 mutant targeted by cytolytic T lymphocytes in a human melanoma. *Science (New York, NY)*, 269, 1281.
- WOLTER, F., AKOGLU, B., CLAUSNITZER, A. & STEIN, J. 2001. Downregulation of the Cyclin D1/Cdk4 Complex Occurs during Resveratrol-Induced Cell Cycle Arrest in Colon Cancer Cell Lines. *The Journal of Nutrition*, 131, 2197-2203.
- WOLTER, F., CLAUSNITZER, A., AKOGLU, B. & STEIN, J. 2002. Piceatannol, a Natural Analog of Resveratrol, Inhibits Progression through the S Phase of the Cell Cycle in Colorectal Cancer Cell Lines. *The Journal of Nutrition*, 132, 298-302.
- WOLTER, F., TURCHANOWA, L. & STEIN, J. 2003. Resveratrol-induced modification of polyamine metabolism is accompanied by induction of c-Fos. *Carcinogenesis*, 24, 469-474.
- WONG, R. 2011. Apoptosis in cancer: from pathogenesis to treatment. *Journal of experimental & clinical cancer research : CR*, 30, 87.
- WOOD, J. G., ROGINA, B., LAVU, S., HOWITZ, K., HELFAND, S. L., TATAR, M. & SINCLAIR, D. 2004. Sirtuin activators mimic caloric restriction and delay ageing in metazoans. *Nature*, 430, 686-689.
- YAAR, R., JONES, M., CHEN, J. F. & RAVID, K. 2004. Animal models for the study of adenosine receptor function. *Journal of cellular physiology*, 202, 9-20.
- YANG, B., ESHLEMAN, J. R., BERGER, N. A. & MARKOWITZ, S. D. 1996. Wild-type p53 protein potentiates cytotoxicity of therapeutic agents in human colon cancer cells. *Clinical Cancer Research*, 2, 1649-1657.

YANG, J. H., HSIA, T. C., KUO, H. M., CHAO, P. D., CHOU, C. C., WEI, Y. H. & CHUNG, J. G. 2006. Inhibition of lung cancer cell growth by quercetin glucuronides via G2/M arrest and induction of apoptosis. *Drug metabolism and disposition: the biological fate of chemicals*, 34, 296-304.

YOUSUF, S., ATIF, F., AHMAD, M., HODA, N., ISHRAT, T., KHAN, B. & ISLAM, F. 2009. Resveratrol exerts its neuroprotective effect by modulating mitochondrial dysfunctions and associated cell death during cerebral ischemia. *Brain research*, 1250, 242-253.

YU, C., SHIN, Y., CHOW, A., LI, Y., KOSMEDER, J., LEE, Y., HIRSCHELMAN, W., PEZZUTO, J., MEHTA, R. & VAN BREEMEN, R. 2002. Human, Rat, and Mouse Metabolism of Resveratrol. *Pharmaceutical research*, 19, 1907-1914.

ZHANG, Q., ZHAO, X.-H. & WANG, Z.-J. 2009. Cytotoxicity of flavones and flavonols to a human esophageal squamous cell carcinoma cell line (KYSE-510) by induction of G<sub>2</sub>/M arrest and apoptosis. *Toxicology in vitro*, 23, 797-807.

ZYKOVA, T. A., ZHU, F., ZHAI, X., MA, W. Y., ERMAKOVA, S. P., LEE, K. W., BODE, A. M. & DONG, Z. 2008. Resveratrol directly targets COX-2 to inhibit carcinogenesis. *Molecular carcinogenesis*, 47, 797-805.

## Chapter 8. Publications and conferences

- Polycarpou, E., Meira, L.B., Carrington, S., Tyrrell, E., Modjtahedi, M., and Carew, M.A. (2013). Resveratrol-3-O-D-glucuronide and resveratrol-4'-O-D-glucuronide inhibit colon cancer cell growth: evidence for a role of A3 adenosine receptors, cyclin D1 depletion and G1 cell cycle arrest. *Molecular Nutrition and Food Research* (Available Online 7<sup>th</sup> May 2013).
- Resveratrol 3- and 4' glucuronide inhibit colon cancer cell growth: evidence for a role of adenosine receptors, AMP-activated kinase and cell cycle arrest.

Elena Polycarpou and Mark Carew.

Resveratrol 2012 Conference, University of Leicester, December 2012

- Resveratrol metabolites inhibit colon cancer cell growth.

Elena Polycarpou, Izabel Villela, Lisiane Meira, Chris Fry, Elizabeth Tyrrell, Simon Carrington, Helmout Modjtahedi and Mark Carew

5<sup>th</sup> International Conference on Polyphenols and Health, Sitges, Barcelona, Spain, October 2011